



**HAL**  
open science

# Combining electroencephalography and functional magnetic resonance imaging for neurofeedback

Lorraine Perronnet

► **To cite this version:**

Lorraine Perronnet. Combining electroencephalography and functional magnetic resonance imaging for neurofeedback. Medical Imaging. Université de Rennes, 2017. English. NNT : 2017REN1S043 . tel-01661583

**HAL Id: tel-01661583**

**<https://theses.hal.science/tel-01661583v1>**

Submitted on 12 Dec 2017

**HAL** is a multi-disciplinary open access archive for the deposit and dissemination of scientific research documents, whether they are published or not. The documents may come from teaching and research institutions in France or abroad, or from public or private research centers.

L'archive ouverte pluridisciplinaire **HAL**, est destinée au dépôt et à la diffusion de documents scientifiques de niveau recherche, publiés ou non, émanant des établissements d'enseignement et de recherche français ou étrangers, des laboratoires publics ou privés.

**THÈSE / UNIVERSITÉ DE RENNES 1**  
*sous le sceau de l'Université Bretagne Loire*

pour le grade de

**DOCTEUR DE L'UNIVERSITÉ DE RENNES 1**

*Mention : Informatique*

**Ecole doctorale MATHSTIC (« Mathématiques et Sciences et  
Technologies de l'Information et de la Communication »)**

présentée par

**Lorraine PERRONNET**

Préparée à l'unité de recherche IRISA UMR CNRS 6074 / Inria Rennes  
Nom développé de l'unité : VisAGes - INSERM U1228  
Composante universitaire : Université de Rennes 1

---

**Combinaison de  
l'électroencéphalo-  
graphie et de  
l'imagerie par  
résonance  
magnétique  
fonctionnelle pour le  
neurofeedback**

**Thèse soutenue à Rennes  
le 7 septembre 2017**

devant le jury composé de :

**Olivier BERTRAND**

Directeur de recherche, Inserm, Université Lyon 1 /  
*Président du jury*

**Dimitri VAN DE VILLE**

Professeur associé, EPFL / *Rapporteur*

**François CABESTAING**

Professeur, Université Lille 1 / *Rapporteur*

**François VIALATTE**

Professeur associé, ESPCI Paris / *Examineur*

**Maureen CLERC**

Directeur de recherche, Inria / *Examineur*

**Fabien LOTTE**

Directeur de recherche, Inria / *Examineur*

**Christian BARILLOT**

Directeur de recherche, CNRS / *Directeur de thèse*

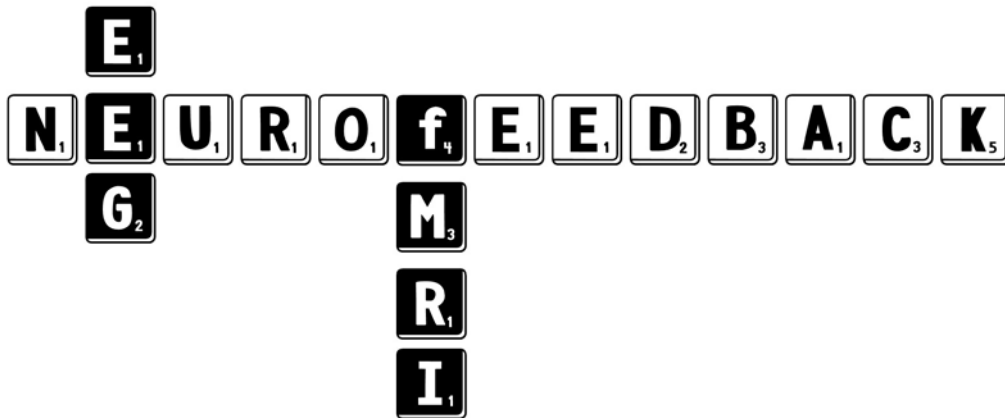
**Anatole LECUYER**

Directeur de recherche, Inria / *Directeur de thèse*



COMBINING EEG AND FMRI FOR NEUROFEEDBACK

LORRAINE PERRONNET





"Those who believe in telekinetics, raise my hand."

— Kurt Vonnegut

"The belief that there is only one truth and that oneself is in possession of it, seems to me the deepest root cause of all that is evil in the world."

— Max Born

I dedicate this work to the two entities of which I am one of the sum, my parents Robert- and -Bertille<sup>1</sup> Perronnet <sup>2</sup>. I owe you almost everything, I guess "almost" being the positive  $\Delta$  corresponding to the fact that the whole is greater than the sum of its parts. Maybe we can discuss that later, now that I have time (... really?).

<sup>1</sup> Note how one is elegantly the continuity of the other

<sup>2</sup> And how our family name sounds as strong as a bone



## ACKNOWLEDGMENTS

---

*Dreams are nothing more than wishes  
And a wish is just a dream  
You wish to come true, woo woo*

*If only I could have a puppy  
I'd call myself so very lucky  
Just to have some company  
To share a cup of tea with me*

*I'd take my puppy everywhere  
La, la, la-la I wouldn't care  
And we would stay away from crowds  
And signs that said no dogs allowed  
Oh we, I know he'd never bite me  
Whoa de lo.....  
We, I know he'd never bite me*

*If only I could have a friend  
To stick with me until the end  
And walk along beside the sea  
Share a bit of moon with me*

*I'd take my friend most everywhere  
La, la, la-la I wouldn't care  
We would stay away from crowds  
With signs that said no friends allowed  
Oh we, we'd be so happy to be  
Whoa de lo.....  
We, we'd be so happy to be together*

— The Puppy Song by Harry Nilsson

Commençons l'hymne des mille et un mercis avec les étoiles du système *Thèse*.

Mes tout premiers remerciements vont bien évidemment à mon duo de directeurs : [Anatole](#) et [Christian](#) (C&A). Vous avez sacrément bien fait la paire et je m'estime chanceuse d'avoir eu deux directeurs complémentaires et s'entendant aussi bien. Anatole, sans tes qualités de manager et tes pouvoirs de remotivation des troupes, je ne sais pas comment je serais arrivée jusqu'au bout. Je fais courir la rumeur selon laquelle tu pourrais ressusciter un thésard mort de déprime :) Merci de toujours commencer nos entrevues par la même question tournée vers la personne en face de toi. Là je suis au bout de ma vie, mais je dirais que sur une échelle de 1 à 7, je suis à 6.4 (record!!) ! Ivresse de la fatigue, ou soulagement d'être arrivée jusqu'au bout ? Christian, merci pour ta détermination, ton pragmatisme mais aussi pour tes grandes idées. Merci à vous deux pour votre optimisme à toute épreuve, pour votre disponibilité régulière malgré vos emplois du temps chargés et pour votre vision stratégique malgré le terrain à nous tous initialement largement inconnu du champ de ma thèse. J'es-



père vraiment avoir hérité ne serait-ce que d'une once de votre optimisme et de votre capacité à présenter les choses sous un angle positif.

A mes encadrants à distance [Maureen](#) et [Fabien](#). Merci pour votre bienveillance et pour vos regards et conseils scientifiques toujours avisés. Merci aussi pour tout ce que vous faites qui contribue à faire vivre la recherche sur les BCI en France et merci d'être un modèle à suivre pour nous les petits padawans du domaine. Merci à [BCI-LIFT](#)!

Merci à [Dimitri Van De Ville](#) et à [François Cabestaing](#) d'avoir été rapporteurs de ma thèse, à [François Vialatte](#) d'avoir été examinateur et à [Olivier Bertrand](#) d'avoir présidé le jury durant ma soutenance de thèse. J'ai été honorée de soutenir ma thèse devant vous tous.

Merci à la [région Bretagne](#) et au [Labex Cominlabs](#) d'avoir financé mes trois années de thèse.

Merci aux assistantes de Visages et Hybrid, [Angélique](#), [Armelle](#) et [Nathalie](#), toujours agréables, réactives et à l'écoute.

Merci à [toutes les personnes qui se sont portées volontaires](#) pour nos expériences de neurofeedback et aux [manips radios](#) de la plateforme Neurinfo qui nous ont si bien assistés durant les expériences et qui ont fait preuve de beaucoup de patience et de dévouement.

Merci aux médecins, [Jean-Marie Batail](#), [Dominique Drapier](#), [Isabelle Bonan](#) et à leurs étudiants, [Maxence](#) et [Simon](#) pour les moments d'échanges. Je vous souhaite beaucoup de réussite avec les essais sur patients. Merci aussi à [Jean-Arthur Micoulaud-Franchi](#) pour son regard érudit, original et aiguisé sur le neurofeedback et merci à la [section Next de l'AFPBN](#) pour tous les efforts que vous mettez en place afin de structurer la recherche et la pratique autour du neurofeedback en France. Vivement la troisième *Journée Nationale sur le Neurofeedback*.

Merci à la [startup Mensia et tous ses membres](#) pour la qualité de leur démarche et de leur travail autour du développement de solutions de neurofeedback performantes, accessibles et attrayantes.

Au tour du système *Collègues* maintenant.

Merci à tous les membres de l'[équipe Visages](#). To [Marsel](#). You and I know it hasn't always been easy but I am glad you were part of the Hemisfer project. Without you, none of this would have been possible. Thank you for all your work, your professionalism and sincerity. I wish you all the best in your Biotrial adventure! Merci à [Elise](#) et [Isabelle](#) pour votre sympathie, vos compétences, votre disponibilité et pour le travail considérable que vous réalisez autour de la plateforme Neurinfo. Merci à [Pierre](#), [Olivier](#) et [Emmanuel](#) d'être toujours là pour aider les autres. Merci à [Pierre-Yves](#) mon co-bureau intermittent, vapoteur, bavard et absolument intéressant de par sa culture et sa curiosité scientifique et générale. Merci à ma co-bureau [Saman](#) pour sa douceur et sa générosité. Et merci à [Francesca](#) ma co-bureau des derniers jours d'avoir fait bonne impression :). Merci à [Michi](#) et [Yao](#) pour leur immuable amicalité et pour notre passion partagée pour Biocoop :). Merci aux membres des débuts, en particulier [Lucas](#) et [Thomas](#) pour avoir mis l'ambiance! Bon courage à ceux qui vont prendre la relève : [Mathis](#), [Giulia](#) et les autres qui arriveront après.

Merci à tous les membres de l'[équipe Hybrid](#). Désolée de n'avoir été qu'un fantôme dans les couloirs qui se matérialisait uniquement pendant les séminaires d'équipe et séminaires au vert. Malheureusement je n'ai pas pu partager mon

corps en deux. Mais je peux multiplier mes mercis par 1000 :) Merci aux pétillantes et compétentes [filles du BCI](#) : [Cam](#) et [Nataliya](#)! Même si je sais que c'est pas pareil, combien de fois je me suis sentie nulle à côté avec mon neurofeedback, mon EEG, mon IRMf et mon taux de publications rikiki comparé aux vôtres :D Vous déchirez les filles! Bonne suite et amusez-vous bien! [Jussi](#). I could actually have added you to the previous corpus of greetings :D Good luck friend, and thank you for the mustard (and the (too rare) crazy conversations)! Merci aux autres BCI guys, [Andéol](#), [Jonathan](#) et [Hakim](#) et à tous les autres côté VR! C'était cool de pouvoir profiter de l'ambiance de cette riche équipe! Et merci aussi à tout ceux que je n'ai pas cité et que j'ai croisé de près ou de loin durant ces dernières années!

Aparté (parce qu'un cerveau n'est rien sans un corps).

Merci à [l'Inria](#) d'avoir financé une partie de mon alimentation bio. Vive les légumes! Merci à [Samuel](#), mon professeur de shiatsu pour ta générosité, ta facétie et merci de nous avoir appris à donner et recevoir les pressions qui font descendre la pression. Merci aux [profs du 36 Boulevard](#) et de [Form Station](#), à mes profs de danse [Hazel](#) et [Elais](#), et à ma prof de yoga [Héloïse](#). Merci à [Marko](#) pour les quelques cours de violon qui ont vraiment changé quelque chose en moi.

Pour finir, au tour des systèmes *amies* et *famille*.

Merci à toutes les [amies de mon petit cercle](#) qui représentent chacune une belle part de mon camembert affectif! Ma [Lou](#), l'amie la plus cool, débrouillard et fidèle qui soit. C'est vrai qu'on est pas beaucoup moins cernées d'incertitudes qu'il y a quelques années, mais c'est peut-être pas si grave parce qu'on accomplit quand même des choses, non? En tout cas, je sais pas où on va mais on y va! Bienvenue à ma petite filleule [Space Jahm Jahm](#)!! Ma [Sara](#), si tu savais comme je suis heureuse de m'être inscrite au cours d'Hazel et d'avoir croisé ton regard hésitant ce jour là. Tu es un vrai cadeau. A présent, ikimashôô! Ma poussine [Anaïs](#). Toi aussi, je ne regrette pas cette soirée pourrie d'un mois de janvier où je t'ai rencontré dans le métro avec la bande de hispters thaïlandais. C'était toi que j'allais ne pas oublier! Ma [Maud](#). Tu déchires! Je suis fière de connaître une fille comme toi avec tant de magie dans ses mains et de personnalité derrière ses yeux et partout ailleurs. Merci infiniment pour les cartoons qui égayent et allègent le (déjà pas si lourd) poids de ce manuscrit :) Ma [Chacha](#), merci d'être encore là. Merci à ma douce [Cécile](#). Merci à toutes les [filles de la danse](#) avec qui on a bien rigolé et fait tournoyer nos jupes! Merci à ma voisine [Isabelle](#) et à [Manon](#) pour votre gentillesse.

Un infini merci à [mes parents](#) du bout du monde pour votre confiance aveugle d'amour et votre soutien à nul autre pareil. Malgré la distance, c'est inestimable de vous avoir. C'est évident que sans vous je ne serais jamais arrivée jusque là. Merci à [mon frère](#) et à [Nerea](#) de n'être pas trop loin pour que je puisse venir vous voir. Merci à mes trois petits basques [Eneko](#), [Unax](#) et [Alaitz](#) pour vos bêtises, vos petites mains, vos grands sourires et les leçons de basque. Je ne pensais pas que le jeu du "krokrodil" aurait autant de succès. Merci de pousser toujours plus loin les possibilités de ce jeu avec vos âmes d'enfants.

Enfin, [Jawzee](#), merci pour tout. Merci d'avoir été là malgré la distance. Du premier au dernier jour, tes bras ont cara-collé en tête des lieux les plus réconfortants pour moi. Oui, et merci à ta famille de m'avoir accueillie.



## ABSTRACT

---

NF is the process of feeding back real-time information to an individual about his/her ongoing brain activity, so that he/she can train to self-regulate neural substrates of specific behavioral functions. NF has been extensively studied for brain rehabilitation of patients with psychiatric and neurological disorders. However its effective deployment in the clinical armamentarium is being held back by the lack of evidence about its efficacy.

One of the possible reason for the debated efficacy of current approaches could be the inherent limitations of single imaging modalities. Indeed, most NF approaches rely on the use of a single modality, EEG and fMRI being the two most widely used. While EEG is inexpensive and benefits from a high temporal resolution (millisecond), its spatial resolution (centimeters) is limited by volume conduction of the head and the number of electrodes. Also source localization from EEG is inaccurate because of the ill-posed inverse problem. In a complementary way, fMRI gives access to the self-regulation of specific brain regions at high spatial resolution (millimeter) but has low temporal resolution (second).

Combined EEG-fMRI has proven much valuable for the study of human brain function, however it has rarely been exploited for NF purpose. In the context of NF, combining EEG and fMRI enables cross-modal paradigm evaluation and validation. But more interestingly it opens up avenues for the development of new NF approaches that would mix both modalities, either at the calibration phase or to provide a bimodal NF signal. Combined EEG-fMRI poses numerous challenges with regard to basic physiology, study design, data quality, analysis/integration and interpretation. These challenges are even greater if EEG and fMRI are both to be used simultaneously for online NF computation, because of the real-time constraint and the difficulty to find a task design compatible with EEG and fMRI' diverging natures.

The theoretical part of this PhD dissertation aims at identifying methodological aspects that differ between EEG-NF and fMRI-NF and at examining the motivations and strategies for combining EEG and fMRI for NF purpose. Among these combination strategies, we choose to focus on bimodal EEG-fMRI-NF as it seems to be one of the most promising approach and is mostly unexplored. The feasibility of this approach was recently demonstrated and opened an entire new field of investigation. First and foremost, we would like to address the following questions: what is the added value of bimodal NF over unimodal NF; are there any specific mechanisms involved when learning to control two NF signals simultaneously; how to integrate EEG and fMRI to derive a single feedback ? The experimental part of this PhD dissertation therefore focuses on the development and evaluation of methods for bimodal EEG-fMRI-NF. In order to conduct bimodal NF experiments, we start by building up a real-time EEG-fMRI platform. Then in a first study, we compare for the first time bimodal EEG-fMRI-NF with unimodal EEG-NF and fMRI-NF. Eventually, in a second study, we introduce and evaluate two integrated feedback strategies for EEG-fMRI-NF.



## RÉSUMÉ

---

Le neurofeedback (NF) est une technique consistant à renvoyer à un individu des informations sur son activité cérébrale en temps réel, lui permettant ainsi d'apprendre à mieux en contrôler certains aspects pour la réorganiser de manière durable. Des effets spécifiques sur les fonctions émotionnelles, cognitives ou comportementales du sujet sont supposés accompagner l'entraînement par NF, ce qui fait du NF une technique prometteuse pour la rééducation du cerveau de patients souffrant de troubles neurologiques ou psychiatriques et pour l'optimisation de la performance chez les sujets sains. Le NF a été étudié comme outil de rééducation cérébrale dans un grand nombre de troubles neurologiques et psychiatriques. Pourtant, son déploiement au sein de l'arsenal thérapeutique est restreint par le manque de preuves concluantes sur sa réelle efficacité. Les limitations inhérentes aux modalités de mesures de l'activité cérébrale pourraient être une des raisons à l'origine de cette efficacité débattue. En effet, la plupart des approches de NF reposent sur l'exploitation d'un seul type de modalité, l'EEG et l'IRMf étant les plus répandues. Alors que l'EEG est peu coûteux et bénéficie d'une haute résolution temporelle (milliseconde), sa résolution spatiale (quelques centimètres) est limitée par la conduction volumique de la tête et le nombre d'électrodes employées. De plus, la localisation de sources à partir de l'EEG est imprécise du fait qu'elle constitue un problème inverse mal posé. De manière complémentaire, l'IRMf rend possible l'auto-régulation de régions cérébrales spécifiques avec une haute résolution spatiale (millimètres) mais pâtit d'une faible résolution temporelle (seconde). La combinaison de l'EEG et de l'IRMf s'est révélée fructueuse dans l'étude des fonctions cérébrales chez l'homme, pourtant elle a rarement été exploitée pour des applications de NF. Dans le cadre du NF, elle permet d'évaluer et de valider différents paradigmes de manière transmodale. Mais surtout, elle ouvre un champ de possibilités pour le développement de nouvelles approches de NF qui mélangeraient les deux modalités, soit à l'étape de calibration soit pour produire un signal de NF bimodal. La combinaison de l'EEG et de l'IRMf pose de nombreux défis relatifs à la physiologie, au design expérimental, à la qualité des données, ainsi qu'à leur analyse/intégration et leur interprétation. Ces défis sont d'autant plus grands si l'EEG et l'IRMf sont destinés à être utilisés simultanément pour le calcul du signal de NF, du fait de la contrainte de temps-réel et de la difficulté de définir des tâches expérimentales compatibles avec les natures divergentes de l'EEG et de l'IRMf. La partie théorique de cette thèse vise à identifier les aspects méthodologiques qui diffèrent entre le NF-EEG et le NF-IRMf ainsi qu'à examiner les motivations et les stratégies pour combiner l'EEG et l'IRMf dans le cadre du NF. Parmi ces différentes stratégies de combinaison, nous avons choisi de nous focaliser sur le NF-EEG-IRMf bimodal car il apparaît comme une approche prometteuse et n'a quasiment pas été étudié. La faisabilité de cette approche a récemment été démontrée, faisant ainsi place à un tout nouveau champ d'investigation. Cette thèse vise à répondre aux questions suivantes : quelle est la valeur ajoutée du NF bimodal par rapport au NF unimodal ; existe-t-il des mécanismes spécifiques engagés lorsqu'un individu apprend à contrôler deux signaux de NF ; comment

intégrer l'EEG et l'IRMf pour produire un seul feedback? La partie expérimentale de cette thèse se focalise donc sur le développement et l'évaluation de méthodes de NF-EEG-IRMf. Afin de conduire des expériences de NF bimodal, nous commençons par mettre en place une plateforme EEG-IRMf temps-réel. Ensuite, dans une première étude, nous comparons les effets du NF-EEG-IRMf, du NF-EEG et du NF-IRMf. Enfin, dans une seconde étude nous proposons et évaluons deux types de feedbacks intégrés pour le NF-EEG-IRMf.

## PUBLICATIONS

---

Below is a list of the publications and communications that have been carried out during this PhD:

- Perronnet, Lorraine**, Anatole Lécuyer, Marsel Mano, Elise Bannier, Fabien Lotte, Maureen Clerc, & Christian Barillot (2017). “Unimodal Versus Bimodal EEG-fMRI Neurofeedback of a Motor Imagery Task.” In: *Frontiers in Human Neuroscience* 11, p. 193. DOI: [10.3389/fnhum.2017.00193](https://doi.org/10.3389/fnhum.2017.00193).<sup>3</sup> <sup>3</sup> Journal paper
- Perronnet, Lorraine**, Anatole Lécuyer, Fabien Lotte, Maureen Clerc, & Christian Barillot (2016). “Entraîner son cerveau avec le neurofeedback / Brain Training with Neurofeedback.” In: *Brain-Computer Interfaces 1: Foundations and Methods*. Ed. by Maureen Clerc, Laurent Bougrain, & Fabien Lotte. John Wiley & Sons, Inc., pp. 271–292. DOI: [10.1002/9781119144977.ch13](https://doi.org/10.1002/9781119144977.ch13).<sup>4</sup> <sup>4</sup> Book chapter
- Mano, Marsel, Anatole Lécuyer, Elise Bannier, **Lorraine Perronnet**, Saman Noorzadeh, & Christian Barillot (2017). “How to build a hybrid neurofeedback platform combining EEG and fMRI.” In: *Frontiers in Neuroscience* 11, p. 140. DOI: [10.3389/FNINS.2017.00140](https://doi.org/10.3389/FNINS.2017.00140).<sup>5</sup> <sup>5</sup> Journal paper
- Perronnet, Lorraine**, Anatole Lécuyer, Fabien Lotte, Maureen Clerc, & Christian Barillot (2017b). “Neurofeedback unimodal ou bimodal ? Intérêt de l’EEG et de l’IRMf.” In: *2ème journée nationale sur le neurofeedback*. ESPCI Paris, France, January 2017.<sup>6</sup> <sup>6</sup> Invited talk
- Perronnet, Lorraine**, Anatole Lécuyer, Fabien Lotte, Maureen Clerc, & Christian Barillot (2017a). “EEG-fMRI neurofeedback of a motor imagery task.” In: *22nd Annual Meeting of the Organization for Human Brain Mapping (OHBM 2016)*. Palexpo, Geneva, Switzerland, June 2017.<sup>7</sup> <sup>7</sup> Poster
- Mano, Marsel, Elise Bannier, **Lorraine Perronnet**, Anatole Lécuyer, & Christian Barillot (2017). “Platform for Hybrid EEG-fMRI Neurofeedback Studies.” In: *22nd Annual Meeting of the Organization for Human Brain Mapping (OHBM 2016)*. Palexpo, Geneva, Switzerland, June 2017.<sup>8</sup> <sup>8</sup> Poster
- Perronnet, Lorraine**, Anatole Lécuyer, Marsel Mano, Elise Bannier, Fabien Lotte, Maureen Clerc, & Christian Barillot (2016). “HEMISFER: Hybrid Eeg-MrI and Simultaneous neuro-FeedBack for brain Rehabilitation.” In: *1ère journée nationale sur le neurofeedback*. ICM, Paris, France, January 2016.<sup>9</sup> <sup>9</sup> Poster
- Bannier, Elise, Marsel Mano, Robert Stoermer, Isabelle Corouge, **Lorraine Perronnet**, Jussi Lindgren, Anatole Lécuyer, & Christian Barillot (2015). “On the feasibility and specificity of simultaneous EEG and ASL MRI at 3T.” In: *Proceedings of ISMRM 2015*. Toronto, Canada, May 2015.<sup>10</sup> <sup>10</sup> Abstract





# CONTENTS

---

Résumé en français	1
<b>1 GENERAL INTRODUCTION</b>	<b>9</b>
1.1 What is neurofeedback ?	9
1.2 Time for NF to go multimodal ?	9
1.3 Combining EEG and fMRI for NF	11
1.4 Goals of this thesis	13
1.5 Chapter-by-chapter overview	14
<b>2 STATE-OF-THE-ART ON NEUROFEEDBACK</b>	<b>17</b>
2.1 Introduction	17
2.2 How does it work?	19
2.2.1 Design of an NF training program	19
2.2.2 Course of a NF session: when the eyes "look" at the brain	20
2.2.3 A learning procedure that we still do not fully understand	21
2.3 60 years of history	22
2.3.1 Yesterday: too premature an infatuation	22
2.3.2 Today: diversification of approaches	23
2.4 Where NF meets BCI	25
2.5 Applications	26
2.6 Conclusion	29
<b>3 COMBINING EEG AND FMRI FOR NEUROFEEDBACK</b>	<b>31</b>
3.1 When to do simultaneous recordings ?	31
3.2 When EEG and fMRI agree and disagree	32
3.3 Methodological comparison of EEG-NF and fMRI-NF	34
3.4 Literature review of EEG/fMRI NF studies	37
3.5 Taxonomy for EEG/fMRI NF studies	40
3.6 Conclusion	42
<b>4 HOW TO BUILD A REAL-TIME EEG-FMRI PLATFORM FOR BIMODAL NEUROFEEDBACK</b>	<b>43</b>
4.1 General description of a real-time EEG-fMRI platform for bimodal neurofeedback	43
4.1.1 NF Unit	44
4.1.2 Neurofeedback Presentation	50
4.2 Illustrative Example: Bimodal Neurofeedback Platform at Neuroinfo	51
4.2.1 EEG subsystem	51
4.2.2 FMRI subsystem	52
4.2.3 NF Unit	52
4.2.4 Display	55
4.2.5 Real-time performance	55
4.2.6 Preparing the subject for EEG-fMRI scanning	56
4.3 Discussion	57

4.4	Conclusion . . . . .	58
5	UNIMODAL VERSUS BIMODAL EEG-FMRI NEUROFEEDBACK OF A MOTOR-IMAGERY TASK	59
5.1	Methods . . . . .	59
5.1.1	Experimental procedure . . . . .	59
5.1.2	Data acquisition/technical setup . . . . .	62
5.1.3	Real-time data processing . . . . .	62
5.1.4	Working hypotheses . . . . .	64
5.1.5	Offline analysis . . . . .	65
5.2	Results . . . . .	67
5.2.1	fMRI data analysis . . . . .	67
5.2.2	EEG data analysis . . . . .	70
5.2.3	Questionnaire . . . . .	71
5.3	Discussion . . . . .	71
5.4	Conclusion . . . . .	76
6	LEARNING 2-IN-1: TOWARDS INTEGRATED EEG-FMRI-NEU- ROFEEDBACK	77
6.1	Introduction . . . . .	77
6.2	Material and methods . . . . .	79
6.2.1	Experimental protocol . . . . .	79
6.2.2	Data acquisition . . . . .	81
6.2.3	Real-time data processing . . . . .	81
6.2.4	Calibration phase . . . . .	82
6.2.5	Offline analysis . . . . .	83
6.3	Results . . . . .	84
6.4	Discussion . . . . .	87
6.5	Conclusion . . . . .	90
7	CONCLUSION AND PERSPECTIVES	91
7.1	General conclusion . . . . .	91
7.2	Perspectives: variations around bimodal NF . . . . .	92
7.2.1	Reinforce our findings . . . . .	92
7.2.2	Multi-sensory bimodal NF . . . . .	93
7.2.3	Integrate EEG and fMRI at earlier stages of the NF loop . . . . .	93
7.2.4	Mixed protocols . . . . .	94
7.2.5	Investigate other modality couples . . . . .	94
7.2.6	Investigate other integrated feedback paradigms . . . . .	94
7.2.7	Going towards clinical applications . . . . .	95
7.3	Last words . . . . .	96
A	PHD COMICS	97

## LIST OF FIGURES

---

FIGURE 1	Boucle de neurofeedback . . . . .	3
FIGURE 2	Base physiologique de l'EEG/MEG et de l'IRMf . . . . .	4
FIGURE 3	Vue d'ensemble des contributions de cette thèse . . . . .	6
Figure 9	Neurofeedback loop . . . . .	10
Figure 10	Physiological basis of EEG/MEG and fMRI . . . . .	12
Figure 11	Overview of contributions . . . . .	14
Figure 17	Example of an EEG-NF environment . . . . .	21
Figure 18	60 years of NF history . . . . .	25
Figure 19	Separate versus simultaneous EEG-fMRI . . . . .	31
Figure 20	EEG micro-states (from Koenig et al. (2002)) . . . . .	33
Figure 21	Methods for fMRI feature extraction . . . . .	36
Figure 22	EEG-fMRI-NF protocol for emotional regulation . . . . .	39
Figure 23	Taxonomy of EEG/fMRI NF studies . . . . .	41
Figure 24	Abstract diagram of an EEG-fMRI NF platform . . . . .	44
Figure 25	Unimodal and bimodal NF scenarios . . . . .	47
Figure 26	Generic diagram of a real-time EEG processing pipeline . . . . .	48
Figure 27	Generic diagram of a real-time fMRI processing pipeline . . . . .	49
Figure 28	Neurofeedback visualization examples . . . . .	51
Figure 29	System synchronization . . . . .	54
Figure 30	Detailed diagram of the real-time EEG-fMRI NF platform . . . . .	54
Figure 31	System installation pictures . . . . .	55
Figure 32	Hardware and software delays . . . . .	56
Figure 33	Experiment preparation . . . . .	57
Figure 34	Experimental procedure . . . . .	61
Figure 35	Real-time multimodal EEG/fMRI-NF setup . . . . .	63
Figure 36	Working hypotheses . . . . .	65
Figure 37	BOLD activation maps at group level . . . . .	68
Figure 38	fMRI laterality group mean . . . . .	69
Figure 39	Post-hoc fMRI activations . . . . .	70
Figure 40	EEG laterality group mean . . . . .	71
Figure 41	Post-hoc EEG activations group mean . . . . .	72
Figure 42	Summary of the statistical analysis results . . . . .	73
Figure 43	Levels of integration of multimodal information . . . . .	78
Figure 44	Integrated feedback strategies . . . . .	80
Figure 45	Experimental protocol . . . . .	80
Figure 46	Activations maps in both groups . . . . .	84
Figure 47	Activations maps in each group . . . . .	85
Figure 48	Difference of activation . . . . .	85
Figure 49	Online group mean . . . . .	86
Figure 50	Posthoc group mean . . . . .	86
Figure 51	Individual online means . . . . .	88
Figure 56	Bimodal NF paradigms . . . . .	95

## LIST OF TABLES

---

Table 1	Methodological comparison of EEG-NF and fMRI-NF	35
---------	---	----

## ACRONYMS

---

ADHD	Attention Deficit Hyperactivity Disorder
ANOVA	ANalysis Of VAriance
ASL	Arterial Spin Labelling
BCG	Ballisto-CardioGram
BCI	Brain-Computer Interface
BOLD	Blood-Oxygen Level Dependent
CNS	Central Nervous System
CSP	Common Spatial Pattern
EEG	Electro-Encephalography
EPI	Echo-Planar Imaging
ERD	Event-Related Desynchronization
ERP	Event-Related Potential
FLD	Fisher's Linear Discriminant analysis
fMRI	functional Magnetic Resonance Imaging
fNIRS	functional Near-Infrared Spectroscopy
GLM	General Linear Model
HRF	Hemodynamic-Response Function
ICA	Independent Component Analysis
kMI	kinesthetic Motor Imagery
LDA	Linear Discriminant Analysis
LFP	Local Field Potential
LORETA	LOW RESolution brain electromagnetic Tomography
MDD	Major Depressive Disorder
MEG	Magneto-Encephalography

MI Motor Imagery  
MR Magnetic Resonance  
NF NeuroFeedback  
PCA Principal Component Analysis  
PTSD Post-Traumatic Stress Disorder  
QEEG Quantitative EEG  
ROI Region of interest  
rtfMRI real-time fMRI  
SCP Slow Cortical Potential  
SMR Sensori-Motor Rhythm  
SNR Signal-to-Noise Ratio  
TCP/IP Transmission Control Protocol/Internet Protocol  
TMS Transcranial Magnetic Stimulation  
TR Time Repetition  
TTL Transistor-Transistor Logic



## RÉSUMÉ EN FRANÇAIS

---

### QU'EST-CE QUE LE NEUROFEEDBACK ?

Cette question n'est pas aussi innocente qu'elle en a l'air. Faire une thèse sur le neurofeedback s'apparente en quelque sorte à étudier une légende vivante et à contribuer à la maintenir en vie. N'eût été que pour la curiosité de découvrir l'histoire trouble du NF et pour le défi de démêler la confusion planant sur ce qu'est vraiment le NF, cette thèse en aurait valu la peine. Mais participer à l'écriture d'un chapitre de la saga du NF aura aussi été une passionnante aventure.

Présenté simplement, le neurofeedback est un procédé consistant à renvoyer à un individu de l'information sur son activité cérébrale en temps réel, afin qu'il/elle s'entraîne à contrôler les substrats neuronaux de certaines fonctions<sup>11</sup>. Le NF a été étudié de manière extensive pour la rééducation de patients souffrant de troubles neurologiques et psychiatriques et pour l'optimisation de la performance chez des sujets sains<sup>12</sup>. Dans certains pays le NF est aussi utilisé par des praticiens mais leurs pratiques ne reflètent pas nécessairement l'état de la recherche<sup>13</sup>.

Le domaine du neurofeedback est très proche de celui des interfaces cerveau-machine (ICM) dans le sens où les deux approches sont basées sur l'exploitation en temps réel de mesures de l'activité cérébrale. Dans le cas du NF, le but est orienté vers le développement d'un contrôle interne (auto-régulation) tandis que le but des ICM traditionnelles est orienté vers la communication et le contrôle d'objets externes (orthèse, ordinateur, ...) <sup>14</sup>. De façon intéressante, les applications des ICM sont historiquement dérivées du NF. Pourtant, il arrive que la communauté ICM batte froid à la communauté NF et rechigne à utiliser le terme "neurofeedback" lorsqu'ils sont pourtant en train d'en faire. En effet, la communauté ICM a récemment commencé à concevoir des ICM pour la rééducation cérébrale alors que c'est justement le but du NF. Ce type d'ICM est appelée "*ICM réparatrice*" en opposition avec les traditionnelles "*ICM d'assistance*" et peut être considéré comme équivalent au NF<sup>15</sup>. Parce que le NF et les ICM sont si proches et complémentaires, cette thèse prend en considération à la fois la littérature du NF et des ICM. Il existe cependant des différences méthodologiques entre les deux domaines qu'il sera important de prendre en considération<sup>16</sup>.

### TEMPS VENU POUR LE NF MULTIMODAL ?

De nos jours, il existe encore un grand besoin de nouvelles méthodes pour le traitement des troubles neurologiques et psychiatriques<sup>17</sup>. En effet, certains patients répondent mal aux traitements classiques ou souffrent de forts effets secondaires. Pour les moins chanceux, il n'existe parfois pas de solution viable. En exploitant la plasticité cérébrale et les capacités d'auto-régulation du patient, le NF apparaît comme une alternative non-invasive prometteuse ou comme complément aux traitements existants tels que les médicaments, la neuro-chirurgie, la psychothérapie et les techniques de stimulation passives. Le NF laisse même

<sup>11</sup> Par exemple la régulation des émotions, la motricité, l'attention, la perception de la douleur, la sensation de dépendance ...

<sup>12</sup> **Dichotomie #1** : applications cliniques versus non cliniques, cf. [Section 2.5](#)

<sup>13</sup> **Dichotomie #2** : la pratique du NF versus la recherche en NF, cf. [Chapter 2](#)

<sup>14</sup> **Dichotomie #3** : NF et ICM (HUSTER et al., 2014)

<sup>15</sup> NF  $\equiv$  restorative BCI  $\neq$  assistive BCI

<sup>16</sup> Cf. [Section 2.4](#) pour plus d'explications sur les similitudes et les différences entre NF et ICM

<sup>17</sup> Comme par exemple : les AVC, la dépression, les troubles anxieux, le TDAH, l'épilepsie, la douleur chronique, l'addiction, la schizophrénie, les acouphènes, l'autisme, les migraines, ...



espérer pouvoir obtenir des effets bénéfiques à long terme avec peu ou pas d'effets secondaires. Cependant, l'histoire du NF depuis ses débuts à aujourd'hui montre que le chemin vers la terre promise du NF est une route longue et sinueuse. On ne met pas si facilement le cerveau d'une personne à sa disposition...

La recherche sur le NF remonte aux années 50 avec les travaux pionniers de Joe Kamiya à l'Université de Chicago sur le conditionnement opérant des ondes alpha de l'EEG chez l'homme. Certaines chercheurs<sup>18</sup> font même remonter les origines du NF à la première démonstration de conditionnement classique de l'EEG humain par le psychologue français Gustave Durup et le neurophysiologiste français Alfred Fessard dans les années 30<sup>19</sup>, ce qui veut dire peu de temps après que l'EEG de l'homme fut décrit pour la première fois par Hans Berger dans les années 20. On pourrait dire que dès qu'on trouve une nouvelle manière de mesurer l'activité cérébrale on a une nouvelle manière de la contrôler, du moment qu'on peut en extraire assez rapidement des informations utiles. Aux débuts des années 2000, longtemps après la première démonstration du NF-EEG, l'avènement de l'IRMf temps-réel rendit possible le NF-IRMf<sup>20</sup>. Celui-ci donna accès à l'auto-régulation des régions profondes du cerveau avec une haute résolution spatiale, ce qui n'était pas possible avec le NF-EEG. Une décennie plus tard, la magnétoencéphalographie (MEG)<sup>21</sup> et la spectroscopie proche infrarouge fonctionnelle (SPIR)<sup>22</sup> s'ajoutèrent à la liste des modalités de NF. A ce jour, l'EEG et l'IRMf sont les modalités les plus utilisées dans la recherche et offrent une variété d'approches<sup>23,24</sup>. Le NF-EEG se décline en : NF traditionnel qui cible des bandes de fréquences à une ou deux électrodes; NF des potentiels corticaux lents; NF z-score qui consiste à normaliser différentes métriques provenant d'un EEG quantitatif; ou le NF LORETA qui se focalise sur un signal reconstruit à partir d'une région corticale d'intérêt. De son côté, le NF-IRMf a essentiellement évolué en passant des approches ciblant une seule région à des approches multivariées. La [Figure 1](#) illustre les boucles fermées du NF-EEG et du NF-IRMf.

Malgré la variété d'approches de NF qui ont été développées et étudiées sur un large panel d'applications au cours de toutes ces années d'existence, la méthodologie optimale et l'efficacité du NF restent aujourd'hui débattues. Actuellement, l'application la plus convaincante du NF-EEG est dans le traitement du trouble de l'attention avec hyperactivité chez l'enfant pour lequel des essais contrôlés et randomisés ainsi qu'une série de méta-analyses ont été publiés. Le faible niveau d'évidence du NF résulte probablement de l'insuffisance d'études remplissant les critères de la médecine basée sur la preuve (petite taille d'échantillon, manque de conditions contrôle, pas de randomisation ou de double aveugle, ...), de l'hétérogénéité des approches utilisées par différentes études, et du manque de connaissance sur les mécanismes sous-tendant le NF qui fait qu'il est difficile d'établir un corpus de bonnes pratiques. Cet état de fait est en train de changer car les études de NF deviennent de plus en plus rigoureuses<sup>25</sup> et car un nouveau type d'études émergent tentant de comprendre les mécanismes du NF<sup>26</sup> et de résoudre différents aspects méthodologiques<sup>27</sup>.

Il se pourrait bien que le manque d'efficacité des approches actuelles soit aussi en partie lié aux limitations inhérentes aux modalités de mesures qui sont employées de manière unimodale<sup>28</sup>. En effet, la plupart des approches de NF exploitent une seule modalité de mesure de l'activité cérébrale parmi l'EEG,

<sup>18</sup> (Martijn ARNS, BATAIL et al., 2017)

<sup>19</sup> **Dichotomie #4** : conditionnement classique versus opérant. Le conditionnement est un concept de psychologie comportementale qui a trait au façonnage des comportements. Le conditionnement classique consiste à émettre un signal neutre avant le déclenchement d'une réponse réflexe (i.e. les comportements involontaires et automatiques) de sorte qu'à terme le signal neutre devienne déclencheur du réflexe (association). Le conditionnement opérant consiste à récompenser et/ou punir un comportement volontaire afin de le renforcer ou de le diminuer. Le conditionnement opérant est traditionnellement considéré comme jouant un rôle central dans le processus de NF. Mais récemment, la compréhension des processus de NF a évolué vers des modèles plus complexes impliquant à la fois des processus volontaires et involontaires.

<sup>20</sup> (S.-S. YOO & JOLESZ, 2002a)

<sup>21</sup> (LAL et al., 2005; SUDRE et al., 2011)

<sup>22</sup> (MIHARA et al., 2012; KOBER, WOOD et al., 2014)

<sup>23</sup> (HAMMOND, 2011; SULZER et al., 2013)

<sup>24</sup> **Dichotomie #5** : EEG et IRMf

<sup>25</sup> (SULZER et al., 2013; STOECKEL et al., 2014; THIBAUT, LIFSHITZ & RAZ, 2016)

<sup>26</sup> (NINAUS et al., 2013; SITARAM, ROS et al., 2016; EMMERT, KOPEL, SULZER et al., 2016; BIRBAUMER, RUIZ & SITARAM, 2013; KOBER, WITTE et al., 2013)

<sup>27</sup> (EMMERT, KOPEL, KOUSH et al., 2017; KRAUSE et al., 2017; SORGER, KAMP et al., 2016; SEPULVEDA et al., 2016)

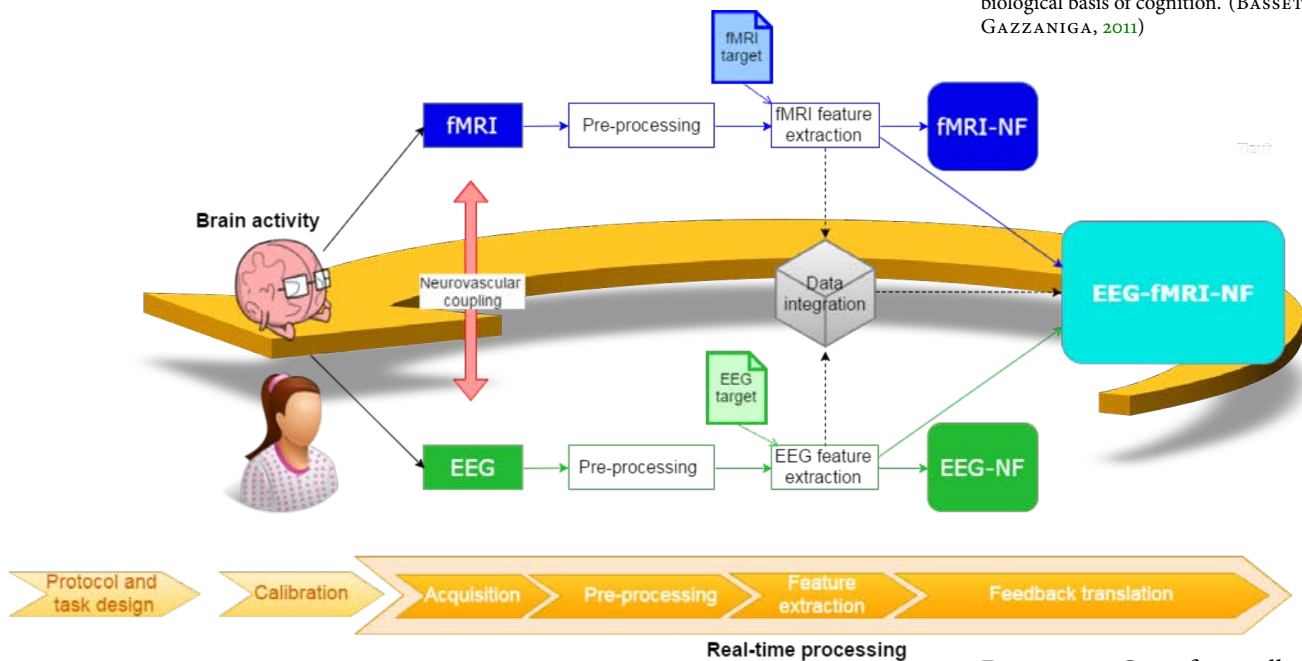
<sup>28</sup> (BIESSMANN et al., 2011; FAZLI, DAHNE et al., 2015)

l'IRMf, la SPIR ou la MEG. Chacune de ces modalités est sensible à des phénomènes biophysiques particuliers liés à l'activité cérébrale et présente des limitations physiologiques et techniques propres<sup>29</sup>. Étant donné la complexité de l'activité cérébrale qui se propage à différentes échelles spatiales et temporelles, personne ne devrait douter qu'il faudrait plus d'un seul dispositif de mesure pour la capter dans ses moindres subtilités<sup>30</sup>.

Combiner plusieurs modalités de mesure pourrait permettre de surmonter certaines limitations des modalités individuelles, extraire des informations plus riches et précises sur l'activité cérébrale et développer des approches de NF plus efficaces. En particulier, la combinaison de l'EEG et de l'IRMf est prometteuse car elle pourrait permettre d'allier la haute résolution temporelle de l'EEG à la haute résolution spatiale de l'IRMf. Dans la communauté ICM, le champ des

<sup>29</sup> (BIESSMANN et al., 2011)

<sup>30</sup> Dire que l'activité cérébrale est complexe est un euphémisme (BULLMORE et al., 2009). On estime que le cerveau humain possède 86 milliards de neurones (16 milliards dans le cortex cérébral, 69 dans le cervelet) (HERCULANO-HOUZEL, 2009) qui déchargent 0.1 - 200 fois par seconde. "It is a complex temporally and spatially multiscale structure that gives rise to elaborate molecular, cellular, and neuronal phenomena that together form the physical and biological basis of cognition." (BASSETT & GAZZANIGA, 2011)



ICM hybrides a récemment émergé<sup>31</sup>, le terme "hybride" faisant référence à une combinaison multimodale de capteurs. Une ICM hybride est définie comme la combinaison de deux ICM ou d'au moins une ICM et d'un autre dispositif comme par exemple un dispositif de biofeedback<sup>32</sup>. Elles peuvent être conçues pour fonctionner de manière simultanée ou séquentielle. Leur but est essentiellement d'améliorer l'usabilité et/ou la performance de l'ICM. Dans la littérature, la plupart des ICM hybrides combinant deux ICM sont basées sur des paradigmes EEG. Mais certains travaux combinant EEG et SPIR ont aussi été proposés<sup>33</sup> et ont montré une performance accrue. Ces résultats encourageants suggèrent qu'utiliser des approches hybrides/multimodales pour le NF pourrait permettre de dépasser l'efficacité des approches unimodales. Si la portabilité et le coût du dispositif sont des critères critiques pour les ICM d'assistance car elles sont destinées à être utilisées de manière fréquente, ces critères sont moins décisifs en NF. C'est une raison pour laquelle la communauté ICM (lorsqu'elle ne fait pas du NF) est plus portée à investiguer la combinaison de l'EEG et de la SPIR plutôt que celle de l'EEG et de l'IRMf.

FIGURE 1 – Cette figure illustre la boucle fermée du NF-EEG, du NF-IRMf et du NF-EEG-IRMf, les étapes préparatoires hors-ligne telles que "Design de la tâche et du protocole" et "Calibration", ainsi que les concepts issus de la littérature de l'EEG-IRMf tels que le "couplage neurovasculaire" et l'"intégration de données"

<sup>31</sup> (PFURTSCHELLER, B. Z. ALLISON et al., 2010; AMIRI, FAZEL-REZAI & ASADPOUR, 2013)

<sup>32</sup> (PFURTSCHELLER, B. Z. ALLISON et al., 2010)

<sup>33</sup> (FAZLI, MEHNERT et al., 2012; BUCCHINO, KELES & OMURTAG, 2016)

## COMBINER L'EEG ET L'IRMf POUR LE NF

<sup>34</sup> "marry the blind (EEG) and the lame (fMRI)"

<sup>35</sup> Vous pouvez essayer de lire cette phrase dans l'autre sens si vous préférez voyager dans le temps de la manière directe

L'EEG et l'IRMf sont complémentaires dans leurs forces, leurs limitations et dans la nature de leurs signaux<sup>34</sup> (see [Figure 10](#)). L'EEG reflète la somme des potentiels post-dendritiques synchronisés d'un grand nombre de cellule pyramidales. Elle bénéficie d'une haute résolution temporelle (millisecondes) qui lui permet de détecter les rythmes du cerveau qui vont des ondes delta (0.5 - 4Hz) aux ondes gamma (> 30Hz). Cependant, sa résolution spatiale (centimètres) est limitée par la conduction volumique de la tête, par le nombre d'électrodes et par le fait que le problème inverse de reconstruction de sources est mal posé. De son côté, l'IRMf mesure indirectement l'activité cérébrale au moyen de l'effet "dependant du niveau d'oxygène" (BOLD). L'IRMf est sensible aux propriétés magnétiques du sang qui changent en fonction de la concentration locale en oxygène qui varie en réponse au besoin en énergie des neurones qui s'activent<sup>35</sup>. Elle offre une résolution spatiale très appréciée (millimètres) de tout le cerveau. Mais sa résolution temporelle est limitée par le temps nécessaire pour acquérir un volume complet du cerveau ( $\geq$  centaines de millisecondes), et par le fait que le pic de la réponse hémodynamique est retardé de 4 à 6 secondes de l'onset neuronal et que cette réponse hémodynamique agit comme un filtre passe-bas qui lisse la réponse neuronale.

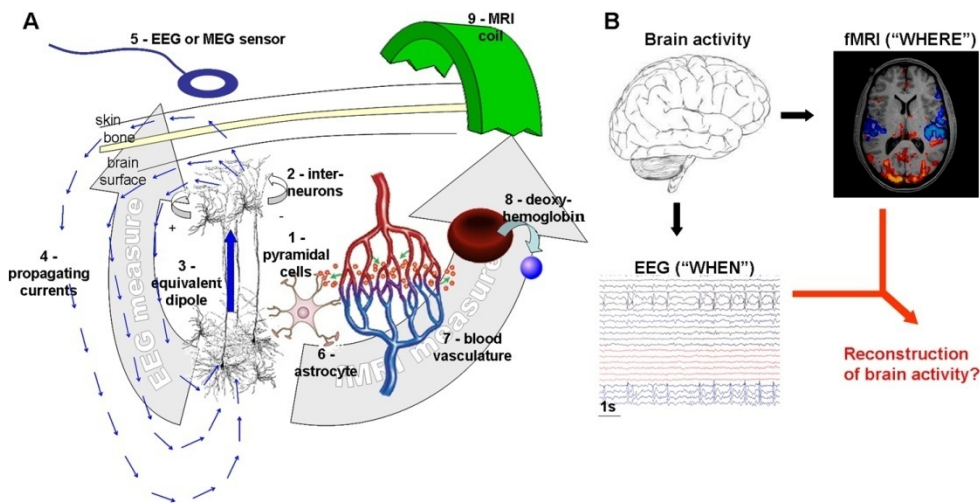


FIGURE 2 – Base physiologique de l'EEG/MEG et de l'IRMf (DE-NEUX, 2011)

<sup>36</sup> (IVES, WARACH & SCHMITT, 1993)

Le développement de l'EEG-IRMf combiné a été initialement motivé par les applications en épilepsie afin de localiser les sources neuronales des décharges épileptiques. La première étude EEG-IRMf a eu lieu en 1992<sup>36</sup>. A cette époque, l'EEG et l'IRMf devaient être enregistrés de manière alternée pour des raisons de sûreté du sujet et du matériel et de qualité des données. En effet, les ondes de radio-fréquences qui oscillent rapidement couplées au puissant champ magnétique statique de l'aimant induisent des courants dans les objets conducteurs, ce qui peut produire un échauffement au niveau des électrodes, endommager les tissus ou le matériel et introduire des artefacts dans les données. Au début des années 2000, le développement de dispositifs EEG compatibles avec l'environnement de l'IRM fait à partir de matériaux non ferro-magnétiques et le développement d'algorithmes de réduction des artefacts rendirent possible l'acqui-

tion simultanée de l'EEG et de l'IRMf. Depuis, l'EEG-IRMf combiné a trouvé sa place dans la planification pré-chirurgicale de l'épilepsie et a significativement contribué à avancer la compréhension du cerveau humain pendant l'état de repos, le sommeil et lors de tâches cognitives.

Dans le contexte du NF, la combinaison de l'EEG et de l'IRMf ouvre des possibilités pour la validation transmodale des paradigmes mais aussi et surtout *pour le développement d'approches de NF qui mélangeraient les deux modalités, soit à la phase de calibration soit en ligne pour renvoyer un NF bimodal, ou utilisées de manière alternative*. Au moment où cette thèse a commencé (fin 2013), très peu d'études de NF avaient eu recours à l'EEG-IRMf combiné. Pourtant toutes ces études avaient des motivations différentes et exploitaient des approches différentes ce qui illustre la variété de possibilités que l'EEG-IRMf a à offrir dans le cadre du NF. Parmi ces études, deux en particulier ont tracé deux grandes directions pour l'usage combiné de l'EEG et de l'IRMf pour le NF. La première étude par Meir-Hasson et al.<sup>37</sup> a introduit l'idée du NF-EEG informé par l'IRMf en proposant une méthode qui produit une empreinte EEG utilisée pour prédire le signal l'IRMf d'une région profonde. La seconde étude par Zotev et al. a présenté la première preuve de concept du NF-EEG-IRMf bimodal qui consiste à renvoyer simultanément au sujet un NF basé simultanément sur l'EEG et l'IRMf<sup>38</sup>. Bien qu'étant des contributions significatives, ces travaux pionniers présentaient des limitations qui laissaient largement la place à des améliorations et approfondissements. La méthode de Meir-Hasson et al. est avantageuse car elle limite le recours coûteux à l'IRMf mais est réductrice dans le sens où elle n'utilise qu'une seule électrode EEG et n'exploite pas complètement le potentiel des deux modalités. Les travaux de Zotev et al. sont les premiers à proposer de renvoyer simultanément un NF-EEG et un NF-IRMf en partant de la supposition que cette approche pourrait s'avérer plus efficace que les approches unimodales. Cependant cette hypothèse n'a pas été testée. Il n'est donc pas clair quelle est la valeur ajoutée de cette nouvelle approche et si des mécanismes spécifiques sont à l'oeuvre lorsqu'un sujet apprend à réguler deux signaux plutôt qu'un.

<sup>37</sup> (MEIR-HASSON, KINREICH et al., 2013)

<sup>38</sup> (ZOTEV, PHILLIPS et al., 2014a)

## OBJECTIFS DE CETTE THÈSE

Cette thèse adresse les questions suivantes :

- *Pourquoi et comment combiner l'EEG et l'IRMf dans le cadre du NF et quelles sont les stratégies les plus prometteuses ?*
- *Quelles sont les contraintes méthodologiques de l'EEG et de l'IRMf qu'il faut particulièrement considérer lors de la conception d'un protocole de NF-EEG-IRMf ?*
- *Comment développer une plateforme expérimentale de NF-EEG-IRMf ?*
- *Quelle est la valeur ajoutée du NF-EEG-IRMf comparé au NF-EEG et au NF-IRMf, et existe-t-il des mécanismes spécifiques à l'oeuvre lorsqu'un sujet apprend à contrôler deux signaux d'origine cérébrale plutôt qu'un seul ?*
- *Comment intégrer et représenter l'EEG et l'IRMf au sein d'un seul feedback ?*

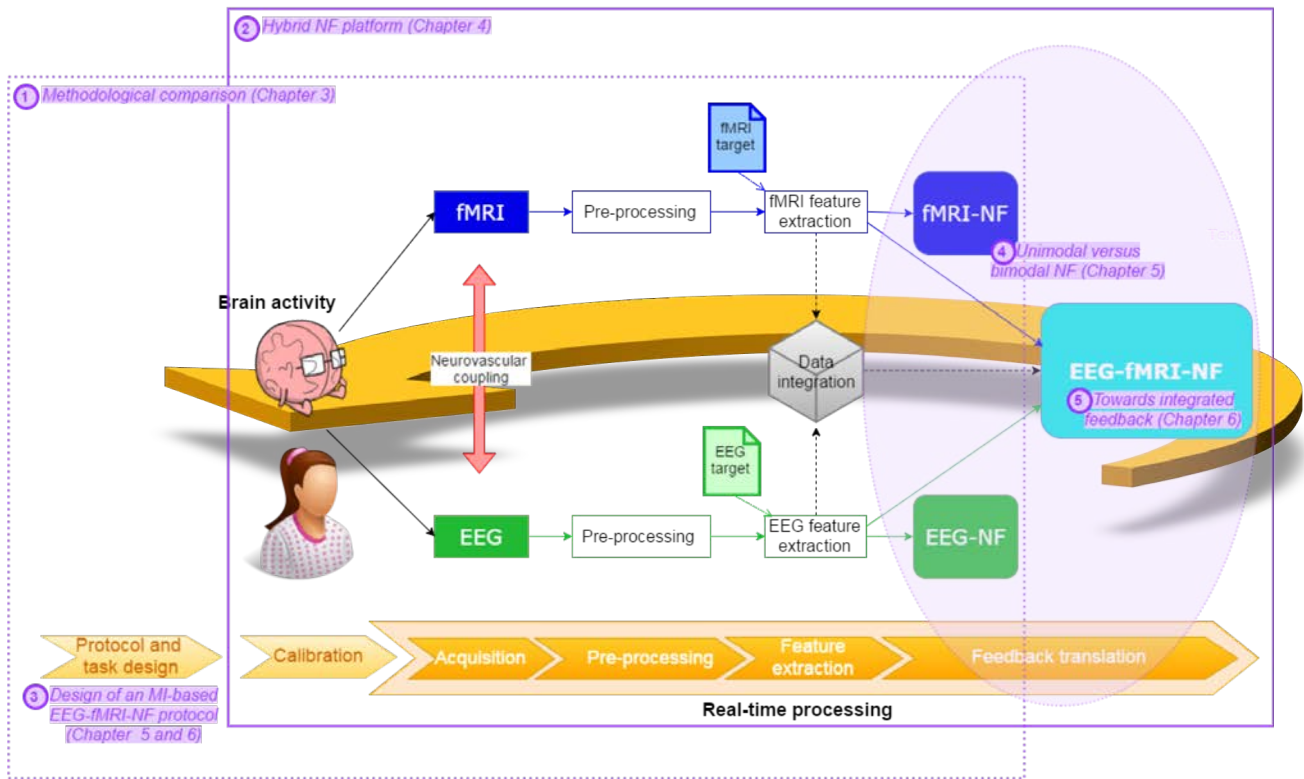


FIGURE 3 – Vue d'ensemble des contributions de cette thèse

A partir de l'étude de la complémentarité entre l'EEG et l'IRMf, cette thèse propose dans un premier temps d'analyser les contraintes spécifiques que chacune de ces modalités imposent sur le design expérimental d'un protocole de NF, et d'identifier les motivations et les stratégies pour combiner ces deux modalités dans le cadre du NF (cf. contribution ① de Figure 11). Par la suite, parmi ces différentes stratégies de combinaison, nous proposons de nous focaliser sur l'investigation, la conception et l'évaluation de méthodes pour le NF-EEG-IRMf bimodal car il apparaît comme une des stratégies les plus prometteuses et n'a quasiment pas été explorée. Pour cela, nous commençons par mettre en place une plateforme EEG-IRMf temps réel capable de fournir un NF dans des conditions unimodales et bimodales (cf. contribution ② de Figure 11). Ensuite, nous procédons à la partie expérimentale de cette thèse. Dans une première étude nous évaluons la valeur ajoutée du NF-EEG-IRMf bimodal comparé au NF-EEG et au NF-IRMf (contribution ④ de Figure 11). Enfin dans une deuxième étude nous introduisons et évaluons de stratégies de feedback intégrés pour le NF-EEG-IRMf (contribution ③ de Figure 11). Nos protocoles et études sont élaborés dans le contexte de l'entraînement à l'imagerie motrice, car cela n'a pas encore été fait et car les activations EEG et IRMf des régions motrices sont bien connues et représentent donc un bon point de départ pour le développement et l'évaluation de nouvelles méthodes (contribution ③ in Figure 11). Les contributions de cette thèse sont indiquées en violet sur la Figure 11.



## PLAN DE CETTE THÈSE

Le **Chapitre 2** présente un état de l'art du neurofeedback. Nous y décrivons la mise en place d'un programme d'entraînement par NF et le déroulement typique d'une session de NF ainsi que les mécanismes sous-tendant le NF. Ensuite nous y retraçons l'histoire du NF de manière à comprendre l'origine de sa parfois mauvaise réputation et appréhender la diversité des approches existantes. Nous discutons aussi de comment les champs du NF et des ICM pourraient se rapprocher avec le développement des ICM "réparatrices". Enfin, nous présentons les applications du NF en détaillant l'état de la recherche sur quelques unes de ses applications cliniques majeures.

Le **Chapitre 3** pose les bases pour comprendre comment l'EEG et l'IRMf peuvent être combinés dans le cadre du NF. Nous commençons par expliquer dans quelles situations l'EEG et l'IRMf doivent être acquis de manière simultanée et comment les signaux BOLD et électrophysiologiques sont reliés. Ensuite nous dressons une comparaison méthodologique du NF-EEG et du NF-IRMf qui sera particulièrement utile pour la conception de protocole de NF-EEG-IRMf. Enfin, nous passons en revue de manière exhaustive le corpus d'études de NF ayant exploités l'EEG et l'IRMf et proposons une taxonomie de ce type d'études.

Le **Chapitre 4** décrit comment mettre en place une plateforme EEG-IRMf temps-réel capable de fournir un NF bimodal. La première partie de ce chapitre décrit les composants matériels, logiciels et logiques d'une telle plateforme et identifie certains de ses aspects critiques tels que la synchronisation de l'EEG et de l'IRMf et les artefacts. Ce chapitre est destiné à être utilisé comme un guide pour les laboratoires qui souhaiteraient mettre en place leur propre plateforme EEG-IRMf pour conduire des expériences de NF bimodal. La seconde partie de ce chapitre donne un exemple illustratif en décrivant la plateforme que nous avons déployé à Neurinfo (CHU Pontchaillou, Rennes, France) et les choix d'implémentation spécifiques que nous avons faits. Les deux études expérimentales présentées dans cette thèse (Chapitre 5 et 6) ont été conduites à l'aide de cette plateforme. Le contenu de ce chapitre a été essentiellement rédigé par Marsel Mano, l'ingénieur qui a développé cette plateforme.

Le **Chapitre 5** présente la première étude de NF-EEG-IRMf réalisée dans le cadre de cette thèse. Cette étude vise à évaluer la valeur ajoutée du NF-EEG-IRMf comparé au NF-EEG et au NF-IRMf. A cette fin, nous introduisons un protocole de NF-EEG-IRMf pour l'entraînement à l'imagerie motrice et employons un design intra-sujets dans lequel chaque participant réalise la tâche d'imagerie motrice dans trois conditions de NF : NF-EEG, NF-IRMf et NF-EEG-IRMf. Ces conditions sont évaluées en terme d'intensité des activations EEG et IRMf.

Le **Chapitre 6** présente la seconde étude de NF-EEG-IRMf réalisée dans le cadre de cette thèse. Dans cette étude, on introduit deux stratégies de feedback intégré pour le NF-EEG-IRMf et étudions leurs effets sur une tâche d'imagerie motrice au moyen d'un design inter-groupes. Un feedback intégré permet de représenter l'EEG et l'IRMf avec un seul feedback au lieu de deux feedbacks

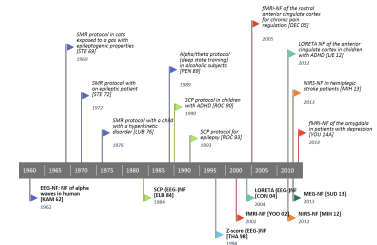


FIGURE 4 – Le **Chapter 2** retrace plus de 60 ans de recherche dans le domaine du NF.

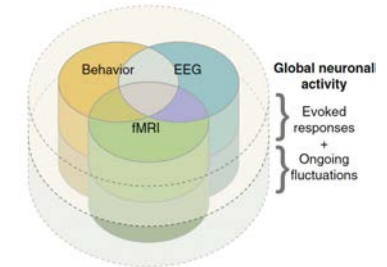


FIGURE 5 – Le **Chapter 3** discute des aspects importants pour la combinaison de l'EEG et de l'IRMf dans le cadre du NF.

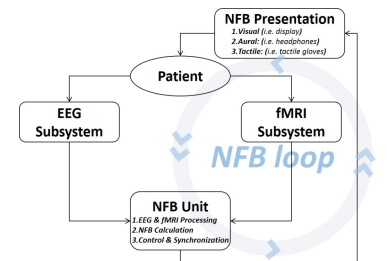


FIGURE 6 – Le **Chapter 4** décrit comment mettre en place une plateforme EEG-IRMf temps-réel pour faire des expériences de NF bimodal.

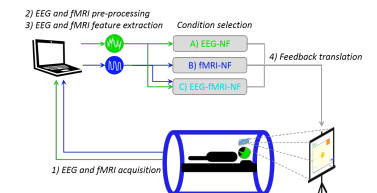


FIGURE 7 – Le **Chapter 5** présente une étude dans laquelle les participants ont réalisé une tâche d'imagerie motrice avec NF unimodal et bimodal.

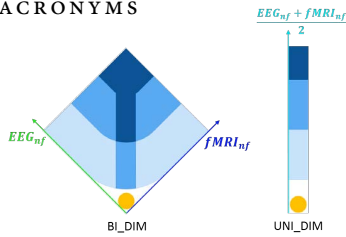


FIGURE 8 – Le [Chapter 6](#) présente une étude dans laquelle on évalue les effets de deux stratégies de feedback intégré pour le NF-EEG-IRMf.

séparés, ce que nous supposons être sous-optimal en terme de charge cognitive et de possibilités pour définir une cible de NF bimodal. Le premier feedback intégré est un graphe bi-dimensionnel (2D) dans lequel chaque dimension représente l'information provenant d'une modalité. Le second feedback intégré est une jauge uni-dimensionnelle (1D) qui intègre les deux informations en une seule. Tout comme dans la première étude, les conditions de NF sont évaluées en terme d'intensité des activations EEG et IRMf.

Le [Chapitre 7](#) résume les contributions de cette thèse et discute des perspectives qu'elle laisse entrevoir.

## GENERAL INTRODUCTION

*"Never permit a dichotomy to rule your life."*

— Pablo Picasso

## 1.1 WHAT IS NEUROFEEDBACK ?

This question is not as innocent as it seems. Doing a PhD on neurofeedback is somehow like studying a living legend, and making this legend live. Had it been only for the thrill of discovering the intrigue of neurofeedback history, and the fuss of untangling the confusion about what NF is, it would have been worth it. Yet, trying to play a part in the NF saga was also very much compelling.

Putting it simply, neurofeedback is the process of feeding back real-time information to an individual about his/her ongoing brain activity, so that he/she can train to self-regulate neural substrates of specific behavioral functions<sup>1</sup>. NF has been extensively studied for brain rehabilitation of patients with psychiatric and neurological disorders and for peak performance training of healthy subjects<sup>2</sup>. NF is also being used by practitioners in some countries but their practice does not necessarily reflect the research<sup>3</sup>.

Neurofeedback has a lot in common with brain-computer interfaces (BCIs) in the way that both approaches exploit brain activity measures in real-time. In NF, the purpose is directed towards an internal control (self-regulation) while the purpose of traditional BCIs is directed towards communication and control of external objects (orthosis, computer, ...)<sup>4</sup>. Interestingly, BCI applications were historically derived from NF. Yet it sometimes happen that the BCI community gives the NF community a cold shoulder and does not dare to use the NF word even when they are actually doing NF. Indeed, the BCI community has recently started developing BCIs designed for brain rehabilitation, just like NF. Such BCIs are coined "*restorative BCIs*" as opposed to traditional "*assistive BCIs*" and can be considered as an equivalent of NF<sup>5</sup>. Because NF and BCI are so related and complementary, this thesis is taking in consideration both the NF and the BCI literature. However there exist differences in methodological aspects between the two fields that will be important to consider<sup>6</sup>.

## 1.2 TIME FOR NF TO GO MULTIMODAL ?

Nowadays there is still a great need for the development of new methods for the treatment of neurological and psychiatric disorders<sup>7</sup>. Some patients do not respond well to classical treatments or suffer from strong side-effects. For the most unfortunate, there might even be no viable cure. By exploiting neuroplasticity together with the self-regulation ability of the patient, NF appears to be a promising non-invasive alternative or complement to existing treatments such as pharmacological treatments, neurosurgery, psychotherapy and passive stim-

<sup>1</sup> For example emotion regulation, motor performance, attention, pain perception, craving ...

<sup>2</sup> **Dichotomy #1:** clinical versus non-clinical applications of NF, see [Section 2.5](#)

<sup>3</sup> **Dichotomy #2:** NF practice versus NF research, see [Chapter 2](#)

<sup>4</sup> **Dichotomy #3:** NF and BCI (Huster et al., 2014)

<sup>5</sup> NF  $\equiv$  restorative BCI  $\neq$  assistive BCI

<sup>6</sup> See [Section 2.4](#) for more explanations about the similarities and differences between NF and BCI

<sup>7</sup> Examples include: stroke, depression, anxiety disorders, ADHD, epilepsy, chronic pain, addiction, schizophrenia, tinnitus, autism, migraines, ...



ulation techniques. NF even makes one dream of long-term efficacy with little or no side-effects. However, looking back at NF history, the path to the promised land of NF turned out to be very long and winding. One does not put so easily someone's brain at his/her own disposal.

NF research dates back to the late 50s with the seminal work of Joe Kamiya at the University of Chicago on the operant conditioning of EEG alpha waves. Some researchers<sup>8</sup> even date it back to the first demonstration of classical conditioning of the human EEG by french psychologist Gustave Durup and french neurophysiologist Alfred Fessard in the 30s<sup>9</sup>, that means not long after the human EEG was first described by Hans Berger in the 20s. One could argue that as soon as one gets a new way to measure the brain activity, one has a new way to self-control it, providing one can extract fast enough something meaningful from it. Many years after the first demonstration of EEG-NF, in the early 2000's, the advent of real-time fMRI allowed the birth of fMRI-NF<sup>10</sup>. fMRI-NF gave access to the self-regulation of deep brain regions with high spatial resolution, which was not possible with EEG-NF. A decade later, magnetoencephalography (MEG)<sup>11</sup> and functional near-infrared spectroscopy (fNIRS)<sup>12</sup> were added to the list of possible NF modalities. To this day, EEG and fMRI are the most common modalities in NF research and offer a variety of approaches<sup>13,14</sup>. EEG-NF is available as traditional amplitude-based NF that targets frequencies at one or two electrodes, slow cortical potentials (SCP) NF, z-score NF that consists in normalizing different quantitative EEG (QEEG) metrics, or LORETA NF that targets reconstructed signal from cortical regions of interest. For its part, fMRI-NF has mainly evolved from single-region to multivariate approaches.

<sup>8</sup> (Martijn Arns, Batail, et al., 2017)

<sup>9</sup> **Dichotomy #4:** classical versus operant conditioning. Conditioning is a concept from behavioral psychology that relates to the shaping of behaviors. Classical conditioning involves placing a neutral signal before a reflex (i.e. involuntary and automatic behaviors) so that eventually the neutral signal will trigger the reflex (association). Operant conditioning involves applying reinforcement and/or punishment after a voluntary behavior in order to strengthen or weaken it. The latter has traditionally been thought to play a central role in the NF process. But recently, the understanding of NF process has switched to more complex models involving both voluntary and involuntary mechanisms.

<sup>10</sup> (S.-S. Yoo & Jolesz, 2002a)

<sup>11</sup> (Lal et al., 2005; Sudre et al., 2011)

<sup>12</sup> (Mihara et al., 2012; Kober, Wood, et al., 2014)

<sup>13</sup> (Hammond, 2011; Sulzer et al., 2013)

<sup>14</sup> **Dichotomy #5** (the golden one): EEG and fMRI

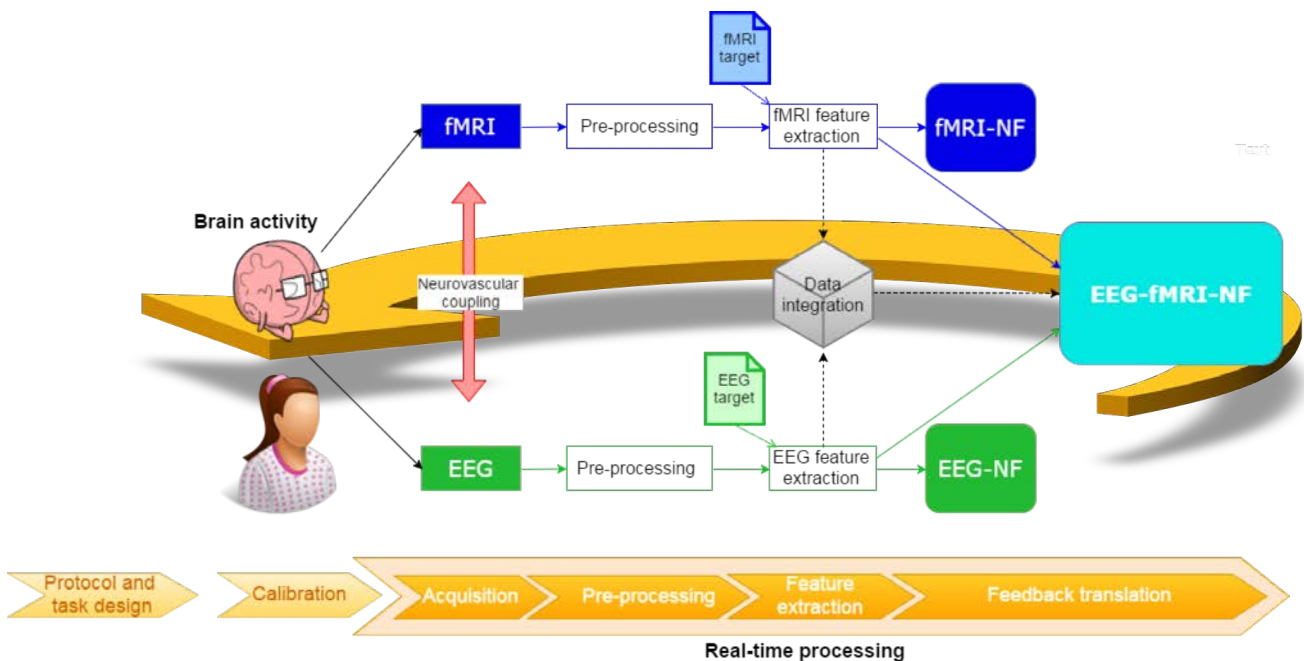


Figure 9 – This figure illustrates the closed loop of EEG-NF, fMRI-NF, and EEG-fMRI-NF, preparatory offline steps "Protocol and task design", and "Calibration", as well as combined EEG-fMRI concepts such as neurovascular coupling and data integration

Despite the fact that over the years many NF approaches have been developed and studied for a large range of applications, the optimal methodology

and the effectiveness of NF remains debated. Currently, the most convincing application of NF is in the treatment of attention-deficit hyperactivity disorder (ADHD) in children with EEG-NF, for which controlled, randomized trials and an initial set of meta-analyses have been published. The limited level of evidence of NF is likely to be a result of insufficient evidence-based criteria of NF studies (small sample size, lack of control, no randomization, no double-blind trials, ...), of the heterogeneity of approaches used in different studies, and of the lack of knowledge about the underlying mechanisms of NF which makes it difficult to establish methodological guidelines. This state of affairs is actually changing as increasingly rigorous approaches are becoming the new standard<sup>15</sup>, and as new studies are delving into the mechanisms<sup>16</sup> as well as the methodological aspects of NF<sup>17</sup>.

Another possible reason for the lack of efficiency of current approaches might be the inherent limitations of single imaging modalities<sup>18</sup>. Indeed, most NF approaches rely on the use of a single brain imaging modality among EEG, fMRI, fNIRS or MEG. Each of these modalities is sensitive to a particular biophysical phenomenon related to brain activity and comes with its own technical and physiological limitations<sup>19</sup>. Given the complexity of brain activity that sparks at different spatial and temporal scales, no one should doubt that it would take more than one device to catch it within its smallest nooks<sup>20</sup>.

Combining modalities could allow to overcome some of the limitations of single modalities, extract richer and more accurate information about the ongoing brain activity and therefore enable to develop more effective NF approaches. In particular, the combination of EEG and fMRI is most promising as it allows to combine the high temporal resolution of EEG together with the high spatial resolution of fMRI.

In the BCI community, the field of hybrid BCI has recently emerged<sup>21</sup>, the term "hybrid" referring to a multimodal combination of sensors. A hybrid BCI is defined as the combination of two BCIs or of at least a BCI and another system such as another biofeedback system (like an electromyogram for example)<sup>22</sup>. They can be designed to work simultaneously or sequentially. Their purpose is mostly to augment the usability and/or the performance of the BCI. Most of the hybrid BCIs combining two BCIs that have been proposed in the literature relied only on EEG paradigms, but some hybrid BCI combining EEG and fNIRS have also been proposed<sup>23</sup> and have shown enhanced performance. These encouraging results suggest that using hybrid/multimodal approaches for NF could outperform the efficiency of unimodal approaches. If the portability and cost of the device are critical criteria for assistive BCI because they are meant to be used on a frequent basis, these criteria are less decisive in NF. This is a reason why the BCI community (when they are not doing NF) is more likely to investigate the combination of EEG and fNIRS than the one of EEG and fMRI.

### 1.3 COMBINING EEG AND FMRI FOR NF

EEG and fMRI are complementary in their strengths and limitations and in the nature of their signals<sup>24</sup> (see Figure 10). EEG reflects the sum of synchronized post-dendritic potentials of pyramidal cells. It benefits from a high temporal (milliseconds) resolution which makes it able to detect the rhythms of the brain

<sup>15</sup> (Sulzer et al., 2013; Stoeckel et al., 2014; Thibault, Lifshitz, & Raz, 2016)

<sup>16</sup> (Ninaus et al., 2013; Sitaram, Ros, et al., 2016; Emmert, Kopel, Sulzer, et al., 2016; Birbaumer, Ruiz, & Sitaram, 2013; Kober, Witte, et al., 2013)

<sup>17</sup> (Emmert, Kopel, Koush, et al., 2017; Krause et al., 2017; Sorger, Kamp, et al., 2016; Sepulveda et al., 2016)

<sup>18</sup> (Biessmann et al., 2011; Fazli, Dahne, et al., 2015)

<sup>19</sup> (Biessmann et al., 2011)

<sup>20</sup> Saying that brain activity is complex is a bit of an understatement (Bullmore et al., 2009). The human brain is estimated to have about 86 billion neurons (16 billions in the cerebral cortex, 69 in the cerebellum) (Herculano-Houzel, 2009) that fire between 0.1 - 200 times per second. "It is a complex temporally and spatially multi-scale structure that gives rise to elaborate molecular, cellular, and neuronal phenomena that together form the physical and biological basis of cognition." (Bassett & Gazzaniga, 2011)

<sup>21</sup> (Pfurtscheller, B. Z. Allison, et al., 2010; Amiri, Fazel-Rezai, & Asadpour, 2013)

<sup>22</sup> (Pfurtscheller, B. Z. Allison, et al., 2010)

<sup>23</sup> (Fazli, Mehnert, et al., 2012; Buccino, Koles, & Omurtag, 2016)

<sup>24</sup> "marry the blind (EEG) and the lame (fMRI)"

which range from delta (0.5 - 4Hz) to gamma (>30Hz). However, its spatial resolution (centimeters) is limited by volume conduction of the head and the number of electrodes. Also source localization from EEG is inaccurate because of the ill-posed inverse problem. On its part, fMRI indirectly measures the brain activity through the blood oxygen-level dependent (BOLD) effect. fMRI is sensitive to the magnetic properties of the blood which change with its oxygen concentration which varies in order to supply energy to the neurons when they are active<sup>25</sup>. It offers a much appreciated spatial resolution (millimeters) of the whole brain. However its temporal resolution is limited by the time required to acquire one brain volume (>=hundreds of milliseconds or seconds), and the fact that the hemodynamic response peak is delayed of 4-6s from the neuronal onset and that it acts like a low-pass filter that smears out the neuronal response.

<sup>25</sup> You may try reading this sentence backwards if you prefer traveling time the forward way

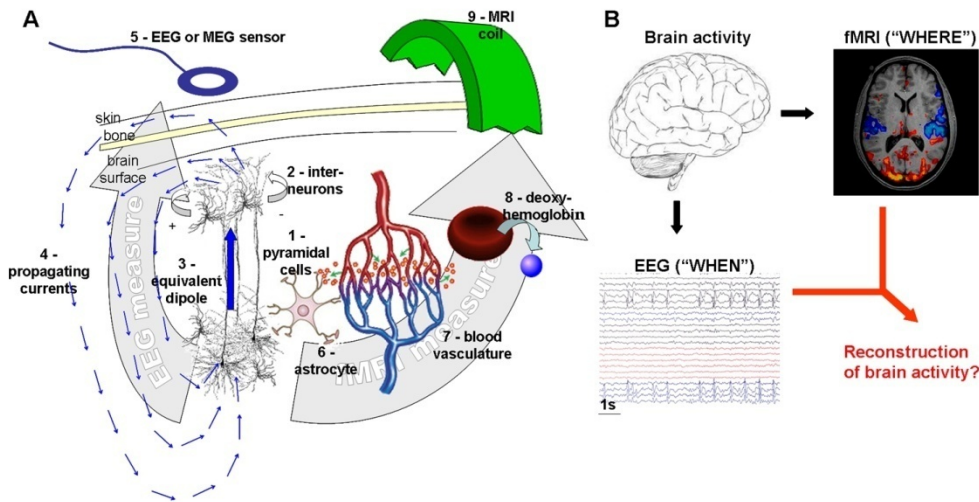


Figure 10 – Physiological basis of EEG/MEG and fMRI (from (Deneux, 2011))

<sup>26</sup> (Ives, Warach, & Schmitt, 1993)

The development of combined EEG-fMRI was initially motivated by applications in epilepsy in order to localize neural sources of epileptic discharges. The first EEG-fMRI study took place in 1992<sup>26</sup>. At that time, EEG and fMRI had to be recorded separately in an interleaved manner for subject and hardware safety and data quality issues. Indeed the rapidly changing radio-frequency pulses coupled to the strong static magnetic field induce currents into electrically conductive objects that can produce heating at the electrode sites, damage tissues or hardware and introduce artifacts in the data. By early 2000s the development of MR-compatible EEG devices made of non-magnetic materials and the development of artifact reduction algorithms made it possible to simultaneously acquire EEG and fMRI. From that time on, combined EEG-fMRI has found its place in pre-surgical planning for epilepsy and has significantly contributed to advance the study of resting-state, sleep, and cognitive brain function.

In the context of NF, combined EEG-fMRI opens up new avenues for cross-modal paradigm validation and *most interestingly for the development of new NF approaches that would mix both modalities, either at the calibration phase or for online use to provide a bimodal NF signal, or used alternatively*. By the time this PhD started (late 2013), very few NF studies had resorted to combined EEG-fMRI, yet all of them had different motivations and relied on different approaches which illustrate the variety that EEG-fMRI has to offer. Most notewor-

thy, two important studies have drawn two main directions for the combined use of EEG and fMRI for NF. The first study by Meir Hasson et al.<sup>27</sup> introduced the idea of fMRI-informed EEG-NF through a method that produces an EEG fingerprint used to predict specific fMRI deep regional activation. The second study by Zotev et al. made the first proof-of-concept of bimodal EEG-fMRI-NF in which simultaneous EEG and fMRI is being fed back to the participant<sup>28</sup>. Despite representing important milestones, these pioneering works had limitations that left room for improvement and further research. The method by Meir-Hasson et al. is advantageous in that it minimizes the expensive resort to fMRI but it is reductive in that it uses only one EEG electrode and does not fully exploit the potential of both modalities. The work by Zotev et al. is the first one to propose to simultaneously provide EEG-NF together with fMRI-NF and hypothesized that such an approach could be more efficient than the unimodal approaches. However this hypothesis was not evaluated. Therefore it was not clear what was the added value of EEG-fMRI-NF and if specific mechanisms were involved when learning to regulate two signals instead of one.

At this point, it is important to note that the combined use of EEG and fMRI inevitably poses numerous challenges and pitfalls with regard to basic physiology, study design, data quality, analysis/integration and interpretation. This is even more the case if EEG and fMRI are both to be used in the online computation of NF, because of the real-time constraint and the difficulty to come up with a task design compatible with EEG and fMRI' diverging natures

<sup>27</sup> (Meir-Hasson, Kinreich, et al., 2013)

<sup>28</sup> (Zotev, Phillips, et al., 2014a)

#### 1.4 GOALS OF THIS THESIS

This PhD addresses the following questions:

- *Why and how should we combine EEG and fMRI for NF and which strategies are more promising ?*
- *What are the important methodological constraints of EEG and fMRI that should be taken into account when designing an EEG-fMRI-NF protocol ?*
- *How to build an experimental platform that can provide EEG-fMRI-NF ?*
- *What is the added value of EEG-fMRI-NF compared to unimodal EEG-NF and fMRI-NF, and are there specific mechanisms involved when learning to control two signals instead of one?*
- *How to integrate and represent EEG and fMRI in a single feedback ?*

Building on the understanding of how EEG and fMRI complement each other, this dissertation first proposes to analyze the specific constraints that they impose on NF experimental design, and to identify the different motivations and approaches for combining both modalities for NF purpose (contribution ① in Figure 11). Then, among these different combination approaches, we propose to focus on the investigation, design and evaluation of methods for bimodal EEG-fMRI-NF for it seems to be one of the most promising approach and is mostly unexplored. We start by building a real-time EEG-fMRI platform that is able to provide NF in unimodal and bimodal conditions (contribution ② in Figure 11). Next we proceed with experimentation. In a first study, we evaluate the added value of bimodal EEG-fMRI-NF compared to unimodal EEG-



NF and fMRI-NF (contribution ④ in Figure 11). Eventually, in a second study we introduce and evaluate two integrated feedback strategies for bimodal EEG-fMRI-NF and study their effects (contribution ⑤ in Figure 11). Our protocols and studies are devised in the context of motor-imagery training, as this has never been done before and because EEG and fMRI motor patterns are well-known and therefore represent a good starting point for the development and evaluation of new methods (contribution ③ in Figure 11). The contributions of this dissertation are highlighted in purple in Figure 11.

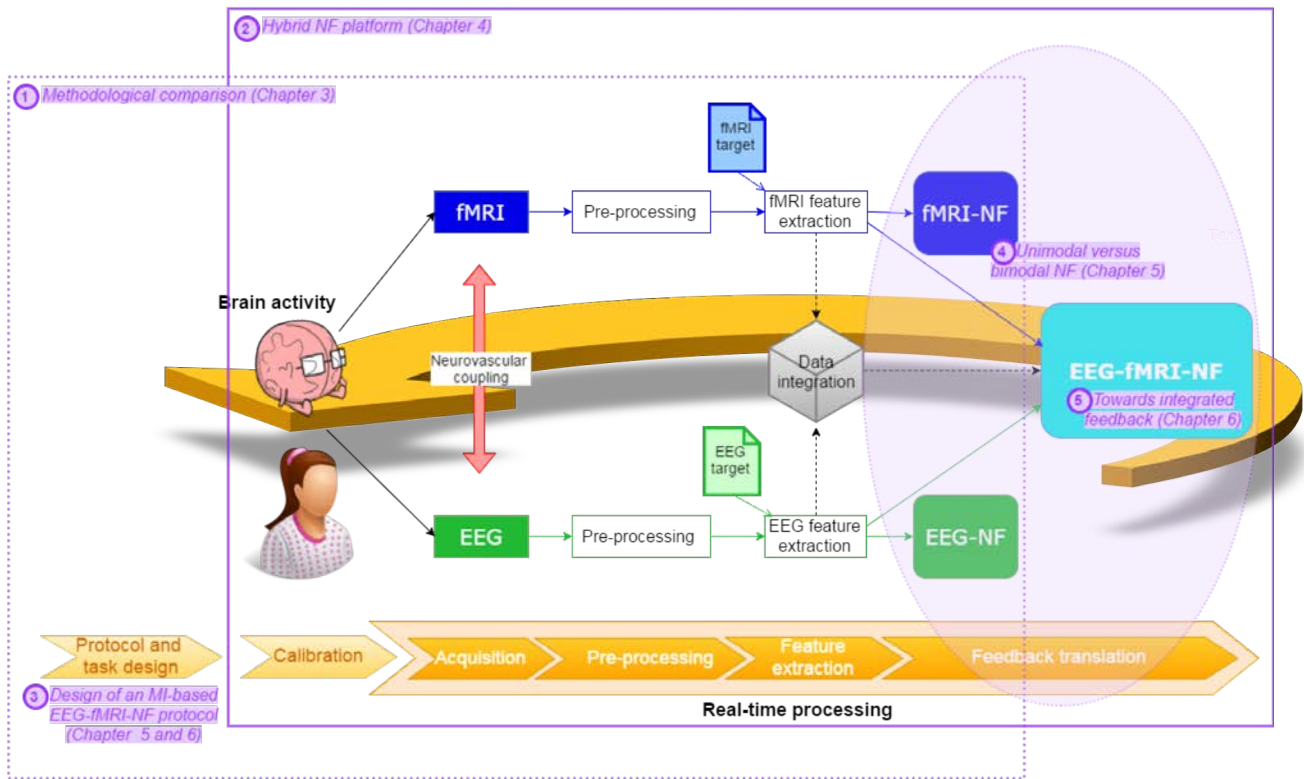


Figure 11 – Overview of contributions

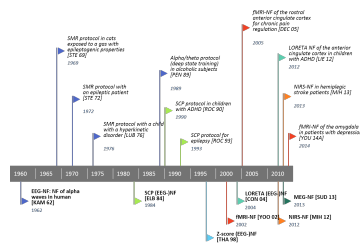


Figure 12 – Almost 60 years of NF research are retraced in Chapter 2.

**Chapter 2** provides a comprehensive state-of-the-art of neurofeedback. It describes the design of a (practical) NF training program, and the typical course of a (practical and research-oriented) NF session, as well as the underlying mechanisms of NF. It also retraces the history of NF, explaining the origin of its questionable reputation and providing a foothold for understanding the diversity of existing approaches. It also discusses how the fields of NF and BCIs might potentially overlap in future with the development of "restorative" BCIs. Finally, it presents a few applications of NF, and summarizes the state of research of some of its major clinical applications.

**Chapter 3** lays the foundations for understanding why and how EEG and fMRI should be combined for NF purpose. We start by explaining under which conditions EEG and fMRI should be acquired simultaneously, and how elec-

trophysiological and BOLD signals are known to be related. Next we make out a methodological comparison of EEG-NF and fMRI-NF that will be particularly useful when designing bimodal EEG-fMRI-NF protocols. We then review exhaustively the limited corpus of NF studies that have exploited EEG and fMRI together and eventually propose a taxonomy of such studies.

**Chapter 4** describes how to build a real-time EEG-fMRI platform for bimodal NF. The first part gives a general description of the different hardware, software and logical components of such a platform and outlines some of its critical aspects such as EEG-fMRI synchronization and artifacts. It is intended to be used as a guide for any laboratory who would like to setup their own real-time EEG-fMRI platform to perform bimodal NF experiments. The second part gives an illustrative example of such a setup by presenting our own EEG-fMRI NF platform deployed at Neurinfo's facilities (CHU Pontchaillou, Rennes, France) and the specific implementation choices we made. The two experimental studies reported in this dissertation (Chapter 5 and 6) were conducted with that platform. The content of this chapter was written mainly by Marsel Mano, the engineer who implemented the platform.

**Chapter 5** presents the first EEG-fMRI-NF study that we performed. This study aimed at evaluating the added value of bimodal EEG-fMRI-NF as compared to unimodal EEG-NF and fMRI-NF. To this end, we introduce a motor imagery-based bimodal EEG-fMRI-NF protocol and employ a within-subject design in which each participant performed the MI task in three different NF conditions: EEG-NF, fMRI-NF and EEG-fMRI-NF. The conditions are evaluated in terms of activation levels of the EEG and fMRI patterns.

**Chapter 6** presents the second EEG-fMRI-NF study that we performed. In this study we introduce two integrated feedback strategies for EEG-fMRI-NF and study their effects on a motor imagery task with a between-group design. Our integrated feedback strategies allow to represent EEG and fMRI in a single feedback instead of representing them in two separate feedbacks, which we assume is suboptimal both in terms of the subject's cognitive load and of the potential for bimodal NF target definition. The first integrated feedback strategy consists in a two-dimensional (2D) plot in which each dimension depicts the information from one modality. The second integrated feedback strategy consists in a one-dimensional (1D) gauge that integrates both types of information even more by merging them into one. Similarly to the previous study, we evaluate the two NF conditions in terms of how well they allow to regulate EEG and fMRI.

**Chapter 7** summarizes the contributions of this thesis and discusses prospects for future work.

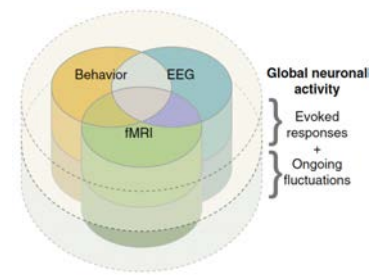


Figure 13 – Chapter 3 discusses relevant aspects of combined EEG-

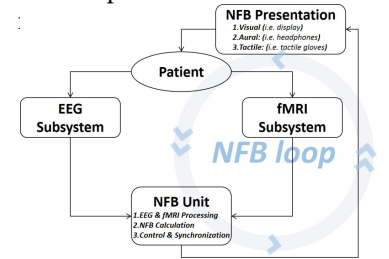


Figure 14 – In Chapter 4, we describe how to build a real-time EEG-fMRI platform for bimodal NF.

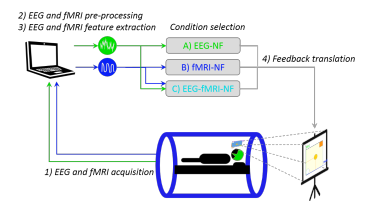


Figure 15 – Chapter 5 presents a study in which participants performed NF in unimodal and bimodal conditions.

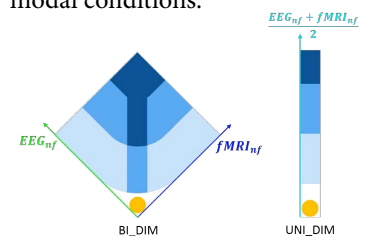


Figure 16 – In Chapter 6, two-integrated EEG-fMRI feedback strategies are studied.



"You have power over your mind - not outside events. Realize this, and you will find strength."

— Marcus Aurelius

*Prelude* This chapter provides a comprehensive state-of-the-art of the field of neurofeedback. It describes the design of a (practical) NF training program, and the typical course of a (practical and research-oriented) NF session, as well as the underlying mechanisms of NF. It also retraces the history of NF, explaining the origin of its questionable reputation and providing a foothold for understanding the diversity of existing approaches. It also discusses how the fields of NF and BCIs might potentially overlap in future with the development of "restorative" BCIs. Finally, it presents a few applications of NF, and summarizes the state of research of some of its major clinical applications.

## 2.1 INTRODUCTION

Neurofeedback (NF) is a *biofeedback* technique that involves providing information to an individual about his or her brain activity in the form of visual, auditory or tactile feedback, updated in real time. For example, individuals can be shown a gauge showing their frontal beta activity as an indicator of their concentration level. NF allows subjects to exploit their self-regulation ability to develop an optimal mental strategy for achieving an objective expressed in terms of brain activity. The sensory feedback informs the user whether his/her cerebral activity is getting closer or further away from the objective. Thus, NF is a way to perform *operant conditioning* of the brain activity, with feedback acting as reinforcement. The goal of NF training is for users to learn to improve how they regulate certain aspects of their cerebral activity, so that this activity may be reorganized sustainably. NF is comprised of different training protocols, each targeting a specific brain pattern, such as the ones related to concentration, relaxation, the imagination of movements, or the visualization of positive memories. It may be used as a tool for exercising the brain and optimizing performance in healthy subjects, or for *rehabilitation* in the case of patients with brain disorders. Over the 60 years of its existence, NF has been studied in a very large range of clinical and non-clinical applications (see [Section 2.5](#)). Even so, its effectiveness in each of these applications remains to be proven and properly differentiated from a placebo effect. Currently, the most convincing application of NF is in the treatment of attention-deficit hyperactivity disorder (*ADHD*) in children, for which randomized controlled trials (RCT) and an initial set of meta-analyses have been published<sup>1</sup>. A number of studies also seem to agree on the potential of NF for treating pharmaco-resistant epilepsy<sup>2</sup>. Despite the preliminary nature of this research, some practitioners in the United States and Canada already use NF, claiming to be able to treat a vast panel of physical, men-

The content of this chapter was published as a book chapter: Perronnet, Lorraine, Anatole Lécuyer, Fabien Lotte, Maureen Clerc, & Christian Barillot (2016). "Brain Training with Neurofeedback." In: *Brain-Computer Interfaces 1: Foundations and Methods*. Ed. by Maureen Clerc, Laurent Bougrain, & Fabien Lotte. John Wiley & Sons, Inc., pp. 271–292. DOI: [10.1002/9781119144977.ch13](https://doi.org/10.1002/9781119144977.ch13).

<sup>1</sup> (Arns, Ridder, & Strehl, 2009)

<sup>2</sup> (Tan et al., 2009)



tal and cognitive disorders. Thus NF exists in two different forms: the current state of research, and its practical applications. These two forms are not necessarily mutually representative. In France, the clinical research community has long been suspicious of this technique, and has only recently begun to consider it more closely. Let us note at this point that the Neuroptimal method, originating in Canada and claiming to be based on NF, has started to gain momentum in France over the last few years. Our position on this method is that it is not an NF technique, as it claims to reorganize the brain passively, whereas NF requires the subject to undertake a conscious and voluntary learning process. Furthermore, the method is not supported by any officially recognized study. Whereas other biofeedback techniques are based on the activity of the peripheral nervous system (cardiac rhythm, muscle tension, skin conductivity), NF focuses on the activity of the central nervous system. This activity can be measured in real time using various non-invasive methods, such as electroencephalography (EEG), functional magnetic resonance imaging (fMRI), near-infrared spectroscopy (NIRS) and magnetoencephalography (MEG). Most of the work published since the early days of NF in the sixties has been based on EEG. There is a considerable body of literature in this area; we shall denote it NF-EEG, but it is sometimes also referred to as "EEG biofeedback". Although EEG is currently the only modality used by NF practitioners, it is limited by a lack of specificity due to low spatial resolution. Research has therefore turned to other modalities that allow the activity of different regions of the brain to be more precisely targeted. Since the turn of the millennium, the strongly dynamic research into fMRI-NF appears to hold promising results for treating depression<sup>3</sup> and chronic pain<sup>4</sup> by virtue of its capacity to provide real-time imagery of activity in deep brain structures. More recently, it was demonstrated that NF-NIRS<sup>5</sup> and MEG-NF<sup>6</sup> are technologically feasible.

As BCIs, NF relies on a closed loop that exploits brain activity in real time, specifically by: acquisition of a signal originating from the brain, signal preprocessing (noise removal, filtering), extraction of relevant features that allow the state or intent of the subject to be recognized, translation into feedback to close the loop and to allow the subject to adapt in real time. Even though the two approaches of NF and BCIs share very similar technologies, their original purposes were very different: BCIs allow the subject to control an *external object* such as a computer, an orthosis or a robotic limb, whereas NF allows subjects to acquire control over *themselves*. Although some BCIs, e.g. spontaneous BCIs, involve a learning process, and so require the subject to perform cerebral self-regulation, this self-regulation is ultimately not the purpose of the exercise. Both NF and BCIs emerged during the sixties and seventies from works studying operant conditioning of brain activity. Those works revealed that humans<sup>7,8</sup> and animals<sup>9,10</sup> are capable of learning to generate specific brain patterns, assuming that they are informed or rewarded when they are successful in doing so. This reward is indispensable for animals<sup>11</sup> and secondary but recommended for human subjects. Following these discoveries, two multidisciplinary communities formed, uniting clinicians, neurologists, psychologists and engineers among others, each with the objective of meeting a specific set of needs:

- The objectives of the NF community were the self-regulation of brain patterns for treating neurological and psychiatric disorders and the optimization of performance. The NF community diversified and refined the targeted

<sup>3</sup> (K. D. Young et al., 2014)

<sup>4</sup> (DeCharms et al., 2005)

<sup>5</sup> (Mihara et al., 2012)

<sup>6</sup> (Sudre et al., 2011)

<sup>7</sup> (Kamiya, 1962)

<sup>8</sup> (M.B Serman & Friar, 1972)

<sup>9</sup> (Wyrwicka & Maurice B. Serman, 1968)

<sup>10</sup> (Fetz, 1969)

<sup>11</sup> (Fetz, 1969)

brain patterns, demonstrated the benefits of learning, and also studied self-regulation processes and the optimization of psycho-experimental learning factors.

- The BCI community instead focused on implementing control and communication interfaces for handicapped persons, investing their efforts into developing tools for signal processing and for classifying brain patterns to optimize reliability and degrees of freedom of BCIs.

Over the last few years, invasive BCIs have attracted attention after several spectacular demonstrations with tetraplegic patients<sup>12,13</sup>, and non-invasive BCIs have become increasingly popular thanks to new applications in video games and virtual reality<sup>14</sup>. On the other hand, NF still suffers from a reputation of new age technique in some scientific circles, a black mark inherited from the outcry of the media in early days of NF in the sixties (see [Section 2.3](#)) that is proving difficult to overcome. As a field of study, NF can appear impenetrable due to the abundance of unreliable information and the diversity of existing protocols and applications. There has nonetheless been a revival in the number of publications in recent years, and a renewed approach indicating that interest in the potential of NF is picking up.

<sup>12</sup> (Pfurtscheller, Guger, et al., 2000)

<sup>13</sup> (Hochberg et al., 2012)

<sup>14</sup> (Lecuyer et al., 2008)

## 2.2 HOW DOES IT WORK?

### 2.2.1 *Design of an NF training program*

NF is comprised of protocols that target brain patterns assumed to underpin specific sets of physical, mental or cognitive functions. We shall describe NF such as it is practiced in NF institutes, whether or not the scope is clinical in nature. Currently, only EEG-based variants of NF are used in practical applications. NF training programs are organized into several stages, the practical aspects of which vary depending on the needs of the subject and the equipment and software used by the practitioner. These stages are generally as follows:

1. **Diagnosis:** this first stage involves identifying the symptoms suffered by the subject, or the function that the subject wishes to improve, in order to establish the target of the training process in functional terms. Generally, this begins with an examination of the patient's medical history, and then, depending on the target disorder or the desired objective, a series of specific, standardized tests are administered, in the form of questionnaires or psychological, neurological or physiological examinations.
2. **Choice of NF protocol:** in the second stage, an EEG-NF protocol is defined to suit the subject's needs; in other words, the electrical activity in the brain that the training process will target is established. This activity corresponds to a certain brain measurement, which is assumed to be indicative of or to act upon the function that the subject wishes to improve. During training, this measurement will be displayed to the subject in the form of feedback; the subject will then attempt to manipulate the measurement towards a desired value or in a desired direction. The simplest type of measurement available is the power in a frequency band measured at an electrode, for example the

power of mu waves in the motor regions for a task of movement imagination. However, more complex metrics that reflect the exchange of information between two or more regions may also be used, such as the coherency or asymmetry measured between two electrodes. Over more than 60 years of research, a large number of protocols have been studied, and are now offered by NF clinics in response to a wide array of conditions (although official research has not yet provided sufficient proof of their effectiveness). The definition of the protocol can be made using *a priori* knowledge from the literature and the experience of the practitioner, or by a *personalized* process for each patient, or a combination of these two approaches. The personalized approach requires additional tests, and particular tools and expertise. For example, certain practitioners use quantified EEGs, which involves comparing the subject's EEG to a database of healthy subjects to detect potential abnormalities which can then be targeted during training<sup>15</sup>.

<sup>15</sup> (Budzynski et al., 2009)

3. **Session planning:** there must be sufficiently many sessions for the first effects to be visible (the subject explores the strategies), and also so that the changes endure in the long term (the subject repeats and attempts to maintain an effective strategy; with practice this becomes ever-easier). The required number of sessions (between 20 and 40<sup>16,17</sup>) depends on the severity of the subject's symptoms, his or her learning skills and motivation levels, but also the chosen target pattern, which may be more or less difficult to master.

<sup>16</sup> (Hammond, 2011)

<sup>17</sup> (Gruzelier, 2014c)

### 2.2.2 Course of a NF session: when the eyes "look" at the brain

Once the NF training program has been established, the training sessions can commence. In this section, we shall describe the typical course of an NF session, which holds both in practice and in research contexts. Figure 17 shows an example of an EEG-NF environment. Over the course of a session of NF, which generally lasts less than an hour to account for the subject's fatigue levels, the subject sits in front of a screen except for fMRI-NF where the subject is lying down in the MR tube, potentially with earphones or, in rarer occasions, connected to a tactile interface. The subject is asked to perform a mental task, such as: concentrating, relaxing, thinking of something positive, or imagining a movement in the right hand. Sometimes, the subject is not given any explicit instruction<sup>18</sup> other than to attempt to control the feedback using the mental strategy that he or she finds most effective. The equipment (traditionally EEG, but alternatively fMRI, NIRS, MEG) records brain signals, which are then processed by an algorithm. The algorithm cleans the signals from any artifacts created by movement or noise from the environment. It then extracts a relevant metric related to the requested task/targeted function, and translates this metric into feedback that indicates to the subject how well the task was performed (as a score), and in which direction he or she must focus subsequent efforts (with an arrow). The feedback is an objective indicator of what is happening the subject's mind. Typically, the screen displays a gauge that fills or empties depending on the subject's performance, but various other forms of feedback are also possible such as sounds with different pitches, the motion of an orthesis, or an interface with a video game or virtual reality. The practitioner remains at the subject's side, observing and guiding the subject by providing advice about

<sup>18</sup> (Kober, Witte, et al., 2013)

mental strategies, encouragement, or by helping the subject to relax. The practitioner also monitors the subject's performance, and if necessary adjusts the parameters of the protocol, such as the difficulty of the task (reinforcement threshold) or the properties of the feedback. In order to ensure that skills acquired during training *transfer* to everyday life, the subject may be asked to attempt to regulate activity without feedback at certain points in the session, and also to practice outside of the sessions.



Figure 17 – Example of an EEG-NF environment

### 2.2.3 A learning procedure that we still do not fully understand

Even if NF was shown to have positive effects on behavior and cognition more than 60 years ago<sup>19</sup>, the mechanisms underlying brain self-regulation during NF training are barely understood<sup>20,21</sup>. This lack of understanding at a fundamental level is why it has been difficult to establish good practices. Methodological aspects, even essential ones such as the optimal form and frequency of feedback, are still being debated<sup>22</sup>. NF is generally viewed as a *learning procedure* based on principles of *operant conditioning*<sup>23</sup> (the feedback acts as reinforcement) and *neuroplasticity* (via the training program and session repetition) and relying on a *voluntary and conscious* involvement on the part of the subject. But these principles do not seem to fully describe the NF process. Recently, certain authors have questioned the central role of operant conditioning and conscious and voluntary action of the subject within the NF procedure. They suggest that NF is instead an instance of *implicit* learning (automatic subconscious process, similar to acquiring the ability to perform a new movement)<sup>24,25</sup>, or even a *dual-process* mechanism with both conscious and subconscious components<sup>26</sup>.

A small set of studies have begun to explore the brain mechanisms that are at play during a NF session, as well as the factors that might affect the subject's performance<sup>27</sup>. For example, the study performed by Ninaus<sup>28</sup> showed that when

<sup>19</sup> (Kamiya, 1962)

<sup>20</sup> (Birbaumer, Ruiz, & Sitaram, 2013)

<sup>21</sup> (Niv, 2013)

<sup>22</sup> (Emmert, Kopel, Koush, et al., 2017; Krause et al., 2017; Sorger, Kamp, et al., 2016; Sepulveda et al., 2016)

<sup>23</sup> (Sherlin et al., 2011)

<sup>24</sup> (Birbaumer, Ruiz, & Sitaram, 2013)

<sup>25</sup> (Ninaus et al., 2013)

<sup>26</sup> (Ute Strehl et al., 2014)

<sup>27</sup> (Ninaus et al., 2013; Sitaram, Ros, et al., 2016; Emmert, Kopel, Sulzer, et al., 2016; Birbaumer, Ruiz, & Sitaram, 2013; Kober, Witte, et al., 2013)

<sup>28</sup> (Ninaus et al., 2013)

<sup>29</sup> (Kober, Witte, et al., 2013)

individuals attempt to control a gauge that they believe is an indicator of their own brain activity, they activate regions of the brains that are involved in *self-referential* processes and *cognitive control*, which does not occur when the subject observes the gauge passively. Another study<sup>29</sup> observed that individuals without any specific mental strategy could increase their sensorimotor rhythm (SMR) more successfully than those who reported adhering to a specific strategy, an observation that supports the hypothesis of implicit learning. Questioning the influence of *mental strategies* and *explicit instructions* appears to be particularly relevant when considering the component of voluntary involvement of the subject in the NF process. Other factors non-specific to neurofeedback can also influence the subject's performance: motivation levels, concentration levels, moods, relaxation, the user's ability to limit muscle-related artifacts, the user's loci of control, or even the therapist-patient relationship. Understanding the role of these specific and non-specific factors in facilitating NF learning should allow more effective NF protocols to be established, and better-controlled studies to be designed<sup>30</sup>.

<sup>30</sup> (Ute Strehl et al., 2014)

## 2.3 60 YEARS OF HISTORY

### 2.3.1 *Yesterday: too premature an infatuation*

<sup>31</sup> (Kamiya, 1962)

The principle of NF was demonstrated for the first time in humans by James Kamiya at the University of Chicago in 1962<sup>31</sup>. In order to discover whether individuals are capable of recognizing spikes of occipital alpha activity in their own brains, he attempted to train a volunteer by providing verbal confirmation each time that the volunteer produced alpha activity. As a result, the subject not only became capable of recognizing the apparition of alpha waves, but also acquired the ability to generate them at will. At the time, research into modified states of consciousness was particularly fashionable. One important study reported that zen monks had particularly elevated alpha activity levels during meditation<sup>32</sup>. Working from this observation, alpha wave NF was further explored with the goals of reducing anxiety<sup>33</sup> and stress, as well as inducing states of relaxation or deep meditation and stimulating creativity. In parallel to this research into alpha NF, in 1969, Barry Sterman from the University of California discovered by accident the therapeutic potential of NF for treating epilepsy<sup>34</sup>. During a study that he was performing for NASA on the epileptogenic properties of a certain type of rocket fuel (hydrazine), he observed that among 50 cats exposed to hydrazine, 10 were particularly resistant to seizures. It just so happened that these same cats had been trained to increase their sensorimotor rhythm (SMR = 11-15Hz) by NF in a previous series of experiments<sup>35</sup>. The fact that this result was observed in animals is particularly significant, as it proves that the effects of NF training cannot be simply reduced to a placebo effect. Encouraged by this surprising discovery, Sterman extended the study of the protocol to humans<sup>36</sup>. For 3 months, twice a week, he trained one of his female colleagues, 23 years, who was suffering from generalized epileptic seizures. After training was complete, he observed a reduction of seizures coupled with an increase in SMR rhythm and a reduction in slower categories of wave. Treatment was continued until the subject recovered completely, and the young woman even managed to obtain her driving licence. In 1976, Lubar<sup>37</sup> showed the benefits of the SMR protocol

<sup>32</sup> (Kasamatsu & Hirai, 1966)

<sup>33</sup> (Hardt & Kamiya, 1978)

<sup>34</sup> (Sterman, LoPresti, & Fairchild, 1969)

<sup>35</sup> (Wyrwicka & Maurice B. Sterman, 1968)

<sup>36</sup> (M.B Sterman & Friar, 1972)

<sup>37</sup> (Joel F. Lubar & Margaret N. Shouse, 1976)



with symptoms of hyperactivity and distractability in a child with hyperkinetic disorder. He started by training the child to increase his SMR rhythm, and observed an improvement in the symptoms. Then, conversely, he trained the child to reduce his SMR rhythm using the experimental ABA model, and the symptoms resurfaced. He then successfully replicated this study with 4 children suffering from ADHD<sup>38</sup>.

The results of Kamiya's research were published in 1968 in an article of *Psychology Today*<sup>39</sup>, and the idea that alpha NF could be used to attain a meditative state aroused a great deal of enthusiasm. Unfortunately, this publication, while introducing the concept of NF to the general public, also triggered a premature and unregulated propagation of the technology. Even though NF was in a stage of early infancy, an industry rapidly formed around it, producing NF kits that promised to allow users to learn to control their brain waves, and reach illumination without needing to invest years into the practice of meditation. As can be expected, these poor-quality devices were essentially smokescreens, and the validity of the link between NF alphas and meditation had not been properly established by scientific studies.

### 2.3.2 *Today: diversification of approaches*

Thus, the beginnings of NF were marked by scientific discoveries that were both surprising and promising, but also by the parallel development of a new age industry based without rigorous foundations, which caused NF to be marginalized and relegated to the status of pseudoscience. The resulting lack of financing placed a considerable brake upon research, which was confined to a set of few laboratories working in isolation. Despite the poor reputation afflicting NF within the scientific community at the end of the seventies, research continued, initially in sparse increments, before gradually expanding into a dynamic field of research with an ever-growing number of publications. The available protocols and practical procedures diversified, benefiting from technical advancements in the quality of EEG devices, brain imaging (fMRI), computer processing capacities and scientific advancements in neurophysiology and electrophysiology. Protocols were developed to extend the range of targets to the rest of the EEG frequency spectrum (other than alpha and SMR), including the outer frequency bands, which generally require specialized measuring equipment. The hypnagogic state induced by the alpha/theta protocol was thought to have potential for treating depression and anxiety resulting from alcoholism, and post-traumatic stress disorder<sup>40</sup>, as well as for stimulating creativity<sup>41</sup>. NF with high-frequency gamma waves, which has only been studied recently as it requires high-performance measuring equipment, seems on the other hand to act upon the cognitive performance<sup>42</sup>. In the 1980s, a new type of NF developed, breaking from traditional forms of NF that use EEG frequencies, based on the studies on self-regulation of slow cortical potentials (SCP)<sup>43</sup>. These potentials are well-known as indicators of the level of cortical excitability. In the 1990s, NF of SCP was studied in populations of patients suffering from ADHD<sup>44</sup> and epilepsy<sup>45</sup>. Despite promising results, deployment of the technique was limited for the longest time for reasons of equipment and the level of mastery required to correctly measure SCP<sup>46</sup>. In the early 1990s, certain practitioners pursuing the idea of normalizing the EEG activity of their patients began to use quan-

<sup>38</sup> (M N Shouse & J F Lubar, 1979)

<sup>39</sup> (Kamiya, 1968)

<sup>40</sup> (Peniston & Kulkosky, 1989)

<sup>41</sup> (Gruzelier, 2014b)

<sup>42</sup> (Keizer et al., 2010)

<sup>43</sup> (Elbert et al., 2012)

<sup>44</sup> (B. Rockstroh et al., 1990)

<sup>45</sup> (Brigitte Rockstroh et al., 1993)

<sup>46</sup> (Ute Strehl, 2009)

<sup>47</sup> (Budzynski et al., 2009)

<sup>48</sup> (Budzynski et al., 2009)

<sup>49</sup> (R. Thatcher, 1998)

<sup>50</sup> (Congedo, Joel F. Lubar, & Joffe, 2004)

<sup>51</sup> (Cannon et al., 2009)

<sup>52</sup> (Liechti et al., 2012)

<sup>53</sup> (White, Congedo, & Ciorciari, 2014)

<sup>54</sup> (Robert W. Cox, Jesmanowicz, & James S. Hyde, 1995)

<sup>55</sup> (S.-S. Yoo & Jolesz, 2002a)

<sup>56</sup> (Weiskopf et al., 2003)

<sup>57</sup> (Sulzer et al., 2013)

<sup>58</sup> (DeCharms et al., 2005)

<sup>59</sup> (K. D. Young et al., 2014)

<sup>60</sup> (Mihara et al., 2012)

<sup>61</sup> (Sudre et al., 2011)

titative EEG to choose the target of NF<sup>47</sup>. With this development, the targets of the protocols were extended to include metrics other than the amplitude of a frequency band in a given region, traditionally measured with a monopolar setup. Certain practitioners used bipolar setups, for example to target the coherency between two regions if it is identified as atypical by quantitative EEG<sup>48</sup>. Towards the end of the nineties, Thatcher<sup>49</sup> introduced the Z-score (EEG-)NF (BrainMaster) based on this data obtained from quantitative EEG, which allows multiple different metrics to be trained simultaneously, such as the absolute power, the power ratio, the coherency, the phase delay or even the asymmetry. Breaking away from the classical approach of EEG-NF that is based on using one or two EEG channels, the LORETA (EEG-)NF or tomographic (EEG-)NF suggested by Congedo in 2004<sup>50</sup> uses a fully-equipped EEG headset with 19 electrodes for reconstructing and targeting deep sources of activity in real time with the LORETA method. The behavioral, cognitive and electrophysiological effects of this type of NF were first observed and described by Cannon et al.<sup>51</sup>. Later, Liechti et al.<sup>52</sup> evaluated the effectiveness of tomographic NF of the anterior cingulate cortex for treating ADHD, and Maurizio et al. (Maurizio et al., 2014) compared it with biofeedback of electromyographic activity. Z-score (EEG-)NF was recently combined with tomographic NF leading to Z-score LORETA (EEG-)NF (Koberda et al., 2013; R. W. Thatcher, 2013). While source-based EEG neurofeedback using source localization methods has been demonstrated (Congedo et al., 2004), offering potential for an improved spatial precision of a training region, these methods remain limited by the susceptibility of source localization methods to artifacts, the inability to isolate neighboring but functionally separate sources, and the spatial precision offered. Perhaps for these reasons, the capacity for learned regulation using these methods has been inconsistently shown (Maurizio et al., 2014). Blind-source-separation (BSS) -based neurofeedback way recently introduced in order to address the limitations of previous source-based neurofeedback that relied on source localization methods which are highly susceptible to artifacts and unable to isolate neighboring but functionally separate sources<sup>53</sup>.

Finally, in the last few years, the NF community has begun to explore new variants. The development of real-time fMRI<sup>54</sup> led to the noteworthy milestone of fMRI-NF<sup>55</sup>. The major benefit of this technique over EEG-NF is that it provides high spatial resolution access to deep brain structures housing complex functions such as emotions, memory and pain. fMRI-NF can target any brain region with millimeter precision, allowing users to train their BOLD activity, reflecting blood oxygen concentration, which is indirectly correlated with neuronal activity. The feasibility of this kind of NF was first shown in the anterior cingulate cortex<sup>56</sup>, and since then has been demonstrated in numerous other regions of the brain<sup>57</sup>. In 2005, de Charms<sup>58</sup> reported findings of pain reduction in patients with chronic pain after learning to control BOLD activity in the rostral anterior cingulate cortex over the course of 4 sessions. Recent work has suggested promising results of fMRI-NF in the amygdala for depression<sup>59</sup>. fMRI-NF is currently only used in research contexts, and requires wider-scale study before it can be integrated into therapeutic programs. More recently, the investigation of NIRS-NF<sup>60</sup> has begun, which could potentially provide a portable alternative method that is less expensive than fMRI-NF, although restricted to superficial brain structures and lower spatial resolutions. Finally, MEG-NF<sup>61</sup> is

still in its infancy, and wide-scale application is not currently conceivable due to the costs involved and the low number of MEG equipment sets in operation (only 5 in France). MEG could however be used as a preliminary to EEG-NF in order to define more precisely the target of treatment. Figure 18 summarizes the emergence of the various types of neurofeedback, and the therapeutic trials with which they are canonically associated.

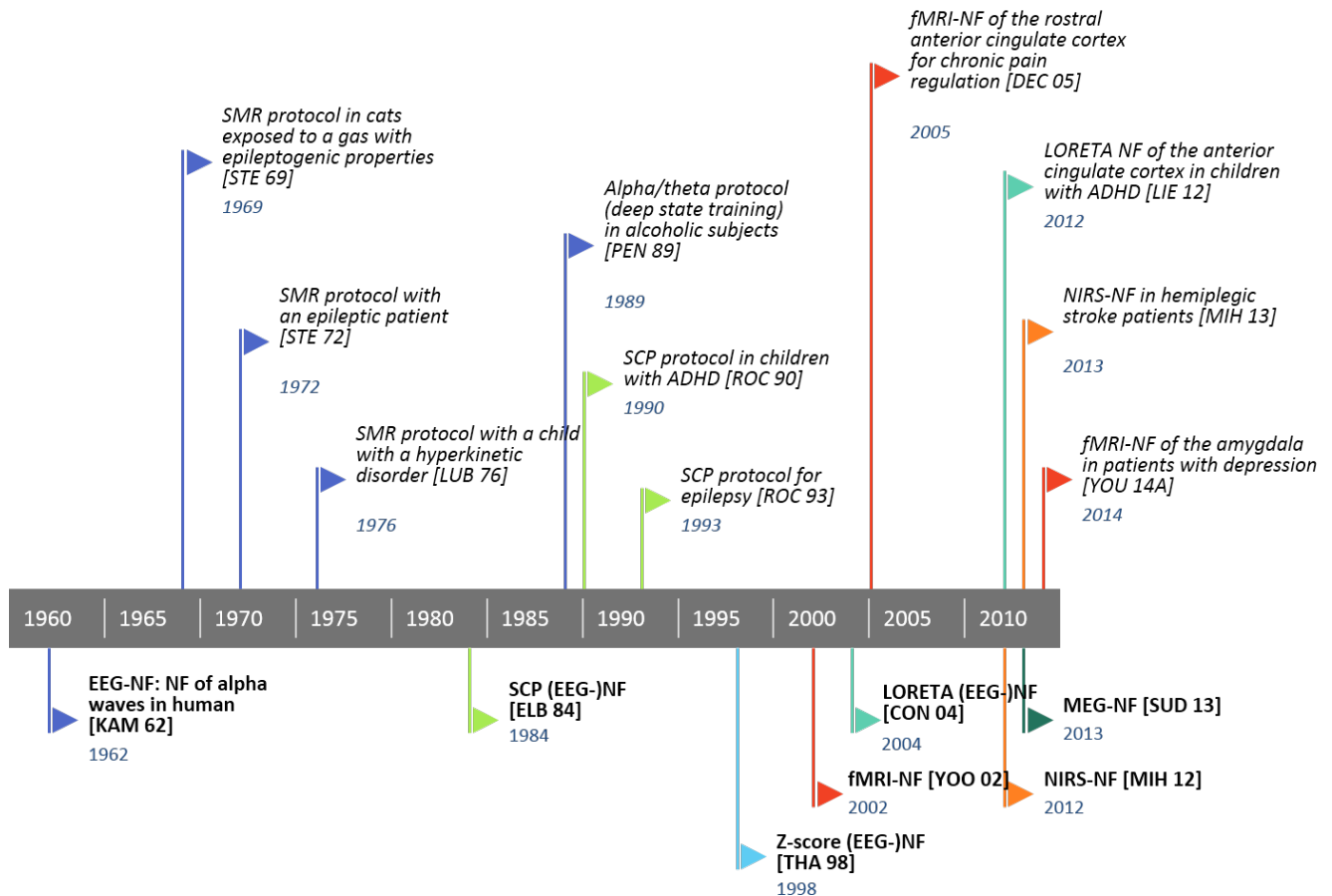


Figure 18 – 60 years of NF history: below, the proofs of feasibility of various types of NF, above, their canonical therapeutic trials.

## 2.4 WHERE NF MEETS BCI

In the scientific literature, the various ways that the terms NF and BCI are used reveal the diversity of authors' conceptions about these topics according to their original fields of study. For example, sometimes BCI is used to refer to the technology and NF is used to refer to applications<sup>62</sup>, which could be interpreted to imply that BCIs are an implementation of the concept of NF. NF is also relatively often presented as a special case of BCIs<sup>63</sup> with a minimal closed loop (no command sent to an external object). In some instances, albeit less frequently, this picture is inverted, so that BCIs are presented as a special case of NF<sup>64</sup>. Indeed, the behavior of objects in BCIs could itself be viewed as a kind of feedback. Finally, in some cases both terms are used in tandem, such as in some reviews of the state of the art that group the therapeutic applications of NF and BCIs into

<sup>62</sup> (Yan N. et al., 2008; Huster et al., 2014)

<sup>63</sup> (J. R. Wolpaw & E. W. Wolpaw, 2011)

<sup>64</sup> (Neuper & Pfurtscheller, 2010; Grosse-Wentrup, Mattia, & Oweiss, 2011)



<sup>65</sup> (Birbaumer, Ramos Murguialday, et al., 2009)

the same category<sup>65</sup>. This particular usage of terminology rightly highlights the similarities of the two approaches and the fact that clinical applications of BCIs have historically been derived from work on NF.

<sup>66</sup> (Huster et al., 2014)

Yet, how we already stressed it, NF and BCI traditionally have different primary purposes, NF being used as a way to develop internal control while BCI are primarily meant to yield a control over external objects (orthoses, computer, ...). This translates into methodological discrepancies, such as the fact that traditional NF exploits a small number of electrodes and rarely relies on machine learning methods for feature selection while they play a major role in BCI<sup>66</sup>. Feature selection might actually be the stage at which assistive BCI and NF practices differ the most. When designing assistive BCI, the goal is usually to maximize the degrees of freedom of the BCI while minimizing the time required for calibration. To this end, BCI heavily rely on signal processing and machine learning techniques for the feature selection step. Implicitly, the brain patterns used in BCI are likely selected based on their robustness, rapidity and ease of evocation by the user. On the opposite, NF rarely relies on machine learning and classification techniques for feature selection but rather on physio-pathological models, a priori knowledge about abnormal patterns, brain structure and function, or normalization databases and applies little or no individual adaptation. The targeted brain patterns are selected for their presumed functional rehabilitation power and it can take long before the user becomes able to control them well.

<sup>67</sup> (B. Allison, 2011)

<sup>68</sup> (J. R. Wolpaw & E. W. Wolpaw, 2011)

Recently, the definition of BCI has been extended to account for new kinds of application<sup>67</sup>. The modern definition of a BCI was given by Wolpaw in 2011<sup>68</sup>: “A BCI is a system that measures central nervous system activity and converts it into artificial output that replaces, restores, enhances, supplements, or improves natural CNS (central nervous system) output and thereby changes the ongoing interactions between the CNS and its external or internal environment.” Unlike the traditional definition of BCI<sup>69</sup>, this definition admits the family of applications linked to brain rehabilitation, which until now had fallen exclusively under NF. This definition of BCIs therefore fully encompasses NF. The specific term “restorative BCI” has even emerged to describe BCIs designed for purposes of brain rehabilitation, as opposed to the term “assistive BCI”, describing BCIs that serve purposes of communication and control. These “restorative BCIs” are thus indeed equivalent to the definition of NF. The reason that this term was introduced despite the prior existence of the term “neurofeedback” is likely that the BCI community has chosen to boycott the label “neurofeedback” due to its connotation of pseudoscience. In BCI literature, restorative BCIs currently focus in essence on the motor rehabilitation of stroke victims<sup>70</sup>. Note that patients with motor deficits (cerebral palsy, strokes, amyotrophic lateral sclerosis, multiple sclerosis, muscular dystrophy, bone marrow lesions, etc.) were historically the primary target audience of the first (assistive) BCIs. But applications of restorative BCIs tend to involve restoring functions that are physical (other than motor), cognitive, and emotional in nature<sup>71</sup>, just like NF.

<sup>69</sup> (J. R. Wolpaw & Birbaumer, 2002)

<sup>70</sup> (Birbaumer, Ramos Murguialday, et al., 2009; Grosse-Wentrup, Mattia, & Oweiss, 2011; Ang & Guan, 2015; Dokkum, Ward, & Laffont, 2015)

<sup>71</sup> (J. R. Wolpaw & E. W. Wolpaw, 2011)

## 2.5 APPLICATIONS

The traditional purpose of NF has always had two components, on the one hand oriented towards *therapeutic* applications for treating *psychiatric and neurological disorders*, and on the other towards *optimizing the performance* of healthy

subjects. Since the brain is the control center of physical, mental and cognitive functions, and NF acts directly upon brain mechanisms that govern or contribute to these control processes, the potential scope of NF is vast. This is reflected in the panel of applications for which NF has already been explored:

- **Therapeutic applications:** ADHD, epilepsy, depression, anxiety, learning disorders, sleeping disorders, autism, post-traumatic stress disorder, addiction, chronic pain, tinnitus, migraines, Alzheimer's, Parkinson's, schizophrenia, ...<sup>72</sup>;
- **Non-therapeutic applications:** mental rotation, attention, memory, visual skills, musical performance, performance of surgical tasks, sportive performance, cognitive deterioration, meditation<sup>73</sup>.

Although there is a large range of variety in the studies performed, the results obtained are preliminary in nature, except in the domain of ADHD, where NF is currently in the process of achieving sufficient levels of proof. Indeed, most NF studies are case studies, or have methodological flaws that limit the scope of their conclusions. Maintaining quality levels in NF studies aiming to demonstrate the effectiveness of an NF protocol in improving a given disorder or function is therefore a substantial multidisciplinary *methodological challenge*. NF has long suffered from a lack of scientific credibility inherited from the rapid failure of alpha NF in the seventies, but also from the poor quality of early studies that were not reproducible, with very few subjects in poorly controlled experimental conditions. Today, it has been clearly established that in order for an NF protocol to be proven effective in a given application, it must first be subjected to rigorous experimentation that observe the principles of evidence-based medicine: significant numbers of subjects, use of control groups (in particular placebo groups<sup>74</sup>), randomization, double-blind trials, studies by multiple research groups, evaluation of physiological, psychological and behavioral effects in the short, medium and long term<sup>75</sup>. Given that NF training programs often require over thirty sessions to obtain sustainable results, and that these sessions must be multiplied by the number of subjects in the study, the resources required to properly meet all of these requirements soon become colossal. The only domain in which these requirements have started to be met is that of ADHD.

By exploiting the self-regulation capacity of its users, NF could potentially find its place as a non-invasive or *complementary* alternative to other treatments, such as pharmacological treatments, neurosurgery, psychotherapy and passive stimulation techniques (like transcranial magnetic stimulation (TMS) and transcranial direct current stimulation tDCS). Below, we shall describe the state of the art for the major therapeutic applications of NF.

**ADHD** ADHD is the clinical application of NF that has been studied in the most depth by far. The protocols that have been shown to be beneficial are the theta/beta protocols (inhibition of theta and facilitation of beta at the fronto-central electrodes), SMR and SCP. One meta-analysis<sup>76</sup> of over fifteen RCT studies with a total of 1194 patients concluded that EEG-NF could be considered an “effective and specific” alternative to usual treatments based on stimulants (methylphenidate and amphetamines), which are limited by their short-term

<sup>72</sup> (Birbaumer, Ramos Murguialday, et al., 2009; Hammond, 2011; Niv, 2013; Wyckoff & Birbaumer, 2014)

<sup>73</sup> (Gruzelier, 2014a; Gruzelier, 2014b; Scharnowski & Weiskopf, 2015)

<sup>74</sup> (Martijn Arns, Heinrich, & Ute Strehl, 2014)

<sup>75</sup> (Robineau et al., 2017)

<sup>76</sup> (Arns, Ridder, & Strehl, 2009)

mode of action and potential side-effects. The authors of the meta-analysis report a large effect size on symptoms of inattention and impulsiveness, and a medium effect size on hyperactivity. However, the effect sizes were found to be smaller in better-controlled studies, i.e. studies with a placebo control group<sup>77</sup>. Additional RCTs with placebo groups are still necessary, particularly double-blind studies, to identify more precisely the effectiveness of NF. As for the duration of the effects of treatment, several studies have shown that the effects of the SCP and theta/beta protocols persisted after the last session of NF, for 6 months<sup>78</sup> and for 2 years<sup>79</sup>.

<sup>77</sup> (Arns, Ridder, & Strehl, 2009)

<sup>78</sup> (Gani, 2009; Leins et al., 2007)

<sup>79</sup> (Gani, 2009)

**Epilepsy** Roughly one-third of patients suffering from epilepsy do not respond to anti-convulsives, and cannot be treated by operation due to the localization of their epileptic foci. NF could represent a viable alternative for these patients. Epilepsy was the first therapeutic application of NF to be discovered<sup>80</sup>. The protocols that seem best-adapted to epileptic patients are the SMR and SCP protocols. One meta-analysis<sup>81</sup> of 174 patients over 10 studies (9 SMR, 1 SCP) showed that the frequency of seizures decreased in 74% of the patients. One study even observed persistent effects 9 years after treatment with NF<sup>82</sup>. Despite these encouraging results, larger-scale trials are required to prove that NF is effective in cases of pharmaco-resistant epilepsy.

<sup>80</sup> (Serman, LoPresti, & Fairchild, 1969)

<sup>81</sup> (Tan et al., 2009)

<sup>82</sup> (Ute Strehl et al., 2014)

**Depression** Unlike existing therapies (psychotherapy, antidepressants, electroshock therapy) and more modern alternatives (vagus nerve stimulation, TMS), one of the unique aspects of NF is that patients suffering from depression are placed in the role of actors in their healing process, demonstrating to themselves that they have the capacity to influence their own brain activity, and consequently their psychological states. The EEG-NF protocol that has been studied in most depth for depression aims to regulate the frontal asymmetry of alpha waves, based on the hypothesis that in some patients suffering from depression, the right prefrontal lobe associated with withdrawal behavior is hyperactive, whereas the left prefrontal lobe associated with approach behavior is hypoactive. Although several studies appear to report an improvement in depression scores following the application of this protocol<sup>83</sup>, these studies have a number of methodological flaws such as: low patient numbers, low initial depression scores, limited number of evaluation criteria for describing effects on depression, lack of control for unspecific effects. Furthermore, the specificity of the frontal asymmetry marker is still subject to debate. As emotional circuits involve deep and complex networks, it is possible that traditional EEG-NF is not sufficient to regulate this kind of circuit. One LORETA NF study<sup>84</sup> showed that reducing rapid beta wave activity (18-30 Hz) in the corticolimbic/paralimbic regions of patients suffering from major depression was correlated with an improvement in depression-related symptoms. fMRI-NF might also be promising for treating depression, giving its capacity to target the deep regions of the emotional circuit such as the amygdala and the ventrolateral prefrontal cortex<sup>85</sup>. A recent study also showed that it is possible to simultaneously combine EEG-NF of frontal asymmetry and fMRI-NF of the amygdala<sup>86</sup>, which could allow the effects of both protocols to be combined.

<sup>83</sup> (S. W. Choi et al., 2011; Peeters et al., 2014)

<sup>84</sup> (Paquette, Beauregard, & Beaulieu-Prévost, 2009)

<sup>85</sup> (K. D. Young et al., 2014)

<sup>86</sup> (Zotey, Phillips, et al., 2014a)

**Motor rehabilitation following a stroke** It is an established fact that the imagination of a movement activates regions and circuits similar to those activated by effectively performing the same movement<sup>87</sup>. By practicing imagining movements, individuals with paralysis after a stroke directly utilize the damaged motor regions in the brain, stimulating neuronal plasticity. It is assumed that practice can help them progressively recover motor function. To allow patients to overcome the phenomenon known as "learned non-use" and to achieve actual recovery of motor control in the affected limb, closing the sensorimotor loop during NF seems crucial<sup>88</sup>. Visual or audio feedback is generally not sufficient for this, and instead tactile feedback should be used. This feedback should be well-calibrated to fit the subject's intended movement, for example using an orthosis<sup>89</sup> or by combining NF with function electrical stimulation (FES)<sup>90</sup>.

<sup>87</sup> (Sharma & Baron, 2013a)

<sup>88</sup> (Dokkum, Ward, & Laffont, 2015)

<sup>89</sup> (Shindo et al., 2011; Ramos-Murguialday et al., 2013)

<sup>90</sup> (B. M. Young, Williams, & Prabhakaran, 2014)

<sup>91</sup> (Lotte, Larrue, & Mühl, 2013)

<sup>92</sup> (Hwang, Kwon, & Im, 2009)

**NF for controlling BCIs** As remarked by Lotte et al.<sup>91</sup>, "*using BCIs is a skill*". Indeed, before being able to operate a BCI (especially a spontaneous BCI) with a given brain pattern, e.g. by imagining moving the left or right hand, subjects must first learn to generate this pattern reliably<sup>92</sup>. Subjects can achieve this through hours of mental practice, but it is difficult for them to be certain that they are practicing the correct tasks, and that they are orienting their efforts in the correct direction. NF provides users with an objective representation of the pattern, allowing them to practice controlling it in more favorable learning conditions. NF-based practice is therefore an indispensable preliminary stage for the usage of certain BCIs, such as spontaneous BCIs.

## 2.6 CONCLUSION

NF is a technique that involves measuring the brain activity of a subject, and communicating this information to the subject in real time so that he or she may learn to control one specific aspect of it. Until recently, the primary distinction between this technique and BCIs was essentially the fact that the objective of NF is self-control, whereas BCIs (in the classical sense of assistive BCIs) aim to control objects external to the user. Today, this distinction has begun to fade, as the field of applications of BCIs has been extended to include BCIs for brain rehabilitation, given the name of "restorative BCIs". We might therefore hope to see the NF and BCI communities come closer together in future thanks to a transfer of experience and knowledge. For example, the NF community might benefit from the more sophisticated processing tools and feedback forms developed for BCIs, while the BCI community might benefit from the learning and brain self-regulation principles used in NF.

Although certain forms of EEG-NF are already used by practitioners who boast of innumerable benefits, NF is still an experimental technique. Among all of the EEG-NF protocols suggested over the course of 60 years in response to a very wide panel of applications, only the SCP, SMR and theta/beta protocols for treating ADHD have begun to attain sufficient levels of proof. Outside of this special case, it seems that traditional NF approaches based on EEG with one or two channels are limited by the quality and the low specificity of the recorded information. Thus, in order to better target the activity of certain regions of the brain, researchers have developed new NF techniques that use larger numbers of EEG electrodes (LORETA-NF with a full EEG headset) or using other equip-

<sup>93</sup> (K. D. Young et al., 2014)

<sup>94</sup> (DeCharms et al., 2005)

<sup>95</sup> (Sulzer et al., 2013)

<sup>96</sup> (Zotев, Phillips, et al., 2014a)

ment (fMRI-NF, MEG-NF, NIRS-NF). The most noteworthy of these newer techniques is fMRI-NF, which gives access to the self-regulation of specific brain regions with high spatial resolution. fMRI-NF already shows promise for treating emotional disorders<sup>93</sup>, chronic pain<sup>94</sup>, and other disorders<sup>95</sup>. Recently, a study demonstrated the feasibility of simultaneous EEG-NF and fMRI-NF<sup>96</sup> leading the way for the development of new multimodal NF approaches that could potentially outperform unimodal NF approaches. Studies questioning the mechanisms at work in NF are another active area in the current state of NF, which should lead to the development of more effective protocols. Last, in order to prove the effectiveness of these protocols in specific conditions and to justify their integration into treatment programs, large-scale RCT will be indispensable. There are currently far too few such studies.

*"L'union fait la force. Oui. Mais la force de qui ?"*

— Emile-Auguste Chartier, dit Alain

*Prelude* This chapter lays the foundations for understanding why and how EEG and fMRI should be combined for NF purpose. We start by explaining under which conditions EEG and fMRI should be acquired simultaneously, and how electrophysiological and BOLD signals are known to be related. Next we make out a methodological comparison of EEG-NF and fMRI-NF that will be particularly useful when designing bimodal EEG-fMRI-NF protocols. We then review exhaustively the limited corpus of NF studies that have exploited EEG and fMRI together and eventually propose a taxonomy of such studies.

### 3.1 WHEN TO DO SIMULTANEOUS RECORDINGS ?

When recording EEG inside an MR, EEG is affected by strong artifacts<sup>1</sup> that can be hard to remove, especially in real-time. Separate acquisition of the EEG and the fMRI presents the big advantage of not generating such artifacts. In some cases, the EPI acquisition can be triggered based on an event detected from the EEG, as was done in the first studies on epilepsy (interleaved recordings). As pointed out by Jorge et al., event-related designs cannot be optimized simultaneously for EEG and fMRI<sup>2</sup>. Simultaneous acquisition ensures that BOLD and EEG data correspond to the exact same experimental situation, thus preventing from uncontrolled effects of novelty processing, learning or experimental variability related to preparation time, task experience, sensory stimulation and recording environment that necessarily affect the subject's mood, attention, expectation, motivation and behavior<sup>3</sup>. Advantages and drawbacks of the two approaches are summarized in [Figure 19](#).

<sup>1</sup> The main artifacts are the gradient and the ballisto-cardiogram artifact. Their origin is explained in [4.1.1.1](#)

<sup>2</sup> (Jorge, Grouiller, et al., 2015)

<sup>3</sup> (Debener et al., 2006)

Protocol feature	Separate	Simultaneous
Optimal signal quality	Yes	No
Possibility to optimize design	Yes	No
Avoidance of order effects	No	Yes
Identical sensory stimulation	No	Yes
Identical subjective experience	No	Yes
Identical behavior	No	Yes
Direct temporal correlation of EEG and fMRI signals	No	Yes

Considering the technical issues of the simultaneous acquisition of EEG and fMRI, such an experimental setting should be used essentially in cases where the EEG is expected to vary significantly during the span of the experience and even preferably if these variations are to be exploited online, by example for the detection of events or study of inter-session variability. This is potentially the case for NF studies. If the experiment can be repeated many times with a high

Figure 19 – Benefits and drawbacks of separate vs simultaneous EEG-fMRI recordings (from Debener et al. (2006))



degree of reliability, then data can be acquired separately.

### 3.2 WHEN EEG AND FMRI AGREE AND DISAGREE

Although fMRI is to this day the most widely used tool in human cognitive neuroscience, the relationship between the BOLD signal and the neuronal activity is still not fully understood<sup>4</sup>. The active process that links transient local neuronal activity to an orchestrated increase in local blood flow is called neurovascular coupling<sup>5</sup>. Over the past two decades, many studies have combined electrophysiological and hemodynamic measurements to investigate the neurovascular coupling in animals and humans (healthy subjects and patients) in various experimental conditions (rest, sensory stimulation, cognitive tasks...).

**Partial non-linearity of the BOLD signal** Within a limited dynamic range of stimulus conditions, the BOLD signal appears to be linearly coupled to neuronal activity<sup>6</sup>. In other situations non linear-coupling has been observed. In some networks, the BOLD saturates before the neuronal activity, while in some other networks it can be the opposite.

**BOLD reflects LFP rather than spike rate** Animal studies combining invasive electrophysiological (LFP: local field potentials and MUA: multiunit activity) and hemodynamic recordings<sup>7</sup> consistently report a tight correlation between the BOLD signal and LFP<sup>8</sup> rather than with action potentials<sup>9,10</sup>. This finding was also replicated in simultaneous intracranial EEG (icEEG)-fMRI data recorded during the pre-surgical evaluation of patients with drug-resistant epilepsy<sup>11</sup>. More specifically the study by Murta et al. suggested that the amplitude of the BOLD signal depends more on the duration of the underlying LFP than on the degree of neuronal activity synchrony (reflected by the amplitude of the LFP)<sup>12</sup>.

**Colocalization of electrophysiological and hemodynamic sources** At the mesoscopic and macroscopic scale, it has been observed that of electrophysiological and hemodynamic source locations matched well in different brain areas and under different conditions<sup>13</sup>.

**BOLD correlates with gamma oscillations** Many studies have described a positive correlation between the BOLD signal and gamma activity<sup>14</sup> and a negative correlation with lower-frequency (alpha, beta)<sup>15</sup>. The study by Scheeringa et al. additionally reveals that alpha/beta and gamma band neural dynamics contribute independently to the BOLD signal<sup>16</sup>. The study by Magri et al. suggested that the amplitude of the BOLD signal reflects the relationship between alpha and gamma power, while the latency of BOLD with respect to significant changes in gamma power reflects the relationship between beta and gamma bands<sup>17</sup>. The study by Engell et al. indicates that hemodynamic changes measured by fMRI reflect non-phase-locked changes in high frequency power rather than the phase-locked ERP<sup>18</sup>.

However these principles should be considered carefully as the directions of EEG-BOLD signal correlations might vary across brain regions, time, brain states and EEG frequency band<sup>19</sup>.

<sup>4</sup> (Nikos K Logothetis & Wandell, 2004; Nikos K. Logothetis, 2008; Riera & Sumiyoshi, 2010; Ekstrom, 2010; Hillman, 2014)

<sup>5</sup> (Hillman, 2014; Huneau, Benali, & Chabriat, 2015)

<sup>6</sup> (Shmuel, 2009)

<sup>7</sup> fMRI or optical imaging

<sup>8</sup> LFP reflect input synaptic activity and intralaminar cortical processing

<sup>9</sup> Action potentials reflect output spiking activity

<sup>10</sup> (N K Logothetis et al., 2001; J. B. M. Goense & Nikos K. Logothetis, 2008; Niessing, 2005; Viswanathan & Freeman, 2007)

<sup>11</sup> (Mukamel et al., 2005; Lachaux et al., 2007; Nir et al., 2007; Murta, Chaudhary, et al., 2016)

<sup>12</sup> (Murta, Chaudhary, et al., 2016)

<sup>13</sup> (M. J. Rosa, Daunizeau, & Karl J. Friston, 2010; Horowitz et al., 2004; Lachaux et al., 2007; Siero et al., 2013)

<sup>14</sup> Gamma oscillations are associated with local neuronal processing

<sup>15</sup> (Scheeringa et al., 2011; Mulert & Lemieux, 2010; Lachaux et al., 2007; Magri et al., 2012)

<sup>16</sup> (Scheeringa et al., 2011)

<sup>17</sup> (Magri et al., 2012)

<sup>18</sup> (Engell, S. Huettel, & McCarthy, 2012)

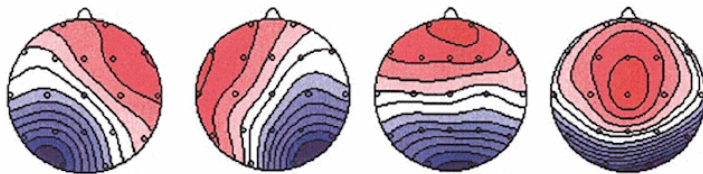
<sup>19</sup> (S. A. Huettel et al., 2004; Michels et al., 2010; Engell, S. Huettel, & McCarthy, 2012)

**Negative BOLD has a specific neurovascular origin** Some studies suggest that negative BOLD responses have a neuronal component to their physiological origin (rather than resulting from a pure vascular phenomenon) and that positive and negative BOLD signals have different neurovascular coupling mechanisms<sup>20</sup>. As the BOLD response attests of the balance between oxygen supply and consumption, in situations where the neural activity is exceptionally high (such as in hippocampal neurons during epileptic seizures by example<sup>21</sup>), it is possible for the oxygen consumption to exceed the supply and thus to result in negative BOLD response. The initial dip of the HRF is an example of this phenomenon.

**Non-neuronal contributions to the BOLD signal** Blood flow in the brain is regulated by neurons and glial cells, in particular astrocytes which act as intermediary between neurons and the vasculature<sup>22</sup>. BOLD signal might therefore also be affected by glial activity. A study by Schulz et al showed that glial activations prolongs the BOLD response potentially by prolonging the dilation of the blood vessels.<sup>23</sup>

The BOLD signal has also been shown to be influenced by physiological parameters<sup>24</sup>. The study by Sumiyoshi et al. indicates that coupling or potential decoupling of BOLD and gamma oscillations is strongly influenced by systemic physiological parameters (mostly heart rate), which dynamically reflect the baseline state of the subject<sup>25</sup>.

**Coupling at rest** Some studies have found correlations between the BOLD signal and LFP during resting-state<sup>26</sup>. More precisely, the study by Ma et al. suggested that resting-state BOLD is coupled to excitatory neural activity<sup>27</sup>. Functional connectivity analysis of resting state fMRI have enabled to identify 4 large-scale functional default networks showing stable hemodynamic signatures of about 10 seconds<sup>28</sup>. These networks have been attributed to phonological processing, visual imagery, attention reorientation, and subjective processing. On the other end, the study of the stability of EEG scalp topography reveals 4 EEG microstates (see Figure 20) whose durations span between 80 and 120 milliseconds<sup>29</sup>. Interestingly, despite their different temporal scales, EEG microstates and BOLD resting-state networks have been found to be significantly correlated<sup>30</sup>.



<sup>20</sup> (J. Goense, Merkle, & Nikos K. Logothetis, 2012; Mullinger et al., 2014; Maggioni et al., 2016)

<sup>21</sup> (Schridde et al., 2008)

<sup>22</sup> (Howart2014; Attwell et al., 2010; Huneau, Benali, & Chabriat, 2015)

<sup>23</sup> (Howart2014; Schulz et al., 2012)

<sup>24</sup> (Sumiyoshi et al., 2012; Pfurtscheller, Schwerdtfeger, et al., 2017)

<sup>25</sup> (Sumiyoshi et al., 2012)

<sup>26</sup> (Shmuel & Leopold, 2008; Magri et al., 2012; Ma et al., 2016)

<sup>27</sup> (Ma et al., 2016)

<sup>28</sup> (Britz, Van De Ville, & Michel, 2010)

<sup>29</sup> (Koenig et al., 2002)

<sup>30</sup> (Britz, Van De Ville, & Michel, 2010; Yuan, Zotev, et al., 2012)

Figure 20 – EEG micro-states (from Koenig et al. (2002))

**Decoupling situations** Several studies have described situations in which the BOLD signal and the underlying neural activity were dissociated<sup>31</sup>. Decoupling can be observed for different reasons:<sup>32</sup>:

- In terms of source locations, it is possible that the neuronal population responsible for the EEG signal do not collocate with the vascular tree supplying

<sup>31</sup> (Ekstrom, 2010)

<sup>32</sup> (M. J. Rosa, Daunizeau, & Karl J. Friston, 2010)



the blood to these neurons and that triggers the associated BOLD change;

- fMRI changes without EEG correlates (EGG-blind fMRI sources) can be explained by different reasons:
  - some processes require energetic support through blood (such as neurotransmitter synthesis, glial cell metabolism, maintenance of the steady-state potential) and will thus trigger a BOLD change but do not generate electrical activity;
  - non synchronized electrophysiological activity;
  - closed source configuration invisible to EEG.
- EEG changes without fMRI correlates (fMRI-blind EEG sources): fMRI might be blind to transient electrophysiological activity.
- signal detection failures.

In some cases, the decoupling between electrophysiological and hemodynamic/metabolic activity can be a sign of a pathology in itself<sup>33</sup>. Alterations of the BOLD fMRI signal with ageing and disease have been described in the literature<sup>34</sup>.

As a last remark, even in cases where the hemodynamic and electrical sources are not correlated, due to global influence of endogenous condition a functional but not necessarily anatomical overlap can exist.

<sup>33</sup> (Huneau, Benali, & Chabriat, 2015; Girouard, 2006)

<sup>34</sup> (D'Esposito, Deouell, & Gazzaley, 2003; Schridde et al., 2008; Girouard, 2006)

### 3.3 METHODOLOGICAL COMPARISON OF EEG-NF AND fMRI-NF

Though EEG and fMRI are the two most widespread modalities in NF research, EEG-NF and fMRI-NF are rarely studied with regard to each other. Yet there is no guarantee that the body of work can easily be transferred from one procedure to the other. Though there are general mechanisms involved in both procedures, the different natures of EEG and fMRI impose different constraints on the design of NF protocols. Extrapolating, it is conceivable that as a consequence they could have different areas of specialization and be better suited to the regulation of different kind of brain patterns and even brain functions. [Table 1](#) elucidates some general and methodological aspects of EEG-NF<sup>35</sup> and fMRI-NF<sup>36</sup>, three of which we will delve more into: NF signal, task design and duration, and Number of training sessions.

<sup>35</sup> (Enriquez-Geppert, Huster, & Herrmann, 2017; Gruzeliier, 2014c)

<sup>36</sup> (Sulzer et al., 2013)

**NF signal** EEG-NF and fMRI-NF literatures offer a wide variety of methods to compute the NF signal which basically range from spatially univariate to spatially multivariate methods (though multivariate methods are more often used for "brain reading"<sup>37</sup> applications). [Figure 21](#) illustrates how different fMRI feature extraction methods integrate the BOLD signal in the spatial and temporal dimensions. Given the low temporal resolution of fMRI, the compromise between the quality and the instantaneous representativity of the NF signal is sometimes hard to find. Some methods construct an online model that is updated either on a sliding-window or incrementally. Among univariate fMRI methods<sup>38</sup>, online version of the general linear model allows to model noise confounds. Multivariate methods are capable of exploiting the full information

<sup>37</sup> "specific mental states or representational content is decoded from fMRI activity patterns after performing a training phase" (Goebel, 2012)

<sup>38</sup> (Robert W. Cox, Jesmanowicz, & James S. Hyde, 1995; Gembris et al., 2000; Bagarinao et al., 2003a; DeCharms et al., 2005; Nakai et al., 2006b; Hinds, Ghosh, Todd W. Thompson, et al., 2011)

	EEG-NF	fMRI-NF
<b>Neurophysiological origin</b>	Sum of synchronized post-synaptic dendritic potential	Blood oxygen level dependent
<b>Equipment cost</b>	100 - 20 000 euros (60 000 euros for MR-compatible EEG device)	1 - 5 million euros + 300 euros/h
<b>Spatial resolution</b>	centimeters	millimeters
<b>Sensitivity depth</b>	~ 4 centimeters	Whole brain
<b>Temporal resolution</b>	Milliseconds	Few hundreds of milliseconds (TR) + 4-6 seconds hemodynamic delay
<b>Duration of stable states at rest</b>	EEG microstates last about 80 - 120 ms	fMRI resting-state network are stable over 5-10 sec
<b>Signal drift origin (Morcom &amp; Fletcher, 2007)</b>	Eye movement, deep breathing, sweating	Scanner instabilities (Smith et al., 1999), brain physiology (Yan et al., 2009)
<b>Feature selection</b>	Usually based on the literature linking abnormal brain oscillations to specific symptoms) with possibilities to personalize the feature. Machine learning techniques are rarely used.	Functional and/or anatomical localizer
<b>NF signal (types of feature)</b>	<ul style="list-style-type: none"> <li>• Amplitude of specific frequency bands at one, two electrode sites</li> <li>• SCP</li> <li>• Amplitude ratio between different frequency bands at one, two, or more electrode sites</li> <li>• Z-score NF allows to target absolute/relative power, ratios, coherence, phase, ...</li> <li>• Source-based (source localization Loreta NF, BSS-NF)</li> </ul>	<ul style="list-style-type: none"> <li>• Average percent signal change in ROI</li> <li>• Differential signal between the ROI and a large background region to cancel out global changes due to arousal, breathing, heart rate and head movements</li> <li>• Effective connectivity</li> </ul> <p>(More details can be found in <a href="#">Figure 21</a> )</p>
<b>Baseline estimation</b>	The same baseline can be used over many sessions or it can be calculated at the beginning of each session	Usually the baseline is updated at every block which partly removes low-frequency drift (if blocks are not too long). Detrending and high pass filtering can also be applied online to remove the low-frequency drift.
<b>Task design</b>	Block, continuous/self-paced (Scherer et al., 2007), event-related	Block
<b>Task duration</b>	Usually about 2-5 minutes but can be much shorter (few seconds for MI) or much longer (tens of minutes for deep state NF)	15-45 seconds
<b>Number of training sessions</b>	20 - 40	5 - 10

Table 1 – Comparison of general and methodological aspects of EEG-NF and fMRI-NF

<sup>39</sup> (Eklund et al., 2010; LaConte, 2011; Sitaram, S. Lee, et al., 2011; Soldati, Vince D. Calhoun, et al., 2013; Koush, Maria Joao Rosa, Robineau, Heinen, W. Rieger, et al., 2013; Zilverstand et al., 2014a; Koush, Meskaldji, et al., 2015)

<sup>40</sup> (Sorger, Kamp, et al., 2016)

<sup>41</sup> (J. H. Lee et al., 2009; J. J. Yoo et al., 2012)

<sup>42</sup> (Sorger, Dahmen, et al., 2009)

<sup>43</sup> (Sorger, Kamp, et al., 2016)

present in the data<sup>39</sup>. Looking at the fMRI-BCI community, some interesting methodological works have been proposed that can give ideas to the fMRI-NF community. Sorger et al.<sup>40</sup> proposed different ways of increasing the degrees of freedom in encoding separate intentions for an fMRI-BCI: spatial features that implement different types of mental tasks<sup>41</sup>, temporal features that use different encoding time intervals<sup>42</sup>, a combination of spatial and temporal features, and magnitudinal features that encode gradual BOLD amplitude<sup>43</sup>. These works suggest that it might be possible to implement new kind of NF designs that would allow to regulate different aspects of the brain response.

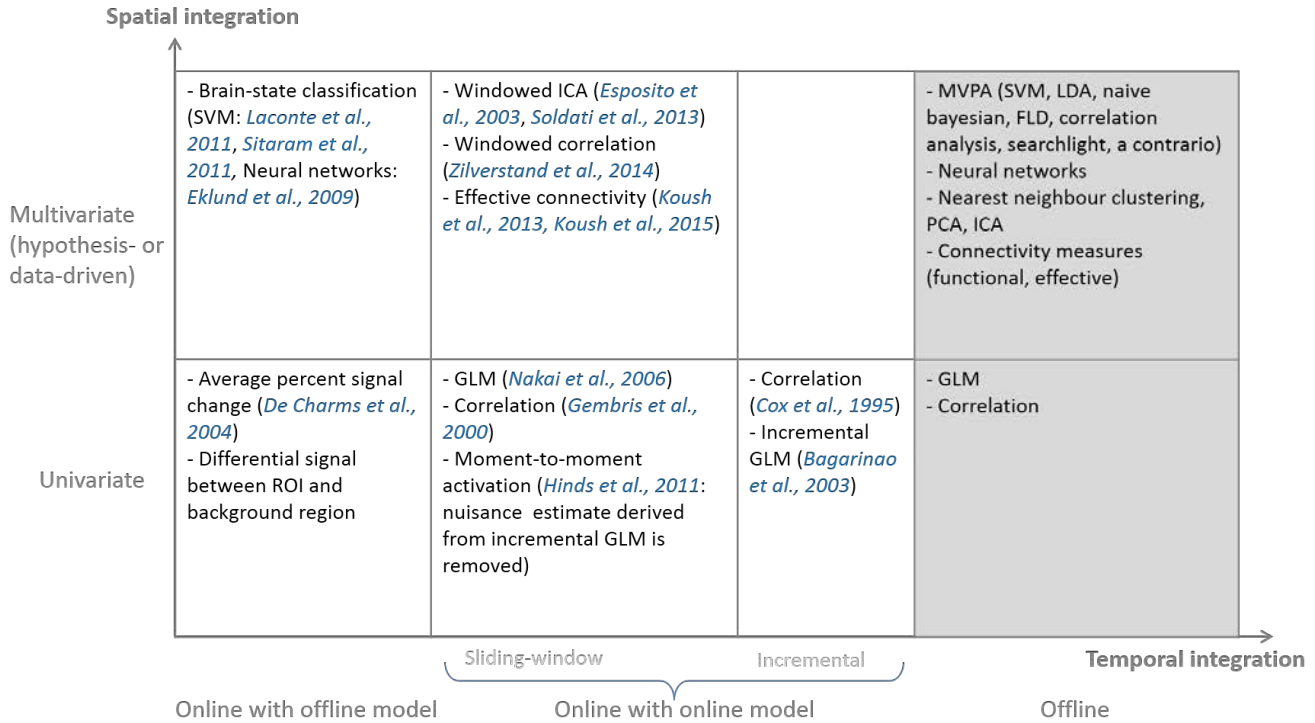


Figure 21 – Methods for fMRI feature extraction grouped by their spatio-temporal integration

**Task design and task duration** Thanks to its higher temporal resolution, EEG gives good flexibility on the type of design and task duration. During long tasks (> 1 minute), the trainer can even interact with the user to suggest strategies. On the opposite, it seems harder to implement fMRI-NF protocols with short tasks, event-related or asynchronous design because of the slow BOLD dynamics and the limited temporal resolution of fMRI. For the same task, EEG-NF and fMRI-NF protocols can vary greatly. For example, most MI-based EEG-NF/BCI rely on the Graz-MI protocol<sup>44</sup> and use pretty short tasks, around 5 seconds long<sup>45</sup>. Meanwhile MI-based fMRI-NF tasks are usually around 20 seconds long<sup>46</sup> (except in <sup>47</sup> in which the MI tasks are 5 seconds long). This example highlights the fact that designing an EEG-fMRI-NF protocol compatible with EEG and fMRI constraints is a real challenge<sup>48,49</sup>.

<sup>44</sup> (Pfurtscheller & Neuper, 2001)

<sup>45</sup> (Ono et al., 2014; Prasad et al., 2010; Kaiser et al., 2011)

<sup>46</sup> (Berman et al., 2012; Chiew, LaConte, & Graham, 2012; Johnson & Hartwell, 2012)

<sup>47</sup> (S. S. Yoo et al., 2008)

<sup>48</sup> (Warbrick, Reske, & Shah, 2013)

<sup>49</sup> "Considering the distinct timescales of EEG and fMRI responses, experimental paradigms must be carefully designed to highlight the phenomena of interest in each modality, while dealing with potential sensitivity and specificity compromises. (Jorge, Van der Zwaag, & Figueiredo, 2014)

**Number of training sessions** The number of NF sessions needed to achieve long-lasting self-regulation and functional outcomes is thought to be higher with EEG-NF than with fMRI-NF. This could be due to the fact that EEG features are noisier and less specific than fMRI features, especially in traditional EEG-NF methods which target single electrode sites that are likely influenced by large scale EEG dynamics involving several brain regions and processes<sup>50</sup>. NF pioneer Niels Birbaumer also hypothesizes that metabolic activity can be more easily and rapidly controlled than electrophysiological activity because *"the brain processes information from its vascular system but has no sensors for its neuroelectric responses"*<sup>51,52</sup>.

<sup>50</sup> (White, Congedo, & Ciorciari, 2014)

<sup>51</sup> (Birbaumer, Ramos Murguialday, et al., 2009)

<sup>52</sup> See [Birbaumer's interview on GoCognitive](#)

### 3.4 LITERATURE REVIEW OF EEG/FMRI NF STUDIES

In the recent years, a dozen NF studies have reported the use of EEG and fMRI. In this section, we review their motivations and approaches.

**Lévesque et al. 2006** <sup>53</sup> Lévesque et al. conducted a fMRI study to measure the effect of NFT on the neural substrates of selective attention in children with ADHD. Fifteen children were randomly assigned to the NF or to the control group. fMRI was acquired 1 week before the beginning of the NF training and 1 week after the end of this training, while children performed a counting stroop task. Before NF, the counting stroop task was associated with significant loci of activation in the left superior parietal lobule in both groups. After NF, for both groups, the counting stroop task was still associated with significant activation of the left superior parietal lobule. But only children from the experimental group showed significant activation of the right anterior cingulate cortex (ACC). These results suggested that in ADHD children, NF has the capacity to normalize the functioning of the ACC, a key neural substrate of selective attention.

<sup>53</sup> (Lévesque, Beauregard, & Mensour, 2006)

**Kinreich et al. 2012** <sup>54</sup> In a 2012 study by Kinreich et al., 30 healthy subjects underwent two sessions of theta/alpha EEG-NF (usually used for deep relaxation training in anxiety and mood disorders), the first outside of the MRI scanner, and the second inside of the MRI scanner. For each subject, the 3 most responsive out of the 8 occipital electrodes were chosen for NF in the second session based on the result of the first session. After these 2 NF sessions, subjects were then categorized into responders and non responders based on their performance in modulating their theta/alpha ratio which was also validated by looking at their heart rate variability. Offline EEG-informed fMRI analysis of the responders data then revealed brain networks correlated to the modulation of alpha, theta and theta/alpha. The analysis showed correlated and inversely correlated activity in cortical and subcortical areas involved in sensory, attention and emotion regulation.

<sup>54</sup> (Kinreich, Podlipsky, Intrator, et al., 2012)

Later on, the same authors conducted another study<sup>55</sup> in which they used a theta/alpha NF protocol to rapidly induce the transition into pre-sleep and simultaneous fMRI to reveal state-dependent neural activity. They identified four different periods that designated the neural dynamics of the transition into pre-sleep. Pre-sleep initiation was found to depend on reduced activation in subcortical regions involved in sensory gating (e.g. medial thalamus). In contrast,

<sup>55</sup> (Kinreich, Podlipsky, Jamsky, et al., 2014)

pre-sleep sustainment relied on opposite activation of anterior versus posterior salience network. The authors argued that this opposition could stand for shifting from extra- to intrapersonal neural processing, respectively.

<sup>56</sup> (Ros et al., 2013)

**Ros et al. 2013** <sup>56</sup> performed an EEG-fMRI study on 34 healthy participants to study the brain plasticity induced by a single session of EEG-NF. The participants underwent a 30 min session of EEG-NF for alpha reduction *preceded and followed* by two fMRI scans of an auditory oddball task designed to evaluate attention and mind wandering levels. The connectivity analysis showed that the NF session induced increased connectivity of the dorsal anterior cingulate cortex within the salience network, which was correlated to decreased alpha amplitude, itself correlated to decreased mind wandering.

<sup>57</sup> (Meir-Hasson, Kinreich, et al., 2013)

**Meir-Hasson et al. 2013** <sup>57</sup> introduced a framework for constructing an EEG predictor model called "EEG finger-print" (EFP) of localized fMRI-BOLD activity. The suggested framework is based on a time/frequency representation of the EEG data with varying time-delay and consists in applying a ridge regression method to fMRI and EEG data acquired simultaneously to derive a subject-specific predictor (electrodes, frequencies and delays) of BOLD activity in a certain region. The authors demonstrated the ability of the method by deriving an EFP of the amygdala (amygdala-EFP) and showing that it can predict activity in this deep limbic region and be used as an EEG-NF target for emotional self-regulation<sup>58</sup>. Following on the idea of reducing the need for fMRI scanning, the authors further extended their method in order to construct a common EFP (cEFP), that is a single model that would be valid across different individuals and different sessions and could thus be used without the need for prior fMRI scanning<sup>59</sup>.

<sup>58</sup> (Cavazza et al., 2014; Cohen et al., 2016; Meir-Hasson, Keynan, et al., 2016)

<sup>59</sup> (Keynan et al., 2016; Meir-Hasson, Keynan, et al., 2016)

<sup>60</sup> (Zotev, Phillips, et al., 2014a)

**Zotev et al. 2014** <sup>60</sup> presented for the first time a NF paradigm based on the regulation of both electrophysiological and hemodynamic activity, which the authors call rtfMRI-EEG-NF. In this proof-of-concept, 6 healthy subjects underwent simultaneous EEG-NF and fMRI-NF, based on two protocols that were previously proposed for training emotional self-regulation with potential application to depression: the EEG-NF protocol for regulation of frontal asymmetry in the high-beta (21-30 Hz) band, and the fMRI-NF protocol for activation of the left amygdala which is well known for its role in the processing of negative stimuli. During the NF training, subjects were instructed to use a conscious strategy based on retrieval of happy autobiographical memories intended to induce positive emotions.

The experiment was conducted with a 8-channel MRI head coil array and a 32-channel MR-compatible EEG cap. Experimental choices were constrained in order to limit the EEG-fMRI artifacts on the EEG-NF signal. First, an EPI sequence with 64×64 acquisition matrix was used instead of a higher resolution sequence with 96×96 acquisition matrix. Secondly, the high-beta band was chosen instead of the alpha band (which is more classically used for asymmetry training in depression) as it was less affected by BCG artifact and random motion artifacts. Thirdly, the electrodes F3 and F4 were chosen to measure the frontal high-beta power asymmetry because they are the less sensitive to mus-

cle, saccadic, BCG and random motion artifacts.

Two feedback bars were presented to the subject, the first bar representing the BOLD level of the LA-ROI which was updated every 2 seconds and the second bar representing the frontal asymmetry in the high beta band which was updated every 0.4 seconds. The block design consisted in alternation of 3 conditions: a Rest condition (for baseline update), a Happy Memories condition involving neurofeedback, and a Count condition consisting in a subtraction task. Each block lasted 40 seconds.

Figure 22 gives a summary of the experimental protocol used in the study.

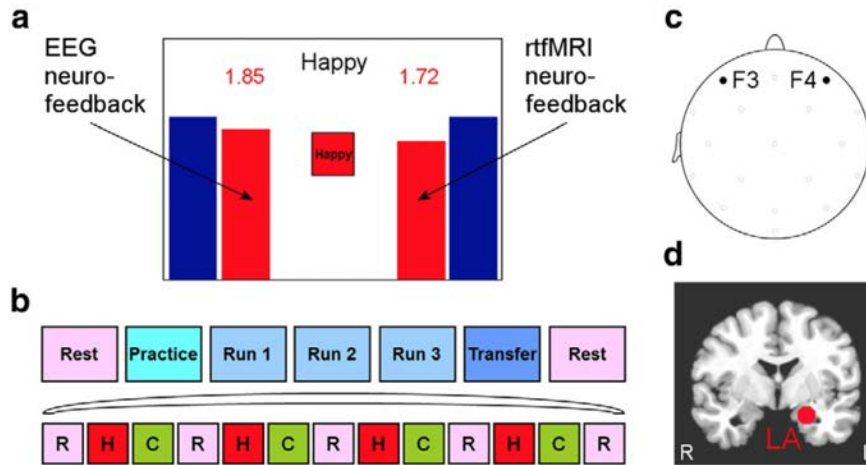


Figure 22 – EEG-fMRI-NF experimental protocol for emotional self-regulation described (from Zotev, Phillips, et al. (2014a))

Real-time artifact correction was based on average artifact subtraction. Residual gradient and BCG artifacts and then muscle and rapid eye movement artifacts were removed with offline ICA. By comparing results at these different stages of artifact correction, the authors evaluated that after the real-time EEG processing, the average EEG power (which is actual signal used for NF) still contained about 50% of gradient and BCG artifacts contribution, and 20% of muscle artifacts, meaning that the regulation was learned on a signal with a very low SNR. The authors identify real-time removal of non stationary artifacts (random head movements, cardiac waveform variations, muscle activity) as one of the main challenge for EEG-fMRI-NF. In addition to being difficult to correct, these kind of artifacts tend to be correlated with the commitment of the subject to the experimental task. Even if these artifacts can be removed quite accurately with ICA there is currently no algorithm for real-time ICA. The authors claimed that the combined protocol could be more efficient than either the EEG-NF or the fMRI-NF protocol performed separately. It is indeed easily conceivable assuming that the EEG-NF and the fMRI-NF protocols are functionally compatible and not entirely redundant, that they might have mutually consistent and complementary therapeutic effects when used in simultaneous combination.

Following their previous work on healthy patients, the authors conducted a pilot study<sup>61</sup> using simultaneous EEG during fMRI-NF training of the amygdala in MDD patients. Their results demonstrated that frontal alpha asymmetry showed temporal correlations with amygdala BOLD activity and suggest that EEG-nf of frontal EEG alpha asymmetry could be compatible with amygdala-

<sup>61</sup> (Zotev, Yuan, et al., 2016)



based fMRI-NF.

<sup>62</sup> (Zich et al., 2015)

**Zich et al. 2015** A recent study by Zich et al.<sup>62</sup> showed that MI-based EEG-NF allowed subjects not only to generate stronger EEG response at the motor electrodes, but also that the BOLD activity observed in the sensorimotor regions in simultaneous fMRI recordings was higher during MI with EEG-NF as compared with MI training alone. Interestingly, the study revealed that the contralateral activity in EEG and fMRI were correlated while the laterality patterns were not. The finding that EEG and fMRI signatures of MI are not redundant suggests a potential for bimodal EEG-fMRI-NF. The authors stressed the need of conducting an exhaustive comparison of unimodal and bimodal neurofeedback in order to understand the specific contribution of each modality: “*only a systematic within-subject comparison using simultaneous EEG-fMRI data acquisition and providing fMRI-based feedback, EEG-based feedback and a hybrid feedback based on both modalities, would provide exact information about the validity of each recording modality*”.

These different studies illustrate the variety of motivations and strategies for combining EEG and fMRI for NF purpose.

### 3.5 TAXONOMY FOR EEG/FMRI NF STUDIES

From the previous literature review we just made, we propose a taxonomy (illustrated in [Figure 23](#)) of the different configurations for combining EEG and fMRI in NF studies and their corresponding motivations:

- **fMRI before/after EEG-NF:** Using fMRI before and after EEG-NF can be used to evaluate functional outcomes of the EEG-NF training. This can be done either at resting-state<sup>63</sup> or during a cognitive task such as an odd-ball task or a counting stroop task<sup>64</sup>.
- **EEG before/after fMRI-NF:** Similarly to the previous configuration, EEG could be used before and after fMRI-NF to evaluate functional outcomes of the fMRI-NF training. To our knowledge the use of this configuration has not been reported in the literature.
- **Passive fMRI during EEG-NF:** Recording passive fMRI during EEG-NF allows to evaluate and validate the EEG-NF protocol and to find BOLD correlates of the EEG-NF training. This configuration is the one that is most often encountered in the literature<sup>65</sup>. However it has the disadvantage that EEG must be cleaned online from MR and BCG artifact and that the quality of the online signal used for NF might be limited.
- **Passive EEG during fMRI-NF:** Recording passive EEG during fMRI-NF allows to evaluate the fMRI-NF protocol and to identify electrophysiological correlates of the fMRI-NF training<sup>66</sup>. In this configuration EEG artifact correction is performed offline. This approach can be used to explore EEG correlates of fMRI-NF that could be used as potential targets for EEG-NF or EEG-fMRI-NF.

<sup>63</sup> (Ros et al., 2013)

<sup>64</sup> (Lévesque, Beauregard, & Mensour, 2006)

<sup>65</sup> (Kinreich, Podlipsky, Intrator, et al., 2012; Kinreich, Podlipsky, Jamshy, et al., 2014; Cavazza et al., 2014; Zich et al., 2015; Shtark et al., 2015)

<sup>66</sup> (Zotev, Yuan, et al., 2016)

- **fMRI-informed EEG-NF:** The EEG-NF feature is enhanced by integrating fMRI information. The model is usually built from preliminary simultaneous EEG-fMRI data <sup>67</sup> and then purposed to be used for EEG-NF without fMRI.
- **EEG-informed fMRI-NF:** The fMRI-NF feature is enhanced by incorporating information from EEG as constraint or predictor. To our knowledge this has not been investigated in the literature. However, if this is to be done online, then at this price, one could rather do bimodal EEG-fMRI-NF instead as it would exploit the full information from the available EEG and fMRI data.
- **EEG-fMRI-NF:** Complementary EEG and fMRI features are used simultaneously to provide NF<sup>68</sup>. EEG has to be cleaned online from gradient and BCG artifacts. A bimodal EEG-fMRI-NF protocol can be considered as a merge of an EEG-NF and an fMRI-NF protocol which are mutually compatible or that are exploited in a way that makes them work efficiently together. Therefore taking in consideration the methodological comparison between EEG-NF and fMRI-NF in [Section 3.3](#) will be useful when designing a bimodal EEG-fMRI-NF protocol.
- **Alternating EEG-NF and fMRI-NF:** EEG-NF and fMRI-NF could be used alternatively in different trials, runs or sessions in order to combine the advantages of both approaches while avoiding the technical challenges of simultaneous acquisition. To our knowledge this has never been investigated.

<sup>67</sup> (Meir-Hasson, Kinreich, et al., 2013; Keynan et al., 2016; Cohen et al., 2016; Meir-Hasson, Keynan, et al., 2016)

<sup>68</sup> (Zotev, Phillips, et al., 2014a; Perronnet, Lécuyer, Lotte, et al., 2016)

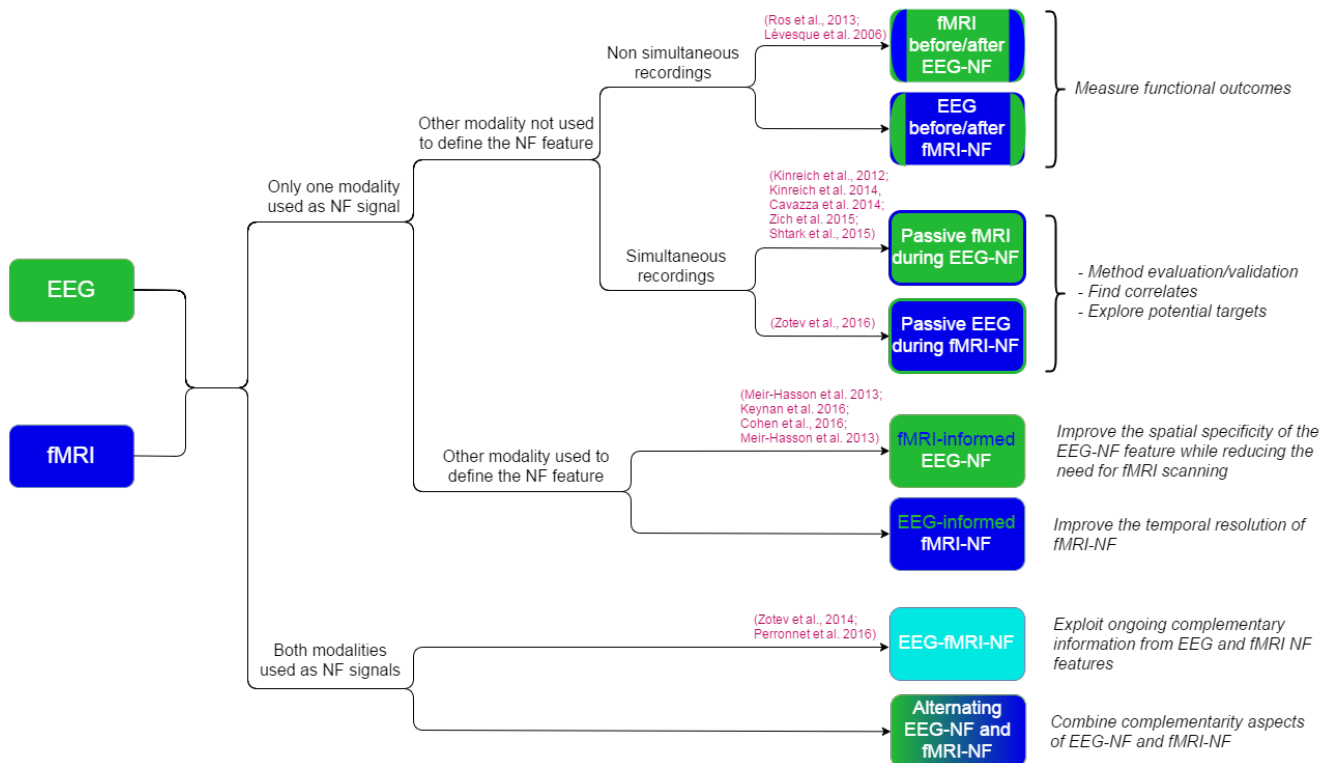


Figure 23 – Taxonomy of the possible use of EEG and fMRI in NF studies



## 3.6 CONCLUSION

In this chapter, we started by presenting general considerations about EEG and fMRI, namely when they should be acquired simultaneously, and how they are known to be related. Next we drew up a methodological comparison of EEG-NF and fMRI-NF in order to identify important aspects that differ between the two. Eventually, we reviewed exhaustively the existing NF studies that have combined EEG and fMRI and we proposed a taxonomy of the different configurations for combining EEG and fMRI in NF studies. Out of this taxonomy, we opt for focusing on bimodal EEG-fMRI-NF as it is particularly promising and mostly unexplored. From the methodological comparison of EEG-NF and fMRI-NF we presented in [Section 3.3](#), we should retain that task design, task duration and the choice of features are key aspects to consider when designing bimodal EEG-fMRI-NF protocols. Indeed the slow BOLD dynamics generally imposes longer task duration while the high temporal resolution and the transient nature of EEG can accommodate shorter tasks. Also the fact that there is a delay between both signals is something to consider. Of course, the solutions and compromises to these considerations will probably be highly task-dependent. Knowing how the EEG and fMRI features are supposed to complement each other, the key will then reside in how we integrate them in order to produce the feedback.

## HOW TO BUILD A REAL-TIME EEG-FMRI PLATFORM FOR BIMODAL NEUROFEEDBACK

---

*"Nothing complements a fast mind better than a slow tongue."*

— Mokokoma Mokhonoana

*Prelude* Before being able to conduct bimodal EEG-fMRI-NF experiments, one is faced with the challenge of setting up a real-time EEG-fMRI experimental platform. If EEG-fMRI has become a relatively accessible technique, turning it into a bimodal NF loop able to acquire EEG and fMRI simultaneously, clean them from artifacts, extract features and communicate feedback to the subject in real-time is no easy task. In this chapter, we describe how to build a real-time EEG-fMRI platform to conduct bimodal EEG-fMRI-NF experiments. The first part gives a general description of the different hardware, software and logical components of such a platform and outlines some of its critical aspects such as EEG-fMRI synchronization, and real-time performance. It is intended to be used as a guide for any laboratory who would like to setup their own real-time EEG-fMRI platform to perform bimodal EEG-fMRI-NF experiments. The second part gives an illustrative example of such a setup by presenting our own EEG-fMRI NF platform deployed at Neurinfo's facilities (CHU Pontchaillou, Rennes, France)<sup>1</sup>. and the specific implementation choices we made. The two experimental studies reported in this thesis (Chapter 5 and Chapter 6) were conducted with that platform.

<sup>1</sup> [Web link to Neurinfo](#)

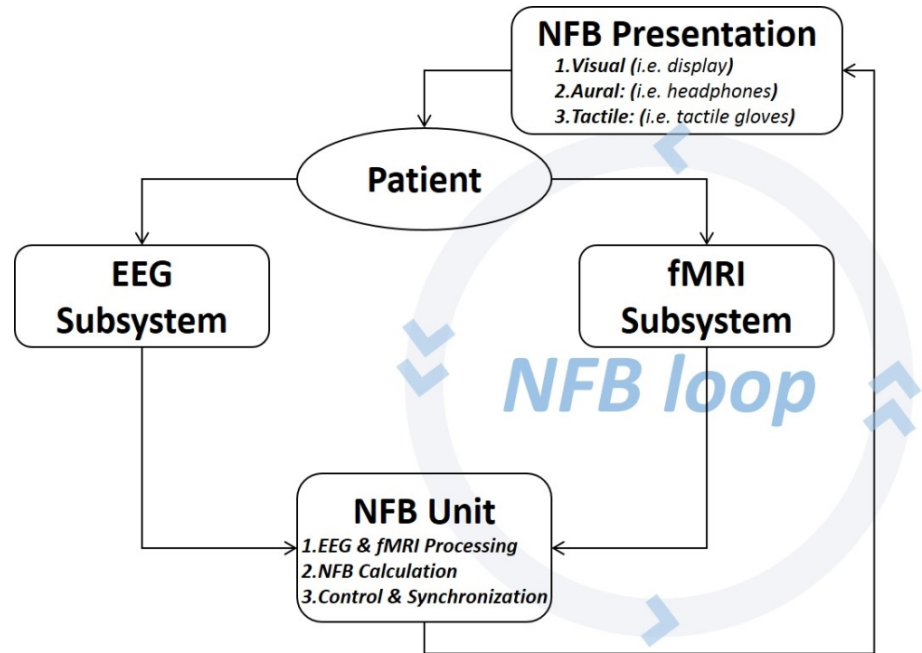
### 4.1 GENERAL DESCRIPTION OF A REAL-TIME EEG-FMRI PLATFORM FOR BIMODAL NEUROFEEDBACK

The abstract diagram of an EEG-fMRI NF platform is shown in [Figure 24](#). Such a platform must have a MR compatible EEG and an fMRI acquisition subsystems. Such subsystems are commercially available (see [Section 4.2.1](#) and [Section 4.2.2](#)) and must be acquired with all the necessary components that enable real-time acquisition.

The platform must also have an *NF Unit* that is capable of: 1) connecting and acquiring brain signals coming from each subsystem in real-time, 2) estimating the NF values from the brain signals, 3) handling the configuration and execution of the experimental protocol, 4) ensuring full synchronization, and 5) establishing continuous communication with the subject. The *NF Unit* is rather a logical unit that can be implemented by using different software modules deployed on one or several computers/servers on a network. The NF loop is closed with the communication device (i.e. display or headphones) which presents the NF to the subject.

The material of this chapter has been published in *Frontiers in Neuroprosthetics* as Mano, Marsel, Anatole Lécuyer, Elise Bannier, Lorraine Perronnet, Saman Noorzadeh, & Christian Barillot (2017). "How to build a hybrid neurofeedback platform combining EEG and fMRI." In: *Frontiers in Neuroscience* 11, p. 140. DOI: [10.3389/FNINS.2017.00140](#). The content of this chapter was mainly written by Marsel Mano, the engineer who implemented the platform.

Figure 24 – Abstract diagram of an EEG-fMRI NF platform. The patient/subject is an integral part of the NF loop. The brain activity generates neurosignals which are read with two subsystems then forwarded to the NF Unit. This unit estimates the NF and then show the results to the subject through the display, thus allowing self-regulation of the brain activity based on the real-time NF.



#### 4.1.1 NF Unit

The *NF Unit* should provide for each modality a real-time processing pipeline that handles signal acquisition and all the necessary methods/algorithms required for NF calculation. Furthermore, it should provide the flexibility of using multimodal or unimodal NF. The following section explains in detail the *NF Unit* components and their functions.

##### 4.1.1.1 The real-time EEG processing pipeline

The exact pipeline architecture and its implementation heavily depend on (i) the NF application(s), (ii) the selected EEG subsystem and (iii) the individual software engineering approach. A generic diagram of the real-time EEG processing pipeline for NF is shown in Figure 26. This diagram is not a rigid design architecture but rather a guideline for the real-time EEG processing flow. Furthermore, its components can be implemented as separate software modules and/or deployed on several processing hardware. The pipeline architecture promotes parallel computing of different signal processing steps, which improves real-time performance.

**Initialization.** The initialization information is usually obtained through a preliminary offline training or calibration session but it can also include a priori information based on empirical knowledge about EEG and/or NF. Depending on the experimental protocol and the selected signal processing techniques, the initialization might include spatial or temporal filters, band power estimates, signal components (i.e. principal or independent components), thresholds, features or NF targets.

**Updates.** Some NF protocols require online updates that complement or even substitute the initialization information throughout the duration of an experiment. These updates can be used to improve the EEG signal filtering, reeval-

uate the extracted features or change the NF targets.

**Pre-processing.** This step includes various preliminary signal processing operations (i.e. artifact and/or baseline removal, dipole extraction, etc.) that aim at improving the signal-to-noise ratio in EEG by minimizing the effect of local and/or global artifacts. Indeed, there are some distinctive EEG artifacts that occur only during simultaneous EEG and fMRI acquisition, which can severely compromise the quality of the EEG signals.

- The *gradient artifacts* are caused by the scanner's alternating gradient magnetic field during an MR acquisition. The very high amplitude and frequency variability range of the gradient magnetic field causes artifacts with amplitude often more than 100 times higher than normal EEG. During an fMRI acquisition the gradient artifact pattern within each Time of Repetition (TR) is ideally identical, which leads to very low inter-volume variability generated gradient artifacts. Hence, the EEG signals recorded within a TR window can be filtered by subtracting the artifact as a template<sup>2</sup>. The template is estimated by averaging a user defined number consecutive equally spaced intervals extracted in phase with the artifact generation. This method causes the randomly distributed EEG signals to be subtracted from the averaged curve, ideally leaving only the external influence of the scanner. For online applications, 5 to 15 shifting consecutive TRs are used to build the template. The template is then subtracted from the following TR window, thus leaving only the filtered EEG signal. It is worth noting that the EEG amplifiers should be very sensitive to small changes in EEG micro currents ( $\sim 0.1\mu V$ ), while also having a large dynamic amplitude range ( $\sim 50000\mu V$ ) in order to record both the EEG with appropriate resolution and the MR artifacts without saturation.
- The *ballistocardiogram (BCG)*<sup>3</sup> artifacts are caused by the micro currents generated by the pulsatile blood flow related movement of the EEG electrodes in the presence of the strong magnetic field of the scanner. Their occurrence is thus strongly related to the subject's heartbeat and their amplitude range is higher than that of normal EEG. The BCG artifacts correction method is very similar to that of gradient artifact. Heartbeats are recorded and detected on a specific channel, then for each channel a template is calculated using 10 to 20 pulse intervals. Finally, the template is removed from the following pulse interval<sup>4</sup>. Depending on the subject's heartbeat variability, the removal of the BCG artifacts can be very challenging and give less than optimal results during real-time applications.
- Another MR specific EEG artifact is caused by the scanner's internal ventilation system. The best way to avoid this artifact is to switch off the ventilation system for the duration the experiment, if this is allowed by the MR scanner manufacturer's guidelines. Otherwise, it can be removed as shown by Nierhaus *et al*<sup>5</sup>.

After removing all the MR specific artifacts, the real-time EEG signal processing is very similar to that of the standard EEG acquired outside of MR.

**Filtering.** This step includes more elaborate signal processing operations in the spatial and temporal domain. Commonly used spatial filtering techniques

<sup>2</sup> (Allen, Josephs, & Turner, 2000)

<sup>3</sup> It is also sometimes called the cardio-ballistic (CB) artifact.

<sup>4</sup> (Allen, Polizzi, et al., 1998)

<sup>5</sup> (Nierhaus et al., 2013)

<sup>6</sup> (Nunez & Westdorp, 1994; Lotte & Guan, 2011; Spencer et al., 1992)

<sup>7</sup> (Subasi & Gursoy, 2010; Pascual-Marqui et al., 2002)

include variants of surface Laplacian, common spatial patterns (CSP), or beamforming<sup>6</sup>. More elaborate techniques that aim at EEG source localization and signal decomposition use various independent component analysis (ICA) methods, inverse modeling, etc.<sup>7</sup>. Temporal filtering is usually based on the spectral analysis of the EEG signals. The majority of the filtering operations requires preliminary training to build subject specific filters and/or mathematical models in order to improve the real-time filtering results.

**Feature extraction.** After filtering, predefined EEG features are extracted. The choice of features highly depends on the NF protocol. The most common features are extracted from the signal power analysis in the frequency domain. The features are then used for the NF calculation (see Section 4.1.1.3).

#### 4.1.1.2 The real-time fMRI processing pipeline

The diagram of a generic real-time fMRI processing pipeline for NF is shown in Figure 27. Similar to EEG, the fMRI pipeline architecture also depends on the application, the fMRI subsystem and software engineering approach.

**Initialization.** The fMRI initialization information is spatial, temporal or a combination of the two. A typical spatial information is a brain region of interest (ROI) that can be selected a priori (i.e. from a brain atlas<sup>8</sup>), extracted offline from previous studies or by a functional localizer preceding the NF session. Examples of temporal information are the experimental design, the hemodynamic response function as well as various temporal filters used for time-series analysis. The fMRI activation mapping techniques yield both spatial and temporal information. There are also some protocols that would take into account different ROIs and their activation order based on dynamic causal models<sup>9</sup>. Initialization may also include information used for NF estimation like target BOLD contrast values or thresholds.

**Updates.** Real-time updates can be used to improve spatial filtering by using voxel clustering in neighboring areas or ROI shape and size changes, to improve temporal filtering (i.e. change online processing parameters or noise filters), or even to dynamically change the NF target(s).

**Pre-processing.** This step includes various mathematical transformations of the fMRI volume series including registration, motion estimation and correction, smoothing and slice-time correction. Their aim is to improve the fMRI signal-to-noise ratio and also to account for signal distortion due to subject's head motion<sup>10</sup>.

**Spatial Filtering.** Global brain activity is seldom the goal of NF. Instead, local activities on specific ROI(s) are usually monitored. Spatial filtering is used to extract the BOLD contrast values of the ROI voxels. This provides focus to the hemodynamic activity of the targeted brain region(s). Furthermore, it also reduces significantly the online computation demand for the following processing steps.

**Temporal Filtering.** The fMRI signal is affected by random noise, physical artifacts from the scanner, subject's motion artifacts or other physiological fluctuations<sup>11</sup>. The random noise can be removed by using Gaussian smoothing or temporal averaging; the scanner drift by linear trend removal, exponential moving average<sup>12</sup>, high-pass filtering, correlation analysis or generalized linear model (GLM) analysis. Global and local physiological fluctuations can also be

<sup>8</sup> (Robert W Cox, 1996; Tzourio-Mazoyer et al., 2002)

<sup>9</sup> (William D Penny et al., 2011; Stephan et al., 2008; Will D Penny et al., 2004)

<sup>10</sup> (Karl J Friston et al., 1995; Jenkinson et al., 2002)

<sup>11</sup> (Bianciardi et al., 2009)

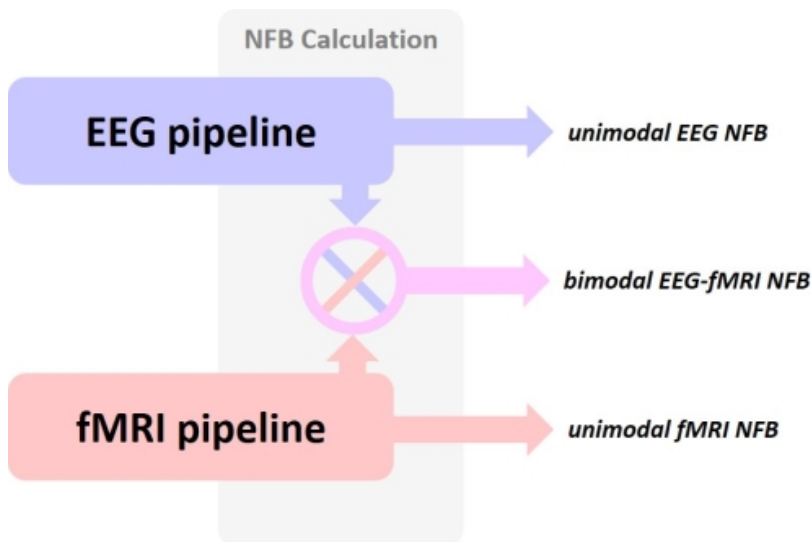
<sup>12</sup> (Koush, Zvyagintsev, et al., 2012; Cui, Bray, & Reiss, 2010; Roberts, 2000)

removed by subtracting background activity, temporal filtering, or again GLM analysis with confound predictors. Standard offline SPM<sup>13</sup> processing uses GLM analysis to linearly fit the whole fMRI time series into a set of specific time-series components pre-defined in the design matrix, followed by an activation mapping process based on statistical and spatial analysis of the GLM results. In real-time experiments, similar modeling like online windowed GLM<sup>14</sup> or the incremental GLM<sup>15</sup>, can be done by using the acquired signal instead of the whole fMRI time series. These methods perform a new GLM based analysis for each new fMRI volume. Other online fMRI methods use correlation analysis<sup>16</sup> or ICA<sup>17</sup>.

**Feature extraction.** Predefined features that will be used for NF estimation, are extracted from the filtered signal. The features, their extraction and how they are used for the NF estimation is determined by the experimental protocol. Commonly, these are statistical observations or inferences over the ROI(s), i.e. the maximum likelihood, z-score or p-values. Some protocols use more elaborated spatial analysis based features like sub-clustering.

#### 4.1.1.3 NF Calculation

The bimodal NF platform must be able to provide also unimodal EEG or fMRI NF by using only one modality (see Figure 25). In this section we will consider some of the most commonly used NF targets for both EEG and fMRI and how to estimate the NF values accordingly.



The NF target or goal is strictly related to the experimental or clinical protocol, hence they can be quite different and used in a variety of applications. Furthermore, they can be either constant or dynamically changed throughout the duration of the experimental session.

Generally, the NF value is estimated using the features extracted from their respective pipelines (see Figure 26 and Figure 27). In unimodal NF, only one set of features is considered, and NF can be estimated as a relative or normalized measure between the current value and the target (i.e. average percent signal change (APSC)<sup>18</sup>), a normalized statistic observations or a connectivity measure<sup>19</sup>. In the case of unimodal EEG-NF protocols that aim at the increase (de-

<sup>13</sup> [Web link to SPM](#)

<sup>14</sup> (Nakai et al., 2006a)

<sup>15</sup> (Bagarinao et al., 2003b)

<sup>16</sup> (Daniel Gembris et al., 2000; Robert W Cox, Jesmanowicz, & James S Hyde, 1995)

<sup>17</sup> (Esposito et al., 2003; Soldati, Vince D Calhoun, et al., 2013a; Soldati, Vince D Calhoun, et al., 2013b; Chiew, 2013)

Figure 25 – The EEG-fMRI platform should be able to provide both unimodal and bimodal NF based on the requirements of the NF protocol. Depending on the protocol, the output can be: a) unimodal EEG NF, b) unimodal fMRI NF, or c) bimodal EEG-fMRI NF. Switching between them could be done with a simple initial configuration.

<sup>18</sup> (Christopher deCharms et al., 2005; Hinds, Ghosh, Todd W Thompson, et al., 2011)

<sup>19</sup> (Koush, Maria Joao Rosa, Robineau, Heinen, Rieger, et al., 2013; Zilverstand et al., 2014b)



crease) of a certain neural oscillation at a specific frequency band and at a specific measuring or source location, the NF value can be the estimation of the relative change of the EEG spectral power related features. Similarly, for unimodal fMRI-NF protocols that aim the increase (decrease) of the hemodynamic activity at a specific ROI, the NF value can be estimated as the relative BOLD contrast change of the ROI voxels. Other fMRI-NF protocols aim to reach a certain signal change at specific brain regions or even spatial augmentation of these regions, in such cases the NF value can be estimated as the relative change of the ROI size<sup>20</sup>. More elaborate protocols rely on the effective connectivity of various ROIs<sup>koush2013connectivity</sup>.

<sup>20</sup> (S.-S. Yoo & Jolesz, 2002b)

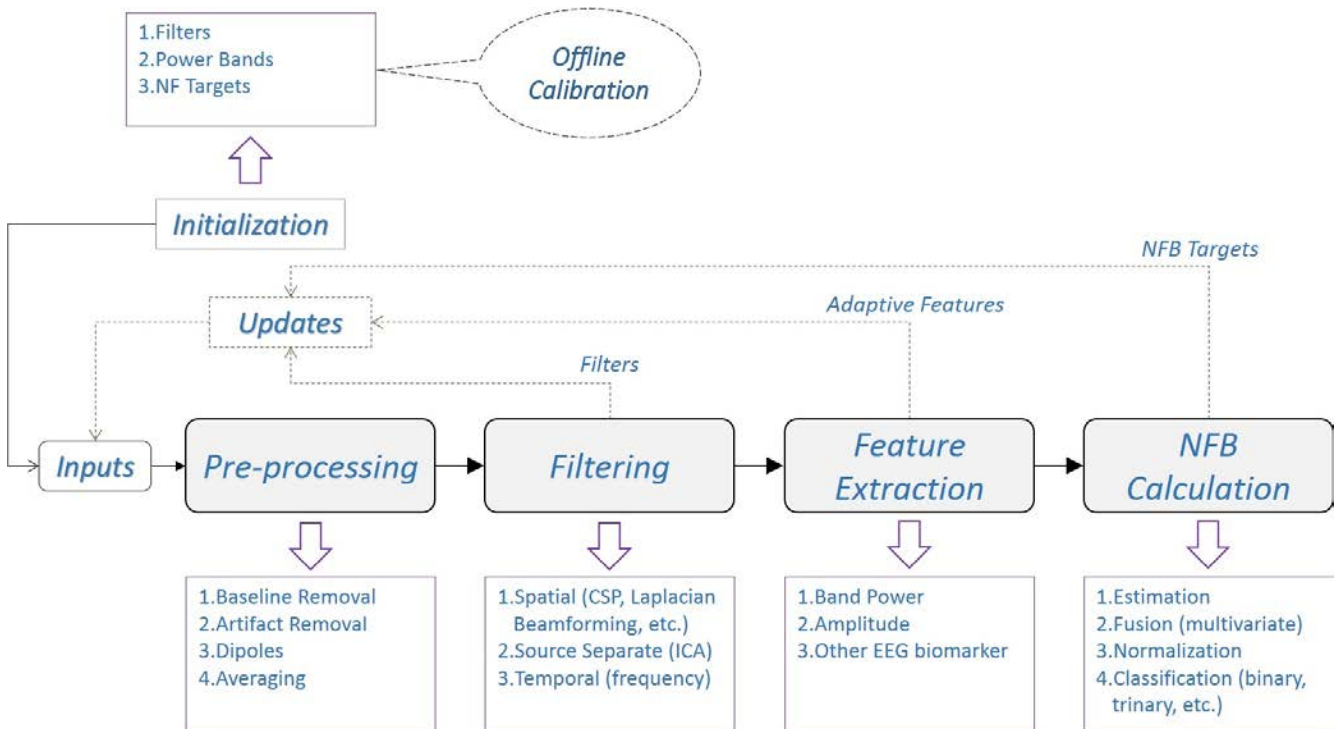


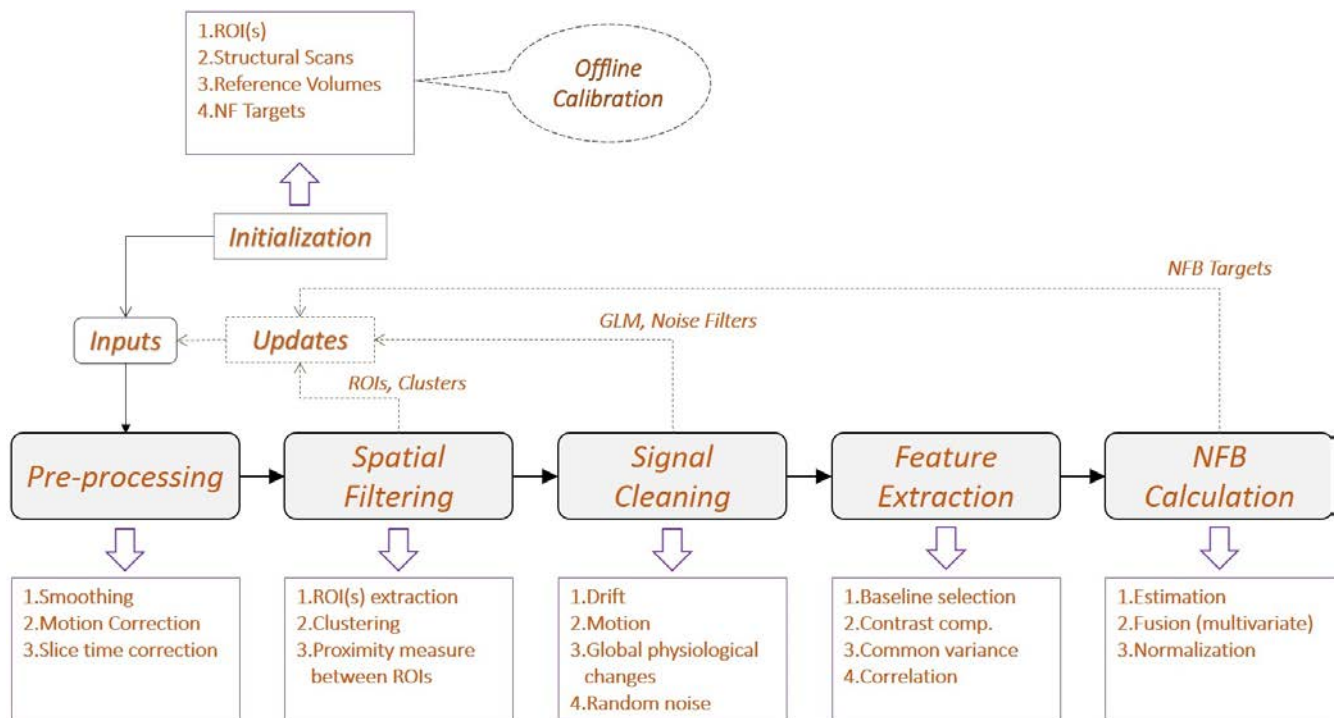
Figure 26 – Generic diagram of a real-time EEG processing pipeline for NF. The (optional) offline calibration, usually performed right before the real-time experiments, is used to obtain initialization information for real-time processing during NF sessions. At each stage of the pipeline there are few examples of signal processing methods, shown inside the purple boxes. The most common types of (optional) updates from each stage are also indicated with dashed lines.

In bimodal protocols, the calculation can be done separately for each modality and then the two NF values are: 1) given as a two dimensional vector [EEG-NF, fMRI-NF], or 2) combined together mathematically to give a one dimensional NF. Another possibility is to combine the features of each modality and use them as the input of a joint model that estimates unidimensional NF. There also exists the possibility to use a joint EEG-fMRI modeling approach to extract features from both EEG and fMRI signals simultaneously and then estimate NF based on the joint features.

#### 4.1.1.4 Synchronization

In bimodal NF, the simultaneous signals coming from each modality should reflect the brain activity occurring during the specific task indicated by the protocol with minimal delay or drift. This demands a high level of synchronization between both subsystems and the protocol. One strategy to achieve such synchronization is by dividing it into two different layers. The first layer shall be





responsible for the acquisition subsystems and the second one for the protocol (see Figure 29).

**Acquisition Synchronization (first layer).** The synchronization starts with the acquisition of the first fMRI scan. At the beginning of each acquisition, the MR platform sends a TTL pulse which marks the start of the online session and is registered as the time reference for all the following events. Immediately after the first pulse, the *NF Unit* starts collecting data from both subsystems using their respective callbacks. To provide real-time acquisition with virtually no delay, the callbacks' frequencies should be equal or higher than their respective subsystems' acquisition frequencies. For example, if EEG is digitized at 250Hz then the callbacks should be  $\geq 250\text{Hz}$ . Similarly, for fMRI acquisitions done at 1Hz the callbacks should be  $\geq 1\text{Hz}$ . For practical reasons both callbacks can be set to the highest acquisition frequency (i.e. EEG's). When the NF protocol is not highly time sensitive, the callback frequencies can be set lower than that of the EEG sub-system in order to allocate more computing time and power for data processing.

In this layer, both the EEG and the fMRI signals have the same starting time marked by the first TTL and are collected synchronously. To ensure continuous synchronization, periodic checks should be implemented in the *NF Unit*, such as buffer overflow, acquisition delays or drifts.

**Protocol Synchronization (second layer).** This layer is necessary for the synchronization of the NF calculation with the acquisition subsystems, and to guarantee that the NF shown to the subject corresponds to the brain activity that was measured following the experiment protocol.

In general, a NF experiment requires the subject to perform a specific mental task that changes the targeted brain activity. An example protocol would be to

Figure 27 – Generic diagram of a real-time fMRI processing pipeline for NF. The same principles shown for EEG in Figure 26 apply also here for fMRI. Furthermore, depending on the fMRI processing method, the spatial and temporal filtering are sometimes interchangeable.

repeat a specific task several times and separate those repetitions with some rest period where the subject can reduce his/her mental activity. Depending on the protocol, at the beginning of the experiment the task interval duration can be either fixed or variable, whilst the rest duration is usually fixed. Thus, the above protocol might be implemented in the two following ways:

- *Fixed task interval.* The task duration is fixed and well known before the experiment starts. For example, a task interval of 20s duration is followed by a rest interval of 20s duration and this block is repeated 10 to 15 times throughout the session.
- *Flexible task interval.* The task duration is variable (i.e.  $task \in [5, 60]s$ ) with respect to the NF result. This means that the task will continue until a certain NF target is achieved. Only when this target is achieved there will be a shift into a rest interval of known duration (i.e.  $rest \in [5, 40]s$ ). This procedure can be repeated 10 to 15 times throughout the session.

The NF value presented to the subject is updated periodically (i.e. every 500ms) by the Update NF callbacks. To ensure synchronization with both acquisitions, these callbacks start simultaneously with the EEG and fMRI callbacks, right after the first TTL pulse.

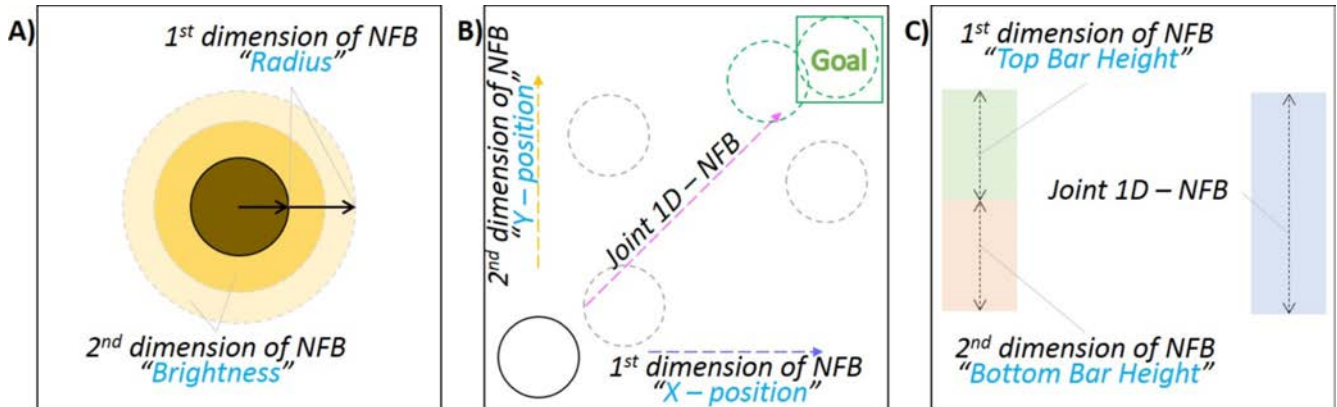
Switching between task and rest intervals is controlled by the protocol callbacks. To ensure synchronization, the protocol callbacks should be triggered simultaneously with their corresponding Update callback, at the end of each interval. This requires for the protocol callback period to be a multiple of the Update NF callback period. In the fixed task interval example above the protocol callback period is invariable (20s), thus the Update NF can be easily set at 500ms or 200ms. In contrast, the second example has a variable protocol callback period. In this case, for synchronization purposes, the protocol period duration will be set at the end of the Update NF callback that occurs right after the target is achieved.

#### 4.1.2 Neurofeedback Presentation

The choice of communication device depends on the type of NF that is being used. Screens or goggles are used for visual, headphones for aural and tactile devices for tactual NF presentations. All these devices must be MR compatible. In the present work we focus on visual presentations, but the same principles can be transferred to any type of presentation and sensing modalities.

The NF presentation needs careful consideration. Complex visualizations might not help the subject or even interfere with the mental task that is being performed during the experiment, instead, simplicity is commonly preferred. Depending on the NF dimensions, there can be various visualization approaches. For example, when a two dimensional visualization is needed, a "Sun" metaphor (see Figure 28(A)) can be used, where the diameter changes based on one of the values (i.e. fMRI) and the brightness changes based on the other (i.e. EEG). The bars in Figure 28(B) can be used to represent either one (left) or two (right) dimensional NF. The animation that uses the motion of the circle into the goal rectangle (see Figure 28(C)) is another two dimensional example. Furthermore, all these representations can be adapted for one dimensional scenarios, by keep-

ing one visualization feature constant and changing the other or simultaneously change both features proportionally to the NF value.



Finally, with the display, the NF loop introduced in Figure 24 is now closed; the NF is sent back to the subject who is now able to change its brain activity based on the received NF. Selecting and integrating together all the components introduced throughout this section is a challenging technical task. So far we have described the different parts of a bimodal platform and their functionality. In the following section we are going to introduce the real-time EEG-fMRI platform that we have built, which we use for bimodal EEG-fMRI-NF experiments.

#### 4.2 ILLUSTRATIVE EXAMPLE: BIMODAL NEUROFEEDBACK PLATFORM AT NEURINFO

In this section we are going to describe the real-time EEG-fMRI platform that we have developed and used in our NF experiments (see Figure 30).

##### 4.2.1 EEG subsystem

Our EEG subsystem is an MR compatible solution from Brain Products<sup>21</sup>. The EEG signals are acquired with a 64-channel cap, equipped with a drop-down electrocardiogram electrode for heart pulse measurements. The cap is connected with two 32-channel battery powered amplifiers via two electrical cables. During experiments, the battery and the amplifiers are placed inside the bore right behind the subject's head (see Figure 31). The amplifiers use fiber optic cables to send the digitized signal to a USB adapter and then to the *NF Unit*. The USB adapter is also connected with the 10 MHz clock of the MR scanner's gradient switching system, via the SyncBox. This connection is necessary for the phase synchronization needed for the MR artifact correction (see Section 4.1.1.1). Furthermore, the *NF Unit* communicates with the USB adapter via parallel connection. The parallel connection is used to send triggers that timely mark the EEG data, for online synchronization control and for offline data analysis. It is worth noting that the installation of the EEG system is done according to the manufacturer recommendation and that different manufacturers might provide different guidelines.

Figure 28 – Neurofeedback visualization examples: (A) Sun metaphor; the Sun's brightness is controlled from one NF value (EEG-NF) whilst the radius from the other value (fMRI-NF). Both the brightness and the radius can be proportionally changed when only one NF value is used. (B) Two variation of bar representations; the addition of the normalized NF values or any of them independently can control the height of the bar. (C) The NF values control the  $x$  and  $y$  positions of the disk. When only one NF value is used, both coordinates change proportionally.

<sup>21</sup> Web link to Brain Products

#### 4.2.2 fMRI subsystem

Our fMRI subsystem is a Nordic-Neurolab (NNL) solution with a Siemens 3T MR scanner. The MR imaging is performed on a Siemens MR scanner (Magnetom 3T Verio, Siemens Healthineers, Erlangen, Germany, VB17) with a 12-ch head coil allowing secure installation of the EEG cap and connection of the bundle to the amplifiers. The NNL hardware solution is used for visual stimulation and synchronization between the MR console and the *NF Unit*. Furthermore, our platform relies on its *Trigger Unit* for the TTL trigger that is sent during MR acquisition.

#### 4.2.3 NF Unit

All the software modules of the *NF Unit* are deployed on two PCs connected on the same LAN with the MR console. Generally, brain activity measurement systems have their corresponding commercial acquisition software. The usage of manufacturer's software in most cases is not only obligatory but also a convenient way to achieve optimal real-time signal acquisition.

##### 4.2.3.1 Acquiring real-time EEG data into the NF unit

In our experiments, *Recorder* is used before the experimental session to configure and setup the EEG acquisition (i.e. channel montages, impedance measurement). Then during the experiments it receives data from the USB adapter (see [Section 4.2.1](#)), pre-filters it and then forwards it for further real-time processing to *RecView* (or similar platforms like Matlab<sup>22</sup> or OpenViBE<sup>23</sup>) using the built-in TCP/IP based Remote Data Access (RDA) feature. Simultaneously, it saves the raw EEG data, the acquisition parameters and the setup information.

*RecView* has specific filters to remove the gradient and the BCG artifacts from the EEG signals and an additional RDA interface to transfer the data to other EEG processing software. The *NF Unit*, collects the data using Matlab (i.e. the *EEG object*), but we have also successfully tested the interface to send real-time EEG data to OpenViBE. The *EEG object* uses the TCP/UDP/IP Matlab Toolbox (pnet<sup>24</sup>) to communicate with *RecView*. The communication protocol is straightforward. At the beginning the RDA server sends the header with the "START" message and the setup information (i.e. number of channels, channel labels, sampling interval). Then, it continuously sends the EEG signals with their event markers, and finally the "STOP" message when the acquisition is stopped.

##### 4.2.3.2 Acquiring real-time fMRI data into the NF unit

The fMRI acquisition is done by certified MR technicians using the MR console software (see [Section 4.2.2](#)). Few sequences are used for imaging depending on the experimental protocols and EEG-fMRI acquisition safety guidelines. All the fMRI series are stored in the console's hard drive at the end of each acquisition.

To the best of our knowledge there does not exist a universal way to acquire real-time fMRI data from all types of scanners, thus it is highly recommended to contact directly the scanner vendor for any available options and/or configurations that could be used. Two ways for real-time fMRI acquisition that were

<sup>22</sup> [Web link to Matlab](#)

<sup>23</sup> [Web link to Openvibe](#)

<sup>24</sup> [Web link to pnet](#)

investigated and tested with our Siemens system, are described here.

- The scanner's software can be configured (using "*ideacmdtool*") to sequentially export single fMRI scans in "dicom" format at a predefined folder using FTP protocol. Then an acquisition software can monitor for new files (i.e. using *FileSystemWatcher*<sup>25</sup> library). In our observations we have noticed jitter in file export, which was more significant for sequences with TR below 2s.
- During an fMRI acquisition, each newly acquired volume's raw data is saved in the console's hard drive. To retrieve these raw data we use a TCP/IP buffer solution from FieldTrip<sup>26</sup>. In brief, this solution consists of an executable server, deployed into the scanner host, and a client running on the *NF Unit*. The server reads each new file and sends it to the client buffer that can be accessed from Matlab.

<sup>25</sup> [Web link to FileSystemWatcher library](#)

<sup>26</sup> [Web link to FieldTrip](#)

In our platform, the later method is employed to transfer the fMRI data over TCP/IP into the *NF Unit* (i.e. the *fMRI object*).

#### 4.2.3.3 Processing the EEG and fMRI data

The EEG signal processing is handled by the *EEG object*. This object is created at the beginning of each experiment and contains all the necessary members to store the signals, events, setup information together with the initialization information and updates. Furthermore, it has additional methods that perform various signal pre-processing, spatial and temporal filtering, and feature extraction (see [Section 4.1.1.1](#)). Similarly, the fMRI data is handled by the *fMRI object*.

In both objects, the extracted features are assigned to respective object's public members in order to be accessible by the *Joint NF*. The *Joint NF* contains calculation methods (i.e. percent signal change, z-Score) for either unimodal or bimodal scenarios. Furthermore, it is equipped with various configuration variables that simplify the optimization of the existing models and templates for the implementation of new ones.

The estimated NF values are used by *Visualize* (see [Figure 30](#)), which controls the display that communicates with the subject. *Visualize* has a collection of visual objects, developed in Psychtoolbox<sup>27</sup>, for: explaining the NF tasks (i.e. texts), showing cues and for animating the NF representation (i.e. 2D/3D objects). It also contains additional audio and visual objects used to communicate with the subject throughout the experiment for various instructions and notifications.

<sup>27</sup> [Web link to Psychtoolbox](#)

#### 4.2.3.4 Control and Synchronization

The last part of the system, the *NF Control*, is a class object developed in Matlab and Java<sup>28</sup>. This object is responsible for starting/stopping the experiment, controlling all other objects' behavior throughout the experiment, synchronization, and finally saving all the experiment data.

<sup>28</sup> [Web link to Java](#)

The *NF Control* constructor is initialized with protocol information (i.e. tasks or conditions, duration, repetition). The input can be given through a GUI for few standard protocols or with custom scripts for more specific ones. The *NF Control* initializes all the objects necessary for the experiment based on the requirements of the input protocol. Thus for unimodal NF only one of the *EEG*



and *fMRI objects* will be initialized, whereas for bimodal NF an *EEG objects* and an *fMRI objects* will be initialized with their respective initialization information. Furthermore, it also defines the method used in *Joint NF* and initializes the *Visualize* objects that are going to be used for presentation.

*NF Control* receives synchronization information from both subsystems, from the *Trigger Unit* of the fMRI subsystem and through *RecView* from the USB adaptor of the EEG subsystem (Figure 30). At each fMRI volume acquisition the scanner sends a TTL signal from the *Trigger Unit*. When *NF Control* receives the first TTL signal, it starts the acquisition callback function(s) (see Figure 29). After the 'Begin' period which is predefined by the protocol, it starts the rest of the callback functions and when the session is over, it stops all the callback functions and saves the data.

Figure 29 – The system synchronization is divided into two layers. The first layer synchronizes the acquisition subsystems by using EEG and fMRI callbacks, and issues periodical controls for de-synchronization, all independently from the NF protocol. The second layer relies on the synchronization of the first layer, and uses protocol and update NF callbacks to ensure the synchronization of the protocol with the acquisition subsystems, the NF calculation and visualization. It uses protocol, update and synchronization controls to detect de-synchronization.

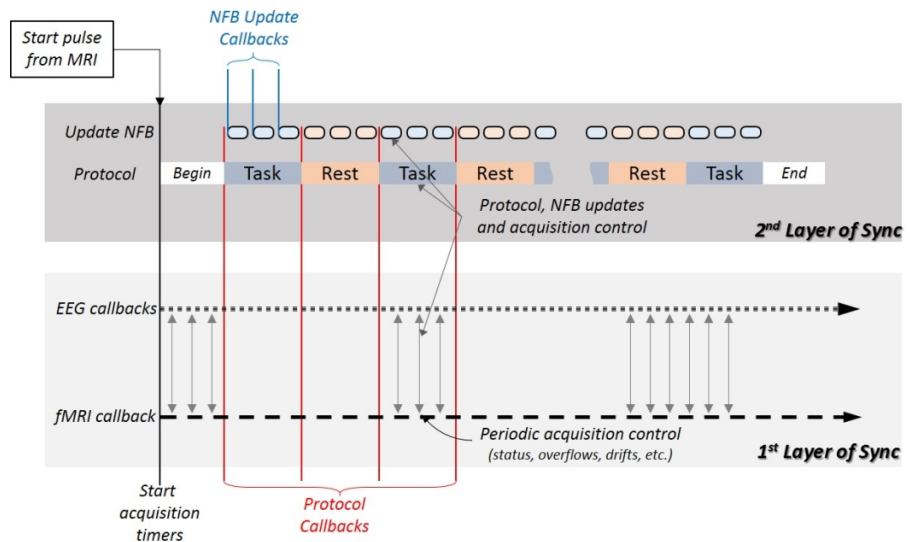
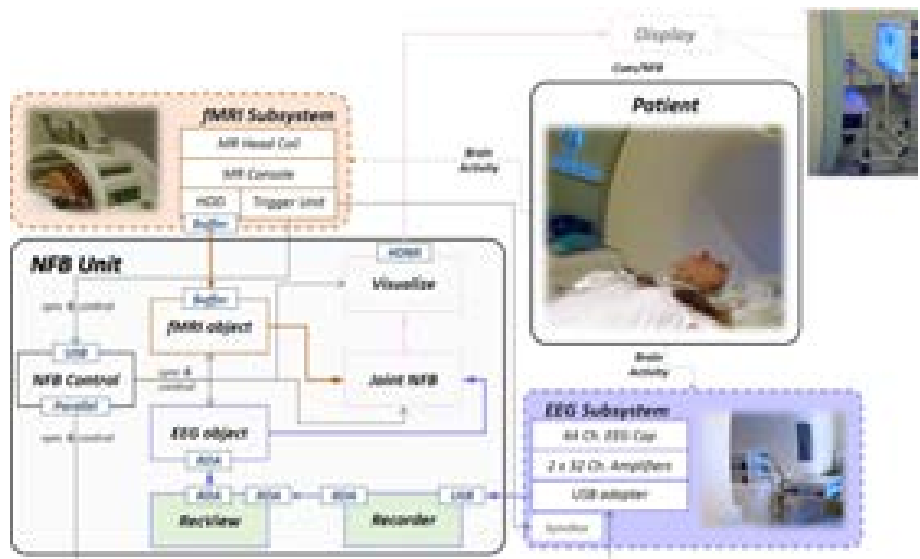


Figure 30 – The detailed diagram of the real-time EEG-fMRI bimodal NF platform at Neurinfo. The EEG (in purple) and fMRI (in orange) signal flow includes the respective subsystems and software modules inside the *NF Unit*. Both pipelines merge at *Joint NF*, which calculates NF and then sends the results to *Visualize*. *Recorder* and *Recview* are the only commercial software, the rest of the *NF Unit* modules are developed in-house (Matlab/C/C++/Java). The *NF Control* exchanges synchronization and control information with the rest of the hardware and software components.



The EEG subsystem records scanner's TTL signals to correct the MR artifact

in *RecView*, thus the EEG data coming from *RecView* already contains the fMRI volume markers. Furthermore, the *NF Control* uses a parallel connection to the USB adapter to send markers to the EEG signals at each protocol callback. These protocol markers are then resent together with the rest of the EEG data to the *EEG object*, with a pre-measured delay that in our implementation is 38-40ms.

All the EEG markers including protocol markers and TTL pulses coming from the scanner are used to periodically control for delays in both layers of synchronization (see [Section 4.1.1.4](#)). The TTL markers are used to check for fMRI acquisition delays or jitter. The same markers, which are recorded on the EEG data for MR correction (see [Section 4.2.1](#)), are used to check for delays in the EEG acquisition and that both subsystems are acquiring data synchronously. The protocol callback markers are used to control the synchronization of the NF updates, and to make sure that the data that is used for the NF update was acquired while the subject was performing the task required by the protocol. When a de-synchronization occurs, the *NF Control* reports it and tries to re-synchronize. If the re-synchronization attempt is unsuccessful the current session is stopped and the stack data is saved.

#### 4.2.4 Display

The communication with the subject lying on the back in the MR bore, is done via an LCD Screen and a rear-facing mirror fixed on the top of the head coil (see [Figure 31](#)(A) and (B)). The 32-inch LCD screen is part of the NNL solution (see [Section 4.2.2](#)); it has a 60Hz input refresh rate and is connected with the *NF Unit* via fiber optic using a DVI to fiber optic converter and powered by an MR compatible power supply.

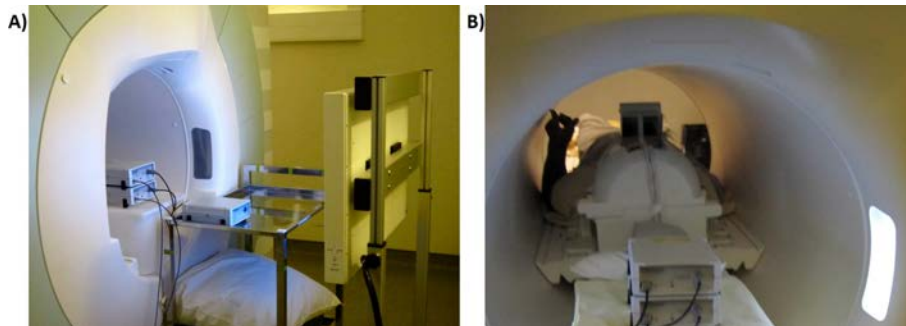


Figure 31 – System installation pictures. (A) Placement of amplifiers, battery and LCD display. (B) Placement of the rear view mirror on the top of the head coil.

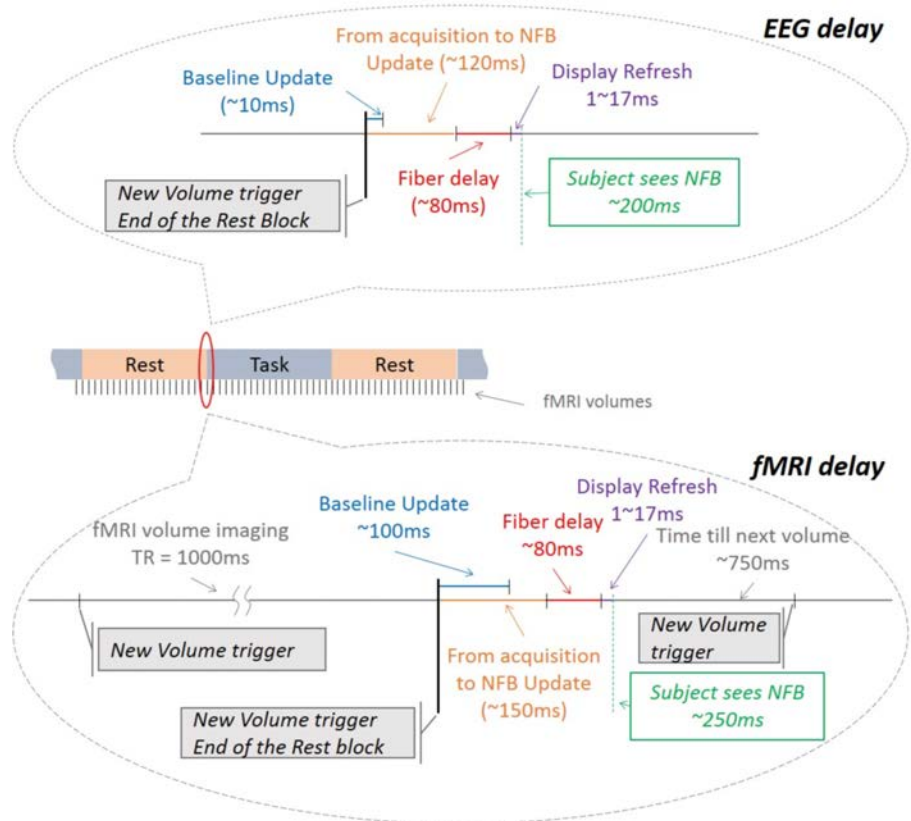
#### 4.2.5 Real-time performance

Real-time tests and experiments have shown very good performance with various pre-processing, filtering, NF calculation and visualization methods. The entire fMRI process from acquisition to NF update takes  $\approx 150$ ms, well below the TR of regular EPI sequences (see [Figure 32](#)). The NF visualization is very fast (1-2ms) and it is done within one screen refresh (i.e. 16,7ms for a 60Hz screen). The screen inside the scanner is connected to the *NF Unit* via optic fiber which minimizes the delay at 80ms (according to the manufacturer's recommendation). Thus the fMRI NF is shown to the subject with a total delay of



$\approx 250$ ms. For EEG this delay is  $\approx 200$ ms.

Figure 32 – Timeline description of all the hardware and software delays for EEG and fMRI. The values include the manufacturer's descriptions and/or the results of the measurements performed in our lab.



Furthermore, at the end of every rest interval the baseline is updated in both EEG and fMRI. These updates take on average less than 20ms for EEG and less than 100ms for fMRI, which is lower than their respective NF update cycles. These delays do not affect each other because: 1) the model updates are done in parallel with the processing of the respective signals and, 2) the EEG and the fMRI pipelines work in parallel.

#### 4.2.6 Preparing the subject for EEG-fMRI scanning

At the beginning of each EEG/fMRI experiment, outside the MR room, a 64 channel EEG cap with adequate size was fitted on the subject's head and conductive gel was applied until electrode impedances were below  $10k\Omega$ . Next, the recording configuration was set up and tested until the acquisition was working properly. Then, the system was disconnected and placed inside the scanner room (see Figure 33). Meanwhile the subject was also put inside the scanner. At this stage, a secondary test was done to control whether the acquisition was still working and that electrodes' impedances had not changed due to the subjects' movements. This procedure was repeated until the acquisition was working, the impedances were within range, and the subject was ready for MRI scanning.

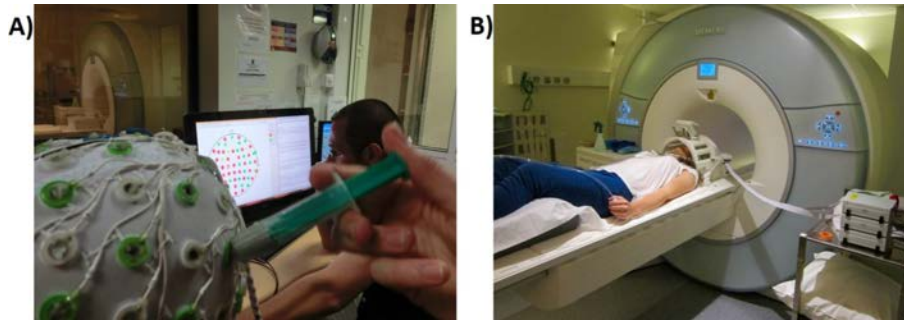


Figure 33 – Subject’s preparation and subsystem installation before the experiment. (A) EEG subsystem installation and impedance check outside the MR room, (B) installation of the MR coil and EEG impedance recheck.

### 4.3 DISCUSSION

Multimodal brain activity monitoring has not only the potential to provide a better understanding of the brain functionality but also to improve NF. But, the simultaneous acquisition and processing of two or more types of neurosignals in real-time can be very challenging. From a technological and safety point of view the challenges of the simultaneous EEG and fMRI acquisition have been addressed before<sup>29</sup>, instead the focus of our present work is on the utilization of the existing EEG and fMRI subsystems in order to build a platform that is capable to perform real-time bimodal NF experiments.

The design and implementation of a real-time EEG-fMRI platform that is capable of acquiring signals, processing, modeling, estimating NF and then communicating with the subjects in real-time has to be carefully considered. Two very different hardware and software subsystems need to work together, fully synchronized and without compromising real-time performance. Throughout this chapter we have particularly emphasized the need for real-time performance and synchronization. We have chosen a two-layer synchronization approach in order to simplify the implementation and to allow flexibility to use the platform for both unimodal and bimodal NF protocols.

Our platform relies on network communication and its modular architecture offers the possibility of distributing the system on different processing units. Inevitably, slow network connection or network congestion might introduce delays in data transmission and for highly time sensitive protocols networking and data transmission aspects need careful consideration. In our implementation, the networking delays, which include the signal acquisition and processing delays (see Figure 32), rely mainly on the manufacturers’ guidelines. Few non-exhaustive tests that we have conducted in general confirmed the manufacturers’ claims.

A similar platform for bimodal EEG and fMRI NF was reported by Zotev et al.<sup>30</sup>. Beyond the choice of subsystem’ manufacturers, operating environment and custom software packages, their platform architecture, components and functionality with respect to the NF process flow, are very similar to the platform introduced here.

A very important future goal in the field of bimodal brain activity monitoring and multimodal NF is the development of good coupling models. Such models have the potential to maximize the information that is extracted from each modality and put it in the context of better understanding the underlying phys-

<sup>29</sup> (Neuner et al., 2014; Ullsperger & Debener, 2010)

<sup>30</sup> (Zotev, Phillips, et al., 2014b)

iological brain activities. Our platform provides fully synchronized simultaneous acquisition and offers easy integration of both modalities at all processing stages. The EEG and fMRI objects provide public members to store the results of each processing step that can be accessed and used in future implementations of coupling models. Furthermore, the initialization information can be customized to input specific modeling information that might be needed for future developments.

There also exist applications that might require additional non neural bio-signals that indirectly represent an estimation of brain activity. For example the galvanic skin response can be used to monitor the stress level of a NF subject. Furthermore, auxiliary sensors can be used to provide additional information for NF or even for monitoring other aspects of the experiments. For example electromyography can be used to monitor the subject's muscular activity when and if a NF protocol requires it. Motion cameras or sensors can be used to better measure the subject's head motion, which currently is estimated by a least squares approach based on the 6 parameter (rigid body) spatial transformation<sup>31</sup>.

<sup>31</sup> (Karl J Friston et al., 1995)

The addition of any new real-time signals needs to be carefully considered in terms of synchronization and computing power. In the current state of the platform the synchronization is solved by using two hierarchical layers. A major advantage of this approach is the possibility to synchronize additional signals with minimum effort, by using the existing layers' infrastructure for acquisition and protocol synchronization. On the other hand, the additional computational power need to be estimated carefully before choosing the hardware/-software configuration. In our implementation, the real-time fMRI processing is the most computationally demanding. With the current hardware configuration there are limitations in the analysis that can be performed in real-time. In the near future, we intend to use a GPU cluster and take advantage of its parallel processing power to perform standard GLM and ICA analysis on full volume fMRI series, or even recent more advanced local multivariate detection methods such as a contrario<sup>32</sup>, in real-time.

<sup>32</sup> (Maumet et al., 2016)

As we showed in this section, there is still remaining challenges and difficulties for improving real-time multimodal brain activity measurement but although not yet very common, the increasing research interest will provide a wide range of applications for multimodal brain research, and many more similar or even more capable platforms should emerge in the following years.

#### 4.4 CONCLUSION

In this chapter, we described a general method for building a real-time EEG-fMRI platform for bimodal NF experiments. Our goal was to share our experience in order to help other researchers build fast and robust platforms, and also provide some minimal technical requirements or features to look for in future commercial systems. Based on those guidelines, we have implemented our own real-time EEG-fMRI platform for bimodal NF. This platform has served for the two experimental studies presented in this dissertation and will continue to be improved and used for experimental and clinical studies.

## UNIMODAL VERSUS BIMODAL EEG-FMRI NEUROFEEDBACK OF A MOTOR-IMAGERY TASK

---

"♪ ♪ ♫ ... One is the loneliest number that you'll ever do.  
Two ... can be as bad as one, it's the loneliest number since the  
number one.

— Harry Nilsson

*Prelude* Neurofeedback approaches usually rely on a single brain imaging modality such as EEG or fMRI which present inherent limitations such as low spatial specificity for EEG and low temporal resolution for fMRI. Recently the feasibility of simultaneous EEG-NF and fMRI-NF (which we refer to as bimodal EEG-fMRI-NF) was demonstrated. It was hypothesized that bimodal EEG-fMRI-NF could be more efficient than EEG-NF or fMRI-NF performed alone. Yet this hypothesis has never been tested and it is therefore not clear what are the advantages of this new approach. The goal of the work presented in this chapter is to evaluate the added value of bimodal EEG-fMRI-NF as compared to unimodal EEG-NF and fMRI-NF. To this end, we introduce a motor imagery-based bimodal EEG-fMRI-NF protocol and compare the activation levels of the MI-related EEG and fMRI patterns that participants were able to reach in three different NF conditions: EEG-NF, fMRI-NF and EEG-fMRI-NF.

### 5.1 METHODS

#### 5.1.1 Experimental procedure

The study was conducted at the Neurinfo platform (CHU Pontchaillou, Rennes France) and was approved by the Institutional Review Board. Ten right-handed NF-naïve healthy volunteers with no prior MI-NF experience (mean age: 28 +/- 5.7 years, 2 females) participated in the study. Throughout the whole experiment, the participants were lying down in the MR bore and wearing a 64 channel MR-compatible EEG cap.

##### 5.1.1.1 Instructions

After signing an informed consent form describing the MR environment, the participants were verbally informed about the goal of the study and of the protocol. They were instructed that during the NF runs, they would be presented with a ball moving in one or two dimensions according to the activity in their motor regions measured with EEG and/or fMRI. They were told that they would have to bring the ball closer to the square in the top-right corner (see [Figure 45](#)) by imagining that they were moving their right-hand. This instruction was reminded in written form on the screen at the beginning of each NF run. More specifically we explained that they would need to perform kinesthetic motor

The material of this chapter was published in *Frontiers in Human Neuroscience* as Perrotet, Lorraine, Anatole Lécuyer, Marsel Mano, Elise Bannier, Fabien Lotte, Maureen Clerc, & Christian Barillot (2017). "Unimodal Versus Bimodal EEG-fMRI Neurofeedback of a Motor Imagery Task." In: *Frontiers in Human Neuroscience* 11, p. 193. DOI: [10.3389/fnhum.2017.00193](https://doi.org/10.3389/fnhum.2017.00193).

imagery (kMI) of their right-hand in order to control the ball. Kinesthetic motor imagery was defined as trying to feel the sensation of the motion rather than visualizing it. We suggested different MI strategies to the participants such as imagining hand clenching or finger tapping, imagining that they were playing the piano, or imagining a hand motion that they were used to perform. They were encouraged to try several strategies and stick with the one that worked best. More specifically, they were informed that the EEG and fMRI measures that would be used to display the feedback were laterality indices. This implied that they would have to maximize the activity in their right-hand region while minimizing it in the left-hand region in order to reach the NF target (get the ball closer to the upper-right square), so that bimanual imagination would not enable them to control the feedback. Participants were informed about the nature of EEG and fMRI signal, and specifically about the 4-6 seconds delay of the hemodynamic response. These general instructions were given verbally at the beginning of the experiment and reminded later if the participant asked for it. Before each NF run, the participants received verbal notice about which dimension/s (horizontal and/or vertical) was/were going to be active in the upcoming run. Participants were asked not to move at all, especially during the course of a run. Video monitoring of the inside of the MR tube allowed to check for whole-body movements of the participant.

The experimental protocol consisted of six EEG-fMRI runs employing a block-design alternating 20s of rest and 20s of task (see [Figure 45](#)):

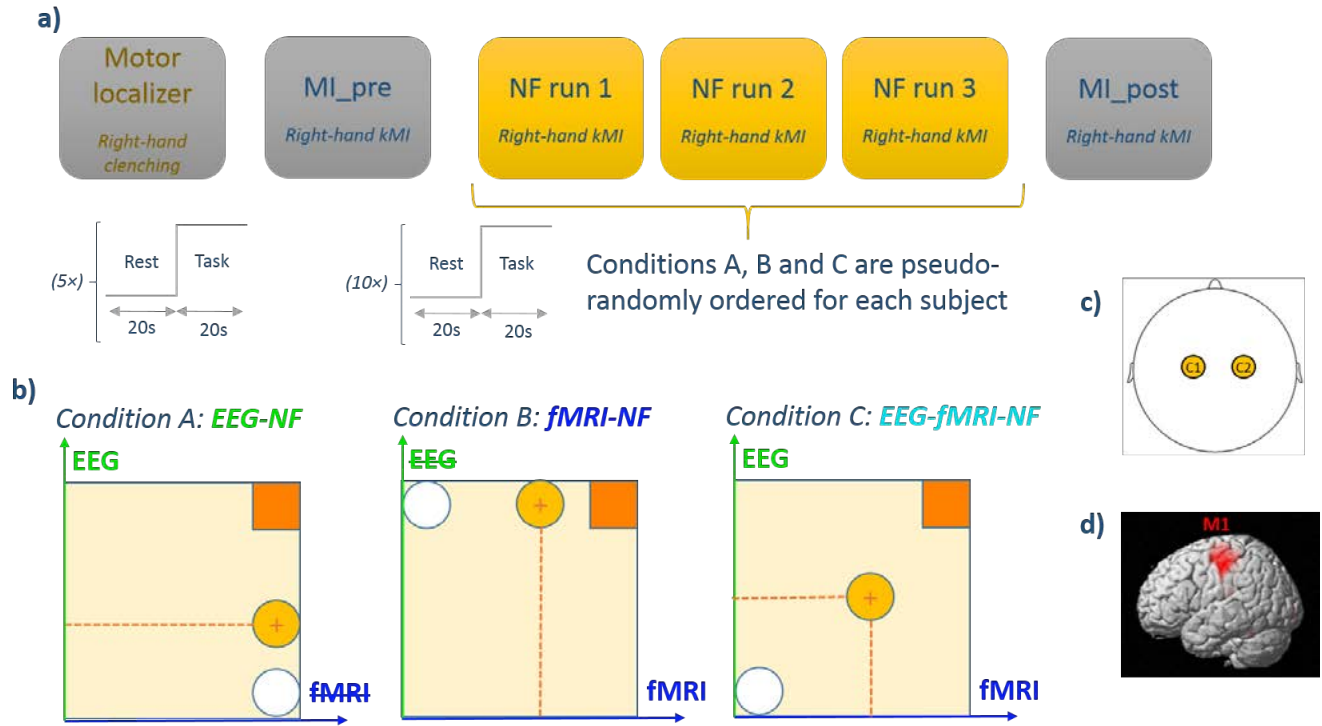
1. a motor localizer run (*MLOC*) lasting 5min 20s
2. a preliminary motor-imagery run without NF (*MI\_pre*) lasting 3min 20s
3. three NF runs (*NF1*, *NF2*, *NF3*) lasting 6min 40s each and corresponding to three different feedback modality conditions (A: *EEG-NF*; B: *fMRI-NF*; C: *EEG-fMRI-NF*) whose order was counter-balanced across participants
4. and a final motor-imagery run without NF (*MI\_post*) lasting 3min 20s.

During rest, the screen displayed a white cross and participants were asked to concentrate on the cross and not on the passed or upcoming task. During task, the screen displayed a cue (“move right”/“imagine right”) as well as the NF ball and target during NF runs. At the end of the experiment, the participants were asked to fill out a questionnaire about their performance, motivation, fatigue, interest, difficulty in performing the NF tasks and specific questions about the bimodal *EEG-fMRI-NF* run. For two participants out of the ten, *MI\_pre* and *MI\_post* could not be acquired due to technical reasons.

During the active blocks of the motor localizer run the participants were asked to perform right-hand clenching at 1Hz. Immediately at the end of this run, the corresponding activation map computed by the MR vendor console (eva\_series GLM file) was used to define a ROI mask over the left primary motor cortex (*M1*) as a  $9 \times 9 \times 3$  voxel ( $18 \times 18 \times 12$  mm<sup>3</sup>) cube centered on the left *M1* voxel with the maximum t-value. The right *M1* ROI was defined by taking the left *M1* ROI symmetric in the sagittal plane. These ROIs were used later during the NF runs for computing the fMRI NF feature.

During the active blocks of the *MI\_pre* run, participants were asked to perform kinesthetic motor imagery of their right-hand. They were suggested to imagine





their right-hand clenching by trying to recall the sensation they had in their right hand when actually executing the movement in the previous run. The goal of this run was for the participants to practice motor imagery. The data from this run was also intended to be used later for assessing the NF learning effect if any.

During the active blocks of the NF runs ( $NF_1$ ,  $NF_2$ ,  $NF_3$ ), the screen displayed a white ball moving in the vertical (condition A), or horizontal (condition B) or both dimensions (condition C) and a square in the top-right corner of the screen representing the target to reach. The same feedback metaphor was used during unimodal and bimodal feedback in order to prevent the occurrence of a confounding effect from the feedback metaphor. The participants were instructed to bring the ball closer to the square by performing kinesthetic motor imagery of their right hand. The ball abscissa depicted a BOLD laterality index (signal difference) between the left and right M1 ROI<sup>1</sup> and was updated every repetition time ( $TR=2s$ ). In a similar fashion, the ball ordinate depicted the laterality index (see Section 6.2.3) between electrodes C1 and C2 in the  $\mu$  (8-12Hz) band and was updated every 250 ms. Figure 45 illustrates the experimental protocol.

Eventually, during the active blocks of the  $MI_{post}$  run, participants were asked to perform motor imagery with the strategy that they found out worked best throughout the NF runs. This run was intended to be used as a transfer run which purpose is that the participant learns to self-regulate in absence of any NF. The data was also intended to be used for assessing the NF learning effect between  $MI_{pre}$  and  $MI_{post}$ .

Figure 34 – Experimental procedure: a) The experimental protocol consisted of 6 EEG-fMRI runs: a motor localizer run, a motor imagery run without NF, three NF runs with different NF conditions, and a post motor imagery run without NF. Each run consisted of a block design with 20s blocks. b) Feedback display for each experimental conditions. Feedback was represented by a ball moving in 1 dimension (condition A and B) or 2 dimensions (condition C). The white circle represents the starting ball position and the yellow circle depicts a possible ball position. Participants are instructed to get the ball closer to the square in the upper-right by performing kinesthetic motor imagery. c) For the EEG feature, we used a laterality index between C1 and C2. d) For the fMRI feature we used a laterality index between left M1 and right M1.

<sup>1</sup> (Chiew, LaConte, & Graham, 2012)

### 5.1.2 Data acquisition/technical setup

EEG and fMRI data were simultaneously acquired with a 64-channel MR-compatible EEG solution from Brain Products (Brain Products GmbH, Gilching, Germany) and a 3T Verio Siemens scanner (VB17) with a 12channel head coil. Foam pads were used to restrict head motion. EEG data was sampled at 5kHz with FCz as the reference electrode and AFz as the ground electrode. fMRI acquisitions were performed using echo-planar imaging (EPI) with the following parameters: repetition time (TR) / echo time (TE) = 2000/23ms,  $210 \times 210\text{mm}^2$  FOV, voxel size =  $2 \times 2 \times 4\text{mm}^3$ , matrix size =  $105 \times 105$ , 32 slices, flip angle =  $90^\circ$ . Visual instructions and feedback were transmitted using the NordicNeuroLab hardware and presented to the participant via an LCD screen and a rear-facing mirror fixed on the coil.

As a structural reference for the fMRI analysis, a high resolution 3D T1 MPRAGE sequence was acquired with the following parameters: TR / TI / TE = 1900 / 900 / 2.26ms, GRAPPA 2,  $256 \times 256\text{mm}^2$  FOV and 176 slabs,  $1 \times 1 \times 1\text{mm}^3$  voxel size, flip angle =  $9^\circ$ .

<sup>2</sup> (Mano et al., 2017)

Our multimodal EEG/fMRI-NF system<sup>2</sup> integrates EEG and fMRI data streams via a TCP/IP socket. The EEG data is pre-processed with BrainVision Recview (Brain Products GmbH, Gilching, Germany) software for gradient and ballistocardiogram (BCG) artifact correction (see Section 6.2.3) and sent to Matlab (The MathWorks, Inc., Natick, Massachusetts, United States) for further processing. The fMRI data is pre-processed online for slice-time correction and motion correction with custom Matlab code adapted from SPM8 (FIL, Wellcome Trust Centre for Neuroimaging, UCL, London, UK). EEG and fMRI NF features are then computed and translated as feedback (vertical and horizontal displacement of the ball) with Psychtoolbox<sup>3</sup>. The fMRI NF dimension is updated every TR (2s, 0.5Hz), while the EEG NF dimension is updated at 8Hz. Figure 35 illustrates the real-time multimodal EEG/fMRI-NF setup.

<sup>3</sup> (Kleiner et al., 2007)

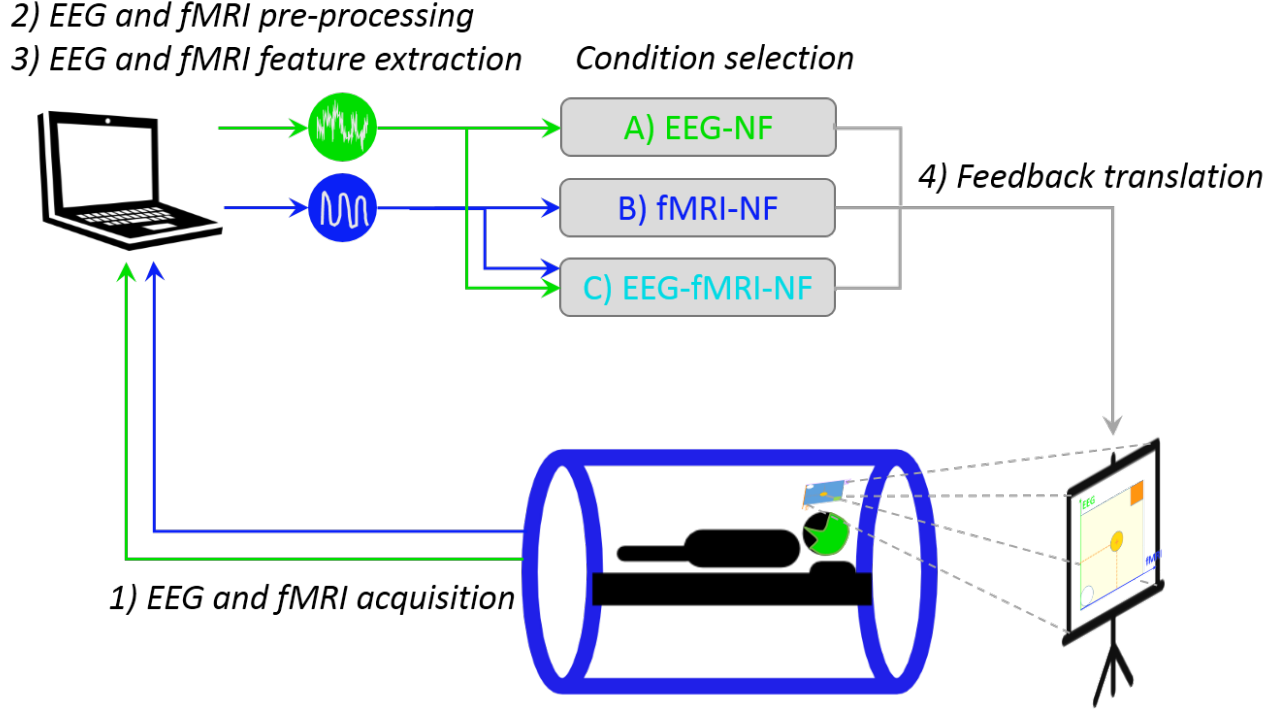
### 5.1.3 Real-time data processing

Online gradient artifact correction and BCG correction of the EEG data were done in BrainVision Recview (Brain Products GmbH, Gilching, Germany) software. The gradient artifact correction in Recview is based on the average artifact subtraction method<sup>4</sup>. We used an artifact subtraction template of 2000ms and 4 templates for template drift correction. The data was then down-sampled to 200Hz and low pass filtered at 50 Hz (48 db slope) with a Butterworth filter. The data were subsequently corrected for BCG artifact<sup>5</sup>. The pulse model was searched in the first 15 seconds of the data. The pulse detection was based on a moving template matching approach with minimal pulse period of 800ms, minimum correlation threshold of 0.7, and amplitude ratio range from 0.6 to 1.2 relative to the pulse model. For pulse correction, a moving template was computed by averaging the 10 previously detected pulses, and the correction was done on a window length of [-100ms, 700ms] relatively to the R-peak. This corrected data was then sent to Matlab. Every 125ms the EEG laterality index

<sup>4</sup> (Allen, Josephs, & Turner, 2000)

<sup>5</sup> (Allen, Polizzi, et al., 1998)





was computed according to the following equation:

$$eeg_{lat}(t) = \frac{nLbp(t) - nRbp(t)}{nLbp(t) + nRbp(t)} \quad (1)$$

Where  $nLbp(t)$  (respectively  $nRbp(t)$ ) is the normalized band power in the  $\mu$  (8-12 Hz) band at the left motor electrode C1 (respectively at the right motor electrode C2) at time  $t$ . We defined  $nLbp$  and  $nRbp$  so that they would be higher than 1 when a desynchronization happened at the corresponding electrode:

$$nLbp(t) = \frac{Lbp(previous\_rest)}{Lbp(t)} \quad (2)$$

$$nRbp(t) = \frac{Rbp(previous\_rest)}{Rbp(t)} \quad (3)$$

Where  $Lbp(t)$  (respectively  $Rbp(t)$ ) is the band power in the  $\mu$  band computed at a bipolar derivation around C1 (respectively C2)<sup>6</sup> on a 2s window and  $Lbp(previous\_rest)$  (respectively  $Rbp(previous\_rest)$ ) is the left baseline (respectively the right baseline) obtained by averaging the  $Lbp$  values (respectively the  $Rbp$  values) over the previous rest block ignoring the first and last second of the block. Eventually, the EEG laterality index  $eeg_{lat}(t)$  was translated as the ordinate of the ball.

The fMRI signal was pre-processed online for motion correction, slice-time correction and then the fMRI laterality index was computed according to the following definition<sup>7</sup>:

Figure 35 – Real-time multimodal EEG/fMRI-NF setup. The participant is lying in the MR tube with a 64-channel MR-compatible EEG cap. EEG and fMRI are simultaneously acquired then pre-processed with custom Matlab code. The EEG and fMRI laterality features are computed and eventually translated as a displacement of the ball on the stimulation screen, the image of which is projected on the mirror mounted on the head coil. Icons made by Freepik from www.flaticon.com

<sup>6</sup> (Neuper, Wörtz, & Pfurtscheller, 2006)

<sup>7</sup> (Chiew, LaConte, & Graham, 2012)

$$fmri_{lat}(t) = \frac{B_{left}(v)}{B_{left}(previous\_rest)} - \frac{B_{right}(v)}{B_{right}(previous\_rest)} \quad (4)$$

Where  $B_{left}(v)$  (respectively  $B_{right}(v)$ ) is the average of the BOLD signal in the left (respectively right) ROI at volume  $v$ , and  $\overline{B_{left}(previous\_rest)}$  (respectively  $\overline{B_{right}(previous\_rest)}$ ) is the left baseline obtained by averaging the signal in the left (respectively right) ROI over the last six volumes (to account for hemodynamic delay) of the previous rest block. The fMRI laterality index was then smoothed by averaging it over the last three volumes and translated as the abscissa of the ball.

#### 5.1.4 Working hypotheses

Our goal is to compare the level of MI-related EEG and fMRI activations elicited during *EEG-NF*, *fMRI-NF* and *EEG-fMRI-NF*. We have made assumptions that are not specific to motor imagery and EEG and fMRI but can be defined for any brain pattern and pair of brain imaging modalities ( $P$ ,  $Q$ ). These assumptions concern the order relations of activation levels in a given modality  $P$  when NF of this modality is given (P-NF), when NF of another modality is given (Q-NF), and when NF of this modality and another is given (P-Q-NF). We hypothesize that:

1. **Generalized NF effect:** activation level in a given modality is significant when NF of this modality is displayed, may it be alone or together with another modality (for the specific application to EEG and fMRI, see below the corresponding refined assumptions 1.a, 1.b, 2.a, 2.b).
2. **Direct NF effect:** As a corollary of the generalized NF effect, activation level in a given modality should be higher when NF of this modality is displayed than when it is not displayed, because in the former case the subject has access to it and can thus better and directly regulate it. (1.c, 1.d, 2.c, 2.d).
3. **Compromise effect:** activation level in a given modality is higher or equal when NF of this modality is displayed alone as when it is displayed with another modality, because in the latter case the subject will also try to regulate the other modality. (1.e, 2.e).

Let  $eeg(NF\_condition)$  be the MI-related EEG activity pattern during *NF\_condition* and

$fmri(NF\_condition)$  the MI-related fMRI activity pattern during *NF\_condition*.

Applying these general assumptions to MI-related EEG and fMRI activations elicited during *EEG-NF*, *fMRI-NF* and *EEG-fMRI-NF* and breaking them in unitary order relations, these yields the following refined assumptions (the ones underlined correspond to the assumptions that we validated in the present study):

- 1.(a)  $eeg(EEG-NF) \gg \mathbf{o}$ : MI-related EEG activations are significant during *EEG-NF*
- (b)  $eeg(EEG-fMRI-NF) \gg \mathbf{o}$ : MI-related EEG activations are significant during *EEG-fMRI-NF*

- (c)  $eeg(EEG-NF) > eeg(fMRI-NF)$ : MI-related EEG activations are higher during EEG-NF than during fMRI-NF
- (d)  $eeg(EEG-fMRI-NF) > eeg(fMRI-NF)$ : MI-related EEG activations are higher during EEG-fMRI-NF than during fMRI-NF
- (e)  $eeg(EEG-NF) \geq eeg(EEG-fMRI-NF)$ : MI-related EEG activations are higher or equal during EEG-NF than during EEG-fMRI-NF
- 2.(a)  $fmri(fMRI-NF) \gg 0$ : MI-related fMRI activations are significant during fMRI-NF
- (b)  $fmri(EEG-fMRI-NF) \gg 0$ : MI-related fMRI activations are significant during EEG-fMRI-NF
- (c)  $fmri(fMRI-NF) > fmri(EEG-NF)$ : MI-related fMRI activations are higher during fMRI-NF than during EEG-NF
- (d)  $fmri(EEG-fMRI-NF) > fmri(EEG-NF)$ : MI-related fMRI activations are higher during EEG-fMRI-NF than during EEG-NF
- (e)  $fmri(fMRI-NF) \geq fmri(EEG-fMRI-NF)$ : MI-related fMRI activations are higher or equal during fMRI-NF than during EEG-fMRI-NF

Figure 36 summarizes the working hypotheses.

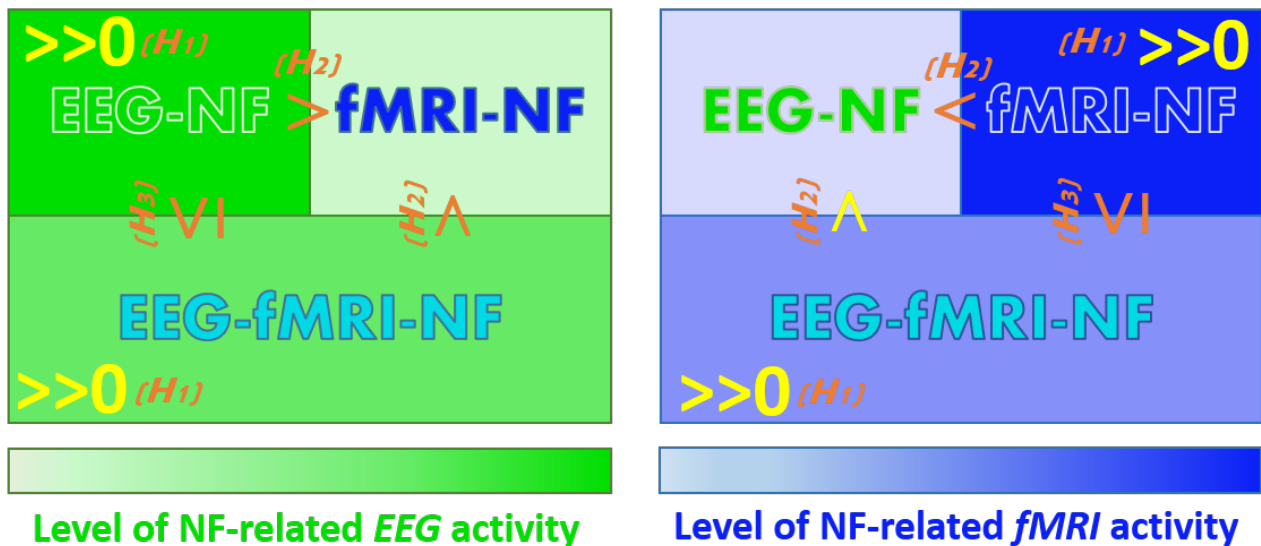


Figure 36 – Working hypotheses. The hypotheses that we validated in this study are in yellow. (H<sub>1</sub>) Generalized NF effect. (H<sub>2</sub>) Direct NF effect. (H<sub>3</sub>) Compromise NF effect.

### 5.1.5 Offline analysis

Data from one participant was excluded because it was too affected by motion artifacts. This participant was one of the two participants for which we could not acquire the *MI\_pre* and *MI\_POST* data. EEG data of *MI\_pre* and *MI\_post* runs from one subject was accidentally lost.

5.1.5.1 *fMRI data analysis*

<sup>8</sup> (Maumet, 2013)

The fMRI data from each of the six runs (*MLOC*, *MI\_pre*, *NF1*, *NF2*, *NF3*, *MI\_post*) was pre-processed and analyzed with AutoMRI<sup>8</sup>, a proprietary software for fMRI analysis automation based on SPM8. Pre-processing included slice-time correction, spatial realignment, co-registration to the 3D T<sub>1</sub>, followed by spatial smoothing with a 8 mm Gaussian kernel. A first-level and second-level general linear model (GLM) analysis was performed. The first-level GLM included the canonical HRF for the task as well as its temporal and dispersion derivatives. For the second-level GLM analysis, the individual data were normalized to the Montreal Neurological Institute (MNI) template and grouped using a mixed effects linear model. The activations maps were corrected for multiple comparisons using Family-Wise error (FWE) correction ( $p < 0.05$  with cluster size  $> 10$  voxels).

In order to compare the level of MI-related fMRI activations between the three NF conditions, we performed a repeated measure ANOVA of the averaged offline fMRI laterality index between the three experimental conditions (A, B and C) and paired t-tests between each pair of conditions. The NF blocks were averaged by considering the last six volumes (out of ten) of the blocks in order to account for the hemodynamic delay. We also performed a post-hoc signal analysis in order to assess the participant- and condition-specific level of activation of the actual fMRI patterns in the motor regions during NF as identified from the individual GLM analysis. For each participant, the post-hoc ROI was defined by running a GLM on the concatenation of *MI\_pre*, *EEG-NF*, *fMRI-NF*, *EEG-fMRI-NF* and *MI\_post* runs (or just the NF runs for subjects who did not perform *MI\_pre*) and taking a  $3 \times 3 \times 3$  box around the maximum of activation (constrained to the left motor area) of the thresholded T-map ( $\text{TASK} > \text{REST}$ ,  $p < 0.05$ , FWE corrected,  $k > 10$ ). For each participant and experimental condition, the registered fMRI values were high-pass filtered (100 seconds) to remove the linear drift, averaged in the ROI and transformed to percent signal change (PSC) using the formulae  $(B_{roi}(v) - m)/m$  where  $m$  is the mean of all  $B_{roi}$  values across the run. Eventually, for each experimental condition the PSC were averaged across the last six volumes of each NF blocks. We then performed a repeated measure ANOVA of this post-hoc feature for the three experimental conditions (A, B and C) and paired t-tests between each pair of conditions. In order to account for any learning effect that could have occurred throughout the consecutive runs, we also computed the repeated measure ANOVA and the paired t-tests on the consecutive runs. For ANOVA and paired t-tests, the PSC values were standardized to z-scores.

5.1.5.2 *EEG data analysis*

<sup>9</sup> (Allen, Josephs, & Turner, 2000)

For offline analysis, EEG signal was pre-processed using BrainVision Analyzer II software: data was cleared from gradient and CB artifact using the artifact subtraction method<sup>9</sup>, down-sampled to 200 Hz, filtered between 8 and 30 Hz using a Butterworth zero phase filter (48 db slope), segmented in 1s segments, and segments affected by motion were removed. The EEG offline laterality index was then computed from this offline cleaned data in Matlab. For each of the three NF conditions (A: *EEG-NF*, B: *fMRI-NF*, C: *EEG-fMRI-NF*), we performed a repeated measure ANOVA of the averaged offline EEG laterality index between

the three experimental conditions (A, B and C) and paired t-tests of the averaged offline EEG laterality index. The NF blocks were averaged by considering the values between the first and the nineteenth second of the block. We also performed a post-hoc analysis whose purpose was to assess the participant- and condition-specific level of activation of the actual EEG patterns over the motor regions during NF as identified with a Common Spatial Pattern (CSP)<sup>10</sup>. For each participant, we computed the pairs of spatial filters that best maximized the difference in  $\mu$  power between rest and NF blocks on the concatenation of *MI\_pre*, *EEG-NF*, *fMRI-NF*, *EEG-fMRI-NF* and *MI\_post* (or just the NF runs for subjects who did not perform *MI\_pre*) using the CSP algorithm<sup>11</sup> on 18 channels located over the motor regions (C<sub>3</sub>, C<sub>4</sub>, FC<sub>1</sub>, FC<sub>2</sub>, CP<sub>1</sub>, CP<sub>2</sub>, FC<sub>5</sub>, FC<sub>6</sub>, CP<sub>5</sub>, CP<sub>6</sub>, C<sub>1</sub>, C<sub>2</sub>, FC<sub>3</sub>, FC<sub>4</sub>, CP<sub>3</sub>, CP<sub>4</sub>, C<sub>5</sub>, C<sub>6</sub>). The first filter  $f_{rest>nf}$  of the pair maximizes the band power during the rest blocks while the second filter  $f_{nf>rest}$  of the pair maximizes the band power during the NF blocks. If the eigenvalue of  $f_{rest>nf}$  was greater than the inverse of the eigenvalue of  $f_{nf>rest}$ <sup>12</sup>, the data was filtered with  $f_{rest>nf}$ ; the band power in the  $\mu$  band was then computed on this filtered data using the periodogram and it was normalized with an event-related desynchronization (ERD)-like formulae  $(\overline{REST} - \text{bandpower}) / \overline{REST}$  with  $\overline{REST}$  being computed by averaging the power on all the baseline blocks from the run. Otherwise, the data was filtered with  $f_{nf>rest}$ ; the band power in the  $\mu$  band was then computed on this filtered data using the periodogram and it was normalized with an event-related desynchronization (ERD)-like formulae  $(\text{bandpower} - \overline{REST}) / \overline{REST}$  with  $\overline{REST}$  being computed by averaging the power on all the baseline blocks from the run. Eventually, for each experimental condition the ERD values were averaged by considering the values between the first and the nineteenth second of each NF blocks. We then performed a repeated measure ANOVA of this post-hoc feature for the three experimental conditions (A, B and C) and paired t-tests between each pair of conditions. In order to account for any learning effect that could have occurred throughout the consecutive runs, we also computed the repeated measure ANOVA and the paired t-tests on the consecutive runs. For ANOVA and paired t-tests, the PSC values were standardized to z-scores.

## 5.2 RESULTS

### 5.2.1 fMRI data analysis

Whole brain analysis of the contrast TASK revealed similar networks of activations during motor execution and motor imagery with the unimodal and bimodal NF conditions.

The motor execution revealed significant activations ( $p < 0.05$ , FWE-corrected) in the primary motor cortex (M<sub>1</sub>), in the premotor cortex and in the cerebellum. All NF conditions exhibited significant activations ( $p < 0.05$ , FWE corrected) in the left and right premotor cortex (PMC) and in the left and right supplementary motor area (SMA). fMRI-NF and EEG-fMRI-NF exhibited significant activations ( $p < 0.05$ , FWE corrected) in the right inferior frontal gyrus (pars opercularis, BA44), right inferior parietal lobule (BA40), right insula (BA47), in the right supramarginal gyrus (BA2), right superior temporal gyrus (BA42). fMRI-NF exhibited significant activations in the left insula (BA47) and in right visual

<sup>10</sup> (Ramoser, Müller-Gerking, & Pfurtscheller, 2000)

<sup>11</sup> (Ramoser, Müller-Gerking, & Pfurtscheller, 2000)

<sup>12</sup> (Blankertz et al., 2008)

cortex (BA19). EEG-fMRI-NF exhibited significant activations in the right primary motor cortex (BA3), in the right middle temporal gyrus (BA37), left IPL (BA40). These activations are illustrated in [Figure 37](#).

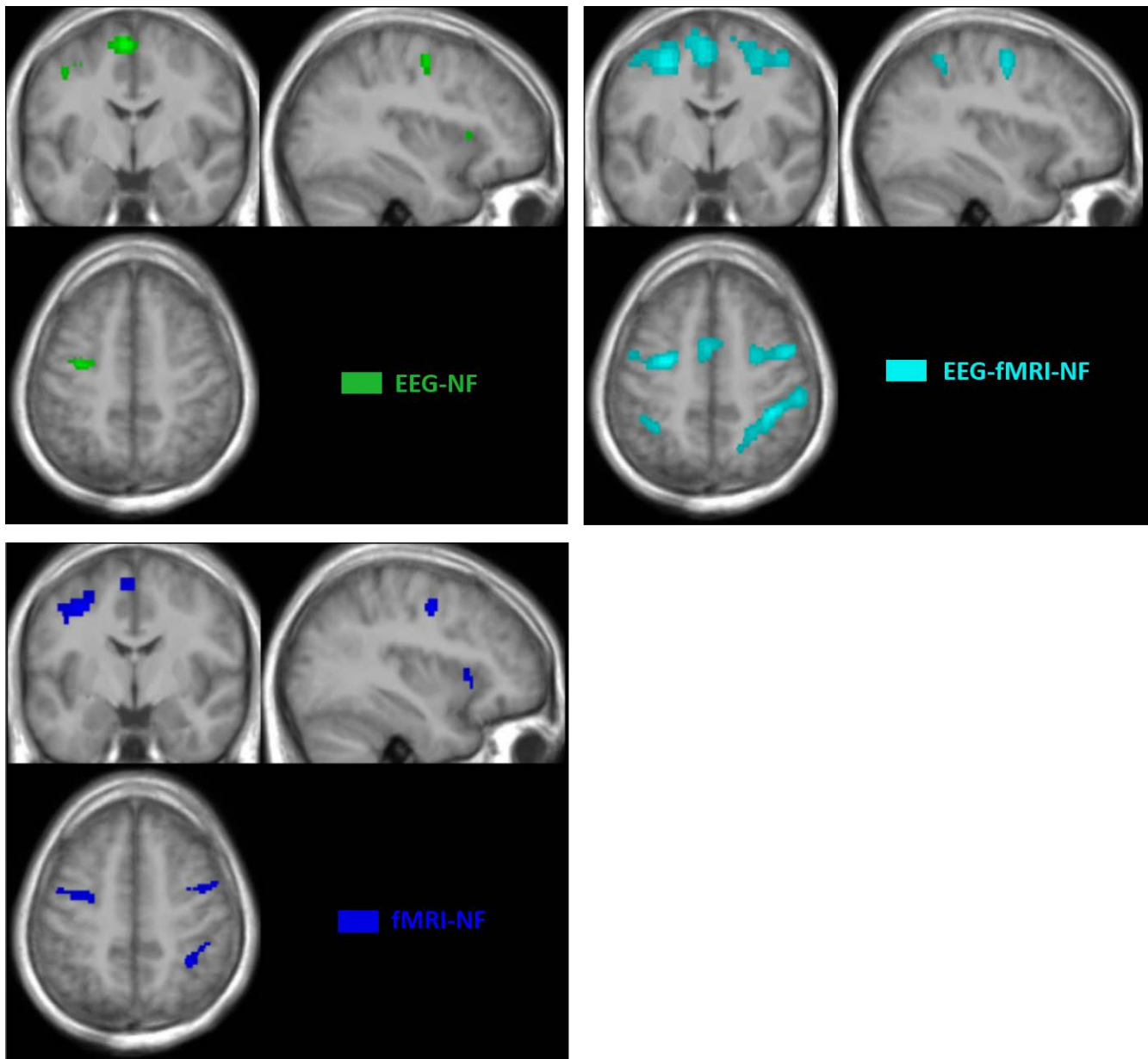


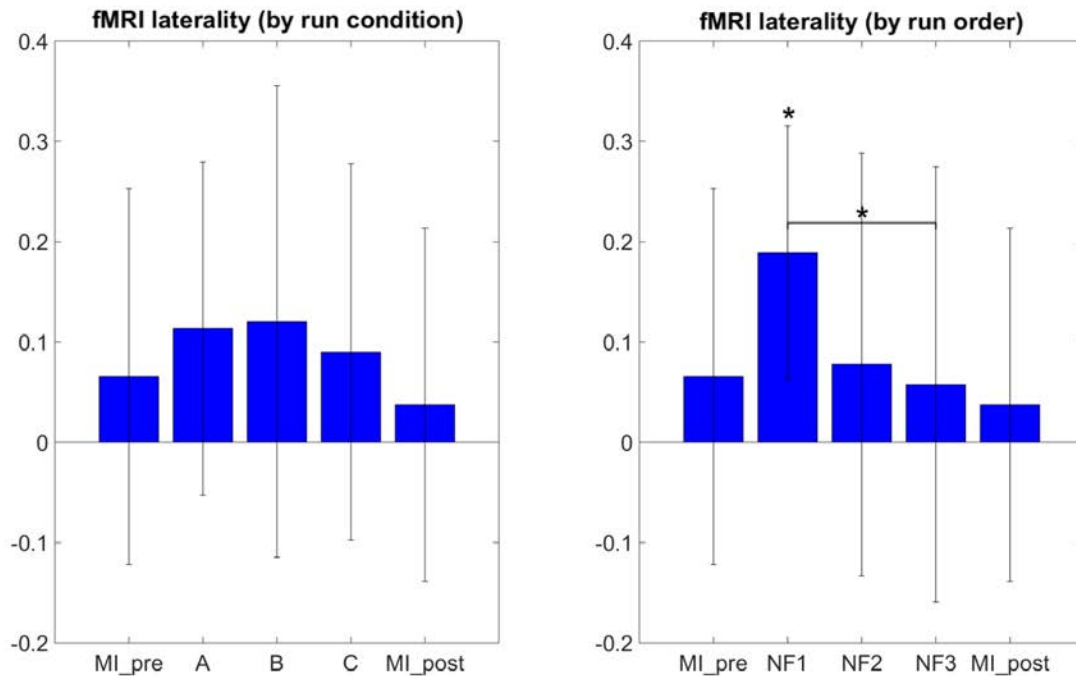
Figure 37 – BOLD activation maps at group level (TASK>REST;  $p > 0.05$  FWE corrected;  $k > 10$  voxels). Green: EEG-NF; Blue: fMRI-NF; Cyan: EEG-fMRI-NF. EEG-fMRI-NF activations are visually larger and more widespread than EEG-NF or fMRI-NF activations.

The results in [Figure 38](#) demonstrate that participants were able to increase their fMRI laterality between the left and right primary motor cortex during NF. The fMRI laterality change was significant in NF1 run ( $t(8) = 4.4832$ ,  $p = 0.0020$ ). Also, fMRI laterality change was significantly different between NF1 and NF3 ( $t(8) = 3.3351$ ,  $p = 0.0103$ ), which suggests that fMRI laterality tended to worsen over the course of the experiment. The results in [Figure 38](#) also illustrate that the fMRI laterality in the primary motor cortex showed high variability across subjects. Therefore the comparison between each pair of conditions did not



show any significant difference. At this point, we can pinpoint that laterality features can be hard to interpret as they reflect a variety of activations patterns combining the left and right ROI<sup>13</sup>. For instance, in Figure 38 the higher level of activity observed during EEG-NF (A) as compared to EEG-fMRI-NF (C) is due to the fact that the group mean activity during EEG-NF was negative in the right hemisphere ROI, though it was close to zero in the left hemisphere ROI. The post-hoc analysis allowed to look directly at the actual activations clusters in order to assess whether there was any significant differences in the level of fMRI activity that would have hid behind the fMRI laterality measure.

<sup>13</sup> (Chiew, LaConte, & Graham, 2012)



It is therefore not surprising that the results in Figure 39 do not show the same tendencies than the results in Figure 38 as they are direct measure of the level of activation in the actual clusters of activations instead of laterality measures. One-way repeated measure ANOVA yielded a significant effect of the NF conditions ( $F(2,8) = 5.4$ ;  $p = 0.0162$ ). The results in Figure 38 show that post-hoc fMRI activations were significantly higher during the EEG-fMRI-NF condition as compared to the EEG-NF condition ( $t(8) = 3.8450$ ,  $p = 0.0049$ ). Post-hoc fMRI activations were significantly higher during MI with NF as compared to MI without NF, which shows the added value of NF. In particular, post-hoc fMRI-NF activations were significantly higher than MI\_pre activations ( $t(7) = 4.0439$ ,  $p = 0.0049$ ). EEG-fMRI-NF activations were significantly higher than MI\_pre activations ( $t(7) = 4.2320$ ,  $p = 0.0039$ ) and significantly higher than MI\_post activations ( $t(7) = 2.8855$ ,  $p = 0.0235$ ). NF1 activations were significantly higher than MI\_pre activations ( $t(7) = 3.4530$ ,  $p = 0.0106$ ). NF2 activations were significantly higher than MI\_pre activations ( $t(7) = 3.8277$ ,  $p = 0.0065$ ). Results are summarized in Figure 42.

Figure 38 – fMRI laterality group mean with standard deviation during task in percent signal change relative to baseline. NF conditions A (EEG-NF), B (fMRI-NF), C (EEG-fMRI-NF) were presented in different order for each subject. On the left side, the means were computed by averaging the data across subjects on each NF conditions A, B, C. On the right the means were computed by averaging the data across subjects on each NF runs by chronological order NF1, NF2, NF3. fMRI laterality was significant in the NF1 run ( $t(8) = 4.1067$ ,  $p = 0.0026$ ). fMRI laterality change was significantly different between NF1 and NF3 ( $t(8) = 3.3351$ ,  $p = 0.0103$ ), which suggests that fMRI laterality tended to worsen throughout the consecutive NF runs.



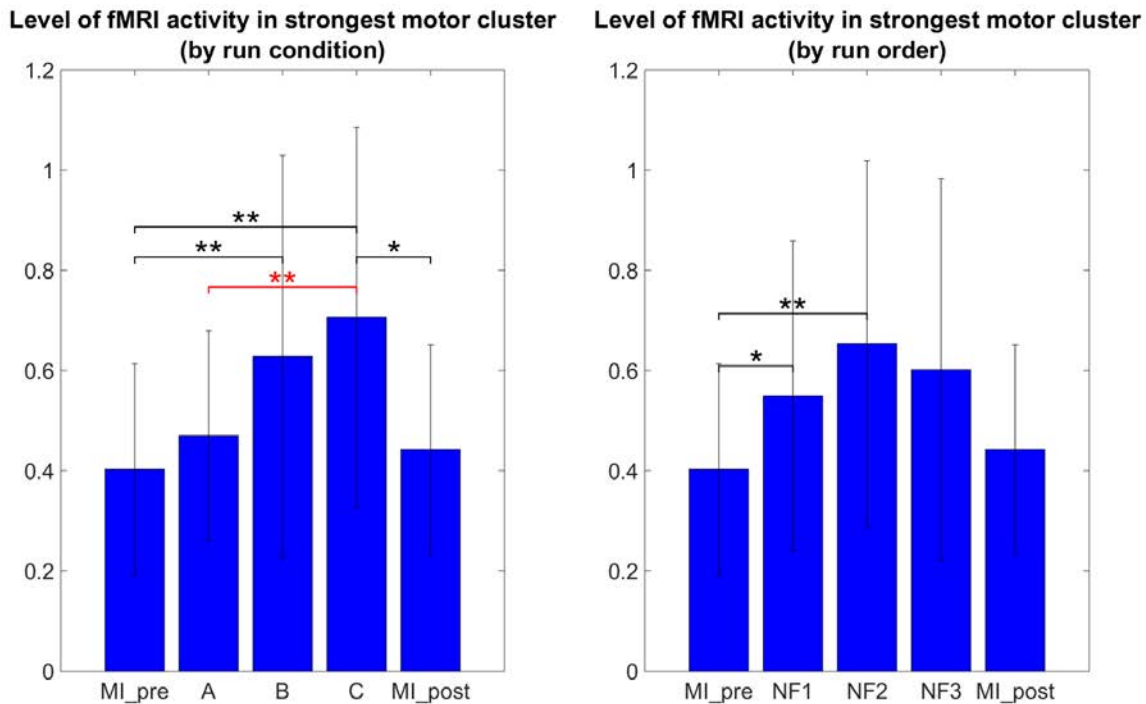


Figure 39 – Post-hoc fMRI activations (defined as activity in strongest motor cluster after GLM) as group mean PSC during task with standard deviation. The post-hoc fMRI activations were significantly higher during the *EEG-fMRI-NF* run than during the *EEG-NF* run ( $t(8) = 3.8450$ ,  $p=0.0049$ ). Also post-hoc fMRI activations were significantly higher during motor imagery with NF than during MI without NF, which shows the added value of NF. For paired t-tests, PSC values were standardized to z-scores. Black significance bars were computed on 8 subjects while red significance bar was computed on 9 subjects.

### 5.2.2 EEG data analysis

The results in Figure 40 demonstrate that participants were able to increase their EEG laterality between C1 and C2 in the  $\mu$  band during NF. The EEG laterality change was significant in the second NF run ( $t(8) = 2.3389$ ,  $p=0.0441$ ). These results also suggest, however without significance, that EEG laterality tended to improve over the course of the experiment. As for the fMRI laterality feature, the EEG laterality between C1 and C2 in the  $\mu$  band showed high variability across subjects. Therefore the comparison between each pair of conditions did not show any significant difference. The post-hoc analysis aimed at looking directly at the actual EEG patterns of activity in order to assess whether there was any significant differences that would have hid behind the EEG laterality measure. However, as illustrated in Figure 41, post-hoc EEG activations did not show any significant differences between the NF conditions either. Post-hoc EEG activations were significantly higher during MI with NF as compared to MI without NF, which shows the added value of NF. In particular, post-hoc *EEG-NF* activations were significantly higher than *MI\_pre* activations ( $t(6) = 3.7907$ ,  $p = 0.0091$ ) and significantly higher than *MI\_post* activations ( $t(6) = 2.5392$ ,  $p = 0.0441$ ). Post-hoc *fMRI-NF* activations were significantly higher than *MI\_pre* activations ( $t(6) = 6.5824$ ,  $p = 0.0006$ ) and significantly higher than *MI\_post* activations ( $t(6) = 2.5195$ ,  $p = 0.0453$ ). Post-hoc *EEG-fMRI-NF* activations were significantly higher than *MI\_pre* activations ( $t(6) = 3.7269$ ,  $p = 0.0098$ ). *NF1* activations were significantly higher than *MI\_pre* activations ( $t(6) = 3.1184$ ,  $p = 0.0206$ ). *NF2* activations were significantly higher than *MI\_pre* activations

( $t(6) = 4.8018, p = 0.0030$ ). *NF3* activations were significantly higher than *MI\_pre* activations ( $t(6) = 6.1116, p = 0.0009$ ) and significantly higher than *MI\_post* activations ( $t(6) = 3.2035, p = 0.0185$ ). Results are summarized in [Figure 42](#).

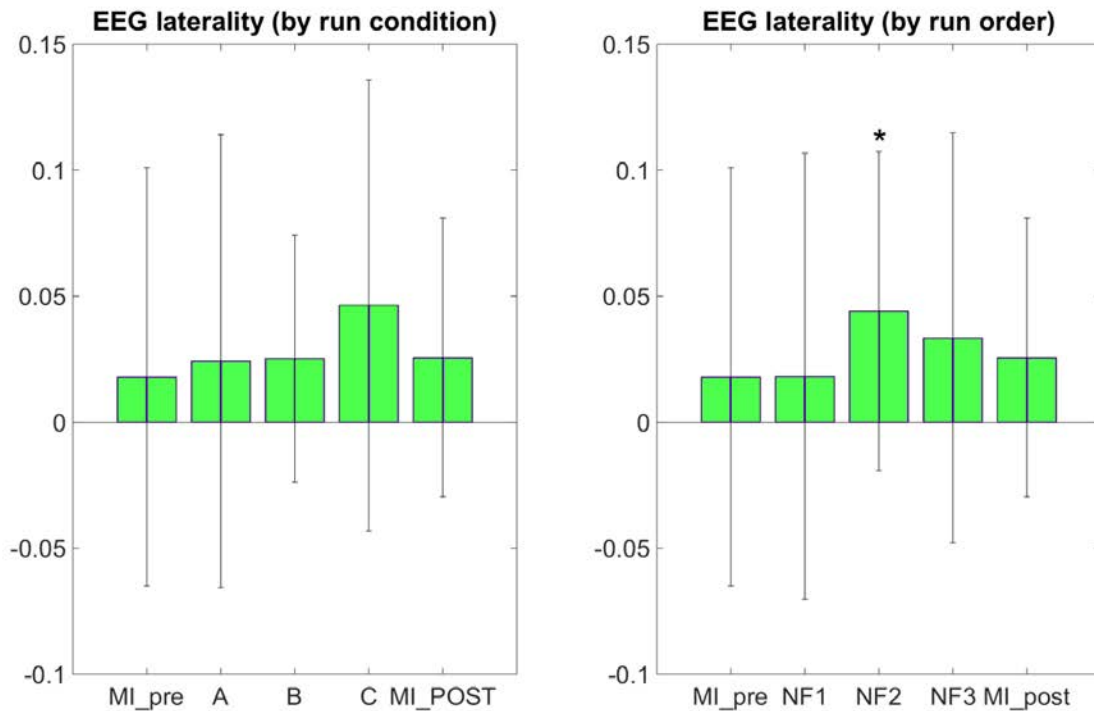


Figure 40 – EEG laterality group mean with standard deviation during task in percent signal change relative to baseline. *NF* conditions A (EEG-*NF*), B (*fMRI-NF*), C (EEG-*fMRI-NF*) were presented in different order for each subject. On the left, the means are computed by averaging the data across subjects on each *NF* conditions A, B, C. On the right the means are computed by averaging the data across subjects on each *NF* runs by chronological order *NF1*, *NF2*, *NF3*. EEG laterality was significant in the second *NF* run ( $t(8) = 2.3389, p = 0.0441$ ). Though not significant, we observe that the EEG laterality tended to improve over the course of the experiment.

### 5.2.3 Questionnaire

In the questionnaire participants were asked specific questions about the *EEG-fMRI-NF* run. Seven participants out of ten reported that they did not feel like they had to perform two regulation tasks. Six participants found that *fMRI* was easier to control than *EEG*; three found that *EEG* was easier; one found no difference. Eight participants out of ten reported to have paid the same attention to both dimensions during the *EEG-fMRI-NF* condition, the two others reported they looked more at the dimension that was harder for them to control (in one case *EEG*, in the other *fMRI*). Five participants out of ten reported that *fMRI* update rate was slow.

## 5.3 DISCUSSION

For the first time, we compared the effects of unimodal *EEG-NF* and *fMRI-NF* with bimodal *EEG-fMRI-NF* in order to assess the potential added value of bimodal *NF* over unimodal *NF*. We tested our hypotheses (cf. section 2.4) by looking at the level of *MI*-related *EEG* and *fMRI* activations during each *NF* conditions. Motor activations as revealed by post-hoc *fMRI* analysis were significantly higher during *EEG-fMRI-NF* than during *EEG-NF* (see [Figure 39](#)).

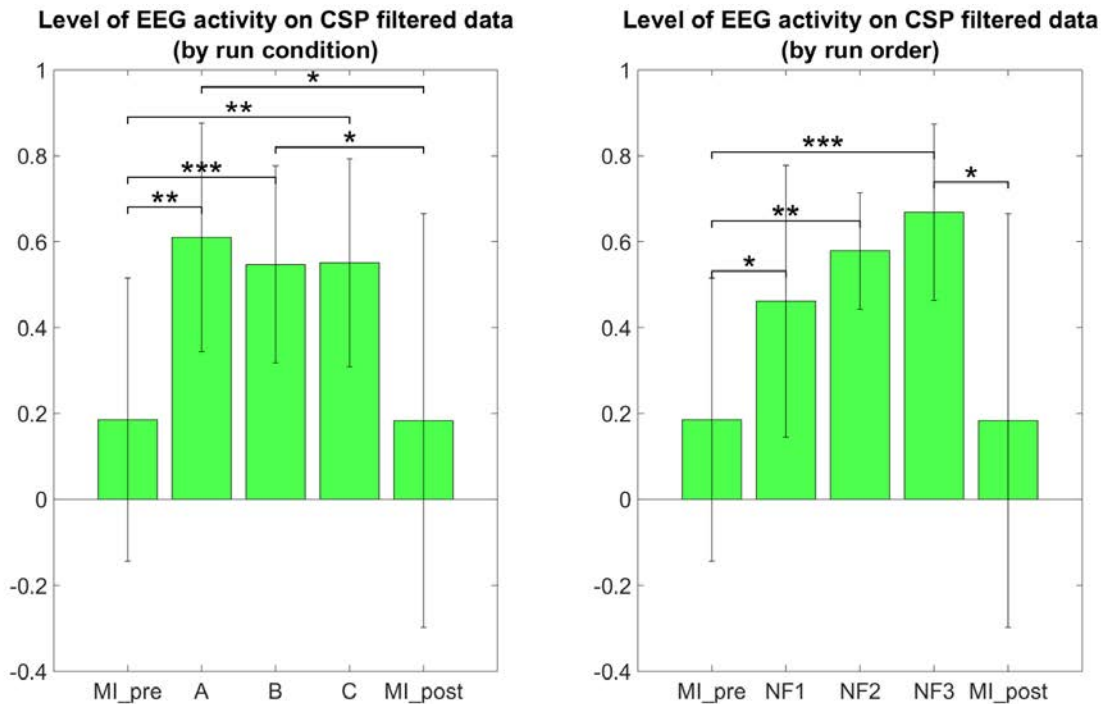


Figure 41 – Post-hoc EEG activations group mean ERD in the  $\mu$  band after CSP filtering. Post-hoc EEG activations were significantly higher during motor imagery with NF than during MI without NF, which shows the added value of NF. There was no significant differences between the 3 NF conditions (A, B, C) nor between the 3 NF runs (NF1, NF2, NF3). For paired t-tests, ERD values were standardized to z-scores. Black significance bars were computed on 7 subjects.

This results partly validated our “direct NF effect” hypothesis and could mean that *EEG-fMRI-NF* specifically triggered more fMRI activations than *EEG-NF* because feedback from fMRI was provided. But it could also mean that bimodal *EEG-fMRI-NF* was more engaging than unimodal *EEG-NF* because subject had to control the feedback in the vertical and horizontal dimension. To disentangle whether *EEG-fMRI-NF* is more specific or simply more engaging than *EEG-NF*, one could use a one-dimensional *EEG-fMRI-NF* feedback that would mix both EEG and fMRI feature in a single gauge and compare it directly to *EEG-NF*. Alternatively, to rule out the engaging factor, one could also compare *EEG-fMRI-NF* with EEG-shamfMRI-NF in which sham fMRI-NF would be provided together with real EEG-NF. Post-hoc EEG activations did not show any significant differences between the different NF conditions. This can be due to the fact that EEG is noisier than fMRI, especially in the MR environment, but it is also possible that it was hard for participants to maintain the  $\mu$  desynchronization throughout the 20 seconds of the NF blocks. The 20s block design was chosen mainly in consideration of the fMRI modality in order to account for the hemodynamic delay. MI-based EEG-NF/-BCI tasks are usually much shorter, around 4 seconds length<sup>14</sup>. The electrophysiology of continuous MI is still not fully understood. Though continuous MI is thought to induce a succession of event-related desynchronizations it can be hard to observe a continuous desynchronization throughout the duration of the continuous MI<sup>15</sup> This highlights the difficulty of designing the task specifically for bimodal *EEG-fMRI-NF* given the different spatio-temporal dynamics of EEG and fMRI. Interestingly, the specific effect of NF in the three NF conditions can be confirmed by the sig-

<sup>14</sup> (Pfurtscheller & Neuper, 2001)

<sup>15</sup> (Rimbert et al., 2015; Jeon et al., 2011)

		EEG		fMRI	
		online	posthoc	online	posthoc
Different from 0	<i>MI_pre</i>	n.s.	n.s.	n.s.	t(7) = 5.4097, p = 0.0010
	<b>A: EEG-NF</b>	n.s.	t(8) = 6.8726, p = 0.0001	n.s.	t(8) = 6.7503, p = 0.0001
	<b>B: fMRI-NF</b>	n.s.	t(8) = 7.1497, p = 0.0001	n.s. tendency (p < 0.1)	t(8) = 4.6955, p = 0.0016
	<b>C: EEG-fMRI-NF</b>	n.s.	t(8) = 6.8361, p = 0.0001	n.s.	t(8) = 5.5974, p = 0.0005
	<b>NF1</b>	n.s.	t(8) = 4.3791, p = 0.0024	t(8) = 4.4832, p = 0.0020	t(8) = 5.3260, p = 0.0007
	<b>NF2</b>	t(8) = 2.3389, p = 0.0441	t(8) = 12.7641, p = 0.0000	n.s.	t(8) = 5.3725, p = 0.0007
	<b>NF3</b>	n.s.	t(8) = 9.7551, p = 0.0000	n.s.	t(8) = 4.7304, p = 0.0015
NF vs no NF	<i>MI_post</i>	n.s.	n.s.	n.s.	t(7) = 5.9860, p = 0.0005
	<b>A vs MI_pre</b>	n.s.	t(6) = 3.7907, p = 0.0091	n.s.	n.s.
	<b>B vs MI_pre</b>	n.s.	t(6) = 6.5824, p = 0.0006	n.s.	t(7) = 4.0439, p = 0.0049
	<b>C vs MI_pre</b>	n.s.	t(6) = 3.7269, p = 0.0098	n.s.	t(7) = 4.2320, p = 0.0039
	<b>A vs MI_post</b>	n.s.	t(6) = 2.5392, p = 0.0441	n.s.	n.s.
	<b>B vs MI_post</b>	n.s.	t(6) = 2.5195, p = 0.0453	n.s.	n.s. tendency (p < 0.1)
	<b>C vs MI_post</b>	n.s.	n.s.	n.s.	t(7) = 2.8855, p = 0.0235
	<b>NF1 vs MI_pre</b>	n.s.	t(6) = 3.1184, p = 0.0206	t(7) = 3.0138, p = 0.0196	t(7) = 3.4530, p = 0.0106
	<b>NF2 vs MI_pre</b>	n.s.	t(6) = 4.8018, p = 0.0030	n.s.	t(7) = 3.8277, p = 0.0065
	<b>NF3 vs MI_pre</b>	n.s.	t(6) = 6.1116, p = 0.0009	n.s.	n.s. tendency (p < 0.1)
	<b>NF1 vs MI_post</b>	n.s.	n.s.	n.s. tendency (p < 0.1)	n.s. tendency (p < 0.1)
	<b>NF2 vs MI_post</b>	n.s.	n.s.	n.s.	n.s. tendency (p < 0.1)
	<b>NF3 vs MI_post</b>	n.s.	t(6) = 3.2035, p = 0.0185	n.s.	n.s.
	Inter NF conditions	<b>A vs B</b>	n.s.	n.s.	n.s.
<b>B vs C</b>		n.s.	n.s.	n.s.	n.s.
<b>A vs C</b>		n.s.	n.s.	n.s.	t(8) = -3.8450, p = 0.0049
Inter NF runs	<b>NF1 vs NF2</b>	n.s. tendency (p < 0.1)	n.s.	n.s. tendency (p < 0.1)	n.s. tendency (p < 0.1)
	<b>NF2 vs NF3</b>	n.s.	n.s.	n.s.	n.s.
	<b>NF1 vs NF3</b>	n.s.	n.s.	t(8) = 3.3351, p = 0.0103	n.s.

nificant difference in the level of post-hoc fMRI and EEG motor activations between the NF runs and the *MI\_pre* and *MI\_post* runs which were done without NF (see Figure 39 and Figure 41). Despite the somehow limited number of subject in our study, these results support our “generalized NF effect” hypothesis. Further work with more subjects should be conducted to even enforce this outcome. In the seminal work on EEG-fMRI-NF<sup>16</sup>, the authors studied a protocol of positive emotion induction with feedback from frontal EEG asymmetry in the beta band and from left amygdala BOLD. As in this related work, we found similar value ranges of the EEG and fMRI features and similar variability. We were however not able to observe significant differences between the three NF conditions by directly looking at the EEG and fMRI laterality features (see Figure 38 and Figure 40). Lateralization of activity in motor regions is known to be an indicator of good motor imagery<sup>17</sup>. Also in stroke rehabilitation, best results are usually obtained when the recovery happens in the ipsi-lesional hemisphere rather than in the contra-lesional one and NF based on laterality indices could allow to promote this kind of recovery<sup>18</sup>. However laterality features are hard to interpret and may have been too hard to regulate significantly in a single session for participants who were not trained to MI before. Regarding the EEG laterality index and given the spatial proximity of the chosen electrode locations C1 and C2, one could wonder if they could be influenced by the same sources. Such sources would be situated in cortices close to the inter-hemispherical midline such as feet sensorimotor area. However, the activity of the hand sensorimotor area is quite far from the midline, so the activity measured by a contralateral electrode will be far stronger than that of an ipsilateral electrode. Given that the neurofeedback was based on a laterality index, there is no chance that activating common sources such as with feet imagination would allow to control

Figure 42 – Summary of the statistical analysis results (t-tests and paired t-tests). Color indicates the level of significance of the tests.

<sup>16</sup> (Zotev, Phillips, et al., 2014a)

<sup>17</sup> (Marchesotti et al., 2016)

<sup>18</sup> (Rehme et al., 2012; Chiew, LaConte, & Graham, 2012)

the neurofeedback. However we do admit that C<sub>3</sub> and C<sub>4</sub> are more common locations for hand movements and might lead to better results. One could also consider computing a CSP filter on calibration data which would allow to define the spatial filtering for the EEG feature at the individual level. Regarding the fMRI laterality index, the right motor ROI was defined approximately by mirroring the left motor ROI. This was done mainly in order not to add more time to the already long experimental protocol. Given the size of the ROI (18 × 18 × 12 mm<sup>3</sup>), there is high chance that the mirror ROI would lie in the right primary motor cortex. However we admit that it would be better to use a functional localizer to define the right motor ROI.

Regarding the “compromise NF effect”, our results did not allow us to get any preliminary insight into our speculations. More experiments with longer NF training and more subjects are needed to confirm the rest of the “direct NF effect” and the “compromise NF effect” assumptions. We can note that in our study, the signal-to-noise ratio (SNR) was the same in unimodal and bimodal NF conditions as EEG and fMRI were simultaneously acquired throughout the whole experiments to assess the cross-modality effects. However, when doing unimodal EEG-NF or fMRI-NF without simultaneous EEG and fMRI recordings, SNR should be better than the one of bimodal EEG-fMRI-NF. This could reinforce the “compromise NF effect”. Artifacts occurring during simultaneous EEG-fMRI are a major limitation of EEG-fMRI-NF<sup>19</sup>. The BCG artifact and motion artifacts from the subject or the environment (vibrations from helium pump and ventilation) are particularly hard to correct. The development of new methods for correcting these artifacts is an ongoing topic of research, but few options are available for online correction<sup>20</sup>. Interestingly, a recent approach consists in using the EEG not only as a brain imaging modality but also as a motion sensor to correct for motion artifact<sup>21</sup>. Another important aspect of the EEG analysis is the choice of the reference. In this work we used the standard reference FCz as it was proven to be efficient for motor imagery<sup>22</sup>. But regarding the fact that the potential of FCz is non-zero, it would be interesting in the future to consider using another reference such as the common average reference (CAR) or reference electrode standardization technique (REST)<sup>23</sup>.

Though the NF features change between the consecutive NF runs and between each pair of NF conditions was not significant, the EEG and fMRI laterality features had asymmetric tendency (see [Figure 38](#) and [Figure 40](#)). Throughout the consecutive NF runs, EEG laterality tended to improve while fMRI laterality tended to worsen. Besides, participants reported on average that the fMRI dimension was easier to control than the EEG dimension, so it is possible that they have put more effort (however not necessarily more attention as they reported) on controlling the EEG dimension. This could explain the learning tendency observed on the EEG laterality feature at the price of a decrease on the fMRI laterality feature. Putting these observations together suggests that during bimodal NF, one feature could be more regulated than the other, possibly the one that is harder to control. We should note however that our study was conducted at a single-session level and that the asymmetric change of the features that we observed could actually be part of a learning scenario in which subjects would by example first learn to regulate one feature, then the other one and eventually manage to regulate both simultaneously. Interestingly, this decrease of performance on NF features was also observed in related works<sup>24</sup> though both on EEG

<sup>19</sup> (Zotев, Phillips, et al., 2014a)

<sup>20</sup> (Allen, Polizzi, et al., 1998; Allen, Josephs, & Turner, 2000; Mayeli et al., 2016; Krishnaswamy et al., 2016; Wu et al., 2016; Meer et al., 2016)

<sup>21</sup> (Jorge, Grouiller, et al., 2015; Wong et al., 2016)

<sup>22</sup> (S. H. Choi et al., 2006)

<sup>23</sup> (Yao, 2001)

<sup>24</sup> (Zotев, Phillips, et al., 2014a)



and fMRI features. This decrease of performance can also be explained as being part of the U-shaped learning curve<sup>25</sup>: by trying new regulation strategies, the cognitive load of the subject suddenly increases and results in a temporary loss of performance. However, it is not yet known how this applies to bimodal NF. Our results thus open interesting questions on how subjects learn to regulate a bimodal NF and on how to define the EEG and fMRI features so that they are complementary enough. The assessment of this complementarity can be based on studies and methods investigating the coupling between BOLD and EEG signal<sup>26</sup> which generally report that BOLD is negatively correlated with low-frequency EEG bands ( $\alpha$ ,  $\beta$ ) and positively correlated with high-frequency EEG bands ( $\gamma$ ). Besides these questions on the learning mechanisms and the inner definition of the features, our observations also raise the issue of whether the two NF signals should be made discriminable or not by the feedback metaphor. Indeed, if the subject was not able to discriminate between both signals, he/she might be less likely to control one signal more than the other.

Feedback design is an important aspect of a neurofeedback protocol and the optimal form of feedback for unimodal NF is still an ongoing topic of research<sup>27</sup>. Though the traditional thermometer metaphor<sup>28</sup> can appear boring for subjects, it has the advantage of being easy to understand. In their pioneering work, Zotev et al<sup>29</sup> have naturally extended the thermometer feedback to the bimodal NF case. We introduced a novel metaphor for EEG-fMRI-NF that integrates both signal into one single feedback in order for the subject to more easily perceive the bimodal NF task as one single regulation task. Though we did not compare our integrated metaphor with a non-integrated one, most of our participants reported that it felt like they had one task to do during bimodal NF. Having two separate feedbacks to control and thus two separate targets to achieve could increase the cognitive load, which is an important aspect of the NF process<sup>30</sup>. Integrating both NF signals in one single feedback can be a way to relieve the cognitive load of the subject. One of the difficulty in combining both NF signals in a single feedback is that EEG and fMRI do not have the same sampling rate. In the present study, the fact that the update rates of the EEG and fMRI dimensions were different might have been disturbing for the participants. Indeed, five participants found that fMRI update rate was slow (16 times slower than EEG). Bringing the EEG and fMRI update rates closer is therefore advisable for future experiments. However, for fMRI, the update rate is constrained by the TR, which cannot be brought much below 1 second. One way to prevent the subject from being disturbed by the different update rates of the two modalities could be to mix the two NF signals in a feedback that would not allow the subject to discriminate between the two signals, like a one-dimensional feedback. Besides the representative advantage of using an integrated feedback metaphor, we believe that it makes it possible to define a truly integrated NF target that would reward brain patterns defined from both modalities. There is different level of “integration” of EEG and fMRI data. In our study, we integrated the two neurofeedback signals in one feedback metaphor in order to provide a bimodal neurofeedback. A more advanced way to provide an integrated bimodal feedback could be to use EEG-fMRI integration methods<sup>31</sup>, such as fMRI-informed EEG analysis, EEG-informed fMRI analysis, or EEG-fMRI fusion. However, despite the wide range of existing methods, these methods are mostly designed for offline use and there is no prospect yet of

<sup>25</sup> (Carlucci & Case, 2013; Gaume et al., 2016)

<sup>26</sup> (Formaggio et al., 2010; Yin, Y. Liu, & Ding, 2016; Murta, Leite, et al., 2015; Yuan, T. Liu, et al., 2010; Murta, Chaudhary, et al., 2016; Dong et al., 2014)

<sup>27</sup> (Cohen et al., 2016)

<sup>28</sup> (Sitaram, Zhang, et al., 2007)

<sup>29</sup> (Zotev, Phillips, et al., 2014a)

<sup>30</sup> (Gaume et al., 2016)

<sup>31</sup> (Sulzer et al., 2013; Jorge, Van der Zwaag, & Figueiredo, 2014)

doing this integration online. In the framework of EEG-fMRI-NF, one could benefit from using these methods offline to study the effects of neurofeedback, guide the choice of the NF features, learn priors for a reconstruction model, learn a predictive<sup>32</sup> or a coupling model.

<sup>32</sup> (Meir-Hasson, Kinreich, et al., 2013)

It is important to stress that in our experiment unimodal and bimodal NF targets were different. The EEG-fMRI-NF target was probably “harder” to reach than the EEG-NF or the fMRI-NF target, as subjects needed to regulate EEG and fMRI simultaneously to reach the target. Thus, by directly integrating the EEG and fMRI NF signals without any fancy fusion technique, brain patterns defined this way from both modalities should already be more specific than those defined from one modality alone. Future experiments involving more subjects and other cognitive tasks will allow to characterize more precisely how EEG and fMRI are modulated in different unimodal and bimodal NF conditions. Eventually, the use of offline EEG-fMRI integration techniques should help understand how to define bimodal EEG-fMRI-NF protocol that make the most of both modalities for therapeutic applications such as stroke, depression, and other psychiatric and neurological disorders.

#### 5.4 CONCLUSION

In this study, we compared for the first time the effects of unimodal EEG-NF and fMRI-NF versus bimodal EEG-fMRI-NF by looking both at EEG and fMRI motor-related activations. We have found that participants were able to regulate MI-related hemodynamic and electrophysiological activity during unimodal EEG-NF and fMRI-NF and during bimodal EEG-fMRI-NF. Notably, we found that MI-related hemodynamic activity was higher during EEG-fMRI-NF than during EEG-NF, unlike fMRI-NF. This result suggests that EEG-fMRI-NF could be more specific or more engaging than EEG-NF alone. We have also observed that during EEG-fMRI-NF one modality could be more regulated than the other, suggesting the existence of self-regulating processes that would be proper to bimodal NF training. Taken together our results shed first light on the added-value of bimodal EEG-fMRI-NF compared to unimodal EEG-NF and fMRI-NF and confirm the interest of the bimodal approach. They also raise interesting questions on the specific mechanisms that might be at stake when subjects learn to regulate a bimodal NF signal and suggest potential for further research.



*"Learning is not a process of accumulation of representations of the environment ; it is a continuous process of transformation of behavior through continuous change in the capacity of the nervous system to synthesize it."*

— Humberto Maturana

*Prelude* By exploiting the complementarity of EEG and fMRI, bimodal EEG-fMRI-NF opens a spectrum of possibilities for defining robust, flexible and more effective NF protocols. However facing this greater amount of information, the question arises of how to integrate and represent the EEG and fMRI information in order to derive a single feedback. In this chapter, we introduce two integrated feedback strategies for EEG-fMRI-NF and study their effects on a motor imagery task with a between group design. Our integrated feedback strategies allow to represent EEG and fMRI in a single feedback instead of representing them in two separate feedbacks, which we assume is suboptimal both in terms of the subject's cognitive load and of the potential for bimodal NF target definition. The first integrated feedback strategy consists in a two-dimensional (2D) plot in which each dimension depicts the information from one modality. The second integrated feedback strategy consists in a one-dimensional (1D) gauge that integrates both types of information even further by merging them into one. We evaluate the two integrated feedback strategies in terms of how well they allow participants to regulate EEG and fMRI.

## 6.1 INTRODUCTION

EEG and fMRI share mutual information yet also contain important singularities, and their overlap is hard to predict. The information coming from EEG and fMRI would therefore benefit from being integrated in order to be used as an efficient feedback. Yet integrating both is a real challenge<sup>1</sup>. Multimodal data integration methods are categorized as asymmetrical (EEG-informed fMRI, fMRI-informed EEG) and symmetrical (data fusion, model-driven or data-driven)<sup>2</sup>. For NF purpose the integration method should be applicable in real-time. As illustrated by [Figure 43](#), the integration of multimodal data can theoretically be made at different levels: the raw measures level, the features level (high level or multivariate), the NF signal level or the feedback level<sup>3</sup>. It is also possible not to integrate EEG and fMRI data and simply show them as two separate/parallel/concurrent feedbacks but we argue that this might be sub-optimal (see below).

Integrating EEG and fMRI at the measures level in real-time does not seem feasible due to the considerable amount of information that it would represent. In hybrid BCI, output of different classifiers are usually passed to a meta-

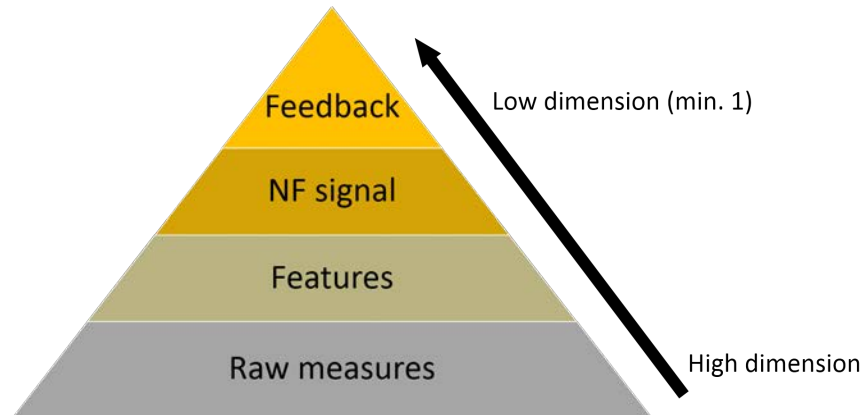
This work will be submitted in a very near future to a peer-review journal.

<sup>1</sup> (Biessmann et al., 2011; Jorge, Van der Zwaag, & Figueiredo, 2014; Fazli, Dahne, et al., 2015; Lahat, Adali, & Jutten, 2015)

<sup>2</sup> (Biessmann et al., 2011; Jorge, Van der Zwaag, & Figueiredo, 2014; Lahat, Adali, & Jutten, 2015; Vince D. Calhoun & Sui, 2016)

<sup>3</sup> (Fazli, Dahne, et al., 2015)

Figure 43 – Possible levels of integration of multimodal information for multimodal NF



<sup>4</sup> (Fazli, Mehnert, et al., 2012; Fazli, Dahne, et al., 2015)

<sup>5</sup> (Krause et al., 2017; Stoeckel et al., 2014; Sollfrank et al., 2016; Darvishi et al., 2017; Ono et al., 2014; Jeunet et al., 2015; Kaufmann & Williamson, 2011)

<sup>6</sup> (Zotev, Phillips, et al., 2014a)

<sup>7</sup> (Gaume et al., 2016)

classifier<sup>4</sup>. In NF it is less common to use a classifier. The feature usually directly constitutes the NF signal. Integrating the EEG and fMRI features at the feedback level is simple, yet could already be powerful. In unimodal NF/BCI studies, few studies have investigated the effect of the feedback representation<sup>5</sup>. In the case of bimodal NF, feedback design might be even more critical as there is more information to display and as the EEG and fMRI bits of information have different spatio-temporal dynamic properties. To our knowledge, no previous work has investigated how to represent both signals and how the representation would affect the simultaneous performance on the EEG and fMRI features. The way both information are represented might have strong implications. For example having an integrated NF target or two separate (concurrent) NF targets for EEG-fMRI-NF, and representing both EEG and fMRI information with one or two degrees of freedom might have significant impact on the way subjects learn to regulate both information at the same time.

In their pioneering work Zotev et al. naturally extended the classical thermometer feedback strategy to the bimodal NF case by juxtaposing two feedback gauges, one for EEG and one for fMRI<sup>6</sup>. Though this has the advantage to clearly and fully represent both features, this could suffer from a few drawbacks. First, it can be hard for the subject to concentrate on both gauges which would not be optimal regarding the subject cognitive load<sup>7</sup>. Also it can be misleading if the subject tries to interpret how both features evolve in time, especially when they go in opposite directions (inconsistencies). Also the fact that the representations of both signals are separated seem to imply that there are two targets to reach. Therefore the regulation task might be perceived by the subject as two simultaneous regulation tasks instead of one. Last, it does not exploit the possibility of using a NF target defined by the state of both features. In contrast, an integrated feedback would represent both EEG and fMRI on a single feedback representation and would have only one NF target characterized by the state of both signals.

In this study, we introduce two integrated feedback strategies (illustrated in Figure 44) for EEG-fMRI-NF and study their effects with a between-group design on a motor-imagery task. The first integrated feedback strategy consists in a *two-dimensional* plot in which each dimension depicts the information from one modality. The second integrated feedback strategy consists in a *one-dimensional* gauge that merges both information into one and therefore has a

higher degree of integration than the bi-dimensional feedback.

## 6.2 MATERIAL AND METHODS

The study was conducted at the Neurinfo platform (CHU Pontchaillou, Rennes, France) and was approved by the Institutional Review Board. Twenty right-handed NF-naive healthy volunteers with no prior MI-NF experience (mean age:  $35 \pm 10.6$  years, 10 females) participated in the study. Participants were randomly assigned to the bi-dimensional (BI\_DIM; mean age:  $37 \pm 14$  years, 5 females) or to the uni-dimensional (UNI\_DIM; mean age:  $33 \pm 6.2$  years, 5 females) group. Throughout the whole experiment, the participants were lying down in the MR bore and wearing a 64 channel MR-compatible EEG cap.

### 6.2.1 *Experimental protocol*

After signing an informed consent form describing the MR environment, the participants were verbally informed about the goal of the study and of the protocol. They were instructed that during the NF runs, they would be presented with a ball moving in two dimensions (for the BI\_DIM group) or in a one-dimensional gauge (for the UNI\_DIM group) according to the activity in their motor regions as measured with EEG and fMRI (see Figure 44). We introduced the bi-dimensional feedback in a previous work (Perronnet, Lécuyer, Mano, et al., 2017) and propose here an upgraded version in which the plot background delineates regions that indicate preferred direction of effort, encouraging the subject to regulate EEG and fMRI equitably. Participants were told that they would have to bring the ball closer to the darker blue areas by imagining clenching their right-hand. This instruction was reminded in written form on the screen at the beginning of each NF run. More specifically we explained the participants that they would need to perform kinesthetic motor imagery (kMI) (Neuper, Scherer, et al., 2005) of their right-hand in order to control the ball. Kinesthetic motor imagery was defined as trying to feel the sensation of the motion rather than only visualizing it. Participants were informed about the nature of EEG and fMRI signal, and specifically about the 4-6 seconds delay of the hemodynamic response. Additionally, for participants in the BI\_DIM group, we explained them that EEG was represented on the left axis while fMRI was represented on the right axis. This implied that when the ball would be on the left side, it would mean that they are controlling more EEG than fMRI, and on the opposite when the ball would be on the right side it would mean that they are controlling fMRI more than EEG. We told them that they should try to control both dimensions, i.e. try to move the ball near the diagonal. These instructions were given verbally at the beginning of the experiment and reminded later if the participant asked for it. Participants were asked not to move at all, especially during the course of a run. Video monitoring of the inside of the MR tube allowed to check for whole-body movements of the participant.

After receiving the instructions and having the EEG cap setup on his/her scalp, the participant was installed in the MR tube where we checked the electrodes impedances one last time in the supine position. The experimental protocol then consisted of: a structural 3D T<sub>1</sub>; a preliminary MI run without NF

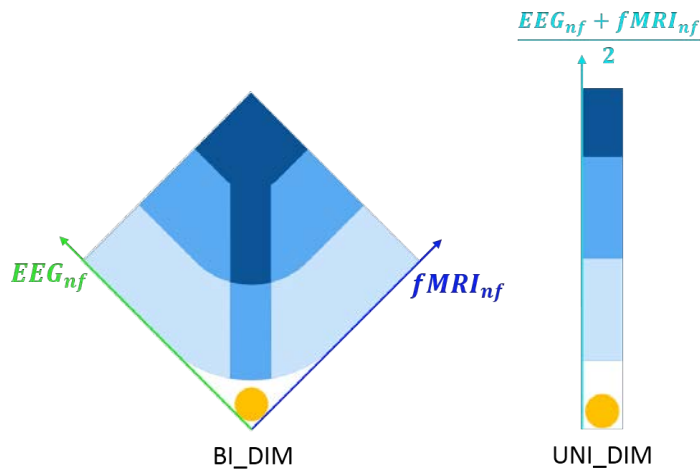


Figure 44 – Integrated feedback display for each group. For the BI\_DIM group, feedback consisted of a ball moving in two dimensions, the left dimension representing the EEG feature and the right dimension representing the fMRI feature. For the UNI\_DIM group, feedback consisted of a ball moving in one dimension for the UNI\_DIM group. Participants were instructed to get the ball closer to the darker blue areas by performing kinesthetic motor imagery of their right hand clenching.

(MI\_pre), the data of which was used to calibrate the NF target (see Section 6.2.4); three NF runs with a one minute break in between each; a post MI run without NF (MI\_post). The five EEG-fMRI functional runs employed a block-design alternating 8 times 20s of rest and 20s of task (see Figure 45).

Figure 45 – The experimental protocol consisted of 5 EEG-fMRI runs: a preliminary motor imagery run without NF (MI\_pre) used for calibration, three NF runs (NF1, NF2, NF3), and a post motor imagery run without NF (MI\_post). Each run consisted of a block design alternating 8 times 20s of rest and 20s of task.



During rest, the screen displayed a white cross and participants were asked to concentrate on the cross and not on the passed or upcoming task block. During task, the screen displayed the cue "Imagine right" as well as the feedback during NF runs. The feedback consisted of a yellow ball moving in a two-dimensional plot for the BI\_DIM group or in a one-dimensional gauge for the UNI\_DIM group. The participants were instructed to bring the ball closer to the darker blue area by performing kinesthetic motor imagery of their right hand clenching. The EEG feature was defined as the event-related desynchronization (ERD) (Pfurtscheller & Lopes da Silva, 1999) in the [8-30Hz] band of the EEG data filtered with a subject specific spatial filter (see Section 6.2.4 and 6.2.3) and was updated every 250ms. The fMRI feature was defined as the mean BOLD in a subject-specific motor region-of-interest (ROI) (see Section 6.2.4 and 6.2.3) and was updated at every repetition time (TR=1s). For the UNI\_DIM group, the ball position was the average of the EEG and fMRI features  $(EEG_{nf} + fMRI_{nf})/2$ . For the BI\_DIM group, the right axis depicted the normalized fMRI feature while the left axis depicted the normalized EEG feature. At the end of the experiment, the participants were asked to fill out a questionnaire about their perceived performance, motivation, fatigue, interest and difficulty in performing the NF task. Figure 45 illustrates the experimental protocol.

### 6.2.2 Data acquisition

EEG and fMRI data were simultaneously acquired with a 64-channel MR-compatible EEG solution from Brain Products (Brain Products GmbH, Gilching, Germany) and a 3T Verio Siemens scanner (VB17) with a 12channel head coil. Foam pads were used to restrict head motion. EEG data was sampled at 5kHz with FCz as the reference electrode and AFz as the ground electrode. fMRI acquisitions were performed using echo-planar imaging (EPI) with the following parameters: repetition time (TR) / echo time (TE) = 1000/23ms, FOV =  $210 \times 210 \text{mm}^2$ , voxel size =  $2 \times 2 \times 4 \text{mm}^3$ , matrix size =  $105 \times 105$ , 16 slices, flip angle =  $90^\circ$ . Visual instructions and feedback were transmitted using the NordicNeuroLab hardware and presented to the participant via an LCD screen and a rear-facing mirror fixed on the coil. As a structural reference for the fMRI analysis, a high resolution 3D T1 MPRAGE sequence was acquired with the following parameters: TR/TI/TE = 1900/900/2.26ms, GRAPPA 2, FOV =  $256 \times 256 \text{mm}^2$  and 176 slabs, voxel size =  $1 \times 1 \times 1 \text{mm}^3$ , flip angle =  $90^\circ$ . Our multimodal EEG/fMRI-NF system (Mano et al. 2017) integrates EEG and fMRI data streams via a TCP/IP socket. The EEG data is pre-processed with BrainVision Recview (Brain Products GmbH, Gilching, Germany) software for gradient and ballistocardiogram (BCG) artifact correction (see Section 6.2.3) and sent to Matlab (The MathWorks, Inc., Natick, Massachusetts, United States) for further processing. The fMRI data is pre-processed online for slice-time correction and motion correction with custom Matlab code adapted from SPM8 (FIL, Wellcome Trust Centre for Neuroimaging, UCL, London, UK). EEG and fMRI NF features are then computed and translated as feedback with Psychtoolbox (Kleiner et al., 2007).

### 6.2.3 Real-time data processing

During NF runs, online gradient artifact correction and BCG correction of the EEG data were done in BrainVision Recview (Brain Products GmbH, Gilching, Germany) software. The gradient artifact correction in Recview is based on the average artifact subtraction method (Allen, Josephs, & Turner, 2000). We used an artifact subtraction template of 2000ms and 4 templates for template drift correction. The data was then down-sampled to 200Hz and low pass filtered at 50 Hz (48 db slope) with a Butterworth filter. The data were subsequently corrected for BCG artifact (Allen, Polizzi, et al., 1998). The pulse model was searched in the first 15 seconds of the data. The pulse detection was based on a moving template matching approach with minimal pulse period of 800ms, minimum correlation threshold of 0.7, and amplitude ratio range from 0.6 to 1.2 relative to the pulse model. For pulse correction, a moving template was computed by averaging the 10 previously detected pulses, and the correction was done on a window length of [-1000ms, 700ms] relatively to the R-peak. This corrected data was then sent to Matlab for feature extraction. The corrected data was filtered with the subject specific spatial filter *FILT* computed during the calibration phase (see Section 6.2.4). The band power in the [8-30Hz] band was then computed on this filtered data using the periodogram and a 2s window size, and it was normalized with the following ERD-like (Pfurtscheller & Lopes da Silva, 1999) formulae:  $EEG_{nf}(t) = reverse \times (\overline{bp(prev\_rest)} -$

$bp(t))/\overline{bp(\text{prev\_rest})}$  where  $bp(t)$  is the power at time  $t$ ,  $\overline{bp(\text{prev\_rest})}$  is the average power over the previous rest block (values between the fourteen and the nineteen seconds) and  $reverse = 1$  if the selected filter  $FILT = f_{rest>task}$  or the default filter (laplacian around C3), or  $reverse = -1$  otherwise. Finally, the EEG feature was smoothed over the last four values, divided by  $EEG_{tresh}$  (see Section 6.2.4) and translated as visual feedback every 250ms.

$$EEG_{nf}(t) = reverse \times \frac{\overline{bp(\text{prev\_rest})} - bp(t)}{\overline{bp(\text{prev\_rest})}}$$

$$fMRI_{nf}(v) = \frac{B_{roi}(v)}{\overline{B_{roi}(\text{prev\_rest})}} - \frac{B_{bg}(v)}{\overline{B_{bg}(\text{prev\_rest})}}$$

The fMRI signal was pre-processed online for motion correction, slice-time correction and then the fMRI NF feature was computed according to the following definition:  $fMRI_{nf}(v) = B_{roi}(v)/\overline{B_{roi}(\text{prev\_rest})} - B_{bg}(v)/\overline{B_{bg}(\text{prev\_rest})}$  where  $B_{roi}(v)$  (respectively  $B_{bg}(v)$ ) is the average BOLD signal in the ROI (respectively in the background (BG)) at volume  $v$ , and  $\overline{B_{roi}(\text{prev\_rest})}$  (respectively  $\overline{B_{bg}(\text{prev\_rest})}$ ) is the ROI (respectively BG) baseline obtained by averaging the signal in the ROI (respectively in the BG) from the fourteenth to the nineteenth second (to account for the hemodynamic delay) of the previous rest block. The background was defined as a large slice (slice 6 out of 16) in deeper regions and used to cancel out global changes. Finally the fMRI feature was smoothed over the last three volumes, divided by  $fMRI_{tresh}$  (see Section 6.2.4) and translated as visual feedback every 1s.

#### 6.2.4 Calibration phase

In order to define subject-specific NF features, right at the end of the MI\_pre run, the MI\_pre EEG and fMRI data were pre-processed and analyzed to extract a spatial filter  $FILT$  and a threshold  $EEG_{tthresh}$  for the EEG NF feature as well as a BOLD ROI and a threshold  $fMRI_{tthresh}$  for the fMRI NF feature.

##### 6.2.4.1 EEG calibration

Right at the end of the MI\_pre run, the MI\_pre data was pre-processed similarly to what was done in real-time (see Section 6.2.3) except that the BCG correction was done semi-automatically. Using the Common Spatial Pattern (CSP) method (Ramoser, Müller-Gerking, & Pfurtscheller, 2000), we then computed the pairs of spatial filters that best maximized the difference in [8-30Hz] power between rest and task blocks on 18 channels located over the motor regions (C3, C4, FC1, FC2, CP1, CP2, FC5, FC6, CP5, CP6, C1, C2, FC3, FC4, CP3, CP4, C5, C6). The first filter  $f_{rest>task}$  of the pair maximizes the power during the rest blocks while the second filter  $f_{task>rest}$  of the pair maximizes the power during the task blocks. If the eigenvalue of  $f_{rest>task}$  was greater than the inverse of the eigenvalue of  $f_{task>rest}$  (Blankertz et al., 2008), then the subject-specific filter  $FILT$  was set to  $f_{rest>task}$ , otherwise it was set to  $f_{task>rest}$ . In case the CSP filter did not look satisfactory (visual inspection to see if the MI\_pre data filtered was correlated with the task), we used a laplacien filter over C3 instead (Nunez, Srinivasan, et al., 1997). The ERD feature was then computed (see Section 6.2.3) and the threshold for the EEG NF was set by computing the ERD threshold that was reached at least 30% of the time.



#### 6.2.4.2 fMRI calibration

MI\_pre fMRI data was pre-processed for slice-time correction, spatial realignment and spatial smoothing with a 6mm Gaussian kernel with SPM8. A first-level general linear model (GLM) analysis modeling the task and the rest was then performed. The fMRI ROI was defined by taking a  $9 \times 9 \times 3$  box around the maximum of activation (constrained to the left motor area) of the thresholded T-map ( $task > rest$ ,  $p < 0.001$ ,  $k > 10$ ). The fMRI feature was then computed on this MI\_pre data (see Section 6.2.3) and the threshold for the fMRI NF was set by computing the value that was reached at least 30% of the time.

#### 6.2.5 Offline analysis

##### 6.2.5.1 EEG analysis

For offline analysis, EEG signal was pre-processed similarly to what was done in real-time (see Section 6.2.3) except that the BCG correction was done semi-automatically.

To analyze how the participants regulated their EEG NF feature, we re-computed the ERD values on offline pre-processed data filtered with the online *FILT* as defined in 6.2.3 except that the baseline was not computed sliding-block-wise, but instead by averaging power values after the first second and before the nineteenth second of all rest blocks. We refer to this feature as "online ERD".

As the amount of calibration data was limited and as participants had no prior MI training, it is possible that the filter from the calibration was suboptimal. Therefore we also extracted the ERD values on data filtered with a posthoc *FILT*. We refer to this feature as "posthoc ERD". The posthoc *FILT* was computed the same way as the online *FILT* (see Section 6.2.4) except that it was computed on the concatenation of MI\_pre, NF1, NF2 and NF3 instead of MI\_pre only.

For statistical analysis, the ERD values were standardized to z-scores by considering for each subject their mean and standard deviation over MI\_pre, NF1, NF2, NF3, MI\_post. For each run the standardized ERD values were averaged by considering the values between the first and the nineteenth second of all NF blocks but the first. The mean ERD over NF1, NF2 and NF3 was averaged to get the mean NF ERD  $\bar{NF}$ . We also considered  $\max_i NF_i$  the best mean ERD over the three NF runs. We refer to the best NF run regarding the EEG feature as  $\max NF_{\text{eeg}}$ .

##### 6.2.5.2 fMRI analysis

The fMRI data from each of the five runs (MI\_pre, NF1, NF2, NF3, MI\_post) was pre-processed and analyzed with AutoMRI (Maumet, 2013), a proprietary software for fMRI analysis automation based on SPM8. Pre-processing included slice-time correction, spatial realignment, co-registration to the 3D T1, followed by spatial smoothing with a 8 mm Gaussian kernel. A first-level and second-level general linear model (GLM) analysis was performed. The first-level GLM included the canonical HRF for the task as well as its temporal and dispersion derivatives. For the second-level GLM analysis, the individual data were normalized to the Montreal Neurological Institute (MNI) template and grouped

using a mixed effects linear model. The activation maps were corrected for multiple comparisons using Family-Wise error (FWE) correction ( $p < 0.05$  with cluster size  $> 10$  voxels).

To analyze how the participants regulated the BOLD signal in the *online ROI*, we extracted the ROI percent signal change (PSC) on offline pre-processed data. For each participant and each run, the registered fMRI values were high-pass filtered (100 seconds) to remove the linear drift, averaged in the online ROI and transformed into PSC using the formulae  $(B_{roi}(v) - m)/m$  where  $m$  is the average of  $B_{roi}$  values from the fourteenth to the nineteenth second. We refer to this feature as "online PSC".

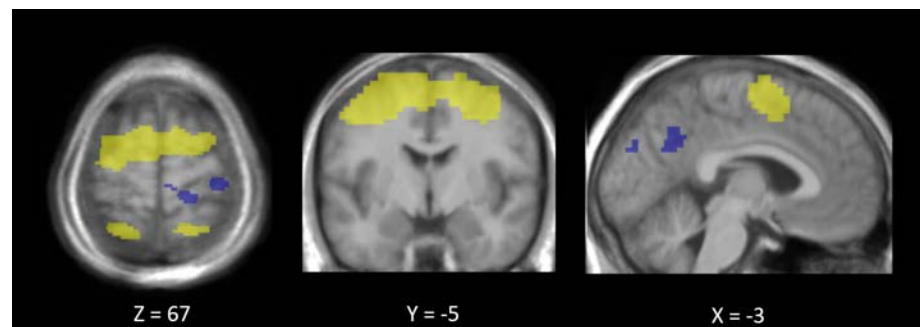
Because NF training affects patterns beyond the one being fed back (Wander et al., 2013; Kopel et al., 2016), the same procedure was done to extract the PSC in a *posthoc ROI* defined by computing individually an average activation map over NF1, NF2 and NF3 and taking a  $9 \times 9 \times 3$  box around the maximum of activation (constrained to the left motor area). We refer to this feature as "posthoc PSC". Finally the PSC values were standardized to z-scores by considering for each subject their mean and standard deviation over MI\_pre, NF1, NF2, NF3, MI\_post. For each run the standardized PSC values were averaged across the last 16 volumes of all NF blocks but the first. The mean PSC over NF1, NF2 and NF3 was averaged to get the mean NF PSC  $\overline{NF}$ . We also considered  $\max_i NF_i$  the best mean PSC over the three NF runs. We refer to the best NF run regarding the fMRI feature as  $\max NF_{fMRI}$ .

#### 6.2.5.3 Statistical analysis

For each group (UNI\_DIM / BI\_DIM), each modality (EEG/fMRI) and level of feature (online/posthoc) we conducted non-parametric Friedman tests of the differences among MI\_pre,  $\overline{NF}$ , MI\_post, as well as Wilcoxon signed-rank tests between  $\overline{NF}$  and MI\_pre and Wilcoxon signed-rank tests (signrank Matlab function) between  $\max_i NF_i$  and MI\_pre with Bonferroni correction (corrected p-value:  $0.05/3$  conditions =  $0.0167$ ). For between group comparison we computed a Wilcoxon test (ranksum Matlab function, equivalent to Mann-Whitney U-test) on  $\overline{NF}$ . The tests were done both for the online PSC and for the posthoc PSC.

## 6.3 RESULTS

Figure 46 – Average activations (in yellow) and deactivations (in blue) over the three NF runs (NF1+NF2+NF3) in both groups (UNI\_DIM + BI\_DIM) thresholded at  $p < 0.05$  FWE corrected



GLM analysis of both groups (UNI\_DIM + BI\_DIM) revealed activations during NF (see Figure 46) in : bilateral premotor cortex (BA 6) including left and right supplementary motor area (SMA), left and right inferior frontal gyrus (pars opercularis rolandic operculum) (BA 44), left and right inferior parietal lobule (IPL), left and right superior parietal lobule (SPL), left and right supra-marginal lobule/gyrus (BA 40,BA 2,BA 48), left and right superior parietal (BA 7, BA 5), bilateral mid-cingulate cortex, left and right precuneus (BA 7). Deactivations were observed in right primary motor cortex (M1), left and right angular gyrus (BA 39), right cuneus (BA 18), left and right precuneus, left middle occipital (BA 10) and in the left inferior parietal lobule (BA 19).

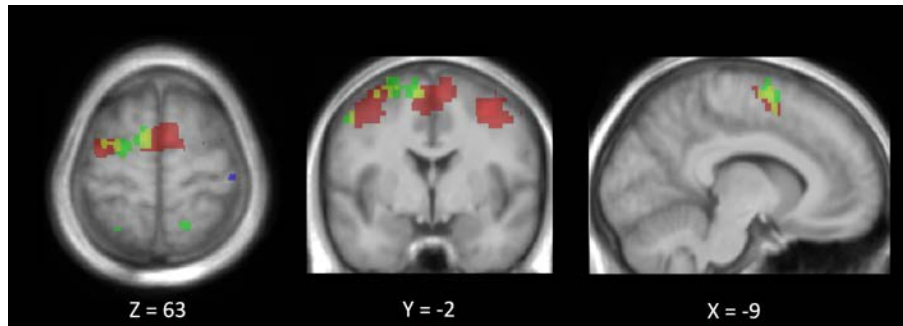


Figure 47 - Average activations over the three NF runs (NF1+NF2+NF3) in each group thresholded at  $p < 0.05$  FWE corrected. Activations of the UNI\_DIM group are shown in red. Activations of the BI\_DIM are shown in green, deactivations of the BI\_DIM group are shown in blue. Yellow corresponds to activations common to UNI\_DIM and BI\_DIM

GLM analysis of the BI\_DIM group during NF revealed activations in (figure 47): Left PMC (BA 6) including SMA, left IPL (BA 40), left SPL (BA 7), right SPL (BA 5, BA 7), right superior occipital (BA 7). Deactivations were observed in right M1, (BA 4), left IPL (BA 19). GLM analysis of the UNI\_DIM group during NF revealed activations in (Figure 47): left and right PMC (BA 6) including left and right SMA, left IPL (BA 40), left superior parietal lobule (BA 40), left and right supra-marginal lobule (BA 2). Deactivations were observed in the right angular gyrus (BA 39).

The BI\_DIM group showed more activations ( $p < 0.001$ , uncorrected) than the UNI\_DIM group in the right superior parietal lobule (BA 7).

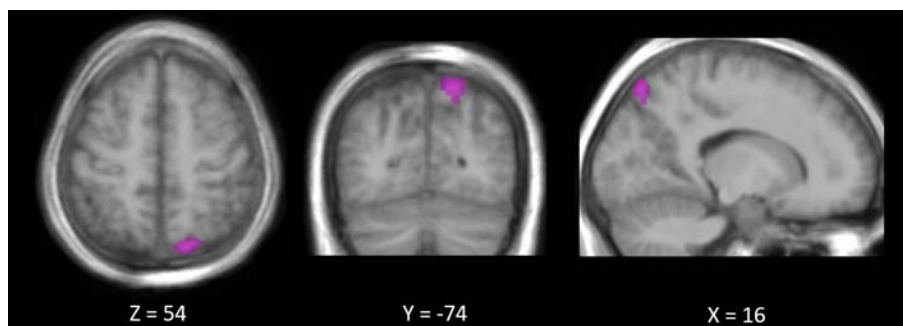


Figure 48 - Group-difference : BI\_DIM > UNI\_DIM thresholded at  $p < 0.001$  uncorrected. The BI\_DIM activated more the right superior parietal lobule (BA7).

Friedman tests between MI\_pre,  $\overline{NF}$  and MI\_post were significant for posthoc EEG in the BI\_DIM group ( $p = 0.045$ ,  $\chi^2(2, 10) = 6.2$ ) and for posthoc fMRI in the BI\_DIM group ( $p = 0.0136$ ,  $\chi^2(2, 10) = 8.6$ ).

Wilcoxon signed rank tests between MI\_pre and maxNF were significant for: online EEG ( $p = 0.0098$ , signedrank = 52) and online fMRI ( $p = 0.0195$ , signe-

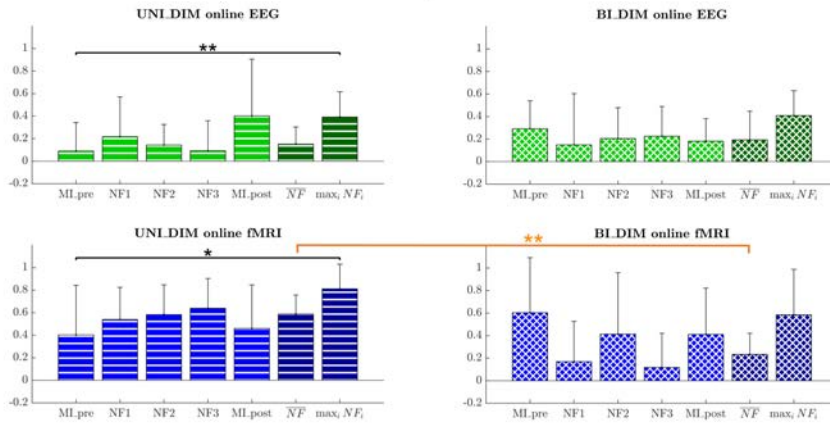
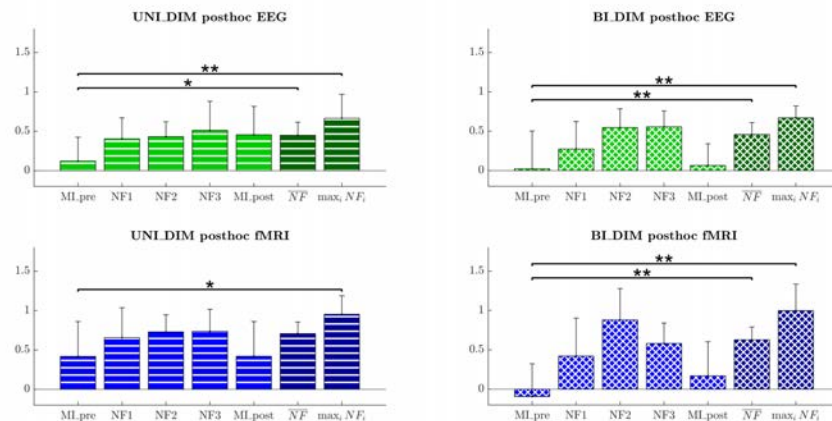


Figure 49 – Group means (EEG/fMRI, online, z-scored) on each run with standard deviation and significance of Wilcoxon tests

drank = 50) in the UNI\_DIM group; posthoc EEG ( $p=0.0020$ , signedrank =55) and posthoc fMRI ( $p=0.0137$ , signedrank =51) in the UNI\_DIM group; and for posthoc EEG ( $p=0.0020$ , signedrank =55) and posthoc fMRI ( $p=0.0020$ , signedrank =55) in the BI\_DIM group. Wilcoxon signed rank tests between MI\_pre and NF were significant for: posthoc EEG ( $p=0.0195$ , signedrank = 50) in the UNI\_DIM group; posthoc EEG ( $p=0.0273$ , signedrank = 49) and posthoc fMRI ( $p=0.0039$ , signedrank = 54) in the BI\_DIM group. Results are summarized in figure 49 and figure 50. During the NF runs the fMRI PSC in the online ROI was significantly higher in the UNI\_DIM group than in the BI\_DIM group (Wilcoxon:  $z = 3.0615$ , ranksum = 146,  $p = 0.0022$ ).

Figure 50 – Group means (EEG/fMRI, posthoc, z-scored) on each run with standard deviation and significance of Wilcoxon tests



Questionnaire : In the BI\_DIM group 5 participants out of 10 found that the blocks were too short (against one who found them too long in the UNI\_DIM group), and 5 participants out of 10 found that the feedback was not a good indicator of their motor imagery (against 0 in the UNI\_DIM group).

## 6.4 DISCUSSION

In the present study we introduced and evaluated two integrated feedback strategies for EEG-fMRI-NF: a 2D plot in which EEG and fMRI are mapped onto each dimension, and a 1D gauge that integrates both information even more by merging them into one. In contrast to representing the EEG and fMRI features with two separate feedbacks, these integrated feedback strategies represent both information in a single feedback with a single NF target. They have the advantage to relieve the cognitive load of the subject, to represent the task has a single regulation task instead of two and to allow to define a NF target characterized by the state of both signals.

*Online and posthoc performance* Overall both strategies allowed participants to up-regulate MI-related EEG and fMRI patterns, as demonstrated by the higher posthoc EEG and fMRI activation levels during maxNF/NF compared to MI\_pre (see Figure 50). The improvement was even more significant on posthoc fMRI in the BI\_DIM group.

Online fMRI activation level during NF were significantly higher in the UNI\_DIM group than in the BI\_DIM group (figure 49) which showed particularly high variability among participants and NF runs. Though the UNI\_DIM worked better than the BI\_DIM regarding the regulation of the initial (online) targets, their performance was moderate. Indeed, the online activation level improvement with respect to MI\_pre was only significant for the UNI\_DIM group in the maxNF run (see Figure 49). The loss of performance on the online fMRI activation level during NF with a bi-dimensional feedback was also observed in our previous study (Perronnet, Lécuyer, Mano, et al., 2017). Our new results thus highlight the fact that the bi-dimensional feedback is harder to control than the uni-dimensional feedback and that this affects online EEG and fMRI activation levels differently, at least on a single-session basis. We hypothesize that this could be due to the higher complexity of the bi-dimensional feedback. This complexity comes from the fact that it has two degrees of freedom which have slightly different update rates (4 Hz and 1 Hz), whose relationship is non-trivial, and one of which is delayed from the other. Subjects therefore need more time to get acquainted with this more complex feedback. By allowing subjects to discriminate between the information coming from EEG and fMRI, the bi-dimensional feedback leads subjects to make interpretations about EEG and fMRI contingency. They might try different strategies and analyze how they affect both dimensions. In particular it can be disturbing when both dimensions seem to present inconsistencies. This could explain why half of the participants in the BI\_DIM group reported that the feedback was not a good indicator of their motor imagery. The hypothesis that the bi-dimensional feedback is more complex and therefore requires more habituation time is supported by the fact that half of the participants in the BI\_DIM group reported they found the training blocks too short (20 seconds) and by participants comments from the BI\_DIM group : *"it is hard to know which mental process will favor EEG activity and which one will favor fMRI activity", "the discrepancy between EEG and fMRI did not help to control the feedback given the small number of trials", "task blocks could have been longer to allow to test different strategies and observe their effect"*. The fact that the loss of performance affected more fMRI than EEG could mean

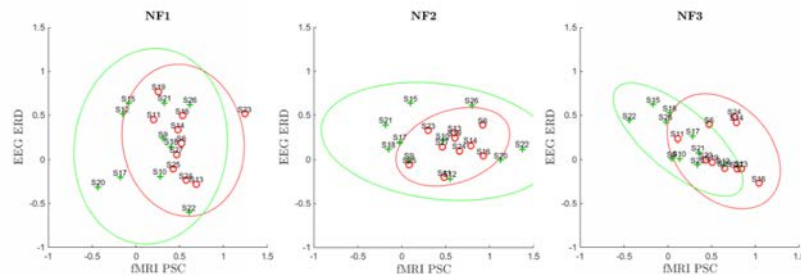


that they focused more on regulating the EEG because feedback from EEG is immediate while feedback from fMRI is delayed. Additionally this could also be due to the fact that the feedback was moving 4 times faster in the EEG dimension.

Looking at the opposite trend between the online and posthoc activation levels of both groups (i.e. higher online fMRI activation levels for UNI\_DIM and higher posthoc fMRI activation levels for BI\_DIM) suggests that participants in the BI\_DIM group could have moved further away from their initial MI\_pre calibration pattern than participants from the UNI\_DIM group. Though the 2D feedback is more complex, it seems to encourage participants to explore mental strategies, interpret their effects on the two feedback dimensions in order to find a strategy that allows to control both dimensions equitably. Training block length might benefit from being adapted to the feedback strategy, with shorter block for the 1D feedback and longer block for the 2D feedback to allow for the exploration and interpretation of inner strategies. The 1D strategy could be well suited during earlier phases of a NF program as it is easier to control, while the 2D strategy could prove valuable in the longer term to reach more specific self-regulation.

*Group distribution across the 3 NF runs* Looking at the distribution of online mean activation levels (figure 51) over the three NF runs shows how the two group populations evolved over the course of the training. In the first run, both populations were rather widespread and distributed along the EEG axis which suggests that participants started by exploring EEG. Participants from the BI\_DIM group were also slightly distributed along the fMRI axis in the first NF run. In the second NF run, both populations were spread along the fMRI axis, which suggests that participants explored fMRI while keeping EEG at a mean level. In the third run, both populations are spread along the central (0.5) isoline, which suggests that participants adopted a strategy that minimized the errors in both dimensions. Overall the progression look similar in both group but the BI\_DIM population is more widespread than UNI\_DIM in NF1 and NF2. This higher variability might once again be due to the higher complexity of the feedback to which participants need to get used.

Figure 51 – Individual means (online EEG ERD and fMRI PSC, z-scored) of all subjects during NF runs. Individuals from the UNI\_DIM group are shown in red. Individuals from the BI\_DIM group are shown in green. We can see how the groups evolved over the NF runs.



*Activation maps* BOLD activation maps show that during NF both groups significantly activated regions from the motor imagery network including premotor areas and posterior parietal areas (figures 47 and 46), as well as regions that have been shown to be consistently active during NF (Emmert, Kopel, Sulzer,



et al., 2016) (mid-cingulate (ACC), supra-marginal (temporo-parietal), dlPFC, premotor). Subcortical and cerebellar regions activations could not be identified as they were out of the field of view. The BI\_DIM group showed more activations ( $p < 0.001$ , uncorrected) than the UNI\_DIM group in the right superior parietal lobule (BA 7). The SPL plays an essential role in many cognitive, perceptive, and motor-related processes (Wang et al., 2015; Culham & Kanwisher, 2001). In particular it has been reported to be activated both during motor execution (ME) and MI (Solodkin et al., 2004; Raffin et al., 2012; Lotze & Halsband, 2006; Héту et al., 2013; Confalonieri et al., 2012; Sharma & Baron, 2013b; Fleming, Stinear, & Byblow, 2010) though greater activation has been observed during MI than ME (Gerardin et al., 2000; Hanakawa et al., 2002). The SPL is known to play a role in guiding motor activity in relation to spatial information (Buneo & Andersen, 2006; Wang et al., 2015; Culham & Kanwisher, 2001) and to be crucial in the generation of mental motor representations (Sirigu et al., 1996). Several studies have demonstrated that impairments to the parietal cortex reduced MI ability (Sirigu et al., 1996; Danckert et al., 2002; McInnes, Friesen, & Boe, 2016). A meta-analysis recently conducted to determine which neurologic disorders/lesions impair or restrict MI ability showed that patients with parietal lobe damage were most impaired (McInnes, Friesen, & Boe, 2016). In MI, the SPL is thought to play a role in facilitating the planning and coordination of imagined movements and/or in indirectly inhibiting M1 through its connection with the SMA (McInnes, Friesen, & Boe, 2016; Kasess et al., 2008; Solodkin et al., 2004). Activations in the SPL have been shown to be more active during visual imagery than during kinaesthetic imagery (Guillot et al., 2009). However we found no significant activation in the occipital regions as would be expected during visual imagery. Therefore it is unlikely that the SPL activation would indicate that participants in the BI\_DIM performed a motor imagery that would have been more visual than kinesthetic. The superior parietal cortex has also been demonstrated to be active during generalized neurofeedback when feedback is presented visually (Sitaram, Ros, et al., 2016; Emmert, Kopel, Sulzer, et al., 2016; Ninaus et al., 2013). However the fact that the SPL was more significantly active in the BI\_DIM group than in the UNI\_DIM group suggest that it is more than a generalized NF effect. This activation could result from both the overlap of the motor imagery task and the self-regulation process (Sitaram, Ros, et al., 2016), both of which could be more intense under the bi-dimensional condition.

Though not shown at the group comparison level, the overlay of UNI\_DIM activations and BI\_DIM activations (see Figure 47) shows that activations in the premotor areas were more widespread and bilateral in the UNI\_DIM group while they were more localized and lateralized to the left hemisphere in the BI\_DIM group. Also, the BI\_DIM group showed significant deactivations in the right primary motor cortex while the UNI\_DIM group did not. Overall, our results suggest that the bi-dimensional feedback triggered more specific activations than the uni-dimensional feedback.

*Defining bimodal NF targets* An integrated feedback allows to reward specific EEG/fMRI pair values and gives flexibility on the definition of the bimodal NF target, depending on the assumed spatio-temporal complementarity of the EEG and fMRI features. In this study, we designed the integrated strategies so that

subjects would have to regulate both EEG and fMRI at the same time in order to reach the NF target. This assumes that such a state is possible. Indeed, neuro-vascular studies show that the electrophysiological and hemodynamic activity are correlated (Formaggio et al., 2010; Gonçalves et al., 2006; Ritter, Moosmann, & Villringer, 2009; Zaidi et al., 2015; Murta, Leite, et al., 2015). For example, a study by (Zaidi et al., 2015) found significant correlations between hemodynamic peak-times of [HbO] and [HbR] signals with the underlying neural activity as measured with intra-cortical electrophysiology in primates, but not for their peak-amplitude. However depending on the type of tasks, the features, and the subjects, this might not necessarily be the case as illustrated in the study by De Vos et al. (De Vos et al., 2013) who reported no correlation between EEG and fMRI of a face processing task. Though it is hard to predict the degree of complementarity and redundancy of the EEG and fMRI features, it might be beneficial to take into consideration the degree of correlation of both features during the calibration phase.

Instead of defining the target on the "intersection" of the EEG and fMRI features, one could think of using a more laxist target defined by their "union", that is the target would be reached when the EEG target or the fMRI target is reached. Such a target would be easier to reach, therefore potentially less specific, but it might be advantageous in order to limit the user frustration when used at the beginning of a protocol for example. Also the "union" strategy could be used in case the EEG and fMRI features would be hardly redundant. This could happen if the mental process being regulated was more complex and involved for example a cognitive regulation and an emotional regulation aspect each of which would be associated to one of the feature. Moreover in the "union" strategy, one could imagine displaying a secondary reward when the pair of EEG and fMRI features would reach the intersection without "penalizing" the subject when he/she does not control for both.

## 6.5 CONCLUSION

Both groups showed higher posthoc EEG and fMRI activation levels during NF as compared to the preliminary condition. Our results demonstrate that integrated EEG-fMRI-NF enables to efficiently regulate EEG and fMRI simultaneously, even when EEG and fMRI are integrated in a 1D feedback. Our results also suggest that the 1D feedback is easier to control on a single-session, while the 2D feedback encourages subjects to explore their strategies to recruit more specific brain patterns.

## CONCLUSION AND PERSPECTIVES

*"We demand rigidly defined areas of doubt and uncertainty !"*  
 — Douglas Adams (The Hitchhiker's Guide to the Galaxy)

## 7.1 GENERAL CONCLUSION

EEG and fMRI are the two most widely used modalities in NF research. They are very much complementary in their advantages and drawbacks. Yet, in the context of NF, they have rarely been used in combination and EEG-NF and fMRI-NF have rarely been studied in regard to each other. Importantly, bringing these two complementary modalities together allows to question the actual limit or validity of standard unimodal NF approaches and understand how they can be improved. The theoretical part of this dissertation aimed at identifying methodological aspects that differ between EEG-NF and fMRI-NF and at examining the motivations and strategies for combining EEG and fMRI for NF purpose. Among these combination strategies, we chose to focus on bimodal EEG-fMRI-NF as it seemed to be one of the most promising approach and had been mostly unexplored. The experimental part of this dissertation therefore focused on the development and evaluation of methods for bimodal EEG-fMRI-NF.

**Chapter 3** In this chapter, we started by presenting general considerations about EEG and fMRI, namely when they should be acquired simultaneously, and how the electrophysiological and hemodynamic activities are known to be related. Next we drew up a methodological comparison of EEG-NF and fMRI-NF in order to identify important aspects that differ between the two. Eventually, we reviewed exhaustively the existing NF studies that have combined EEG and fMRI and we proposed a taxonomy of the different configurations for combining EEG and fMRI in NF studies. Out of this taxonomy, we opted for focusing on bimodal EEG-fMRI-NF as it is particularly promising and mostly unexplored. From the methodological comparison of EEG-NF and fMRI-NF we presented in [Section 3.3](#), one should retain that task design, task duration and the choice of features are key aspects to consider when designing bimodal EEG-fMRI-NF protocols.

**Chapter 4** Before being able to conduct bimodal EEG-fMRI-NF experiments, one is faced with the challenge of setting up a real-time EEG-fMRI experimental platform. If EEG-fMRI has become a relatively accessible technique, turning it into a bimodal NF loop able to acquire EEG and fMRI simultaneously, clean them from artifacts, extract features and communicate feedback to the subject in real-time is no easy task. In this chapter, we described a general method for building a real-time EEG-fMRI platform for bimodal NF experiments. Our goal was to share our experience in order to help other

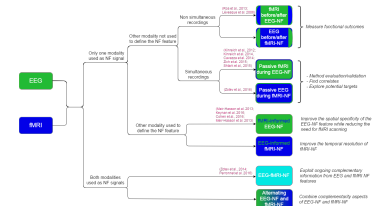


Figure 52 – In [Chapter 3](#) we proposed a taxonomy of EEG/fMRI NF studies.

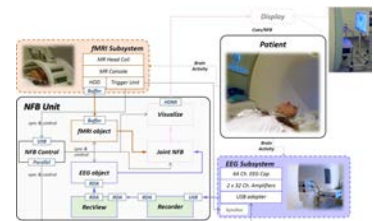


Figure 53 – In [Chapter 4](#) we described our real-time EEG-fMRI platform for bimodal NF.

researchers build fast and robust platforms, and also provide some minimal technical requirements or features to look for in future commercial systems. Based on those guidelines, we have implemented our own real-time EEG-fMRI platform for bimodal NF. This platform has served for the two experimental studies presented in this dissertation and will continue to be improved and used for experimental and clinical studies.

**Chapter 5** The goal of our first experimental study was to evaluate the added-value of bimodal EEG-fMRI-NF as compared to unimodal EEG-NF and fMRI-NF during a motor-imagery task. Healthy participants performed a MI task in three different NF conditions: EEG-NF, fMRI-NF and EEG-fMRI-NF. The conditions were evaluated in terms of activation levels of the MI-related hemodynamic and electrophysiological patterns. We have found that participants were able to regulate MI-related hemodynamic and electrophysiological activity during unimodal EEG-NF and fMRI-NF and during bimodal EEG-fMRI-NF. Notably, we found that MI-related hemodynamic activity was higher during EEG-fMRI-NF than during EEG-NF, unlike fMRI-NF. This result suggests that EEG-fMRI-NF could be more specific or more engaging than EEG-NF alone. We have also observed that during EEG-fMRI-NF subjects could regulate more one modality than the other, which suggests the existence of self-regulation processes that would be proper to bimodal EEG-fMRI-NF training. Our results therefore confirm the interest of the bimodal EEG-fMRI-NF approach and raise interesting questions on the specific mechanisms that might be at stake when subjects learn to regulate a bimodal EEG-fMRI-NF signal.

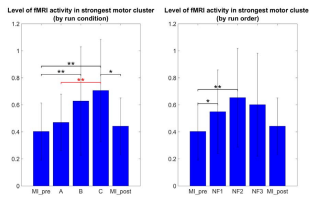


Figure 54 – In [Chapter 5](#), we showed that during a motor-imagery task, MI-related BOLD activity was higher during bimodal EEG-fMRI-NF than during EEG-NF.

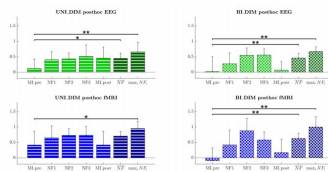


Figure 55 – In [Chapter 6](#), we showed that during a motor-imagery task, integrated EEG-fMRI-NF enables to efficiently regulate EEG and fMRI simultaneously.

**Chapter 6** In our second experimental study we introduced two integrated feedback strategies for EEG-fMRI-NF and studied their effects on a motor imagery task with a between-group design. The first integrated feedback strategy consisted in a two-dimensional (2D) plot in which each dimension depicts the information from one modality. The second integrated feedback strategy consisted in a one-dimensional (1D) gauge that integrates both types of information even more by merging them into one. Both groups showed higher posthoc EEG and fMRI activation levels during NF as compared to the preliminary condition. Our results thus demonstrate that integrated EEG-fMRI-NF enables to regulate EEG and fMRI simultaneously, even when EEG and fMRI are integrated in a 1D feedback. Our results also suggest that the 1D feedback is easier to control (at least on a single-session), while the 2D feedback encourages subjects to explore their strategies to find one that allows to control EEG and fMRI by recruiting more specific brain patterns.

## 7.2 PERSPECTIVES: VARIATIONS AROUND BIMODAL NF

### 7.2.1 Reinforce our findings

Future studies with more subjects, more NF sessions and targeting different brain patterns should allow to characterize more finely the added-value of bimodal EEG-fMRI-NF as compared to unimodal NF, delve more deeply into its specific mechanisms and see how this generalizes to different types of NF targets. Following up on the work we presented in [Chapter 5](#), it would be relevant

to evaluate the rest of the "*direct NF effect*" in order to confirm whether EEG-fMRI-NF allows to trigger stronger EEG activations than fMRI-NF and also to evaluate the "*compromise effect*" in order to figure out whether EEG-fMRI-NF allows to reach similar, lower or greater EEG activation level than EEG-NF (though generally this might be compromised by the fact that EEG SNR is better outside of the MR) and similar, lower or greater fMRI activation level than fMRI-NF. Questioning further the efficiency of the 2D integrated feedback, *using sham control* could allow to disentangle whether higher activation levels are a specific effect of the bimodal NF conveyed bi-dimensionally or a consequence of higher level of arousal/engagement due to the higher complexity of the feedback, or a combination of both. Conducting bimodal NF studies over multiple sessions will allow to *probe the bimodal learning curve*. We hypothesize that different bimodal learning scenarios are plausible, in particular the 2D integrated feedback might lead up to different scenarios in the way subject learn to control both signals.

### 7.2.2 Multi-sensory bimodal NF

The integrated feedback strategies that we proposed in this dissertation are conveyed through the visual modality. It would be interesting to investigate bimodal NF when conveyed through other types of sensory modalities, such as the auditory or tactile ones. Also, EEG and fMRI could be fed back using different sensory modalities<sup>1</sup>. For example EEG which is more transient and noisier could be fed back with auditory feedback while fMRI would be fed back with visual feedback. However, if the EEG and fMRI features are directly mapped onto each sensory modality, this would not allow to produce an integrated feedback as we defined in this dissertation.

<sup>1</sup> (Cohen et al., 2016)

### 7.2.3 Integrate EEG and fMRI at earlier stages of the NF loop

The work presented in this dissertation focused on the possibility of combining EEG and fMRI at the feedback level. In [Chapter 6](#), we briefly discussed other possible levels of integration of EEG and fMRI for bimodal NF. It would be interesting to investigate possibilities of integrating EEG and fMRI at the calibration phase or at earlier stages of the NF loop such as the feature level. A plethora of EEG-fMRI data integration/fusion methods have been described in the literature<sup>2</sup>. Asymmetrical methods which consist in using one modality to inform the other rely on the assumption that EEG and fMRI share common neuronal sources and therefore do not fully exploit their complementarity, which is what we are mostly looking for in bimodal NF. Among symmetrical methods, data-driven methods based for example on independent component analysis, partial least squares, or canonical correlation analysis are interesting in that they leverage fully the information from both modalities while making little assumptions about the nature of the underlying data. Such methods allow to explore potentially unpredictable patterns in the joint data and can be improved by incorporating spatial or temporal priors. However, none of the existing EEG-fMRI integration/fusion methods are currently applicable in real-time. The choice of an EEG-fMRI integration/fusion method that will be most useful for bimodal

<sup>2</sup> (Jorge, Van der Zwaag, & Figueiredo, 2014)

NF and its adaptation for real-time use will constitute a real challenge.

#### 7.2.4 *Mixed protocols*

Once the relative efficiency of unimodal and bimodal NF will be understood well enough, maybe it will be worth considering designing global NF programs that combine unimodal and bimodal NF training sessions. Such a program could for example 1) start with one or a few fMRI-NF session(s) which would allow the subject to develop a mental strategy to regulate a specific brain region, 2) then continue with one or a few EEG-fMRI-NF session(s) so that he/she can keep on practising regulating the fMRI feature while additionally trying to control simultaneously the EEG feature, 3) eventually end with enough EEG-NF sessions to consolidate the effects of the training.

#### 7.2.5 *Investigate other modality couples*

The reason why we focused on the combination of EEG and fMRI for bimodal NF in this dissertation is because these two modalities are most complementary in term of spatial and temporal properties. However, EEG could also be used in combination with fNIRS or MEG for bimodal NF. EEG-fNIRS-NF would be a cheaper and portable alternative to EEG-fMRI-NF. Another big advantage of EEG-fNIRS over EEG-fMRI is the absence of MR-related artifacts affecting the EEG. However EEG-fNIRS-NF would be limited to the surface of the cortex and would not benefit from the improved spatial resolution of EEG-fMRI-NF. It would be interesting to investigate how the motor-imagery based EEG-fMRI-NF protocol we introduced in this dissertation would transfer to EEG-fNIRS-NF.

#### 7.2.6 *Investigate other integrated feedback paradigms*

In this dissertation, we introduced the concept of integrated feedback assuming that representing EEG and fMRI with two separate visual feedbacks would be suboptimal in terms of cognitive load. In order to confirm that hypothesis, it would be necessary to compare our integrated feedback strategies with a separate feedback one.

The other motivation for integrated feedback strategies is that they enable to reward specific EEG-fMRI pair values and gives flexibility on the definition of the bimodal NF target. In this dissertation, we designed our integrated feedback strategies so that subjects would have to regulate both EEG and fMRI at the same time in order to reach the NF target. Theoretically, this narrows the targeted brain pattern and implies that the bimodal target is harder to reach than each unimodal target on its own. Such a bimodal NF target can be seen as being defined on the intersection of the EEG *and* the fMRI features. We refer to this integrated feedback paradigm as "AND". However integrated feedback strategies make it possible to define the bimodal NF target differently. For example, one could define a more laxist target by the "union" of the EEG and fMRI features, that is the target would be reached when the EEG target *or* the fMRI target is reached. We refer to this integrated feedback paradigm as "OR". Such a



target would be easier to reach than an "AND" target therefore potentially less specific, but it might be advantageous in order to limit the user frustration when used at the beginning of a protocol for example. Also the "OR" strategy could be used in case the EEG and fMRI features would be hardly redundant. Another possibility would be to use the EEG and the fMRI features alternatively or in a temporally-varying mixture throughout the trial, run or session. We refer to this integrated feedback paradigm as "Temporal mix". For example, immediate feedback could be favored at the beginning of the trial before the BOLD response reaches its peak. Or the fMRI could be displayed at the end of the trial<sup>3</sup> while EEG would be fed back immediately. Finally, all these approaches could be mixed. For example, when using an "OR" strategy, one could imagine adding an "AND" secondary reward. In this way the subject would be rewarded additionally when the pair of EEG and fMRI features are correlated but would not be "penalized" when they are not. These different kinds of paradigms are illustrated in Figure 56.

<sup>3</sup> (Emmert, Kopel, Koush, et al., 2017; Johnson & Hartwell, 2012)

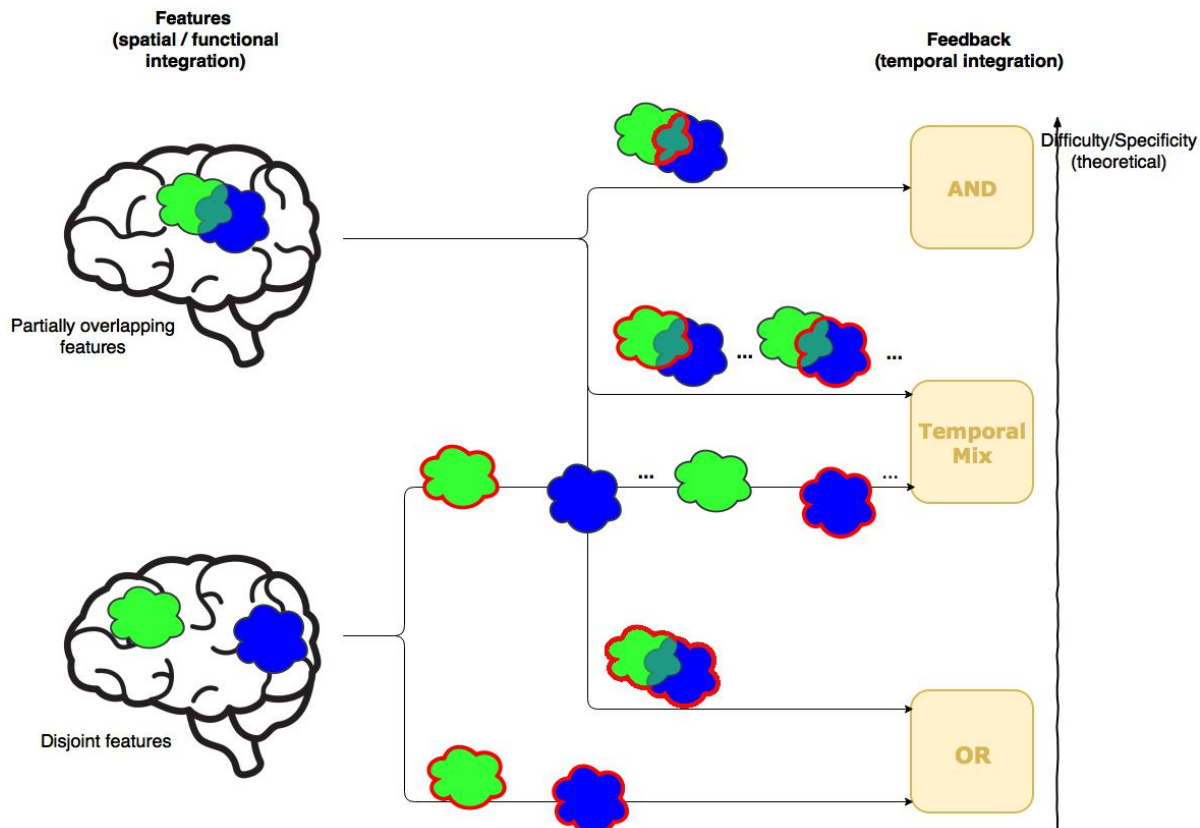


Figure 56 – Bimodal NF paradigms

### 7.2.7 Going towards clinical applications

Regarding potential clinical applications, EEG-fMRI-NF is not much more expensive than fMRI-NF. It surely requires additional efforts in the protocol and task design and its application is also more cumbersome (setup of the EEG cap, data quality, longer calibration). But it could be worth the labor. Our hope is that EEG-fMRI-NF will enable patients to reach stronger, faster and more specific self-regulation and functional outcomes than unimodal approaches. Through-

out this PhD, many discussions with medical doctors were carried out, in particular with Doctor of physical and rehabilitation medicine Isabelle Bonan and Psychiatrists Jean-Marie Batail and Dominique Drapier.

**Motor rehabilitation for stroke patients** Our work on the design of a MI-based EEG-fMRI-NF protocol which we tested on healthy patients is purposed to be eventually adapted to stroke patients. Shortly after the end of this PhD, a pilot study with stroke patients will take place at Neurinfo's facilities. However tailoring our protocol to stroke patients raises additional concerns about target definition, as well as task and feedback design. The main idea would be to target the activity of the perilesional area whose recovery could lead to efficient outcomes. Though this can be easily targeted for fMRI, it is not sure what mental task (motor imagery, execution, other) and what EEG feature it will correspond to. Regarding the feedback, it might be difficult for patients with affected cognitive abilities to concentrate on the 2D feedback. Also, for motor rehabilitation a proprioceptive feedback might be necessary in order to close the motor loop, which leads to think of the possibility of designing multi-sensory multi-modal NF.

**Depression** A systematic review of neuroimaging studies of unipolar depression revealed that two distinct neurocognitive networks are central in the symptomatology of depression, namely the autobiographic memory network (AMN) and the cognitive control network (CCN)<sup>4</sup>. Depressive patients usually exhibits an imbalance between these two networks. The hyperactivity of the AMN is associated with rumination, brooding and self-blame while the under-engagement of the CNN is linked with indecisiveness, negative automatic thoughts, poor concentration and distorted cognitive processing. Using EEG-fMRI-NF could allow to train patients to improve the balance between these two networks. For example, EEG could be used to upregulate the CCN (located in pre-frontal regions), while fMRI could be used to down-regulate the AMN (located more in the limbic region). A pilot study with MDD patients is currently under preparation.

<sup>4</sup> (Rayner, Jackson, & Wilson, 2016)

### 7.3 LAST WORDS

I hope I have demonstrated the flexibility that bimodal EEG-fMRI-NF and integrated feedback strategies can offer even without fancy data integration. This PhD work is only a little step forward, but I hope that many more will continue successfully on this track. Adapting EEG-fMRI integration methods for online use in bimodal NF will surely contribute to increasing the potential of the bimodal NF approach. For those who are still skeptical about this episode of the NF saga, I hope that at least this work will have raised awareness about (or have reminded) the need to question what is it that we show to our participants when we are doing NF (may it be with one, two, or a thousand modalities) telling them this is their brain activity. I look forward to reading the outcome of the first bimodal NF studies with stroke and MDD patients at Neurinfo. Good luck to the relay runners !

I thank my friend **Maud Boulet** for her great work at transposing some moments of my PhD with her magic hand.

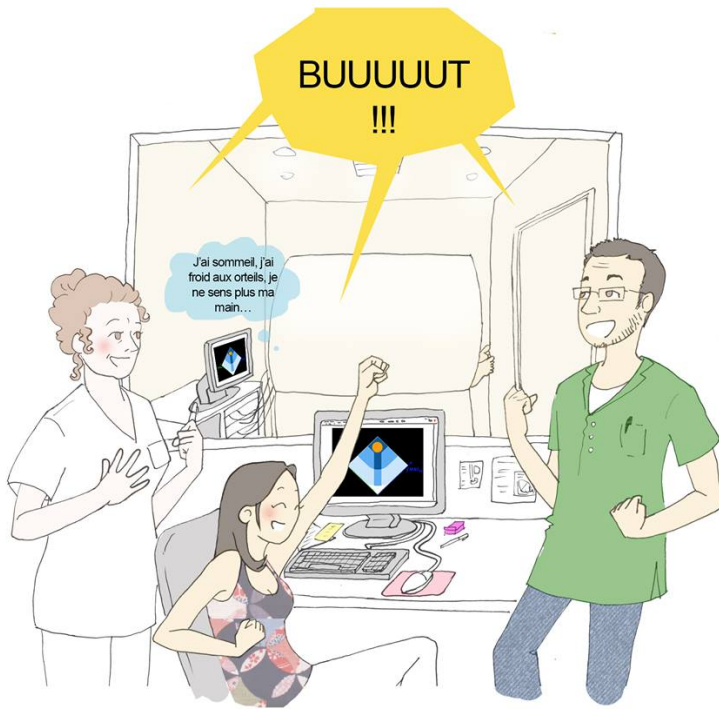
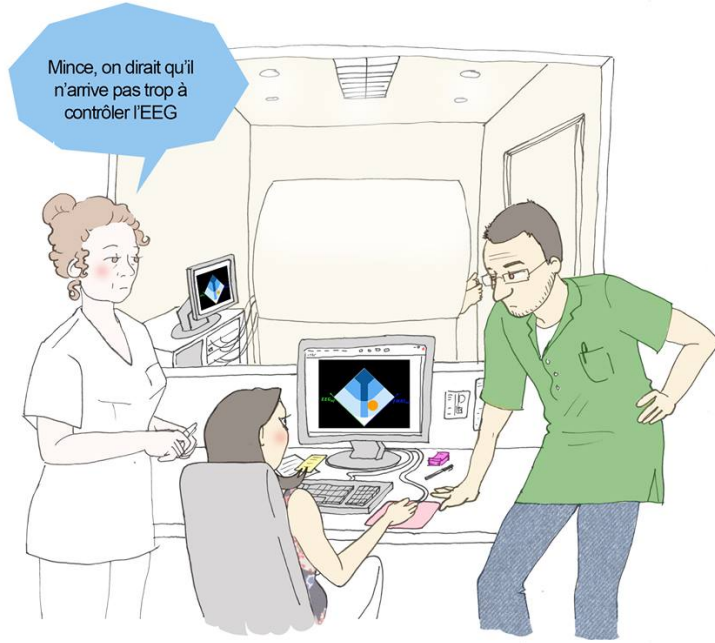
## La thèse commence



A la recherche de volontaires pour mes expériences



# Le neurofeedback-EEG-IRMf: quand ça marche





Perdue dans les données





## BIBLIOGRAPHY

---

- Allen, P J, Oliver Josephs, & Robert Turner (2000). "A method for removing imaging artifact from continuous EEG recorded during functional MRI." In: *NeuroImage* 12.2, pp. 230–9. DOI: [10.1006/nimg.2000.0599](https://doi.org/10.1006/nimg.2000.0599) (cit. on pp. 45, 62, 66, 74, 81).
- Allen, P J, G Polizzi, K Krakow, D R Fish, & L Lemieux (1998). "Identification of EEG events in the MR scanner: the problem of pulse artifact and a method for its subtraction." In: *NeuroImage* 8.3, pp. 229–239. DOI: [10.1006/nimg.1998.0361](https://doi.org/10.1006/nimg.1998.0361) (cit. on pp. 45, 62, 74, 81).
- Allison, Brendan (2011). "Trends in BCI research." In: *XRDS: Crossroads, The ACM Magazine for Students* 18.1, pp. 18–22. DOI: [10.1145/2000775.2000784](https://doi.org/10.1145/2000775.2000784) (cit. on p. 26).
- Amiri, Setare, Reza Fazel-Rezai, & Vahid Asadpour (2013). *A review of hybrid brain-computer interface systems*. DOI: [10.1155/2013/187024](https://doi.org/10.1155/2013/187024) (cit. on pp. 3, 11).
- Ang, Kai Keng & Cuntai Guan (2015). "Brain-Computer Interface for Neurorehabilitation of Upper Limb After Stroke." In: *Proceedings of the IEEE* 103.6, pp. 1–10. DOI: [10.1109/JPROC.2015.2415800](https://doi.org/10.1109/JPROC.2015.2415800) (cit. on p. 26).
- Arns, M, S de Ridder, & U Strehl (2009). "Efficacy of neurofeedback treatment in ADHD: the effects on inattention, impulsivity and hyperactivity: a meta-analysis." In: *Clinical EEG and Neuroscience* 40.3, pp. 180–189 (cit. on pp. 17, 27, 28).
- Arns, Martijn, Jean-Marie Batail, et al. (2017). "Neurofeedback: One of today's techniques in psychiatry?" In: *L'Encéphale* 43.2, pp. 135–145. DOI: [10.1016/j.encep.2016.11.003](https://doi.org/10.1016/j.encep.2016.11.003) (cit. on pp. 2, 10).
- Arns, Martijn, Hartmut Heinrich, & Ute Strehl (2014). "Evaluation of neurofeedback in ADHD: The long and winding road." In: *Biological Psychology* 95.1, pp. 108–115. DOI: [10.1016/j.biopsycho.2013.11.013](https://doi.org/10.1016/j.biopsycho.2013.11.013) (cit. on p. 27).
- Attwell, David, Alastair M Buchan, Serge Charpak, Martin Lauritzen, Brian A. MacVicar, & Eric A Newman (2010). "Glial and neuronal control of brain blood flow." In: *Nature* 468.7321, pp. 232–243. DOI: [10.1038/nature09613](https://doi.org/10.1038/nature09613) (cit. on p. 33).
- Bagarinao, E, K Matsuo, T Nakai, & S Sato (2003a). "Estimation of general linear model coefficients for real-time application." In: *NeuroImage* 19.2, pp. 422–429. DOI: [10.1016/S1053-8119\(03\)00081-8](https://doi.org/10.1016/S1053-8119(03)00081-8) (cit. on p. 34).
- (2003b). "Estimation of general linear model coefficients for real-time application." In: *Neuroimage* 19.2, pp. 422–429 (cit. on p. 47).
- Bassett, Danielle S & Michael S Gazzaniga (2011). *Understanding complexity in the human brain*. DOI: [10.1016/j.tics.2011.03.006](https://doi.org/10.1016/j.tics.2011.03.006) (cit. on pp. 3, 11).
- Berman, Brian D., Silvina G. Horowitz, Gaurav Venkataraman, & Mark Hallett (2012). "Self-modulation of primary motor cortex activity with motor and motor imagery tasks using real-time fMRI-based neurofeedback." In: *Neu-*

- roImage* 59.2, pp. 917–925. DOI: [10.1016/j.neuroimage.2011.07.035](https://doi.org/10.1016/j.neuroimage.2011.07.035). arXiv: [NIHMS150003](https://arxiv.org/abs/NIHMS150003) (cit. on p. 36).
- Bianciardi, Marta et al. (2009). “Sources of functional magnetic resonance imaging signal fluctuations in the human brain at rest: a 7 T study.” In: *Magnetic resonance imaging* 27.8, pp. 1019–1029 (cit. on p. 46).
- Biessmann, Felix, Sergey Plis, Frank C. Meinecke, Tom Eichele, & Klaus-Robert Müller (2011). “Analysis of Multimodal Neuroimaging Data.” In: *IEEE Reviews in Biomedical Engineering* 4, pp. 26–58. DOI: [10.1109/RBME.2011.2170675](https://doi.org/10.1109/RBME.2011.2170675) (cit. on pp. 2, 3, 11, 77).
- Birbaumer, Niels, Ander Ramos Murguialday, Cornelia Weber, & Pedro Montoya (2009). “Neurofeedback and brain-computer interface clinical applications.” In: *International review of neurobiology* 86, pp. 107–117. DOI: [10.1016/S0074-7742\(09\)86008-X](https://doi.org/10.1016/S0074-7742(09)86008-X) (cit. on pp. 26, 27, 37).
- Birbaumer, Niels, Sergio Ruiz, & Ranganatha Sitaram (2013). “Learned regulation of brain metabolism.” In: *Trends in cognitive sciences* 17.6, pp. 295–302. DOI: [10.1016/j.tics.2013.04.009](https://doi.org/10.1016/j.tics.2013.04.009) (cit. on pp. 2, 11, 21).
- Blankertz, Benjamin, Ryota Tomioka, Steven Lemm, Motoaki Kawanabe, & Klaus Robert Müller (2008). “Optimizing spatial filters for robust EEG single-trial analysis.” In: *IEEE Signal Processing Magazine* 25.1, pp. 41–56. DOI: [10.1109/MSP.2008.4408441](https://doi.org/10.1109/MSP.2008.4408441) (cit. on pp. 67, 82).
- Britz, Juliane, Dimitri Van De Ville, & Christoph M Michel (2010). “BOLD correlates of EEG topography reveal rapid resting-state network dynamics.” In: *NeuroImage* 52.4, pp. 1162–70. DOI: [10.1016/j.neuroimage.2010.02.052](https://doi.org/10.1016/j.neuroimage.2010.02.052) (cit. on p. 33).
- Buccino, Alessio Paolo, Hasan Onur Keles, & Ahmet Omurtag (2016). “Hybrid EEG-fNIRS asynchronous brain-computer interface for multiple motor tasks.” In: *PLoS ONE* 11.1. Ed. by Bin He, e0146610. DOI: [10.1371/journal.pone.0146610](https://doi.org/10.1371/journal.pone.0146610) (cit. on pp. 3, 11).
- Budzynski, TH, HK Budzynski, JR Evans, & A Abarbanel (2009). *Introduction to quantitative EEG and neurofeedback: Advanced theory and applications*. Elsevier Science (cit. on pp. 20, 24).
- Bullmore, Ed et al. (2009). *Generic aspects of complexity in brain imaging data and other biological systems*. DOI: [10.1016/j.neuroimage.2009.05.032](https://doi.org/10.1016/j.neuroimage.2009.05.032) (cit. on pp. 3, 11).
- Buneo, Christopher A. & Richard A. Andersen (2006). “The posterior parietal cortex: Sensorimotor interface for the planning and online control of visually guided movements.” In: *Neuropsychologia* 44.13, pp. 2594–2606. DOI: [10.1016/j.neuropsychologia.2005.10.011](https://doi.org/10.1016/j.neuropsychologia.2005.10.011) (cit. on p. 89).
- Calhoun, Vince D. & Jing Sui (2016). *Multimodal Fusion of Brain Imaging Data: A Key to Finding the Missing Link(s) in Complex Mental Illness*. DOI: [10.1016/j.bpsc.2015.12.005](https://doi.org/10.1016/j.bpsc.2015.12.005) (cit. on p. 77).
- Cannon, Rex, Marco Congedo, Joel Lubar, & Teresa Hutchens (2009). “Differentiating a network of executive attention: LORETA neurofeedback in anterior cingulate and dorsolateral prefrontal cortices.” en. In: *The International journal of neuroscience* 119.3, pp. 404–441. DOI: [10.1080/00207450802480325](https://doi.org/10.1080/00207450802480325) (cit. on p. 24).
- Carlucci, Lorenzo & John Case (2013). “On the Necessity of U-Shaped Learning.” In: *Topics in Cognitive Science* 5.1, pp. 56–88. DOI: [10.1111/tops.12002](https://doi.org/10.1111/tops.12002) (cit. on p. 75).

- Cavazza, Marc et al. (2014). “Towards emotional regulation through neurofeedback.” In: *Proceedings of the 5th Augmented Human International Conference on - AH '14*, pp. 1–8. DOI: [10.1145/2582051.2582093](https://doi.org/10.1145/2582051.2582093) (cit. on pp. 38, 40).
- Chiew, Mark (2013). “Development and Application of Methods for Real-Time fMRI Neurofeedback.” PhD thesis. University of Toronto (cit. on p. 47).
- Chiew, Mark, Stephen M LaConte, & Simon J. Graham (2012). “Investigation of fMRI neurofeedback of differential primary motor cortex activity using kinesthetic motor imagery.” In: *NeuroImage* 61.1, pp. 21–31. DOI: [10.1016/j.neuroimage.2012.02.053](https://doi.org/10.1016/j.neuroimage.2012.02.053) (cit. on pp. 36, 61, 63, 69, 73).
- Choi, Sang Han, Minh Lee, Yijun Wang, & Bo Hong (2006). “Estimation of optimal location of EEG reference electrode for motor imagery based BCI using fMRI.” In: *Conference proceedings : ... Annual International Conference of the IEEE Engineering in Medicine and Biology Society. IEEE Engineering in Medicine and Biology Society. Conference 1*, pp. 1193–1196. DOI: [10.1109/IEMBS.2006.260270](https://doi.org/10.1109/IEMBS.2006.260270) (cit. on p. 74).
- Choi, Sung Won, Sang Eun Chi, Sun Yong Chung, Jong Woo Kim, Chang Yil Ahn, & Hyun Taek Kim (2011). “Is alpha wave neurofeedback effective with randomized clinical trials in depression? A pilot study.” In: *Neuropsychobiology* 63.1, pp. 43–51. DOI: [10.1159/000322290](https://doi.org/10.1159/000322290) (cit. on p. 28).
- Christopher deCharms, R et al. (2005). “Control over brain activation and pain learned by using real-time functional MRI.” In: *Proceedings of the National Academy of Sciences of the United States of America* 102.51, pp. 18626–18631 (cit. on p. 47).
- Cohen, Avihay et al. (2016). “Multi-modal Virtual Scenario Enhances Neurofeedback Learning.” In: *Frontiers in Robotics and AI* 3, p. 52. DOI: [10.3389/frobt.2016.00052](https://doi.org/10.3389/frobt.2016.00052) (cit. on pp. 38, 41, 75, 93).
- Confalonieri, Linda, Giuseppe Pagnoni, Lawrence W Barsalou, Justin Rajendra, Simon B Eickhoff, & Andrew J Butler (2012). “Brain Activation in Primary Motor and Somatosensory Cortices during Motor Imagery Correlates with Motor Imagery Ability in Stroke Patients.” In: *ISRN Neurology* 2012, pp. 1–17. DOI: [10.5402/2012/613595](https://doi.org/10.5402/2012/613595) (cit. on p. 89).
- Congedo, Marco, Joel F. Lubar, & David Joffe (2004). “Low-resolution electromagnetic tomography neurofeedback.” In: *IEEE Transactions on Neural Systems and Rehabilitation Engineering* 12.4, pp. 387–397. DOI: [10.1109/TNSRE.2004.840492](https://doi.org/10.1109/TNSRE.2004.840492) (cit. on p. 24).
- Cox, Robert W (1996). “AFNI: software for analysis and visualization of functional magnetic resonance neuroimages.” In: *Computers and Biomedical research* 29.3, pp. 162–173 (cit. on p. 46).
- Cox, Robert W., Andrzej Jesmanowicz, & James S. Hyde (1995). “Real-Time Functional Magnetic Resonance Imaging.” In: *Magnetic Resonance in Medicine* 33.2, pp. 230–236. DOI: [10.1002/mrm.1910330213](https://doi.org/10.1002/mrm.1910330213) (cit. on pp. 24, 34).
- Cox, Robert W, Andrzej Jesmanowicz, & James S Hyde (1995). “Real-Time Functional Magnetic Resonance Imaging.” In: *Magnetic resonance in medicine* 33.2, pp. 230–236 (cit. on p. 47).
- Cui, Xu, Signe Bray, & Allan L Reiss (2010). “Functional near infrared spectroscopy (NIRS) signal improvement based on negative correlation between oxygenated and deoxygenated hemoglobin dynamics.” In: *Neuroimage* 49.4, pp. 3039–3046 (cit. on p. 46).

- Culham, Jody C & Nancy G Kanwisher (2001). *Neuroimaging of cognitive functions in human parietal cortex*. DOI: [10.1016/S0959-4388\(00\)00191-4](https://doi.org/10.1016/S0959-4388(00)00191-4) (cit. on p. 89).
- Danckert, James, Susanne Ferber, Timothy Doherty, Helena Steinmetz, David Nicolle, & Melvyn Goodale (2002). "Selective, Non-lateralized Impairment of Motor Imagery Following Right Parietal Damage." In: *Neurocase* 8.3, pp. 194–204. DOI: [10.1093/neucas/8.3.194](https://doi.org/10.1093/neucas/8.3.194) (cit. on p. 89).
- Darvishi, Sam, Alireza Gharabaghi, Chadwick B Boulay, Michael C Ridding, Derek Abbott, & Mathias Baumert (2017). "Proprioceptive feedback facilitates motor imagery-related operant learning of sensorimotor beta-band modulation." In: *Frontiers in Neuroscience* 11.FEB, p. 60. DOI: [10.3389/fnins.2017.00060](https://doi.org/10.3389/fnins.2017.00060) (cit. on p. 78).
- De Vos, Maarten, Rob Zink, Bobala Hunyadi, Bogdan Mijovic, Sabine Van Huffel, & Stefan Debener (2013). "The quest for single trial correlations in multimodal EEG-fMRI data." In: DOI: [10.0/Linux-x86\\_64](https://doi.org/10.0/Linux-x86_64) (cit. on p. 90).
- Debener, Stefan, Markus Ullsperger, Markus Siegel, & Andreas K Engel (2006). "Single-trial EEG-fMRI reveals the dynamics of cognitive function." In: *Trends in cognitive sciences* 10.12, pp. 558–63. DOI: [10.1016/j.tics.2006.09.010](https://doi.org/10.1016/j.tics.2006.09.010) (cit. on p. 31).
- DeCharms, R Christopher et al. (2005). "Control over brain activation and pain learned by using real-time functional MRI." In: *Proceedings of the National Academy of Sciences of the United States of America* 102.51, pp. 18626–18631. DOI: [10.1073/pnas.0505210102](https://doi.org/10.1073/pnas.0505210102) (cit. on pp. 18, 24, 30, 34).
- Deneux, Thomas (2011). "EEG-fMRI Fusion: Adaptations of the Kalman Filter for Solving a High-Dimensional Spatio-Temporal Inverse Problem." In: *Adaptive Filtering*. InTech. DOI: [10.5772/16490](https://doi.org/10.5772/16490) (cit. on pp. 4, 12).
- D'Esposito, Mark, Leon Y. Deouell, & Adam Gazzaley (2003). "Alterations in the BOLD fMRI signal with ageing and disease: a challenge for neuroimaging." In: *Nature Reviews Neuroscience* 4.11, pp. 863–872. DOI: [10.1038/nrn1246](https://doi.org/10.1038/nrn1246) (cit. on p. 34).
- Dokkum, L E H van, T Ward, & I Laffont (2015). "Brain computer interfaces for neurorehabilitation - its current status as a rehabilitation strategy post-stroke." In: *Annals of physical and rehabilitation medicine* 58.1, pp. 3–8. DOI: [10.1016/j.rehab.2014.09.016](https://doi.org/10.1016/j.rehab.2014.09.016) (cit. on pp. 26, 29).
- Dong, Li et al. (2014). "Simultaneous EEG-fMRI: Trial level spatio-temporal fusion for hierarchically reliable information discovery." In: *NeuroImage* 99, pp. 28–41. DOI: [10.1016/j.neuroimage.2014.05.029](https://doi.org/10.1016/j.neuroimage.2014.05.029) (cit. on p. 75).
- Eklund, Anders, Mats Andersson, Henrik Ohlsson, Anders Ynnerman, & Hans Knutsson (2010). "Using real-time fMRI to control a dynamical system by brain activity classification." In: *2010 20th International Conference on Pattern Recognition* 12.Pt 1, pp. 3665–3669. DOI: [10.1109/ICPR.2010.894](https://doi.org/10.1109/ICPR.2010.894) (cit. on p. 36).
- Ekstrom, Arne (2010). *How and when the fMRI BOLD signal relates to underlying neural activity: The danger in dissociation*. DOI: [10.1016/j.brainresrev.2009.12.004](https://doi.org/10.1016/j.brainresrev.2009.12.004). arXiv: [NIHMS150003](https://arxiv.org/abs/NIHMS150003) (cit. on pp. 32, 33).
- Elbert, Thomas, Brigitte Rockstroh, Werner Lutzenberger, & Niels Birbaumer (2012). *Self-Regulation of the Brain and Behavior*. Ed. by Thomas Elbert, Brigitte Rockstroh, Werner Lutzenberger, & Niels Birbaumer. Berlin, Heidelberg: Springer

- Berlin Heidelberg, p. 360. DOI: [10.1007/978-3-642-69379-3](https://doi.org/10.1007/978-3-642-69379-3) (cit. on p. 23).
- Emmert, Kirsten, Rotem Kopel, Yury Koush, et al. (2017). “Continuous vs. intermittent neurofeedback to regulate auditory cortex activity of tinnitus patients using real-time fMRI - A pilot study.” In: *NeuroImage: Clinical* 14, pp. 97–104. DOI: [10.1016/j.nicl.2016.12.023](https://doi.org/10.1016/j.nicl.2016.12.023) (cit. on pp. 2, 11, 21, 95).
- Emmert, Kirsten, Rotem Kopel, James Sulzer, et al. (2016). “Meta-analysis of real-time fMRI neurofeedback studies using individual participant data: How is brain regulation mediated?” In: *NeuroImage* 124.Pt A, pp. 806–812. DOI: [10.1016/j.neuroimage.2015.09.042](https://doi.org/10.1016/j.neuroimage.2015.09.042) (cit. on pp. 2, 11, 21, 88, 89).
- Engell, Andrew D., Scott Huettel, & Gregory McCarthy (2012). “The fMRI BOLD signal tracks electrophysiological spectral perturbations, not event-related potentials.” In: *NeuroImage* 59.3, pp. 2600–2606. DOI: [10.1016/j.neuroimage.2011.08.079](https://doi.org/10.1016/j.neuroimage.2011.08.079). arXiv: [NIHMS150003](https://arxiv.org/abs/NIHMS150003) (cit. on p. 32).
- Enriquez-Geppert, Stefanie, René J Huster, & Christoph S Herrmann (2017). “EEG-Neurofeedback as a Tool to Modulate Cognition and Behavior: A Review Tutorial.” In: *Frontiers in Human Neuroscience* 11, p. 51. DOI: [10.3389/fnhum.2017.00051](https://doi.org/10.3389/fnhum.2017.00051) (cit. on p. 34).
- Esposito, Fabrizio et al. (2003). “Real-time independent component analysis of fMRI time-series.” In: *Neuroimage* 20.4, pp. 2209–2224 (cit. on p. 47).
- Fazli, Siamac, Sven Dahne, Wojciech Samek, Felix Biebmann, & Klaus Robert Müller (2015). *Learning From More Than One Data Source: Data Fusion Techniques for Sensorimotor Rhythm-Based Brain-Computer Interfaces*. DOI: [10.1109/JPROC.2015.2413993](https://doi.org/10.1109/JPROC.2015.2413993) (cit. on pp. 2, 11, 77, 78).
- Fazli, Siamac, Jan Mehnert, et al. (2012). “Enhanced performance by a hybrid NIRS-EEG brain computer interface.” In: *NeuroImage* 59.1, pp. 519–529. DOI: [10.1016/j.neuroimage.2011.07.084](https://doi.org/10.1016/j.neuroimage.2011.07.084) (cit. on pp. 3, 11, 78).
- Fetz, E. E. (1969). “Operant Conditioning of Cortical Unit Activity.” In: *Science* 163.3870, pp. 955–958. DOI: [10.1126/science.163.3870.955](https://doi.org/10.1126/science.163.3870.955) (cit. on p. 18).
- Fleming, Melanie K., Cathy M. Stinear, & Winston D. Byblow (2010). “Bilateral parietal cortex function during motor imagery.” In: *Experimental Brain Research* 201.3, pp. 499–508. DOI: [10.1007/s00221-009-2062-4](https://doi.org/10.1007/s00221-009-2062-4) (cit. on p. 89).
- Formaggio, Emanuela, Silvia Francesca Storti, Roberto Cerini, Antonio Fiaschi, & Paolo Manganotti (2010). “Brain oscillatory activity during motor imagery in EEG-fMRI coregistration.” In: *Magnetic Resonance Imaging* 28.10, pp. 1403–1412. DOI: [10.1016/j.mri.2010.06.030](https://doi.org/10.1016/j.mri.2010.06.030) (cit. on pp. 75, 90).
- Friston, Karl J, Christopher D Frith, Richard SJ Frackowiak, & Robert Turner (1995). “Characterizing dynamic brain responses with fMRI: a multivariate approach.” In: *Neuroimage* 2.2, pp. 166–172 (cit. on pp. 46, 58).
- Gani, C (2009). “Long term effects after feedback of slow cortical potentials and of Theta/Beta-amplitudes in children with Attention Deficit Hyperactivity Disorder (ADHD).” In: *Thèse de doctorat, Université de Tübingen* (cit. on p. 28).
- Gaume, A., A. Vialatte, A. Mora-Sánchez, C. Ramdani, & François Vialatte (2016). “A psychoengineering paradigm for the neurocognitive mechanisms of biofeedback and neurofeedback.” In: *Neuroscience & Biobehavioral Reviews*. DOI: [10.1016/j.neubiorev.2016.06.012](https://doi.org/10.1016/j.neubiorev.2016.06.012) (cit. on pp. 75, 78).



- Gembris, D, J G Taylor, S Schor, W Frings, D Suter, & S Posse (2000). “Functional magnetic resonance imaging in real time (FIRE): sliding-window correlation analysis and reference-vector optimization.” In: *Magnetic resonance in medicine : official journal of the Society of Magnetic Resonance in Medicine / Society of Magnetic Resonance in Medicine* 43.2, pp. 259–268. DOI: [Doi10.1002/\(SICI\)1522-2594\(200002\)43:2<259::Aid-Mrm13>3.0.Co;2-P](https://doi.org/10.1002/(SICI)1522-2594(200002)43:2<259::Aid-Mrm13>3.0.Co;2-P) (cit. on p. 34).
- Gembris, Daniel, John G Taylor, Stefan Schor, Wolfgang Frings, Dieter Suter, & Stefan Posse (2000). “Functional magnetic resonance imaging in real time (FIRE): Sliding-window correlation analysis and reference-vector optimization.” In: *Magnetic Resonance in Medicine* 43.2, pp. 259–268 (cit. on p. 47).
- Gerardin, E et al. (2000). “Partially overlapping neural networks for real and imagined hand movements.” In: *Cerebral cortex (New York, N.Y. : 1991)* 10.11, pp. 1093–104 (cit. on p. 89).
- Girouard, Helene (2006). “Neurovascular coupling in the normal brain and in hypertension, stroke, and Alzheimer disease.” In: *Journal of Applied Physiology* 100.1, pp. 328–335. DOI: [10.1152/jappphysiol.00966.2005](https://doi.org/10.1152/jappphysiol.00966.2005) (cit. on p. 34).
- Goebel, Rainer (2012). “BrainVoyager - Past, present, future.” In: *NeuroImage* 62.2, pp. 748–756. DOI: [10.1016/j.neuroimage.2012.01.083](https://doi.org/10.1016/j.neuroimage.2012.01.083). arXiv: 4 (cit. on p. 34).
- Goense, Jozien B M & Nikos K. Logothetis (2008). “Neurophysiology of the BOLD fMRI Signal in Awake Monkeys.” In: *Current Biology* 18.9, pp. 631–640. DOI: [10.1016/j.cub.2008.03.054](https://doi.org/10.1016/j.cub.2008.03.054) (cit. on p. 32).
- Goense, Jozien, Hellmut Merkle, & Nikos K. Logothetis (2012). “High-Resolution fMRI Reveals Laminar Differences in Neurovascular Coupling between Positive and Negative BOLD Responses.” In: *Neuron* 76.3, pp. 629–639. DOI: [10.1016/j.neuron.2012.09.019](https://doi.org/10.1016/j.neuron.2012.09.019) (cit. on p. 33).
- Gonçalves, S. I. et al. (2006). “Correlating the alpha rhythm to BOLD using simultaneous EEG/fMRI: Inter-subject variability.” In: *NeuroImage* 30.1, pp. 203–213. DOI: [10.1016/j.neuroimage.2005.09.062](https://doi.org/10.1016/j.neuroimage.2005.09.062) (cit. on p. 90).
- Grosse-Wentrup, Moritz, Donatella Mattia, & Karim Oweiss (2011). “Using brain-computer interfaces to induce neural plasticity and restore function.” In: *Journal of neural engineering* 8.2. DOI: [10.1088/1741-2560/8/2/025004](https://doi.org/10.1088/1741-2560/8/2/025004) (cit. on pp. 25, 26).
- Gruzelier, John H (2014a). “EEG-neurofeedback for optimising performance. I: a review of cognitive and affective outcome in healthy participants.” In: *Neuroscience and biobehavioral reviews* 44, pp. 124–141. DOI: [10.1016/j.neubiorev.2013.09.015](https://doi.org/10.1016/j.neubiorev.2013.09.015) (cit. on p. 27).
- (2014b). “EEG-neurofeedback for optimising performance. II: creativity, the performing arts and ecological validity.” In: *Neuroscience and biobehavioral reviews* 44, pp. 142–158. DOI: [10.1016/j.neubiorev.2013.11.004](https://doi.org/10.1016/j.neubiorev.2013.11.004) (cit. on pp. 23, 27).
- (2014c). “EEG-neurofeedback for optimising performance. III: A review of methodological and theoretical considerations.” In: *Neuroscience & Biobehavioral Reviews* 44, pp. 159–182. DOI: [10.1016/j.neubiorev.2014.03.015](https://doi.org/10.1016/j.neubiorev.2014.03.015) (cit. on pp. 20, 34).
- Guillot, Aymeric, Christian Collet, Vo An Nguyen, Francine Malouin, Carol Richards, & Julien Doyon (2009). “Brain activity during visual versus kines-



- thetic imagery: An fMRI study.” In: *Human Brain Mapping* 30.7, pp. 2157–2172. DOI: [10.1002/hbm.20658](https://doi.org/10.1002/hbm.20658) (cit. on p. 89).
- Hammond, DC (2011). “What is neurofeedback: An update.” In: *Journal of Neurotherapy* 15.4, pp. 305–336. DOI: [10.1080/10874208.2011.623090](https://doi.org/10.1080/10874208.2011.623090) (cit. on pp. 2, 10, 20, 27).
- Hanakawa, T., Ilka Immisch, Keiichiro Toma, Michael A Dimyan, Peter Van Gelderen, & Mark Hallett (2002). “Functional Properties of Brain Areas Associated With Motor Execution and Imagery.” In: *Journal of Neurophysiology* 89.2, pp. 989–1002. DOI: [10.1152/jn.00132.2002](https://doi.org/10.1152/jn.00132.2002) (cit. on p. 89).
- Hardt, J. V. & Joe Kamiya (1978). “Anxiety change through electroencephalographic alpha feedback seen only in high anxiety subjects.” In: *Science* 201.4350, pp. 79–81. DOI: [10.1126/science.663641](https://doi.org/10.1126/science.663641) (cit. on p. 22).
- Herculano-Houzel, Suzana (2009). “The human brain in numbers: a linearly scaled-up primate brain.” In: *Frontiers in Human Neuroscience* 3, p. 31. DOI: [10.3389/neuro.09.031.2009](https://doi.org/10.3389/neuro.09.031.2009) (cit. on pp. 3, 11).
- Hétu, Sébastien et al. (2013). *The neural network of motor imagery: An ALE meta-analysis*. DOI: [10.1016/j.neubiorev.2013.03.017](https://doi.org/10.1016/j.neubiorev.2013.03.017) (cit. on p. 89).
- Hillman, Elizabeth M.C. (2014). “Coupling Mechanism and Significance of the BOLD Signal: A Status Report.” In: *Annual Review of Neuroscience* 37.1, pp. 161–181. DOI: [10.1146/annurev-neuro-071013-014111](https://doi.org/10.1146/annurev-neuro-071013-014111) (cit. on p. 32).
- Hinds, Oliver, Satrajit Ghosh, Todd W. Thompson, et al. (2011). “Computing moment-to-moment BOLD activation for real-time neurofeedback.” In: *NeuroImage* 54.1, pp. 361–368. DOI: [10.1016/j.neuroimage.2010.07.060](https://doi.org/10.1016/j.neuroimage.2010.07.060). arXiv: [NIHMS150003](https://arxiv.org/abs/NIHMS150003) (cit. on p. 34).
- Hinds, Oliver, Satrajit Ghosh, Todd W. Thompson, et al. (2011). “Computing moment-to-moment BOLD activation for real-time neurofeedback.” In: *Neuroimage* 54.1, pp. 361–368 (cit. on p. 47).
- Hochberg, Leigh R et al. (2012). “Reach and grasp by people with tetraplegia using a neurally controlled robotic arm.” In: *Nature* 485.7398, pp. 372–375. DOI: [10.1038/nature11076](https://doi.org/10.1038/nature11076) (cit. on p. 19).
- Horowitz, Silvina G, Bruno Rossion, Pawel Skudlarski, & John C Gore (2004). “Parametric design and correlational analyses help integrating fMRI and electrophysiological data during face processing.” In: *NeuroImage* 22.4, pp. 1587–1595. DOI: [10.1016/j.neuroimage.2004.04.018](https://doi.org/10.1016/j.neuroimage.2004.04.018) (cit. on p. 32).
- Huettel, Scott A et al. (2004). “Linking Hemodynamic and Electrophysiological Measures of Brain Activity: Evidence from Functional MRI and Intracranial Field Potentials.” In: *Cerebral Cortex* 14.2, pp. 165–173. DOI: [10.1093/cercor/bhg115](https://doi.org/10.1093/cercor/bhg115) (cit. on p. 32).
- Huneau, Clément, Habib Benali, & Hugues Chabriat (2015). “Investigating human neurovascular coupling using functional neuroimaging: A critical review of dynamic models.” In: *Frontiers in Neuroscience* 9.DEC, p. 467. DOI: [10.3389/fnins.2015.00467](https://doi.org/10.3389/fnins.2015.00467) (cit. on pp. 32–34).
- Huster, René J, Zacharais N Mokom, Stefanie Enriquez-Geppert, & Christoph S Herrmann (2014). “Brain-computer interfaces for EEG neurofeedback: peculiarities and solutions.” In: *International journal of psychophysiology : official journal of the International Organization of Psychophysiology* 91.1, pp. 36–45. DOI: [10.1016/j.ijpsycho.2013.08.011](https://doi.org/10.1016/j.ijpsycho.2013.08.011) (cit. on pp. 1, 9, 25, 26).

- Hwang, Han-Jeong, Kiwoon Kwon, & Chang-Hwang Im (2009). "Neurofeedback-based motor imagery training for brain-computer interface (BCI)." In: *Journal of neuroscience methods* 179.1, pp. 150–156. DOI: [10.1016/j.jneumeth.2009.01.015](https://doi.org/10.1016/j.jneumeth.2009.01.015) (cit. on p. 29).
- Ives, JR, S Warach, & F Schmitt (1993). "Monitoring the patient's EEG during echo planar MRI." In: *Electroencephalography ...* 87, pp. 417–420 (cit. on pp. 4, 12).
- Jenkinson, Mark, Peter Bannister, Michael Brady, & Stephen Smith (2002). "Improved optimization for the robust and accurate linear registration and motion correction of brain images." In: *Neuroimage* 17.2, pp. 825–841 (cit. on p. 46).
- Jeon, Yongwoong, Chang S. Nam, Young Joo Kim, & Min Cheol Whang (2011). "Event-related (De)synchronization (ERD/ERS) during motor imagery tasks: Implications for brain-computer interfaces." In: *International Journal of Industrial Ergonomics* 41.5, pp. 428–436. DOI: [10.1016/j.ergon.2011.03.005](https://doi.org/10.1016/j.ergon.2011.03.005) (cit. on p. 72).
- Jeunet, Camille, Chi Vi, Daniel Spelmezan, Bernard N'Kaoua, Fabien Lotte, & Sriram Subramanian (2015). "Continuous Tactile Feedback for Motor-Imagery Based Brain-Computer Interaction in a Multitasking Context." In: Springer, Cham, pp. 488–505. DOI: [10.1007/978-3-319-22701-6\\_36](https://doi.org/10.1007/978-3-319-22701-6_36) (cit. on p. 78).
- Johnson, KA & Karen Hartwell (2012). "Intermittent "Real-time" fMRI Feedback Is Superior to Continuous Presentation for a Motor Imagery Task: A Pilot Study." In: *Journal of Neuroimaging* 22.1, pp. 58–66. DOI: [10.1111/j.1552-6569.2010.00529.x](https://doi.org/10.1111/j.1552-6569.2010.00529.x). Intermittent (cit. on pp. 36, 95).
- Jorge, João, Frédéric Grouiller, Rolf Gruetter, Wietske van der Zwaag, & Patrícia Figueiredo (2015). "Towards high-quality simultaneous EEG-fMRI at 7 T: Detection and reduction of EEG artifacts due to head motion." In: *NeuroImage* 120, pp. 143–153. DOI: [10.1016/j.neuroimage.2015.07.020](https://doi.org/10.1016/j.neuroimage.2015.07.020) (cit. on pp. 31, 74).
- Jorge, João, Wietske Van der Zwaag, & Patrícia Figueiredo (2014). "EEG-fMRI integration for the study of human brain function." In: *NeuroImage* 102.P1, pp. 24–34. DOI: [10.1016/j.neuroimage.2013.05.114](https://doi.org/10.1016/j.neuroimage.2013.05.114) (cit. on pp. 36, 75, 77, 93).
- Kaiser, Vera, Alex Kreilinger, Gernot R Müller-Putz, & Christa Neuper (2011). "First steps toward a motor imagery based stroke BCI: New strategy to set up a classifier." In: *Frontiers in Neuroscience* 5.JUL, p. 86. DOI: [10.3389/fnins.2011.00086](https://doi.org/10.3389/fnins.2011.00086). arXiv: [fnins.2011.00086](https://arxiv.org/abs/2011.00086). [10.3389] (cit. on p. 36).
- Kamiya, Joe (1962). "Conditional discrimination of the EEG alpha rhythm in humans." In: *Meeting of the Western Psychological Association* (cit. on pp. 18, 21, 22).
- (1968). "Conscious control of brain waves." In: *Psychology Today* (cit. on p. 23).
- Kasamatsu, a & T Hirai (1966). "An electroencephalographic study on the zen meditation (Zazen)." In: *Psychiatry and Clinical Neurosciences* 20.4, pp. 315–336. DOI: [10.1111/j.1440-1819.1966.tb02646.x](https://doi.org/10.1111/j.1440-1819.1966.tb02646.x) (cit. on p. 22).
- Kasess, Christian H., Christian Windischberger, Ross Cunnington, Rupert Lanzenberger, Lukas Pezawas, & Ewald Moser (2008). "The suppressive influence of SMA on M1 in motor imagery revealed by fMRI and dynamic causal model-

- ing.” In: *NeuroImage* 40.2, pp. 828–837. DOI: [10.1016/j.neuroimage.2007.11.040](https://doi.org/10.1016/j.neuroimage.2007.11.040) (cit. on p. 89).
- Kaufmann, Tobias & John Williamson (2011). “Visually multimodal vs. classic unimodal feedback approach for smr-bcis: a comparison study.” In: *Int. J. ...* 13.2, pp. 80–81 (cit. on p. 78).
- Keizer, André W., Maurice Verschoor, Roland S. Verment, & Bernhard Hommel (2010). “The effect of gamma enhancing neurofeedback on the control of feature bindings and intelligence measures.” In: *International Journal of Psychophysiology* 75.1, pp. 25–32. DOI: [10.1016/j.ijpsycho.2009.10.011](https://doi.org/10.1016/j.ijpsycho.2009.10.011) (cit. on p. 23).
- Keynan, Jakob N. et al. (2016). “Limbic Activity Modulation Guided by Functional Magnetic Resonance Imaging–Inspired Electroencephalography Improves Implicit Emotion Regulation.” In: *Biological Psychiatry* 80.6, pp. 490–496. DOI: [10.1016/j.biopsych.2015.12.024](https://doi.org/10.1016/j.biopsych.2015.12.024) (cit. on pp. 38, 41).
- Kinreich, Sivan, Ilana Podlipsky, Nathan Intrator, & Talma Hendler (2012). “Categorized EEG Neurofeedback Performance Unveils Simultaneous fMRI Deep Brain Activation.” In: *Machine Learning and ...* Pp. 108–115 (cit. on pp. 37, 40).
- Kinreich, Sivan, Ilana Podlipsky, Shahar Jamsky, Nathan Intrator, & Talma Hendler (2014). “Neural dynamics necessary and sufficient for transition into pre-sleep induced by EEG NeuroFeedback.” In: *NeuroImage* 97, pp. 19–28. DOI: [10.1016/j.neuroimage.2014.04.044](https://doi.org/10.1016/j.neuroimage.2014.04.044) (cit. on pp. 37, 40).
- Kleiner, M, D Brainard, D Pelli, A Ingling, R Murray, & C Broussard (2007). “What’s new in Psychtoolbox-3.” In: *Perception* 36.14, p. 1 (cit. on pp. 62, 81).
- Kober, Silvia E, Matthias Witte, Manuel Ninaus, Christa Neuper, & Guilherme Wood (2013). “Learning to modulate one’s own brain activity: the effect of spontaneous mental strategies.” In: *Frontiers in Human Neuroscience* 7. October, p. 695. DOI: [10.3389/fnhum.2013.00695](https://doi.org/10.3389/fnhum.2013.00695) (cit. on pp. 2, 11, 20–22).
- Kober, Silvia E, G. Wood, et al. (2014). “Near-infrared spectroscopy based neurofeedback training increases specific motor imagery related cortical activation compared to sham feedback.” In: *Biological Psychology* 95.1, pp. 21–30. DOI: [10.1016/j.biopsych.2013.05.005](https://doi.org/10.1016/j.biopsych.2013.05.005) (cit. on pp. 2, 10).
- Koberda, J. Lucas, Paula Koberda, Andrew A. Bienkiewicz, Andrew Moses, & Laura Koberda (2013). “Pain Management Using 19-Electrode Z-Score LORETA Neurofeedback.” en. In: *Journal of Neurotherapy* 17.3, pp. 179–190. DOI: [10.1080/10874208.2013.813204](https://doi.org/10.1080/10874208.2013.813204) (cit. on p. 24).
- Koenig, Thomas et al. (2002). “Millisecond by millisecond, year by year: normative EEG microstates and developmental stages.” In: *NeuroImage* 16.1, pp. 41–8. DOI: [10.1006/nimg.2002.1070](https://doi.org/10.1006/nimg.2002.1070) (cit. on p. 33).
- Kopel, Rotem, Kirsten Emmert, Frank Scharnowski, Sven Haller, & Dimitri Van De Ville (2016). “Distributed patterns of brain activity underlying real-time fMRI neurofeedback training.” In: *IEEE Transactions on Biomedical Engineering* 64.6, pp. 1–1. DOI: [10.1109/TBME.2016.2598818](https://doi.org/10.1109/TBME.2016.2598818) (cit. on p. 84).
- Koush, Yury, Djalel-E. Meskaldji, et al. (2015). “Learning Control Over Emotion Networks Through Connectivity-Based Neurofeedback.” In: *Cerebral Cortex* 8.2, bhv311. DOI: [10.1093/cercor/bhv311](https://doi.org/10.1093/cercor/bhv311) (cit. on p. 36).

- Koush, Yury, Maria Joao Rosa, Fabien Robineau, Klaartje Heinen, Sebastian W Rieger, et al. (2013). "Connectivity-based neurofeedback: dynamic causal modeling for real-time fMRI." In: *Neuroimage* 81, pp. 422–430 (cit. on p. 47).
- Koush, Yury, Maria Joao Rosa, Fabien Robineau, Klaartje Heinen, Sebastian W. Rieger, et al. (2013). "Connectivity-based neurofeedback: Dynamic causal modeling for real-time fMRI." In: *NeuroImage* 81, pp. 422–430. DOI: [10.1016/j.neuroimage.2013.05.010](https://doi.org/10.1016/j.neuroimage.2013.05.010) (cit. on p. 36).
- Koush, Yury, Mikhail Zvyagintsev, Miriam Dyck, Krystyna A Mathiak, & Klaus Mathiak (2012). "Signal quality and Bayesian signal processing in neurofeedback based on real-time fMRI." In: *Neuroimage* 59.1, pp. 478–489 (cit. on p. 46).
- Krause, Florian et al. (2017). "Real-time fMRI-based self-regulation of brain activation across different visual feedback presentations." In: *Brain-Computer Interfaces*, pp. 1–15. DOI: [10.1080/2326263X.2017.1307096](https://doi.org/10.1080/2326263X.2017.1307096) (cit. on pp. 2, 11, 21, 78).
- Krishnaswamy, Pavitra, Giorgio Bonmassar, Catherine Poulsen, Eric T. Pierce, Patrick L. Purdon, & Emery N. Brown (2016). "Reference-free removal of EEG-fMRI ballistocardiogram artifacts with harmonic regression." In: *NeuroImage* 128, pp. 398–412. DOI: [10.1016/j.neuroimage.2015.06.088](https://doi.org/10.1016/j.neuroimage.2015.06.088) (cit. on p. 74).
- Lachaux, Jean-Philippe et al. (2007). "A blueprint for real-time functional mapping via human intracranial recordings." In: *PloS one* 2.10, e1094. DOI: [10.1371/journal.pone.0001094](https://doi.org/10.1371/journal.pone.0001094) (cit. on p. 32).
- LaConte, Stephen M (2011). "Decoding fMRI brain states in real-time." In: *NeuroImage* 56.2, pp. 440–54. DOI: [10.1016/j.neuroimage.2010.06.052](https://doi.org/10.1016/j.neuroimage.2010.06.052) (cit. on p. 36).
- Lahat, Dana, Tülay Adali, & Christian Jutten (2015). "Multimodal Data Fusion : An Overview of Methods , Challenges , and Prospects." In: *Proceedings of the IEEE* 103.9, pp. 1449–1477. DOI: [10.1109/jproc.2015.2460697](https://doi.org/10.1109/jproc.2015.2460697) (cit. on p. 77).
- Lal, Thomas Navin et al. (2005). "A Brain Computer Interface with Online Feedback based on Magnetoencephalography." In: *22Nd International Conference on Machine Learning*, pp. 465–472. DOI: [10.1145/1102351.1102410](https://doi.org/10.1145/1102351.1102410) (cit. on pp. 2, 10).
- Lecuyer, A., F. Lotte, R.B. Reilly, R. Leeb, M. Hirose, & M. Slater (2008). "Brain-Computer Interfaces, Virtual Reality, and Videogames." In: *Computer* 41.10, pp. 66–72. DOI: [10.1109/MC.2008.410](https://doi.org/10.1109/MC.2008.410) (cit. on p. 19).
- Lee, Jong Hwan, Jeongwon Ryu, Ferenc A. Jolesz, Zang Hee Cho, & Seung Schik Yoo (2009). "Brain-machine interface via real-time fMRI: Preliminary study on thought-controlled robotic arm." In: *Neuroscience Letters* 450.1, pp. 1–6. DOI: [10.1016/j.neulet.2008.11.024](https://doi.org/10.1016/j.neulet.2008.11.024). arXiv: [NIHMS150003](https://arxiv.org/abs/NIHMS150003) (cit. on p. 36).
- Leins, Ulrike, Gabriella Goth, Thilo Hinterberger, Christoph Klinger, Nicola Rumpf, & Ute Strehl (2007). "Neurofeedback for children with ADHD: a comparison of SCP and Theta/Beta protocols." In: *Applied psychophysiology and biofeedback* 32.2, pp. 73–88. DOI: [10.1007/s10484-007-9031-0](https://doi.org/10.1007/s10484-007-9031-0) (cit. on p. 28).
- Lévesque, Johanne, Mario Beauregard, & Boualem Mensour (2006). "Effect of neurofeedback training on the neural substrates of selective attention in chil-

- dren with attention-deficit/hyperactivity disorder: a functional magnetic resonance imaging study.” In: *Neuroscience letters* 394.3, pp. 216–21. DOI: [10.1016/j.neulet.2005.10.100](https://doi.org/10.1016/j.neulet.2005.10.100) (cit. on pp. 37, 40).
- Liechti, Martina D. et al. (2012). “First clinical trial of tomographic neurofeedback in attention-deficit/hyperactivity disorder: Evaluation of voluntary cortical control.” In: *Clinical Neurophysiology* 123.10, pp. 1989–2005. DOI: [10.1016/j.clinph.2012.03.016](https://doi.org/10.1016/j.clinph.2012.03.016) (cit. on p. 24).
- Logothetis, N K, J Pauls, M Augath, T Trinath, & a Oeltermann (2001). “Neurophysiological investigation of the basis of the fMRI signal.” In: *Nature* 412.6843, pp. 150–7. DOI: [10.1038/35084005](https://doi.org/10.1038/35084005) (cit. on p. 32).
- Logothetis, Nikos K. (2008). “What we can do and what we cannot do with fMRI.” In: *Nature* 453.7197, pp. 869–878. DOI: [10.1038/nature06976](https://doi.org/10.1038/nature06976). arXiv: [0208024 \[gr-qc\]](https://arxiv.org/abs/0208024) (cit. on p. 32).
- Logothetis, Nikos K & Brian A Wandell (2004). “Interpreting the BOLD Signal.” In: *Annual Review of Physiology* 66.1, pp. 735–769. DOI: [10.1146/annurev.physiol.66.082602.092845](https://doi.org/10.1146/annurev.physiol.66.082602.092845) (cit. on p. 32).
- Lotte, Fabien & Cuntai Guan (2011). “Regularizing common spatial patterns to improve BCI designs: unified theory and new algorithms.” In: *IEEE Transactions on biomedical Engineering* 58.2, pp. 355–362 (cit. on p. 46).
- Lotte, Fabien, Florian Larrue, & Christian Mühl (2013). “Flaws in current human training protocols for spontaneous Brain-Computer Interfaces: lessons learned from instructional design.” In: *Frontiers in Human Neuroscience* 7. DOI: [10.3389/fnhum.2013.00568](https://doi.org/10.3389/fnhum.2013.00568) (cit. on p. 29).
- Lotze, Martin & Ulrike Halsband (2006). “Motor imagery.” In: *Journal of Physiology Paris* 99.4-6, pp. 386–395. DOI: [10.1016/j.jphysparis.2006.03.012](https://doi.org/10.1016/j.jphysparis.2006.03.012) (cit. on p. 89).
- Lubar, Joel F. & Margaret N. Shouse (1976). “EEG and behavioral changes in a hyperkinetic child concurrent with training of the sensorimotor rhythm (SMR) - A preliminary report.” In: *Biofeedback and Self-Regulation* 1.3, pp. 293–306. DOI: [10.1007/BF01001170](https://doi.org/10.1007/BF01001170) (cit. on p. 22).
- Ma, Ying et al. (2016). “Resting-state hemodynamics are spatiotemporally coupled to synchronized and symmetric neural activity in excitatory neurons.” In: *Proceedings of the National Academy of Sciences* 113.52, E8463–E8471. DOI: [10.1073/pnas.1525369113](https://doi.org/10.1073/pnas.1525369113) (cit. on p. 33).
- Maggioni, Eleonora et al. (2016). “Investigation of the electrophysiological correlates of negative BOLD response during intermittent photic stimulation: An EEG-fMRI study.” In: *Human Brain Mapping* 37.6, pp. 2247–2262. DOI: [10.1002/hbm.23170](https://doi.org/10.1002/hbm.23170) (cit. on p. 33).
- Magri, C., U. Schridde, Y. Murayama, S. Panzeri, & N. K. Logothetis (2012). “The Amplitude and Timing of the BOLD Signal Reflects the Relationship between Local Field Potential Power at Different Frequencies.” In: *Journal of Neuroscience* 32.4, pp. 1395–1407. DOI: [10.1523/JNEUROSCI.3985-11.2012](https://doi.org/10.1523/JNEUROSCI.3985-11.2012) (cit. on pp. 32, 33).
- Mano, Marsel, Anatole Lécuyer, Elise Bannier, Lorraine Perronnet, Saman Noorzadeh, & Christian Barillot (2017). “How to build a hybrid neurofeedback platform combining EEG and fMRI.” In: *Frontiers in Neuroscience* 11, p. 140. DOI: [10.3389/FNINS.2017.00140](https://doi.org/10.3389/FNINS.2017.00140) (cit. on pp. 43, 62).
- Marchesotti, Silvia, Michela Bassolino, Andrea Serino, Hannes Bleuler, & Olaf Blanke (2016). “Quantifying the role of motor imagery in brain-machine in-



- terfaces.” In: *Scientific reports* 6.7, p. 24076. DOI: [10.1038/srep24076](https://doi.org/10.1038/srep24076) (cit. on p. 73).
- Maumet, Camille (2013). “From group to patient-specific analysis of brain function in arterial spin labelling and BOLD functional MRI.” PhD thesis (cit. on pp. 66, 83).
- Maumet, Camille, Pierre Maurel, Jean-Christophe Ferré, & Christian Barillot (2016). “An a contrario approach for the detection of patient-specific brain perfusion abnormalities with arterial spin labelling.” In: *NeuroImage* 134, pp. 424–433 (cit. on p. 58).
- Maurizio, Stefano et al. (2014). “Comparing tomographic EEG neurofeedback and EMG biofeedback in children with attention-deficit hyperactivity disorder.” In: *Biological psychology* 95, pp. 31–44. DOI: [10.1016/j.biopsycho.2013.10.008](https://doi.org/10.1016/j.biopsycho.2013.10.008) (cit. on p. 24).
- Mayeli, Ahmad, Vadim Zotev, Hazem Refai, & Jerzy Bodurka (2016). “Real-time EEG artifact correction during fMRI using ICA.” In: *Journal of Neuroscience Methods* 274, pp. 27–37. DOI: [10.1016/j.jneumeth.2016.09.012](https://doi.org/10.1016/j.jneumeth.2016.09.012) (cit. on p. 74).
- McInnes, Kerry, Christopher Friesen, & Shaun Boe (2016). *Specific brain lesions impair explicit motor imagery ability: A systematic review of the evidence*. DOI: [10.1016/j.apmr.2015.07.012](https://doi.org/10.1016/j.apmr.2015.07.012) (cit. on p. 89).
- Meer, Johan N. van der et al. (2016). “Carbon-wire loop based artifact correction outperforms post-processing EEG/fMRI corrections-A validation of a real-time simultaneous EEG/fMRI correction method.” In: *NeuroImage* 125, pp. 880–894. DOI: [10.1016/j.neuroimage.2015.10.064](https://doi.org/10.1016/j.neuroimage.2015.10.064) (cit. on p. 74).
- Meir-Hasson, Yehudit, Jakob N. Keynan, et al. (2016). “One-class FMRI-inspired EEG model for self-regulation training.” In: *PLoS ONE* 11.5. Ed. by Christian Schmahl, e0154968. DOI: [10.1371/journal.pone.0154968](https://doi.org/10.1371/journal.pone.0154968) (cit. on pp. 38, 41).
- Meir-Hasson, Yehudit, Sivan Kinreich, Ilana Podlipsky, Talma Hendler, & Nathan Intrator (2013). “An EEG Finger-Print of fMRI deep regional activation.” In: *NeuroImage*. DOI: [10.1016/j.neuroimage.2013.11.004](https://doi.org/10.1016/j.neuroimage.2013.11.004) (cit. on pp. 5, 13, 38, 41, 76).
- Michels, Lars et al. (2010). “Simultaneous EEG-fMRI during a working memory task: Modulations in low and high frequency bands.” In: *PLoS ONE* 5.4. Ed. by Michael H. Herzog, e10298. DOI: [10.1371/journal.pone.0010298](https://doi.org/10.1371/journal.pone.0010298) (cit. on p. 32).
- Mihara, Masahito et al. (2012). “Neurofeedback using real-time near-infrared spectroscopy enhances motor imagery related cortical activation.” In: *PLoS ONE* 7.3. DOI: [10.1371/journal.pone.0032234](https://doi.org/10.1371/journal.pone.0032234) (cit. on pp. 2, 10, 18, 24).
- Morcom, Alexa M & Paul C Fletcher (2007). “Does the brain have a baseline? Why we should be resisting a rest.” In: *NeuroImage* 37.4, pp. 1073–1082. DOI: [10.1016/j.neuroimage.2006.09.013](https://doi.org/10.1016/j.neuroimage.2006.09.013) (cit. on p. 35).
- Mukamel, Roy, Hagar Gelbard, Amos Arieli, Uri Hasson, Itzhak Fried, & Rafael Malach (2005). “Coupling Between Neuronal Firing, Field Potentials, and fMRI in Human Auditory Cortex.” In: *Science* 309.5736, pp. 951–954. DOI: [10.1126/science.1110913](https://doi.org/10.1126/science.1110913) (cit. on p. 32).



- Mulert, Christoph & Louis Lemieux (2010). *EEG - fMRI Physiological Basis, Technique, and Applications*. Springer (cit. on p. 32).
- Mullinger, K. J., S. D. Mayhew, A. P. Bagshaw, R. Bowtell, & S. T. Francis (2014). “Evidence that the negative BOLD response is neuronal in origin: A simultaneous EEG-BOLD-CBF study in humans.” In: *NeuroImage* 94, pp. 263–274. DOI: [10.1016/j.neuroimage.2014.02.029](https://doi.org/10.1016/j.neuroimage.2014.02.029) (cit. on p. 33).
- Murta, Teresa, Ujwal Chaudhary, et al. (2016). “Phase-amplitude coupling and the BOLD signal: A simultaneous intracranial EEG (icEEG) - fMRI study in humans performing a finger-tapping task.” In: *NeuroImage*. DOI: [10.1016/j.neuroimage.2016.08.036](https://doi.org/10.1016/j.neuroimage.2016.08.036) (cit. on pp. 32, 75).
- Murta, Teresa, Marco Leite, David W Carmichael, Patrícia Figueiredo, & Louis Lemieux (2015). “Electrophysiological correlates of the BOLD signal for EEG-informed fMRI.” In: *Human Brain Mapping* 36.1, pp. 391–414. DOI: [10.1002/hbm.22623](https://doi.org/10.1002/hbm.22623) (cit. on pp. 75, 90).
- Nakai, Toshiharu, Epifanio Bagarinao, Kayako Matsuo, Yuko Ohgami, & Chikako Kato (2006a). “Dynamic monitoring of brain activation under visual stimulation using fMRI: the advantage of real-time fMRI with sliding window GLM analysis.” In: *Journal of neuroscience methods* 157.1, pp. 158–167 (cit. on p. 47).
- (2006b). “Dynamic monitoring of brain activation under visual stimulation using fMRI-The advantage of real-time fMRI with sliding window GLM analysis.” In: *Journal of Neuroscience Methods* 157.1, pp. 158–167. DOI: [10.1016/j.jneumeth.2006.04.017](https://doi.org/10.1016/j.jneumeth.2006.04.017) (cit. on p. 34).
- Neuner, Irene, Jorge Arrubla, Jörg Felder, & N Jon Shah (2014). “Simultaneous EEG–fMRI acquisition at low, high and ultra-high magnetic fields up to 9.4 T: Perspectives and challenges.” In: *Neuroimage* 102, pp. 71–79 (cit. on p. 57).
- Neuper, Christa & Gert Pfurtscheller (2010). “Neurofeedback Training for BCI Control.” In: *Brain-Computer Interfaces: Revolutionizing Human-Computer Interaction*, pp. 65–78. DOI: [10.1007/978-3-642-02091-9](https://doi.org/10.1007/978-3-642-02091-9) (cit. on p. 25).
- Neuper, Christa, Reinhold Scherer, Miriam Reiner, & Gert Pfurtscheller (2005). “Imagery of motor actions: Differential effects of kinesthetic and visual-motor mode of imagery in single-trial EEG.” In: *Cognitive Brain Research* 25.3, pp. 668–677. DOI: [10.1016/j.cogbrainres.2005.08.014](https://doi.org/10.1016/j.cogbrainres.2005.08.014). arXiv: [j.cogbrainres.2005.08.014](https://arxiv.org/abs/j.cogbrainres.2005.08.014). [10.1016] (cit. on p. 79).
- Neuper, Christa, Michael Wörtz, & Gert Pfurtscheller (2006). “ERD/ERS patterns reflecting sensorimotor activation and deactivation.” In: *Progress in Brain Research* 159, pp. 211–222. DOI: [10.1016/S0079-6123\(06\)59014-4](https://doi.org/10.1016/S0079-6123(06)59014-4) (cit. on p. 63).
- Nierhaus, Till, Christopher Gundlach, Dominique Goltz, Sabrina D Thiel, Burkhard Pleger, & Arno Villringer (2013). “Internal ventilation system of MR scanners induces specific EEG artifact during simultaneous EEG-fMRI.” In: *NeuroImage* 74, pp. 70–76 (cit. on p. 45).
- Niessing, J. (2005). “Hemodynamic Signals Correlate Tightly with Synchronized Gamma Oscillations.” In: *Science* 309.5736, pp. 948–951. DOI: [10.1126/science.1110948](https://doi.org/10.1126/science.1110948) (cit. on p. 32).
- Ninaus, Manuel et al. (2013). “Neural substrates of cognitive control under the belief of getting neurofeedback training.” In: *Frontiers in human neuroscience* 7.December, p. 914. DOI: [10.3389/fnhum.2013.00914](https://doi.org/10.3389/fnhum.2013.00914) (cit. on pp. 2, 11, 21, 89).

- Nir, Yuval et al. (2007). "Coupling between Neuronal Firing Rate, Gamma LFP, and BOLD fMRI Is Related to Interneuronal Correlations." In: *Current Biology* 17.15, pp. 1275–1285. DOI: [10.1016/j.cub.2007.06.066](https://doi.org/10.1016/j.cub.2007.06.066) (cit. on p. 32).
- Niv, Sharon (2013). "Clinical efficacy and potential mechanisms of neurofeedback." In: *Personality and Individual Differences* 54.6, pp. 676–686. DOI: [10.1016/j.paid.2012.11.037](https://doi.org/10.1016/j.paid.2012.11.037) (cit. on pp. 21, 27).
- Nunez, Paul L, Ramesh Srinivasan, et al. (1997). *EEG coherency I: Statistics, reference electrode, volume conduction, Laplacians, cortical imaging, and interpretation at multiple scales*. DOI: [10.1016/S0013-4694\(97\)00066-7](https://doi.org/10.1016/S0013-4694(97)00066-7) (cit. on p. 82).
- Nunez, Paul L & Andrew F Westdorp (1994). "The surface Laplacian, high resolution EEG and controversies." In: *Brain topography* 6.3, pp. 221–226 (cit. on p. 46).
- Ono, Takashi et al. (2014). "Brain-computer interface with somatosensory feedback improves functional recovery from severe hemiplegia due to chronic stroke." In: *Frontiers in Neuroengineering* 7, p. 19. DOI: [10.3389/fneng.2014.00019](https://doi.org/10.3389/fneng.2014.00019) (cit. on pp. 36, 78).
- Paquette, Vincent, Mario Beauregard, & Dominic Beaulieu-Prévost (2009). "Effect of a psychoneurotherapy on brain electromagnetic tomography in individuals with major depressive disorder." In: *Psychiatry research* 174.3, pp. 231–239. DOI: [10.1016/j.psychres.2009.06.002](https://doi.org/10.1016/j.psychres.2009.06.002) (cit. on p. 28).
- Pascual-Marqui, Roberto D, Michaela Esslen, Kieko Kochi, Dietrich Lehmann, et al. (2002). "Functional imaging with low-resolution brain electromagnetic tomography (LORETA): a review." In: *Methods and findings in experimental and clinical pharmacology* 24.Suppl C, pp. 91–95 (cit. on p. 46).
- Peeters, Frenk, Mare Oehlen, Jacco Ronner, Jim van Os, & Richel Lousberg (2014). "Neurofeedback as a treatment for major depressive disorder—a pilot study." In: *PloS one* 9.3. DOI: [10.1371/journal.pone.0091837](https://doi.org/10.1371/journal.pone.0091837) (cit. on p. 28).
- Peniston, E G & P J Kulkosky (1989). "Alpha-theta brainwave training and beta-endorphin levels in alcoholics." In: *Alcoholism, clinical and experimental research* 13.2, pp. 271–279 (cit. on p. 23).
- Penny, Will D, Klaas E Stephan, Andrea Mechelli, & Karl J Friston (2004). "Modelling functional integration: a comparison of structural equation and dynamic causal models." In: *Neuroimage* 23, S264–S274 (cit. on p. 46).
- Penny, William D, Karl J Friston, John T Ashburner, Stefan J Kiebel, & Thomas E Nichols (2011). *Statistical parametric mapping: the analysis of functional brain images*. Academic press (cit. on p. 46).
- Perronnet, Lorraine, Anatole Lécuyer, Fabien Lotte, Maureen Clerc, & Christian Barillot (2016). "Brain Training with Neurofeedback." In: *Brain-Computer Interfaces 1: Foundations and Methods*. Ed. by Maureen Clerc, Laurent Bougrain, & Fabien Lotte. John Wiley & Sons, Inc., pp. 271–292. DOI: [10.1002/9781119144977.ch13](https://doi.org/10.1002/9781119144977.ch13) (cit. on pp. 17, 41).
- Perronnet, Lorraine, Anatole Lécuyer, Marsel Mano, et al. (2017). "Unimodal Versus Bimodal EEG-fMRI Neurofeedback of a Motor Imagery Task." In: *Frontiers in Human Neuroscience* 11, p. 193. DOI: [10.3389/fnhum.2017.00193](https://doi.org/10.3389/fnhum.2017.00193) (cit. on pp. 59, 79, 87).

- Pfurtscheller, Gert, Brendan Z Allison, et al. (2010). "The hybrid BCI." In: *Frontiers in Neuroscience* 4.April, pp. 1–11. DOI: [10.3389/fnpro.2010.00003](https://doi.org/10.3389/fnpro.2010.00003) (cit. on pp. 3, 11).
- Pfurtscheller, Gert, C. Guger, Gernot Müller, G. Krausz, & Christa Neuper (2000). "Brain oscillations control hand orthosis in a tetraplegic." In: *Neuroscience Letters* 292.3, pp. 211–214. DOI: [10.1016/S0304-3940\(00\)01471-3](https://doi.org/10.1016/S0304-3940(00)01471-3) (cit. on p. 19).
- Pfurtscheller, Gert & Fernando Lopes da Silva (1999). *Event-related EEG/MEG synchronization and desynchronization: Basic principles*. DOI: [10.1016/S1388-2457\(99\)00141-8](https://doi.org/10.1016/S1388-2457(99)00141-8). arXiv: [S1388-2457\(99\)00141-8](https://arxiv.org/abs/10.1016/S1388-2457(99)00141-8). [10.1016] (cit. on pp. 80, 81).
- Pfurtscheller, Gert & Christa Neuper (2001). "Motor imagery and direct brain-computer communication." In: *Proceedings of the IEEE* 89.7, pp. 1123–1134. DOI: [10.1109/5.939829](https://doi.org/10.1109/5.939829) (cit. on pp. 36, 72).
- Pfurtscheller, Gert, Andreas Schwerdtfeger, et al. (2017). "Distinction between neural and vascular BOLD oscillations and intertwined heart rate oscillations at 0.1 Hz in the resting state and during movement." In: *PLoS ONE* 12.1, e0168097. DOI: [10.1371/journal.pone.0168097](https://doi.org/10.1371/journal.pone.0168097) (cit. on p. 33).
- Prasad, Girijesh, Pawel Herman, Damien Coyle, Suzanne McDonough, & Jacqueline Crosbie (2010). "Applying a brain-computer interface to support motor imagery practice in people with stroke for upper limb recovery: a feasibility study." In: *Journal of NeuroEngineering and Rehabilitation* 7.1, p. 60. DOI: [10.1186/1743-0003-7-60](https://doi.org/10.1186/1743-0003-7-60) (cit. on p. 36).
- Raffin, Estelle, Jérémie Mattout, Karen T. Reilly, & Pascal Giroux (2012). "Disentangling motor execution from motor imagery with the phantom limb." In: *Brain* 135.2, pp. 582–595. DOI: [10.1093/brain/awr337](https://doi.org/10.1093/brain/awr337) (cit. on p. 89).
- Ramoser, Herbert, Johannes Müller-Gerking, & Gert Pfurtscheller (2000). "Optimal spatial filtering of single trial EEG during imagined hand movement." In: *IEEE Transactions on Rehabilitation Engineering* 8.4, pp. 441–446. DOI: [10.1109/86.895946](https://doi.org/10.1109/86.895946) (cit. on pp. 67, 82).
- Ramos-Murguialday, Ander et al. (2013). "Brain-machine interface in chronic stroke rehabilitation: a controlled study." In: *Annals of neurology* 74.1, pp. 100–8. DOI: [10.1002/ana.23879](https://doi.org/10.1002/ana.23879) (cit. on p. 29).
- Rayner, Genevieve, Graeme Jackson, & Sarah Wilson (2016). *Cognition-related brain networks underpin the symptoms of unipolar depression: Evidence from a systematic review*. DOI: [10.1016/j.neubiorev.2015.09.022](https://doi.org/10.1016/j.neubiorev.2015.09.022) (cit. on p. 96).
- Rehme, Anne K., Simon B. Eickhoff, Claudia Rottschy, Gereon R. Fink, & Christian Grefkes (2012). "Activation likelihood estimation meta-analysis of motor-related neural activity after stroke." In: *NeuroImage* 59.3, pp. 2771–2782. DOI: [10.1016/j.neuroimage.2011.10.023](https://doi.org/10.1016/j.neuroimage.2011.10.023) (cit. on p. 73).
- Riera, Jorge J & Akira Sumiyoshi (2010). "Brain oscillations: ideal scenery to understand the neurovascular coupling." In: *Current Opinion in Neurology* 23.4, p. 1. DOI: [10.1097/WCO.0b013e32833b769f](https://doi.org/10.1097/WCO.0b013e32833b769f) (cit. on p. 32).
- Rimbert, Sébastien, Laurent Bougrain, Cecilia Lindig-León, & Guillaume Serrière (2015). *Amplitude and latency of beta power during a discrete and continuous motor imageries*. Tech. rep. (cit. on p. 72).
- Ritter, Petra, Matthias Moosmann, & Arno Villringer (2009). "Rolandic alpha and beta EEG rhythms' strengths are inversely related to fMRI-BOLD sig-

- nal in primary somatosensory and motor cortex.” In: *Human Brain Mapping* 30.4, pp. 1168–1187. DOI: [10.1002/hbm.20585](https://doi.org/10.1002/hbm.20585) (cit. on p. 90).
- Roberts, SW (2000). “Control chart tests based on geometric moving averages.” In: *Technometrics* 42.1, pp. 97–101 (cit. on p. 46).
- Robineau, Fabien et al. (2017). “Maintenance of Voluntary Self-regulation Learned through Real-Time fMRI Neurofeedback.” In: *Frontiers in Human Neuroscience* 11, p. 131. DOI: [10.3389/fnhum.2017.00131](https://doi.org/10.3389/fnhum.2017.00131) (cit. on p. 27).
- Rockstroh, B., T. Elbert, W. Lutzenberger, & N. Birbaumer (1990). “Biofeedback: Evaluation and Therapy in Children with Attentional Dysfunctions.” In: *Brain and behavior in child psychiatry*, pp. 345–357 (cit. on p. 23).
- Rockstroh, Brigitte et al. (1993). “Cortical self-regulation in patients with epilepsies.” In: *Epilepsy Research* 14.1, pp. 63–72. DOI: [10.1016/0920-1211\(93\)90075-I](https://doi.org/10.1016/0920-1211(93)90075-I) (cit. on p. 23).
- Ros, Tomas et al. (2013). “Mind over chatter: plastic up-regulation of the fMRI salience network directly after EEG neurofeedback.” In: *NeuroImage* 65, pp. 324–35. DOI: [10.1016/j.neuroimage.2012.09.046](https://doi.org/10.1016/j.neuroimage.2012.09.046) (cit. on pp. 38, 40).
- Rosa, M. J., J. Daunizeau, & Karl J. Friston (2010). “EEG-fMRI integration: a critical review of biophysical modeling and data analysis approaches.” In: *Journal of Integrative Neuroscience* 09.04, pp. 453–476. DOI: [10.1142/S0219635210002512](https://doi.org/10.1142/S0219635210002512) (cit. on pp. 32, 33).
- Scharnowski, Frank & Nikolaus Weiskopf (2015). “Cognitive enhancement through real-time fMRI neurofeedback.” In: *Current Opinion in Behavioral Sciences* 4, pp. 122–127. DOI: [10.1016/j.cobeha.2015.05.001](https://doi.org/10.1016/j.cobeha.2015.05.001) (cit. on p. 27).
- Scheeringa, René et al. (2011). “Neuronal Dynamics Underlying High- and Low-Frequency EEG Oscillations Contribute Independently to the Human BOLD Signal.” In: *Neuron* 69.3, pp. 572–583. DOI: [10.1016/j.neuron.2010.11.044](https://doi.org/10.1016/j.neuron.2010.11.044) (cit. on p. 32).
- Scherer, Reinhold, Alois Schloegl, Felix Lee, Horst Bischof, Janez Janša, & Gert Pfurtscheller (2007). “The self-paced graz brain-computer interface: Methods and applications.” In: *Computational Intelligence and Neuroscience* 2007, p. 79826. DOI: [10.1155/2007/79826](https://doi.org/10.1155/2007/79826) (cit. on p. 35).
- Schridde, Ulrich, Manjula Khubchandani, Joshua E Motelow, Basavaraju G Sanganahalli, Fahmeed Hyder, & Hal Blumenfeld (2008). “Negative BOLD with large increases in neuronal activity.” In: *Cerebral cortex (New York, N.Y. : 1991)* 18.8, pp. 1814–27. DOI: [10.1093/cercor/bhm208](https://doi.org/10.1093/cercor/bhm208) (cit. on pp. 33, 34).
- Schulz, Kristina et al. (2012). “Simultaneous BOLD fMRI and fiber-optic calcium recording in rat neocortex.” In: *Nature Methods* 9.6, pp. 597–602. DOI: [10.1038/nmeth.2013](https://doi.org/10.1038/nmeth.2013) (cit. on p. 33).
- Sepulveda, Pradyumna, Ranganatha Sitaram, Mohit Rana, Cristian Montalba, Cristian Tejos, & Sergio Ruiz (2016). “How feedback, motor imagery, and reward influence brain self-regulation using real-time fMRI.” In: *Human Brain Mapping* 37.9, pp. 3153–3171. DOI: [10.1002/hbm.23228](https://doi.org/10.1002/hbm.23228) (cit. on pp. 2, 11, 21).
- Sharma, Nikhil & Jean-Claude Baron (2013a). “Does motor imagery share neural networks with executed movement: a multivariate fMRI analysis.” In: *Frontiers in human neuroscience* 7. DOI: [10.3389/fnhum.2013.00564](https://doi.org/10.3389/fnhum.2013.00564) (cit. on p. 29).

- Sharma, Nikhil & Jean-Claude Baron (2013b). “Does motor imagery share neural networks with executed movement: a multivariate fMRI analysis.” In: *Frontiers in Human Neuroscience* 7, p. 564. DOI: [10.3389/fnhum.2013.00564](https://doi.org/10.3389/fnhum.2013.00564) (cit. on p. 89).
- Sherlin, Leslie H. et al. (2011). “Neurofeedback and Basic Learning Theory: Implications for Research and Practice.” en. In: *Journal of Neurotherapy* 15.4, pp. 292–304. DOI: [10.1080/10874208.2011.623089](https://doi.org/10.1080/10874208.2011.623089) (cit. on p. 21).
- Shindo, Keiichiro et al. (2011). “Effects of neurofeedback training with an electroencephalogram-based brain-computer interface for hand paralysis in patients with chronic stroke: a preliminary case series study.” In: *Journal of rehabilitation medicine* 43.10, pp. 951–957. DOI: [10.2340/16501977-0859](https://doi.org/10.2340/16501977-0859) (cit. on p. 29).
- Shmuel, Amir (2009). “Locally Measured Neuronal Correlates of Functional MRI Signals.” In: *EEG - fMRI*. Berlin, Heidelberg: Springer Berlin Heidelberg, pp. 63–82. DOI: [10.1007/978-3-540-87919-0\\_4](https://doi.org/10.1007/978-3-540-87919-0_4) (cit. on p. 32).
- Shmuel, Amir & David A. Leopold (2008). “Neuronal correlates of spontaneous fluctuations in fMRI signals in monkey visual cortex: Implications for functional connectivity at rest.” In: *Human Brain Mapping* 29.7, pp. 751–761. DOI: [10.1002/hbm.20580](https://doi.org/10.1002/hbm.20580) (cit. on p. 33).
- Shouse, M N & J F Lubar (1979). “Operant conditioning of EEG rhythms and ritalin in the treatment of hyperkinesis.” In: *Biofeedback and self-regulation* 4.4, pp. 299–312. DOI: [10.1007/BF00998960](https://doi.org/10.1007/BF00998960) (cit. on p. 23).
- Shtark, M. B. et al. (2015). “Synergetic fMRI-EEG Brain Mapping in Alpha-Rhythm Voluntary Control Mode.” In: *Bulletin of Experimental Biology and Medicine* 158.5, pp. 644–649. DOI: [10.1007/s10517-015-2827-7](https://doi.org/10.1007/s10517-015-2827-7) (cit. on p. 40).
- Siero, Jeroen CW, Dora Hermes, Hans Hoogduin, Peter R Luijten, Natalia Petridou, & Nick F Ramsey (2013). “BOLD Consistently Matches Electrophysiology in Human Sensorimotor Cortex at Increasing Movement Rates: A Combined 7T fMRI and ECoG Study on Neurovascular Coupling.” In: *Journal of Cerebral Blood Flow & Metabolism* 33.9, pp. 1448–1456. DOI: [10.1038/jcbfm.2013.97](https://doi.org/10.1038/jcbfm.2013.97) (cit. on p. 32).
- Sirigu, A, J.-R. Duhamel, L Cohen, B Pillon, B Dubois, & Y Agid (1996). “The Mental Representation of Hand Movements After Parietal Cortex Damage.” In: *Science* 273.5281, pp. 1564–1568. DOI: [10.1126/science.273.5281.1564](https://doi.org/10.1126/science.273.5281.1564) (cit. on p. 89).
- Sitaram, Ranganatha, Sangkyun Lee, Sergio Ruiz, Mohit Rana, Ralf Veit, & Niels Birbaumer (2011). “Real-time support vector classification and feedback of multiple emotional brain states.” In: *NeuroImage* 56.2, pp. 753–765. DOI: [10.1016/j.neuroimage.2010.08.007](https://doi.org/10.1016/j.neuroimage.2010.08.007) (cit. on p. 36).
- Sitaram, Ranganatha, Tomas Ros, et al. (2016). “Closed-loop brain training: the science of neurofeedback.” In: *Nature Reviews Neuroscience* 18.2, pp. 86–100. DOI: [10.1038/nrn.2016.164](https://doi.org/10.1038/nrn.2016.164) (cit. on pp. 2, 11, 21, 89).
- Sitaram, Ranganatha, Haihong Zhang, et al. (2007). “Temporal classification of multichannel near-infrared spectroscopy signals of motor imagery for developing a brain-computer interface.” In: *NeuroImage* 34.4, pp. 1416–27. DOI: [10.1016/j.neuroimage.2006.11.005](https://doi.org/10.1016/j.neuroimage.2006.11.005) (cit. on p. 75).



- Smith, Anne M. et al. (1999). "Investigation of Low Frequency Drift in fMRI Signal." In: *NeuroImage* 9.5, pp. 526–533. DOI: [10.1006/nimg.1999.0435](https://doi.org/10.1006/nimg.1999.0435) (cit. on p. 35).
- Soldati, Nicola, Vince D. Calhoun, Lorenzo Bruzzone, & Jorge Jovicich (2013). "ICA analysis of fMRI with real-time constraints: an evaluation of fast detection performance as function of algorithms, parameters and a priori conditions." In: *Frontiers in Human Neuroscience* 7, p. 19. DOI: [10.3389/fnhum.2013.00019](https://doi.org/10.3389/fnhum.2013.00019) (cit. on p. 36).
- Soldati, Nicola, Vince D Calhoun, Lorenzo Bruzzone, & Jorge Jovicich (2013a). "ICA analysis of fMRI with real-time constraints: an evaluation of fast detection performance as function of algorithms, parameters and a priori conditions." In: *Frontiers in human neuroscience* 7, p. 19 (cit. on p. 47).
- (2013b). "The use of a priori information in ICA-based techniques for real-time fMRI: an evaluation of static/dynamic and spatial/temporal characteristics." In: *Frontiers in human neuroscience* 7, p. 64 (cit. on p. 47).
- Sollfrank, T. et al. (2016). "The effect of multimodal and enriched feedback on SMR-BCI performance." In: *Clinical Neurophysiology* 127.1, pp. 490–498. DOI: [10.1016/j.clinph.2015.06.004](https://doi.org/10.1016/j.clinph.2015.06.004) (cit. on p. 78).
- Solodkin, Ana, Petr Hlustik, E. Elinor Chen, & Steven L. Small (2004). "Fine modulation in network activation during motor execution and motor imagery." In: *Cerebral Cortex* 14.11, pp. 1246–1255. DOI: [10.1093/cercor/bhh086](https://doi.org/10.1093/cercor/bhh086) (cit. on p. 89).
- Sorger, Bettina, Brigitte Dahmen, et al. (2009). *Another kind of 'BOLD Response': answering multiple-choice questions via online decoded single-trial brain signals*. DOI: [10.1016/S0079-6123\(09\)17719-1](https://doi.org/10.1016/S0079-6123(09)17719-1) (cit. on p. 36).
- Sorger, Bettina, Tabea Kamp, Nikolaus Weiskopf, Judith Caroline Peters, & Rainer Goebel (2016). *When the brain takes 'BOLD' steps: Real-time fMRI neurofeedback can further enhance the ability to gradually self-regulate regional brain activation*. DOI: [10.1016/j.neuroscience.2016.09.026](https://doi.org/10.1016/j.neuroscience.2016.09.026) (cit. on pp. 2, 11, 21, 36).
- Spencer, Michael E, Richard M Leahy, JC Mosher, & PS Lewis (1992). "Adaptive filters for monitoring localized brain activity from surface potential time series." In: *Signals, Systems and Computers, 1992. 1992 Conference Record of The Twenty-Sixth Asilomar Conference on*. IEEE, pp. 156–161 (cit. on p. 46).
- Stephan, Klaas Enno et al. (2008). "Nonlinear dynamic causal models for fMRI." In: *Neuroimage* 42.2, pp. 649–662 (cit. on p. 46).
- Sterman, M.B & L Friar (1972). "Suppression of seizures in an epileptic following sensorimotor EEG feedback training." In: *Electroencephalography and Clinical Neurophysiology* 33.1, pp. 89–95. DOI: [10.1016/0013-4694\(72\)90028-4](https://doi.org/10.1016/0013-4694(72)90028-4) (cit. on pp. 18, 22).
- Sterman, MB, RW LoPresti, & MD Fairchild (1969). "Electroencephalographic and behavioral studies of monomethylhydrazine toxicity in the cat." In: (cit. on pp. 22, 28).
- Stoeckel, L. E. et al. (2014). "Optimizing real time fMRI neurofeedback for therapeutic discovery and development." In: *NeuroImage: Clinical* 5, pp. 245–255. DOI: [10.1016/j.nicl.2014.07.002](https://doi.org/10.1016/j.nicl.2014.07.002) (cit. on pp. 2, 11, 78).
- Strehl, Ute (2009). "Slow Cortical Potentials Neurofeedback." en. In: *Journal of Neurotherapy* 13.2, pp. 117–126. DOI: [10.1080/10874200902885936](https://doi.org/10.1080/10874200902885936) (cit. on p. 23).



- Strehl, Ute, Sarah M. Birkle, Sonja Wörz, & Boris Kotchoubey (2014). “Sustained Reduction of Seizures in Patients with Intractable Epilepsy after Self-Regulation Training of Slow Cortical Potentials - 10 Years After.” In: *Frontiers in Human Neuroscience* 8.604, pp. 1–7. DOI: [10.3389/fnhum.2014.00604](https://doi.org/10.3389/fnhum.2014.00604) (cit. on pp. 21, 22, 28).
- Subasi, Abdulhamit & M Ismail Gursoy (2010). “EEG signal classification using PCA, ICA, LDA and support vector machines.” In: *Expert Systems with Applications* 37.12, pp. 8659–8666 (cit. on p. 46).
- Sudre, Gustavo, Lauri Parkkonen, Elizabeth Bock, Sylvain Baillet, Wei Wang, & Douglas J. Weber (2011). “RtMEG: A real-time software interface for magnetoencephalography.” In: *Computational Intelligence and Neuroscience* 2011. DOI: [10.1155/2011/327953](https://doi.org/10.1155/2011/327953) (cit. on pp. 2, 10, 18, 24).
- Sulzer, James et al. (2013). “Real-time fMRI neurofeedback: Progress and challenges.” In: *NeuroImage* 76, pp. 386–399. DOI: [10.1016/j.neuroimage.2013.03.033](https://doi.org/10.1016/j.neuroimage.2013.03.033) (cit. on pp. 2, 10, 11, 24, 30, 34, 75).
- Sumiyoshi, Akira, Hideaki Suzuki, Takeshi Ogawa, Jorge J. Riera, Hiroaki Shimokawa, & Ryuta Kawashima (2012). “Coupling between gamma oscillation and fMRI signal in the rat somatosensory cortex: Its dependence on systemic physiological parameters.” In: *NeuroImage* 60.1, pp. 738–746. DOI: [10.1016/j.neuroimage.2011.12.082](https://doi.org/10.1016/j.neuroimage.2011.12.082) (cit. on p. 33).
- Tan, Gabriel et al. (2009). “A meta analysis of EEG biofeedback in treatment of epilepsy.” In: *Clinical EEG and Neuroscience* 40.3, pp. 1–8 (cit. on pp. 17, 28).
- Thatcher, Robert (1998). “Normative EEG Databases and EEG Biofeedback.” In: *Journal of Neurotherapy* 2.4, pp. 8–39. DOI: [10.1300/J184v02n04](https://doi.org/10.1300/J184v02n04) (cit. on p. 24).
- Thatcher, Robert W. (2013). “Latest Developments in Live Z-Score Training: Symptom Check List, Phase Reset, and Loreta Z-Score Biofeedback.” en. In: *Journal of Neurotherapy* 17.1, pp. 69–87. DOI: [10.1080/10874208.2013.759032](https://doi.org/10.1080/10874208.2013.759032) (cit. on p. 24).
- Thibault, Robert T., Michael Lifshitz, & Amir Raz (2016). “The self-regulating brain and neurofeedback: Experimental science and clinical promise.” In: *Cortex* 74, pp. 247–261. DOI: [10.1016/j.cortex.2015.10.024](https://doi.org/10.1016/j.cortex.2015.10.024) (cit. on pp. 2, 11).
- Tzourio-Mazoyer, Nathalie et al. (2002). “Automated anatomical labeling of activations in SPM using a macroscopic anatomical parcellation of the MNI MRI single-subject brain.” In: *Neuroimage* 15.1, pp. 273–289 (cit. on p. 46).
- Ullsperger, Markus & Stefan Debener (2010). *Simultaneous EEG and fMRI: recording, analysis, and application*. Oxford University Press (cit. on p. 57).
- Viswanathan, Ahalya & Ralph D Freeman (2007). “Neurometabolic coupling in cerebral cortex reflects synaptic more than spiking activity.” In: *Nature Neuroscience* 10.10, pp. 1308–1312. DOI: [10.1038/nn1977](https://doi.org/10.1038/nn1977) (cit. on p. 32).
- Wander, Jeremiah D et al. (2013). “Distributed cortical adaptation during learning of a brain-computer interface task.” In: *Proceedings of the National Academy of Sciences* 110.26, pp. 10818–10823. DOI: [10.1073/pnas.1221127110](https://doi.org/10.1073/pnas.1221127110) (cit. on p. 84).
- Wang, Jiaojian et al. (2015). “Convergent functional architecture of the superior parietal lobule unraveled with multimodal neuroimaging approaches.” In: *Human Brain Mapping* 36.1, pp. 238–257. DOI: [10.1002/hbm.22626](https://doi.org/10.1002/hbm.22626). arXiv: [NIHMS150003](https://arxiv.org/abs/NIHMS150003) (cit. on p. 89).

- Warbrick, Tracy, Martina Reske, & N. Jon Shah (2013). "Do EEG paradigms work in fMRI? Varying task demands in the visual oddball paradigm: Implications for task design and results interpretation." In: *NeuroImage* 77, pp. 177–185. DOI: [10.1016/j.neuroimage.2013.03.026](https://doi.org/10.1016/j.neuroimage.2013.03.026) (cit. on p. 36).
- Weiskopf, Nikolaus et al. (2003). "Physiological self-regulation of regional brain activity using real-time functional magnetic resonance imaging (fMRI): methodology and exemplary data." In: *NeuroImage* 19.3, pp. 577–586. DOI: [10.1016/S1053-8119\(03\)00145-9](https://doi.org/10.1016/S1053-8119(03)00145-9) (cit. on p. 24).
- White, David J, Marco Congedo, & Joseph Ciorciari (2014). "Source-based neurofeedback methods using EEG recordings: training altered brain activity in a functional brain source derived from blind source separation." In: *Frontiers in Behavioral Neuroscience* 8, p. 373. DOI: [10.3389/fnbeh.2014.00373](https://doi.org/10.3389/fnbeh.2014.00373) (cit. on pp. 24, 37).
- Wolpaw, Jonathan R & Niels Birbaumer (2002). "Brain-computer interfaces for communication and control." In: *Clinical neurophysiology* 113.6, pp. 767–791 (cit. on p. 26).
- Wolpaw, Jonathan R & Elizabeth W Wolpaw (2011). "Brain-computer interfaces: principles and practice." In: (cit. on pp. 25, 26).
- Wong, Chung Ki, Vadim Zotev, Masaya Misaki, Raquel Phillips, Qingfei Luo, & Jerzy Bodurka (2016). "Automatic EEG-assisted retrospective motion correction for fMRI (aE-REMCOR)." In: *NeuroImage* 129, pp. 133–147. DOI: [10.1016/j.neuroimage.2016.01.042](https://doi.org/10.1016/j.neuroimage.2016.01.042) (cit. on p. 74).
- Wu, Xia, Tong Wu, Zhichao Zhan, Li Yao, & Xiaotong Wen (2016). "A real-time method to reduce ballistocardiogram artifacts from EEG during fMRI based on optimal basis sets (OBS)." In: *Computer Methods and Programs in Biomedicine* 127, pp. 114–125. DOI: [10.1016/j.cmpb.2016.01.018](https://doi.org/10.1016/j.cmpb.2016.01.018) (cit. on p. 74).
- Wyckoff, Sarah & Niels Birbaumer (2014). "Neurofeedback and Brain-Computer Interfaces." In: *The Handbook of Behavioral Medicine*. Oxford, UK: John Wiley & Sons, Ltd, pp. 275–312. DOI: [10.1002/9781118453940.ch15](https://doi.org/10.1002/9781118453940.ch15) (cit. on p. 27).
- Wyrwicka, Wanda & Maurice B. Serman (1968). "Instrumental conditioning of sensorimotor cortex EEG spindles in the waking cat." In: *Physiology & Behavior* 3.5, pp. 703–707. DOI: [10.1016/0031-9384\(68\)90139-X](https://doi.org/10.1016/0031-9384(68)90139-X) (cit. on pp. 18, 22).
- Yan N. et al. (2008). "Designing a brain-computer interface device for neurofeedback using virtual environments." In: *Journal of Medical and Biological Engineering* 28.3, pp. 167–172 (cit. on p. 25).
- Yan, Lirong et al. (2009). "Physiological origin of low-frequency drift in blood oxygen level dependent (BOLD) functional magnetic resonance imaging (fMRI)." In: *Magnetic Resonance in Medicine* 61.4, pp. 819–827. DOI: [10.1002/mrm.21902](https://doi.org/10.1002/mrm.21902) (cit. on p. 35).
- Yao, Dezhong (2001). "A method to standardize a reference of scalp EEG recordings to a point at infinity." In: *Physiological Measurement* 22.4, pp. 693–711. DOI: [10.1088/0967-3334/22/4/305](https://doi.org/10.1088/0967-3334/22/4/305) (cit. on p. 74).
- Yin, Siyang, Yuelu Liu, & Mingzhou Ding (2016). "Amplitude of Sensorimotor Mu Rhythm Is Correlated with BOLD from Multiple Brain Regions: A Simultaneous EEG-fMRI Study." In: *Frontiers in Human Neuroscience* 10, July, pp. 1–12. DOI: [10.3389/fnhum.2016.00364](https://doi.org/10.3389/fnhum.2016.00364) (cit. on p. 75).

- Yoo, Julie J. et al. (2012). “When the brain is prepared to learn: Enhancing human learning using real-time fMRI.” In: *NeuroImage* 59.1, pp. 846–852. DOI: [10.1016/j.neuroimage.2011.07.063](https://doi.org/10.1016/j.neuroimage.2011.07.063). arXiv: NIHMS150003 (cit. on p. 36).
- Yoo, Seung Schik, Jong Hwan Lee, Heather O’Leary, Lawrence P. Panych, & Ferenc A. Jolesz (2008). “Neurofeedback fMRI-mediated learning and consolidation of regional brain activation during motor imagery.” In: *International Journal of Imaging Systems and Technology* 18.1, pp. 69–78. DOI: [10.1002/ima.20139](https://doi.org/10.1002/ima.20139). arXiv: NIHMS150003 (cit. on p. 36).
- Yoo, Seung-Schik & Ferenc A Jolesz (2002a). “Functional MRI for neurofeedback: feasibility study on a hand motor task.” In: *Neuroreport* 13.11, pp. 1377–1381 (cit. on pp. 2, 10, 24).
- (2002b). “Functional MRI for neurofeedback: feasibility study on a hand motor task.” In: *Neuroreport* 13.11, pp. 1377–1381 (cit. on p. 48).
- Young, Brittany M, Justin Williams, & Vivek Prabhakaran (2014). “BCI-FES: could a new rehabilitation device hold fresh promise for stroke patients?” In: *Expert review of medical devices* 11.6, pp. 537–539. DOI: [10.1586/17434440.2014.941811](https://doi.org/10.1586/17434440.2014.941811) (cit. on p. 29).
- Young, Kymberly D et al. (2014). “Real-time FMRI neurofeedback training of amygdala activity in patients with major depressive disorder.” In: *PloS one* 9.2. DOI: [10.1371/journal.pone.0088785](https://doi.org/10.1371/journal.pone.0088785) (cit. on pp. 18, 24, 28, 30).
- Yuan, Han, Tao Liu, Rebecca Szarkowski, Cristina Rios, James Ashe, & Bin He (2010). “Negative covariation between task-related responses in alpha/beta-band activity and BOLD in human sensorimotor cortex: an EEG and fMRI study of motor imagery and movements.” In: *NeuroImage* 49.3, pp. 2596–606. DOI: [10.1016/j.neuroimage.2009.10.028](https://doi.org/10.1016/j.neuroimage.2009.10.028) (cit. on p. 75).
- Yuan, Han, Vadim Zotev, Raquel Phillips, Wayne C Drevets, & Jerzy Bodurka (2012). “Spatiotemporal dynamics of the brain at rest—exploring EEG microstates as electrophysiological signatures of BOLD resting state networks.” In: *NeuroImage* 60.4, pp. 2062–72. DOI: [10.1016/j.neuroimage.2012.02.031](https://doi.org/10.1016/j.neuroimage.2012.02.031) (cit. on p. 33).
- Zaidi, Ali Danish et al. (2015). “Simultaneous epidural functional near-infrared spectroscopy and cortical electrophysiology as a tool for studying local neurovascular coupling in primates.” In: *NeuroImage* 120, pp. 394–399. DOI: [10.1016/j.neuroimage.2015.07.019](https://doi.org/10.1016/j.neuroimage.2015.07.019) (cit. on p. 90).
- Zich, Catharina, Stefan Debener, Cornelia Kranczioch, Martin G. Bleichner, Ingmar Gutberlet, & Maarten De Vos (2015). “Real-time EEG feedback during simultaneous EEG-fMRI identifies the cortical signature of motor imagery.” In: *NeuroImage* 114, pp. 438–447. DOI: [10.1016/j.neuroimage.2015.04.020](https://doi.org/10.1016/j.neuroimage.2015.04.020) (cit. on p. 40).
- Zilverstand, Anna, Bettina Sorger, Jan Zimmermann, Amanda Kaas, & Rainer Goebel (2014a). “Windowed correlation: A suitable tool for providing dynamic fMRI-based functional connectivity neurofeedback on task difficulty.” In: *PLoS ONE* 9.1. Ed. by Essa Yacoub, e85929. DOI: [10.1371/journal.pone.0085929](https://doi.org/10.1371/journal.pone.0085929) (cit. on p. 36).
- (2014b). “Windowed correlation: a suitable tool for providing dynamic fMRI-based functional connectivity neurofeedback on task difficulty.” In: *PLoS One* 9.1, e85929 (cit. on p. 47).

- Zotev, Vadim, Raquel Phillips, Han Yuan, Masaya Misaki, & Jerzy Bodurka (2014a). "Self-regulation of human brain activity using simultaneous real-time fMRI and EEG neurofeedback." In: *NeuroImage* 85, pp. 985–995. DOI: [10.1016/j.neuroimage.2013.04.126](https://doi.org/10.1016/j.neuroimage.2013.04.126). arXiv: [1301.4689](https://arxiv.org/abs/1301.4689) (cit. on pp. [5](#), [13](#), [28](#), [30](#), [38](#), [39](#), [41](#), [73–75](#), [78](#)).
- (2014b). "Self-regulation of human brain activity using simultaneous real-time fMRI and EEG neurofeedback." In: *NeuroImage* 85, pp. 985–995 (cit. on p. [57](#)).
- Zotev, Vadim, Han Yuan, et al. (2016). "Correlation between amygdala BOLD activity and frontal EEG asymmetry during real-time fMRI neurofeedback training in patients with depression." In: *NeuroImage: Clinical* 11, pp. 224–238. DOI: [10.1016/j.nicl.2016.02.003](https://doi.org/10.1016/j.nicl.2016.02.003). arXiv: [1409.2046](https://arxiv.org/abs/1409.2046) (cit. on pp. [39](#), [40](#)).